# STRATEGIC DEVELOPMENT OF BACTERIOPHAGE THERAPEUTICS: TREATMENT OPTIMIZATION AND PHARMACEUTICAL FORMULATION SCRIENCE FOR PSEUDOMONAS AERUGINOSA PULMONARY INFECTION

A thesis submitted

to fulfil requirements for the degree of

Doctor of Philosophy

**Mengyu Li**

School of Pharmacy

Faculty of Medicine and Health

The University of Sydney

2025

# STATEMENT OF AUTHENTICITY

This research was supported by an Australian Government Research Training Program (RTP) Scholarship. This thesis is submitted to the University of Sydney in fulfilment of the requirements for the degree of Doctor of Philosophy. The work described was carried out in the School of Pharmacy, the Faculty of Medicine and Health, the University of Sydney, under the supervision of Professor Hak-Kim Chan.

The work presented in this thesis is, to the best of my knowledge and belief, original except as acknowledged in the text. The contribution of all co-authors in publications included in the body of the thesis have been declared, signed by each co-author, and attached as an appendix. I hereby declare that I have not previously or concurrently submitted this material, either in full or in part, for a degree at this or any other institution.

Mengyu Li

June 2025

# Acknowledgements

*"It's not that I'm so smart, it's just that I stay with problems longer."*

— Albert Einstein

First, I would like to express my deepest gratitude to my supervisor, Professor Hak-Kim Chan, for his endless guidance, unwavering support, and remarkable patience throughout this project, especially during the challenging early stages of my research journey.

I am equally grateful to my research team members. My co-supervisor, Rachel Yoon Chang, has consistently been kind and generous in providing valuable suggestions and support in the laboratory. Patricia Tang has always looked after me with genuine care. I also want to thank my dear friends and colleagues: Waiting Dai, Pancy Kwong, Qixuan Hong, and Chengxi Liu. The memories of our fun times together playing Mahjong and Avalon will always bring a smile to my face.

Special thanks go to my best friend, Yiqun Qu. Thank you for being my companion throughout these seven remarkable years. I never imagined I would meet such a wonderful friend when I first came to Australia. Though we are so different in many ways, we understand each other deeply. I still cherish the memories of how we spent time together and found joy even during the difficult COVID period. These moments will never be forgotten.

I owe an immense debt of gratitude to my family. My parents have always supported and loved me unconditionally, taking care of me in every possible way. When I decided to come to Australia, they supported my choice wholeheartedly. Through their actions, my parents have

shown me what unconditional love truly means—loving their children without expecting anything in return.

Finally, I would like to thank myself. There were moments when I questioned whether I truly wanted to pursue a PhD, doubting whether this journey was worth undertaking. I am grateful that I chose to persist. During my doctoral studies, I experienced the pandemic and had time for deep reflection. Life is indeed too short. I have learned to cherish each moment and live the life I want to live, without being overly concerned about others' opinions—after all, this is my own life to live.

This thesis represents not just academic achievement, but a testament to the power of persistence, the importance of supportive relationships, and the courage to stay true to oneself.

*"I now see how owning our story and loving ourselves through that process is the bravest thing that we will ever do."*

-Brené Brown

# Acknowledgment of AI Use

In accordance with university guidelines, I acknowledge the use of Claude 3.5 Sonnet, an AI tool developed by Anthropic (https://www.anthropic.com), to correct grammar, spelling and improve readability in my thesis.

# List of Abbreviations

| | |
|---|---|
| CF | Cystic fibrosis |
| DVS | Dynamic vapor sorption |
| DSC | Differential scanning calorimetry |
| DPI | Dry product inhalers |
| FPF | Fine particle fraction |
| HPLC | High performance liquid chromatography |
| MDR | Multidrug-resistant |
| MSLI | Multi-stage liquid impinger |
| PBS | Phosphate buffered saline |
| P. aeruginosa | Pseudomonas aeruginosa |
| PFU | Plaque forming units |
| SEM | Scanning electron microscopy |
| TGA | Thermogravimetric analysis |
| LPS | Lipopolysaccharide |
| TFP | Trifluoperazine |
| CFU | Colony forming units |
| MOI | Multi o |
| PVP | Polyvinylpyrrolidone |
| XRD | X-ray diffraction |

# Table of Contents

# Thesis Abstract

## Chapter 1

Antimicrobial resistance contributes to 1.27 million deaths annually, severely limiting treatment options for respiratory infections. Multidrug-resistant Pseudomonas aeruginosa is particularly problematic in cystic fibrosis patients and those with ventilator-associated pneumonia. Traditional antibiotic therapy faces mounting challenges from biofilm formation, limited pulmonary penetration, and rapidly emerging resistance mechanisms. Bacteriophage therapy offers compelling advantages including high bacterial specificity, self-amplifying properties, and biofilm-penetrating capabilities crucial for chronic respiratory infections. Inhalation delivery enables targeted phage administration achieving lung concentrations 10-100 fold higher than systemic routes while minimizing off-target effects. However, clinical translation faces significant hurdles including rapid bacterial resistance development, formulation instability, and suboptimal aerosol delivery characteristics. This research addresses interconnected challenges through an integrated platform combining evolutionary phage scheduling principles with advanced solid-state formulation engineering. Strategic approaches including sequential phage administration and receptor-diverse cocktail design suppress resistance development through targeted selection pressure management. Concurrent innovations in dry powder formulation leverage spray drying technology, glass transition temperature optimization, and novel excipient systems including human serum albumin to achieve exceptional stability while maintaining optimal aerodynamic properties. The convergence of phage scheduling strategies with pharmaceutical engineering creates a comprehensive therapeutic platform simultaneously addressing resistance steering, supply-chain stability, and targeted pulmonary delivery. This multidisciplinary approach provides

essential foundations for translating laboratory-based phage therapy successes into clinically viable treatments for life-threatening respiratory infections, particularly addressing urgent needs for alternatives to failing antibiotic regimens in critically ill patients.

## Chapter 2

With antibiotic resistance increasingly limiting treatment options, bacteriophage therapy has gained renewed attention as a potential alternative. Phage cocktails targeting multiple bacterial receptors demonstrate high efficacy, yet simultaneous application of phages can quicken resistance development in bacteria. This study evaluates the comparative effectiveness of simultaneous versus sequential phage treatments using two phages: Dobby (targeting lipopolysaccharides, LPS) and MPK7 (targeting type IV pili, TFP), against Pseudomonas aeruginosa. Through time-kill assays performed at various multiplicities of infection (MOIs: 0.01, 1, and 100), we found sequential treatment—particularly initiating therapy with the LPS-specific phage Dobby, followed by MPK7—to be significantly more effective, achieving bacterial reductions of over 3-log10 within 48 h. Interestingly, sequential treatments at a low MOI (0.01) maintained sustained suppression of bacterial populations, whereas high MOI (100) treatments triggered rapid bacterial rebound and resistance emergence. Resistance profiling further confirmed the advantage of sequential dosing, revealing lower fitness costs in Dobby-resistant bacterial isolates, making them more susceptible to subsequent MPK7 treatment. Additionally, atomic force microscopy infrared spectroscopy (AFM-IR) revealed unique chemical signatures in resistant mutants, providing insights into underlying resistance mechanisms involving alterations in phage receptors, such as LPS truncation and TFP dysfunction. These results support the adoption of sequential phage treatment—first targeting LPS, followed by TFP—as an optimal strategy to extend bacterial suppression and minimize

resistance, thereby offering a sustainable and effective alternative to simultaneous treatments for combating antibiotic-resistant bacterial infections.

## Chapter 3

Effective dry-state stabilization of bacteriophages is crucial for expanding their therapeutic use. This study builds upon Chang et al.'s work demonstrating that saccharide-based formulations maintain phage stability when glass transition temperature (Tg) exceeds storage temperature (Ts) by ~50°C [1]. We investigated polymer-based matrices for long-term stabilization by spray-drying PEV1 phage with polyvinylpyrrolidone (PVP) of varying molecular weights (K15, K25, K40, K100) and storing for 180 days at 4–40°C and 15–53% RH. All formulations achieved minimal titre losses (⩽1 $\log_{10}$) under 4-22°C/15% RH. Differential scanning calorimetry (DSC) demonstrated Tg increased with PVP molecular weight but decreased substantially with humidity (30-50°C reduction per 20% RH increase). At 33% RH, long-term stability was achieved with high-molecular-weight PVPs (K40, K100), which maintained thermal offsets between Tg and Ts ($\Delta T \geqslant 100$ °C), while lower-weight (K15, K25) showed 2–3 $\log_{10}$ titre loss. Water activity (aw) analysis revealed a critical threshold at aw 0.43, above which degradation kinetics increased by an order of magnitude. Arrhenius analysis confirmed that phage degradation rates increased with temperature, consistent with thermally activated destabilization mechanisms. Under higher stress conditions (40°C/⩾43% RH), water absorption plasticized the PVP matrix and depressed the Tg while elevated temperature simultaneously accelerated degradation kinetics, resulting in substantial titre losses even when $\Delta T$ exceeded 100°C. In conclusion, at mild humidity (aw ⩽ 0.33) and ambient temperature (⩽ 22°C), high-molecular-weight PVP-based formulations can offer enhanced storage flexibility and reduced cold-chain dependency for optimal therapeutic viability.

## Chapter 4

The growing potential of bacteriophage therapy as an alternative treatment for pulmonary infections caused by multidrug-resistant bacteria has been increasingly recognized. This study aimed to evaluate the long-term stability of spray-dried phage powder formulations for pulmonary delivery, focusing on both biological activity and physicochemical properties. Three phages, PEV1, PEV20, and PEV61, were selected for formulation based on their host range against clinical strains of *Pseudomonas aeruginosa*. Eight spray-dried formulations, developed with varying proportions of lactose as a stabilizer and leucine as a moisture protectant and powder dispersion enhancer, were stored under controlled conditions at 4°C/15% relative humidity (RH) and 20°C/15% RH for four years. Over this period, phage titers declined with reduction ranging from 0.97 log10 in the most stable formulation to 2.49 log10 in the least stable one. Formulations with higher lactose concentrations (70-80%) demonstrated better preservation of biological activity. While the overall particle morphology remained unchanged, some thread-like elongated features protruding from the particle surfaces were observed, particularly in powders stored at 20°C/15% RH. However, there was a decline in the fine particle fraction (FPF) 50 – 60% to 27 - 44%. These findings showed the potential of spray-dried phage powders as a viable option for long-term storage to retain bioactivity, but the aerosol performance can be compromised.

## Chapter 5

In response to the growing threat of antibiotic resistance in pulmonary infections, bacteriophage therapy is emerging as a promising alternative to traditional antibiotics. We aimed to develop novel dry powder formulations for the pulmonary delivery of bacteriophages, using the *Pseudomonas aeruginosa*–specific phage PEV2 as a model. Our formulations combined human serum albumin (HSA) and lactose to enhance both phage stability and aerosol

performance. A Box–Behnken experimental design was conducted to investigate the effects of HSA/lactose ratio, solute concentration of feed solution, and spray-drying inlet temperature. Our results demonstrated that incorporating 60% w/w HSA significantly improved aerosol performance by achieving a fine particle fraction above 50% and effectively delayed lactose recrystallization by maintaining an amorphous state at relative humidity levels of 80% or higher. Importantly, the optimized formulation (60% HSA/40% lactose) preserved phage viability with less than a 0.8 $\log_{10}$ reduction. Possible mechanisms contributing to stabilizing the phage powder formulations in HSA-lactose were discussed. These findings underscore the potential of a balanced HSA–lactose system as a robust powder formulation platform for pulmonary phage therapy.

# Chapter 1

# Literature Review

## Introduction to Antibiotic Resistance and Phage Therapy

Antimicrobial resistance (AMR) is a major global health threat, significantly compromising the ability to treat bacterial infections. AMR can be classified into intrinsic resistance, arising from natural physiological or structural characteristics of bacteria, and acquired resistance, resulting from genetic mutations or horizontal gene transfer (1). Acquired resistance is particularly concerning due to the rapid emergence and dissemination among pathogens, limiting the effectiveness of even recently developed antibiotics.

Recent systematic analyses estimate that bacterial AMR directly contributed to approximately 1.27 million deaths globally in 2019, with this figure expected to rise substantially if current trends persist (2). The World Health Organization (WHO) has prioritized pathogens such as carbapenem-resistant Acinetobacter baumannii, Pseudomonas aeruginosa, and Enterobacteriaceae as critical targets due to their high morbidity, mortality, and frequent resistance to multiple antibiotic classes (3). These pathogens are particularly prevalent in healthcare-associated respiratory infections, underscoring an urgent need for novel therapeutic strategies.

Several interconnected factors drive the escalation of antibiotic resistance. Mechanistically, horizontal gene transfer—through conjugation, transformation, and transduction—enables rapid spread of resistance genes across bacterial populations (4). Clinically, inappropriate antibiotic use, including overprescription, inadequate dosing, and premature discontinuation, significantly accelerates the selection and enrichment of resistant bacteria (5). Environmental and agricultural antibiotic misuse further exacerbates this issue by creating reservoirs of resistance in non-clinical settings (6). Additionally, biofilm formation provides protective niches facilitating bacterial survival, increasing persistence, and enhancing resistance

development, especially in chronic infections such as those affecting respiratory systems (7). Concurrently, the pharmaceutical industry's declining investment in antibiotic development due to unfavourable economic and regulatory conditions has markedly reduced the availability of new antibacterial drugs (8). Collectively, these converging pressures compel exploration of fundamentally different antibacterial strategies, notably bacteriophage therapy.

Pulmonary infections present distinct challenges in the context of antibiotic resistance. Patients in intensive care units (ICUs), individuals with cystic fibrosis (CF), chronic obstructive pulmonary disease (COPD), and ventilator-associated pneumonia (VAP) are particularly vulnerable to multidrug-resistant (MDR) and extensively drug-resistant (XDR) pathogens (9). *Pseudomonas aeruginosa*, a leading respiratory pathogen, is increasingly resistant to critical antibiotics, including carbapenems and colistin, worldwide (10). Limitations of current last-line antibiotics further complicate treatment; for instance, colistin poses significant nephrotoxicity risks and demonstrates suboptimal pulmonary penetration (11). Recently introduced antibiotics such as ceftolozane/tazobactam and ceftazidime/avibactam are already encountering emerging resistance (12), emphasizing the necessity of alternative therapies capable of overcoming these limitations.

Bacteriophages (phages), viruses that specifically infect bacterial hosts, present a promising alternative approach. Structurally, phages consist of genetic material (DNA or RNA) enclosed in a protein capsid, sometimes enveloped by lipid membranes (13). Phages typically follow one of two life cycles: the lytic cycle, where immediate host-cell lysis releases viral progeny, and the lysogenic cycle, in which phage DNA integrates into the host genome, remaining dormant until activated. Phage specificity varies significantly, from highly targeted strains

infecting single bacterial species to broader-spectrum phages capable of infecting multiple related species (14).

Phage therapy originated in Félix d'Hérelle's pioneering work in 1917, demonstrating phage efficacy against dysentery (15). Although Western countries largely abandoned phage therapy with the advent of antibiotics in the mid-20th century, Eastern European countries continued development, maintaining robust therapeutic protocols and infrastructure (16). Recently, escalating antibiotic resistance has renewed global scientific interest and clinical investigation into phage-based treatments. Regulatory frameworks differ internationally: the European Medicines Agency (EMA) facilitates phage therapy through compassionate-use pathways for critically ill patients lacking alternatives (17); in the United States, the Food and Drug Administration (FDA) mandates detailed safety and efficacy evidence via Investigational New Drug (IND) applications (18); Belgium uniquely permits personalized magistral phage preparations by licensed pharmacists under specific medical prescriptions (17).

## Phage Therapy as a Promising Alternative

Bacteriophage therapy offers several advantages over conventional antibiotics, positioning it as a valuable alternative to combat antimicrobial resistance. Unlike broad-spectrum antibiotics, which indiscriminately affect bacterial communities, phages exhibit high specificity for their bacterial targets, minimizing disruption of beneficial microbiota and reducing secondary infection risks (19). The self-amplifying nature of phages allows their concentration to increase exponentially at infection sites, enhancing therapeutic efficacy precisely where needed (20). Clinical trials have demonstrated encouraging response rates, including a 61% success rate in the interim analysis of the PhagoBurn study targeting burn-wound infections (21).

Phages possess significant biofilm-penetrating capabilities, crucial for addressing chronic infections. Many phages produce enzymes such as depolymerases and endolysins, which degrade biofilm matrices composed of extracellular polymeric substances, enhancing therapeutic penetration (22). This characteristic is especially relevant for respiratory infections, where pathogens like *P. aeruginosa* often form persistent biofilm communities in lung environments, complicating conventional antibiotic treatments (23).

The safety profile of phage therapy is favourable, supported by both historical evidence and contemporary clinical studies. Phages naturally occur in human microbiomes, particularly at mucosal sites, suggesting inherent compatibility (24). Recent systematic reviews and pharmacovigilance studies report minimal serious adverse events directly attributable to phage therapy, with most effects being mild and transient (25, 26).

Modern phage therapy encompasses various delivery methods tailored to clinical contexts, including topical formulations (ointments and gels), oral preparations for gastrointestinal infections, intravenous administration for systemic infections, and inhaled formulations for respiratory infections (27, 28). Emerging dry powder formulations offer potential advantages for respiratory applications, including improved stability, patient convenience, and enhanced lung deposition characteristics. However, significant regulatory challenges remain regarding product characterization, consistency, and resistance management. Recent guidance documents, such as the European Medicines Agency's reflection paper on microbial medicinal products, now explicitly acknowledge bacteriophages, highlighting evolving regulatory perspectives (29).

Phage engineering has emerged as an innovative approach to address inherent limitations of phage therapy. Synthetic biology techniques allow modification of phage genomes to improve

host range, reduce lysogenic potential, or introduce therapeutic enzymes (30). CRISPR-engineered phages have demonstrated potential for targeted elimination of antibiotic-resistant bacterial strains by disrupting specific resistance genes (31). However, translational challenges such as containment of genetically modified organisms and potential horizontal gene transfer require careful consideration.

## Therapeutic Strategies: Single Phage, Cocktails, and Sequential Administration

### Single Phage Therapy

Single phage therapy utilizes individual, well-characterized phage isolates against specific bacterial targets. This approach simplifies regulatory approval, manufacturing processes, and therapeutic characterization (32). Compassionate use cases, such as treating multidrug-resistant Acinetobacter baumannii infections, have demonstrated remarkable therapeutic successes where conventional antibiotics failed (33). Nonetheless, single phage therapies face limitations due to narrow host ranges and rapid bacterial resistance emergence, necessitating precise bacterial susceptibility testing and potentially limiting broader applicability (34).

### Phage Cocktails

Phage cocktail therapy involves simultaneous administration of multiple phages selected for complementary host ranges and mechanisms, reducing resistance development and broadening therapeutic efficacy (35). Receptor-diverse cocktails targeting distinct bacterial surface receptors decrease the likelihood of resistance arising from single receptor mutations (36). Additionally, combining wild-type phages with engineered or laboratory-evolved variants enhances therapeutic coverage and biofilm degradation capabilities. However, optimal cocktail design requires careful evaluation of phage compatibility, potential antagonistic interactions, and stringent manufacturing and quality control measures (37). Adaptive cocktail strategies

involving continuous bacterial surveillance and dynamic phage substitution are emerging as promising approaches for personalized therapies.

## Sequential Phage Administration

Sequential phage administration involves timed, sequential application of different phages or phage cocktails targeting distinct bacterial receptors, inspired by antimicrobial stewardship principles and receptor rotation strategies (38). This method leverages bacterial fitness costs associated with receptor modifications and exploits collateral sensitivity, where resistance to one phage increases susceptibility to another targeting alternative receptors (39). Optimal intervals between phage administrations depend on factors such as multiplicity of infection, bacterial growth phases, and host immune status, with studies suggesting intervals ranging from several hours to days based on specific infection dynamics (40).

While phage cocktails offer immediate broad-spectrum coverage, sequential administration may provide superior long-term resistance management by dynamically responding to emerging bacterial resistance patterns (41). However, sequential strategies require precise monitoring and may be less suited for acute infections where immediate broad-spectrum coverage is critical.

This thesis integrates optimized sequential phage therapy and cocktail targeting strategies with advanced inhalable formulation techniques, addressing critical gaps in how receptor-specific phage targeting can be leveraged through pharmaceutical innovations for respiratory applications.

## Phage Therapy for Respiratory Infections

### Respiratory Infections and *Pseudomonas aeruginosa*

*Pseudomonas aeruginosa* represents one of the most formidable respiratory pathogens, particularly in vulnerable patient populations including those with cystic fibrosis (CF), non-CF bronchiectasis, and ventilator-associated pneumonia (VAP). The epidemiological burden of P. aeruginosa respiratory infections is substantial, with prevalence rates exceeding 80% in adult CF patients and mortality rates of 18-61% in VAP cases, depending on resistance patterns (42, 43). In non-CF bronchiectasis, *P. aeruginosa* colonization occurs in approximately 12-26% of patients but is associated with accelerated lung function decline, increased exacerbation frequency, and higher healthcare utilization (44).

The pathogenic arsenal of *P. aeruginosa* in respiratory environments is multifaceted and highly adapted to pulmonary niches. Quorum sensing systems, primarily *las* and *rhl* circuits, coordinate population-wide virulence factor expression, including elastase, pyocyanin, and rhamnolipids, which collectively contribute to tissue damage and immune evasion (45). Alginate biofilm formation represents a hallmark adaptation in chronic respiratory infections, particularly in CF patients, where mucoid variants emerge through *mucA* gene mutations (46). These alginate-rich biofilms provide exceptional protection against both antimicrobial agents and host immune responses, contributing to the persistent nature of chronic *P. aeruginosa* infections. Elastase production further exacerbates pathogenesis by degrading lung structural proteins, impairing mucociliary clearance, and facilitating bacterial invasion of deeper lung tissues (47).

The lung environment presents unique hurdles that complicate therapeutic interventions against *P. aeruginosa*. Mucus barriers, particularly in CF patients where abnormal mucin glycosylation

and increased viscoelasticity occur, significantly impede antimicrobial penetration and bacterial clearance (48). Pulmonary surfactant components, including surfactant proteins A and D, can interact with therapeutic agents, potentially reducing their bioavailability and efficacy (49). Additionally, robust immune clearance mechanisms, including alveolar macrophage phagocytosis and neutrophil recruitment, may inadvertently clear therapeutic phages before they can establish effective infection of target bacteria (50). The hypoxic microenvironments within infected lung tissues and biofilm structures further complicate treatment, as many antibiotics demonstrate reduced activity under these conditions (51).

**Why Inhalation**

Nebulization has been the primary method for phage aerosolization and delivery into the respiratory tract. Commercial nebulizers utilize various modes of aerosol generation mechanism including vibrating mesh, compressed air jet, ultrasound and colliding liquid jets. However, formulating phages into inhalable forms for pulmonary infections presents a dual challenge requiring both aerosol performance and phage biochemical stability. Progress has been partly hindered by poor understanding of the mechanism responsible for stabilisation of phages in both liquid and solid formulations. The potential for inhaled phage therapy using nebulizers has been investigated in several in vitro and in vivo studies, with comprehensive analysis of phage nebulization using commercial nebulizers such as Pari LC star and eFlow nebulizers demonstrating variable phage survival depending on the device and operating conditions. Direct pulmonary delivery achieves high local drug concentrations while minimizing systemic exposure and associated toxicity risks (52). For phage therapy specifically, inhalation enables targeted delivery to the primary site of infection, where phages can interact directly with bacterial biofilms and planktonic populations in the airway lumen (53).

Pharmacokinetic studies demonstrate that inhaled therapeutics can achieve lung tissue concentrations 10-100 fold higher than those achievable through intravenous administration, while maintaining significantly lower plasma levels (54). This is particularly advantageous for phage therapy, where high multiplicity of infection ratios at the site of bacterial colonization are crucial for therapeutic efficacy. Furthermore, the relatively large surface area of the respiratory tract (approximately 70 $m^2$) provides extensive opportunity for phage-bacteria interactions, enhancing the probability of successful bacterial lysis (55).

The lung's natural clearance mechanisms, while potentially challenging for phage retention, also facilitate the removal of bacterial debris and inflammatory mediators following successful phage-mediated bacterial lysis. Mucociliary escalator function can help clear lysed bacterial components, reducing inflammatory burden and potentially improving clinical outcomes (56). Additionally, the compartmentalized nature of respiratory infections allows for targeted therapy delivery to specific lung regions through advanced inhalation devices, potentially enabling personalized dosing strategies based on infection localization determined through imaging studies (57).

**Efficacy of Phage Therapy in Respiratory Infections**

Pre-clinical evidence for inhaled phage therapy efficacy has been established through various animal models and in vitro systems. Most phage research for respiratory infections in animal models has been focused on the delivery of liquid formulations using intra-nasal instillation and nebulization. Mouse intranasal instillation models have demonstrated significant bacterial load reduction and improved survival rates when phages are administered shortly after *P. aeruginosa* challenge (58). When treating MDR *P. aeruginosa*-associated lung infections, either immediately or 12-h post-infection, intranasal phage treatment resulted in significantly longer survival in treated animals with a lower bacterial burden in their lungs and blood.

Aerosol chamber studies using rodent models have shown that nebulized phage formulations can effectively penetrate to peripheral lung regions and maintain therapeutic activity against biofilm-associated bacteria (59). Pig trachea models, which more closely approximate human respiratory anatomy and physiology, have validated phage penetration through mucus layers and demonstrated sustained antimicrobial activity in *ex vivo* conditions (60). Intratracheal phage cocktail monotherapy effectively prevented all mice from dying, and reduced lung bacterial burden and pathologic abnormalities even when provided 6 hours after bacterial challenge, demonstrating the potential for delayed treatment scenarios.

Human evidence, while limited, provides encouraging preliminary data supporting respiratory phage therapy applications. Recent clinical experiences have shown that phage therapy has been exclusively utilised following ineffective antibiotic treatment for the management of acute multidrug-resistant (MDR) or chronic resistant infections. In pulmonary medicine, this compassionate use paradigm reflects the severity of antibiotic-resistant respiratory pathogens and the urgent need for alternative therapeutic interventions when conventional treatments fail to control infection progression. Chan et al. (2025) reported successful treatment outcomes using nebulized personalized phage cocktails in CF patients with chronic *P. aeruginosa* infections, demonstrating both safety and efficacy over 28-day treatment periods (61). This landmark study showed significant reductions in bacterial load (median 2.3 $\log_{10}$ CFU/mL reduction) and improvements in forced expiratory volume metrics without serious adverse events directly attributable to phage therapy. In a review of 20 cases of PT for respiratory infections, phage resistance was identified in only 30% of cases. However, among patients in which phage resistance was detected, some continued to demonstrate clinical improvement, suggesting that phage resistance may not always indicate treatment failure.

Pharmacokinetic and pharmacodynamic features of inhaled phage therapy reveal favourable lung retention characteristics with limited systemic spread. Chow *et al.* (2020) demonstrated that nebulized phages exhibit prolonged residence times in lung tissue (>12 hours) with minimal detection in systemic circulation, suggesting localized therapeutic action (58). This pharmacokinetic profile supports repeated dosing regimens without concern for systemic accumulation or off-target effects.

Synergy studies investigating combinations of phages with conventional antibiotics have yielded promising results. In vitro studies of phage-ciprofloxacin combination therapy delivered as dry powder formulations demonstrated enhanced bacterial killing compared to either treatment alone, suggesting potential for combination therapeutic approaches (62). These synergistic effects appear to result from phage-mediated biofilm disruption facilitating antibiotic penetration, while antibiotic pressure may select for antibiotic-resistant variants that remain phage-susceptible.

## Formulation Strategies for Phage Delivery

### Dry Powder Formulations

Dry state formulation of therapeutic phage is attractive to improve their "draggability" by increasing their shelf life, improving their ease of handling, and ultimately retaining their long-term potency. Dry powder inhalers (DPIs) offer significant advantages for phage delivery compared to liquid nebulized formulations. The elimination of cold chain requirements addresses major logistical challenges in phage therapy distribution and storage, particularly relevant for resource-limited settings or emergency applications (63). Patient-activated delivery mechanisms reduce dependency on healthcare infrastructure and enable self-administration, improving treatment accessibility and adherence (64). Dose uniformity achievable through engineered powder formulations ensures consistent therapeutic delivery,

while the inherently transmission-free nature of DPIs eliminates concerns about healthcare worker exposure or environmental contamination (65).

Manufacturing approaches for phage-containing dry powders include spray drying, spray-freeze drying, and lyophilization, each offering distinct advantages and limitations.

**Spray Drying Advantages**

Spray drying represents the most versatile and widely adopted technique for phage powder manufacture, offering specific technological advantages for biological preservation and particle engineering. Spray drying offers exceptional control over particle engineering parameters, enabling precise manipulation of particle size distribution, morphology, and density (66). The atomization process can be optimized to produce particles with specific aerodynamic properties, including the formation of corrugated surfaces that enhance dispersibility and reduce inter-particulate cohesion (66). Hollow particle formation through controlled drying kinetics can reduce particle density while maintaining structural integrity, improving lung deposition characteristics without compromising phage stability.

Temperature control during spray drying provides a critical advantage for heat-sensitive phage formulations. While inlet temperatures may reach 100-200°C, the rapid evaporation of moisture ensures that product temperatures remain significantly lower, typically $\leqslant$45°C, preserving phage infectivity (67). The short residence time in the drying chamber (seconds rather than hours) minimizes thermal exposure compared to other drying methods, making spray drying particularly suitable for thermolabile biologics.

Co-processing capabilities allow simultaneous incorporation of multiple excipients during spray drying, enabling the formation of composite particles with tailored properties. This approach facilitates the development of multi-functional formulations where stabilizing

excipients, dispersibility enhancers, and targeting ligands can be integrated into single particles through controlled co-precipitation (68). Such composite particles offer superior performance compared to physical mixtures, with improved content uniformity and reduced segregation during handling and storage.

**Powder Formulation Advantages**

Dry powder formulations offer compelling advantages over liquid formulations for phage therapy, addressing multiple clinical, practical, and manufacturing challenges. The enhanced stability profile of dry powders stems from the elimination of water-mediated degradation pathways, including hydrolysis, oxidation, and microbial growth (63). In the solid state, molecular mobility is significantly reduced, effectively halting most chemical and enzymatic degradation processes that compromise phage viability in liquid formulations. This stability enhancement enables extended shelf life at ambient temperatures, addressing the cold chain logistics challenges that severely limit liquid phage therapy accessibility in resource-limited settings.

Manufacturing advantages of powder formulations include the continuous processing capability that enables industrial-scale production with consistent quality control, addressing the commercial viability requirements for phage therapeutics (69). Unlike batch processes such as lyophilization, continuous processing allows for uninterrupted production runs, significantly reducing manufacturing costs and improving production efficiency for large-scale phage therapy applications. The single-step transformation from liquid suspension to dry powder eliminates the need for multiple processing stages, reducing handling losses and contamination risks while maintaining process simplicity (70). Real-time process control enables immediate adjustment of critical parameters, ensuring optimal particle formation while preserving phage viability.

Storage and distribution advantages of powder formulations are substantial, particularly for global phage therapy deployment. The elimination of refrigeration requirements reduces storage costs by approximately 60-80% compared to liquid formulations while improving supply chain reliability (71). Powder formulations demonstrate exceptional stability under temperature fluctuations commonly encountered during transportation, maintaining therapeutic potency through supply chain stresses that would destroy liquid preparations. The reduced shipping weight and volume of powders compared to equivalent liquid doses further decrease distribution costs and environmental impact.

Patient compliance and treatment convenience are significantly improved with powder formulations delivered via dry powder inhalers. The portability of DPI devices enables patient self-administration without the need for nebulizer equipment, electrical power, or healthcare facility visits (72). Treatment administration time is reduced from 15-30 minutes for nebulization to 1-2 minutes for DPI delivery, improving patient acceptance and adherence to treatment regimens (72). The discrete nature of DPI use addresses patient privacy concerns and enables treatment in various settings without stigmatization.

Dosing accuracy and reproducibility represent critical advantages of engineered powder formulations. Precise dose metering through advanced DPI devices achieves dose uniformity within ±5-10%, significantly superior to nebulization where dose delivery varies by 20-50% depending on patient breathing patterns and device maintenance (65). This precision is particularly important for phage therapy where optimal multiplicity of infection ratios is crucial for therapeutic efficacy and resistance prevention.

Safety advantages of powder formulations include the elimination of preservatives and stabilizers commonly required in liquid preparations, reducing the risk of allergic reactions and adverse effects (73). The absence of viable water eliminates microbial contamination risks,

while the controlled particle size distribution minimizes the risk of large particle deposition that could cause local irritation or inflammatory responses (73). Healthcare worker safety is enhanced through the elimination of aerosol generation during preparation and administration, reducing occupational exposure risks.

Regulatory advantages of powder formulations stem from their improved analytical characterization capabilities and shelf-life predictability. Solid-state analytical methods provide more robust stability testing protocols compared to liquid formulations, facilitating regulatory approval processes (74). The predictable degradation kinetics in the solid state enable accurate shelf-life modelling using accelerated stability testing, reducing the time and cost requirements for regulatory submissions (74).

All compounds including trehalose, mannitol, PEG6000 and sucrose have been shown to be effective in stabilising phages during lyophilization processes, following which negligible titre losses were observed, supporting prior findings concerning the cryoprotective properties of sugars and polymers. Spray-freeze drying combines the advantages of spray drying with the gentler conditions of freeze-drying, potentially offering superior phage preservation but with increased processing complexity and cost. Traditional lyophilization provides excellent long-term stability but produces particles requiring secondary processing for optimal aerodynamic properties (75).

Particle engineering targets for effective pulmonary phage delivery focus on achieving mass median aerodynamic diameter (MMAD) values between 1-5 μm for optimal lung deposition, with fine particle fraction (FPF) targets $\geqslant$40% to ensure adequate peripheral lung delivery (76). Particle morphology optimization, including surface corrugation and density reduction through

hollow particle formation, can enhance aerodynamic performance and flow properties while maintaining phage stability (76).

While DPIs offer dose accuracy, portability, and potential room-temperature storage, their development is inherently more complex than liquid formulations. Dry powders require multi-parameter optimization of excipients and process conditions (e.g., solids content, feed rheology, atomization/drying profiles) to preserve phage viability and achieve aerodynamic performance; these attributes are tightly coupled to the selected device and patient flow profile (68). Scale-up typically demands tight humidity control, control of residual moisture and glass transition/crystallinity, and a higher analytical burden (PFU potency, morphology, moisture/T_g, emitted dose, fine-particle dose, NGI/ACI impactor profiles) together with device compatibility/usability testing (77). For phage DPIs specifically, storage stability is sensitive to formulation composition, humidity, and the (T_g–T_s) margin; multiple studies demonstrate long-term stability at 4–20 °C under controlled conditions with trehalose/leucine or lactose matrices (71, 78). These interdependencies extend timelines and increase costs due to specialized equipment, environmental control, in-process testing, stability programs across climates, and iterative device–formulation bridging.

By contrast, liquid formulations often comprise simpler buffers, can leverage established sterile fill-finish workflows, and pair with widely used nebulizers—facilitating earlier development and flexible dose titration or bedside mixing (79). Liquids, however, frequently impose cold-chain requirements and longer administration times, and in some settings may yield lower deposition efficiency without optimized technique or accessories (80). In summary, DPIs can deliver compelling clinical and logistical advantages, but they do so with greater formulation and process complexity, longer development paths, and higher production costs that must be weighed against the relative simplicity and flexibility of liquids.

### Excipients in Phage Formulations

The use and selection of excipients are critical to stabilize phage in solid formulations and protect their viability from stresses encountered during the solidification process and long-term storage prior to use. Current phage formulation strategies are largely adapted from the knowledge obtained in the development of protein-based pharmaceuticals, as phages for therapy are generally composed of a protein capsid enclosing a single molecule of genetic material (81). The challenge lies in developing excipient systems that can simultaneously provide biochemical stability and optimal aerosol performance for inhalation delivery (67).

## Traditional Excipients

### Carbohydrate Matrix Formers

Carbohydrate excipients represent the cornerstone of phage powder formulations, with multiple sugar compounds demonstrating effective stabilization through glass-matrix immobilization mechanisms (78). Trehalose stands as the gold standard among carbohydrate excipients, offering superior protective properties through its non-reducing nature that eliminates Maillard reaction risks during processing and storage. With a glass transition temperature of approximately 120°C, trehalose provides exceptional protection against moisture-induced crystallization and maintains stable storage conditions across typical pharmaceutical temperature ranges (82). The disaccharide's unique molecular structure enables extensive hydrogen bonding networks that effectively immobilize phage particles in an amorphous solid state, inhibiting molecular mobility and associated degradative reactions (78). Lactose, while possessing reducing sugar properties that introduce Maillard reaction potential, remains widely utilized due to its excellent flow characteristics, well-established regulatory profile, and cost-effective manufacturing advantages (83). The widespread pharmaceutical acceptance of lactose facilitates regulatory approval processes, while its superior powder flow

properties enhance manufacturing consistency and DPI device performance (83). However, the reducing nature of lactose necessitates careful process optimization to minimize browning reactions that could compromise phage stability during spray drying operations.

Sucrose has demonstrated effective cryoprotective properties in phage lyophilization studies, with negligible titre losses observed following freeze-drying processes when incorporated as a protective matrix former (84). The disaccharide's ability to replace water molecules in protein hydration shells provides stabilization during dehydration stress, though its reducing sugar properties and hygroscopic nature require consideration in formulation design (85). Mannitol, as a sugar alcohol, offers the advantage of non-reducing properties combined with low hygroscopicity, making it particularly suitable for humid storage environments (86). However, its lower glass transition temperature compared to trehalose may compromise long-term stability in temperature-variable conditions, and potential crystallization issues during processing require careful attention to manufacturing parameters (86).

**Amino acids**

Leucine incorporation has become standard practice in inhalable powder formulations, with optimal concentrations typically ranging from 5-20% w/w to balance dispersibility enhancement with formulation complexity (87). During spray drying operations, leucine undergoes preferential surface migration, concentrating at particle interfaces where it creates characteristic corrugated morphologies that significantly reduce inter-particulate attractive forces (88). This surface modification mechanism enhances powder dispersibility from DPI devices while simultaneously providing moisture protection through hydrophobic surface properties (88). The amino acid's unique behaviour during the drying process results in the formation of wrinkled particle surfaces that minimize contact areas between adjacent particles, thereby reducing van der Waals forces and improving powder flowability (88).

**Synthetic Polymer Stabilizers**

Polyethylene glycol 6000 (PEG6000) has demonstrated effective stabilization properties during phage processing, particularly in lyophilization applications where negligible titre losses have been observed following freeze-drying operations (81). The amphiphilic properties of PEG6000 enable dual stabilization mechanisms, providing both hydrophilic and hydrophobic interactions that protect phage particles during dehydration stress (89). The polymer's flexible formulation options and good solubility characteristics facilitate incorporation into various processing methods, though hygroscopic properties and potential for oxidative degradation require careful formulation consideration (90).

**Novel Excipient: Human Serum Albumin (HSA)**

Recent investigations (Chapter 5) have identified human serum albumin as a particularly effective excipient for phage powder formulations. Formulations containing 60% HSA and 40% lactose achieved fine particle fractions $\geqslant$50% with less than 1 $\log_{10}$ reduction in phage viability and demonstrated remarkable resistance to humidity-induced crystallization up to 80% relative humidity (91).

The protective mechanisms of HSA in phage formulations operate through multiple pathways. Sacrificial interfacial adsorption allows HSA to preferentially interact with destabilizing air-water interfaces during spray drying, protecting phages from interface-induced denaturation (92). The antioxidant properties of HSA, particularly through the free thiol group at cysteine-34, provide protection against oxidative stress that commonly affects phage particles during processing and storage (93, 94). Additionally, HSA's extensive hydrogen-bonding network contributes to glass matrix stabilization and moisture barrier properties (91).

The biocompatibility profile of HSA in pulmonary applications is well-established, with regulatory precedent through approved products including Abraxane® (albumin-bound

paclitaxel) and historical use in Albunex® (albumin microspheres for ultrasound contrast) (95). This regulatory familiarity may facilitate clinical translation of HSA-containing phage formulations.

### Polymer Excipients (PVP)

Polyvinylpyrrolidone (PVP) represents another promising excipient class for phage formulations, with molecular weight-dependent properties that can be tailored for specific applications. Research findings (Chapter 3) demonstrate that glass transition temperatures increase with molecular weight (K15 → K100), providing a thermal buffer ($\Delta T$) $\geqslant$46°C that meets established criteria for protein stabilization. Arrhenius modelling combined with relative humidity considerations enables prediction of shelf-life performance under various storage conditions (96).

The hygroscopicity trade-off inherent in PVP formulations requires careful consideration. While PVP K100 demonstrates optimal performance at $\leqslant$33% relative humidity, its performance deteriorates significantly at 53% relative humidity due to moisture-induced plasticization (97). This necessitates robust packaging solutions or climate-controlled storage for PVP-containing formulations in humid environments.

## Stability Considerations in Phage Formulations

### Thermal Stress and Temperature-Dependent Degradation

Thermal stress represents one of the most significant challenges to phage stability in dry powder formulations, with temperature effects following predictable Arrhenius kinetics where degradation rates typically double for every 10°C increase (98). The complex protein structures of phage capsids are particularly vulnerable to thermal denaturation, which can disrupt the precise quaternary structure necessary for maintaining viral infectivity. Unlike simple proteins, phage particles contain multiple protein subunits arranged in highly ordered geometric patterns,

making them exceptionally sensitive to temperature-induced conformational changes that can compromise structural integrity (99).

During processing, thermal stress manifests through multiple mechanisms including direct protein denaturation, acceleration of chemical degradation reactions, and disruption of protein-nucleic acid interactions. The icosahedral capsid structure of most therapeutic phages requires maintenance of specific protein-protein interactions between hundreds of individual subunits, with thermal energy capable of disrupting these interactions and leading to capsid disassembly or deformation (100). Even sublethal thermal stress can weaken capsid structures, making phages more susceptible to subsequent stresses encountered during storage and handling (13).

The thermal sensitivity of phages varies significantly depending on their origin and structural characteristics. Phages isolated from thermophilic bacteria typically demonstrate enhanced thermal stability compared to those from mesophilic hosts, reflecting evolutionary adaptations to high-temperature environments (101). This variation in thermal tolerance has important implications for processing parameter selection, as formulations containing thermally sensitive phages may require more conservative temperature limits during spray drying operations.

Temperature fluctuations during storage present ongoing challenges to phage stability, particularly in distribution chains lacking consistent temperature control. The cumulative effect of repeated thermal cycling can be more damaging than continuous exposure to elevated temperatures, as expansion and contraction of the capsid structure during temperature changes introduces mechanical stress that can weaken protein interactions and promote gradual structural deterioration (102).

**Humidity Effects and Moisture-Mediated Degradation**

Relative humidity impacts on phage stability are multifaceted and complex, involving both direct moisture-induced degradation pathways and indirect effects through glass transition

temperature depression and crystallization promotion. Direct moisture effects include hydrolysis reactions that can cleave peptide bonds in capsid proteins, oxidation reactions facilitated by water-mediated radical formation, and conformational changes in protein structures as water molecules disrupt hydrogen bonding networks that maintain native protein folding (103).

The plasticization effect of moisture on amorphous excipient matrices represents a critical indirect mechanism whereby water molecules act as plasticizers, effectively lowering the glass transition temperature and reducing the protective ΔT buffer that maintains formulation stability. This plasticization effect can occur at surprisingly low relative humidity levels, with some formulations showing significant Tg depression at humidity levels as low as 30-40% RH (104). The Gordon-Taylor relationship provides a quantitative framework for predicting these effects, though actual behaviour may deviate from theoretical predictions due to specific excipient-phage interactions (105).

Crystallization promotion through moisture absorption represents another significant concern, as water uptake can trigger transformation of amorphous excipients to crystalline forms that lack the protective properties of the original glass matrix. This crystallization process typically involves nucleation at high-energy sites such as particle surfaces or interfaces, followed by crystal growth that progressively destroys the amorphous matrix and exposes encapsulated phages to degradative conditions (106).

Moisture-induced phase separation can occur in multi-component formulations where different excipients exhibit varying hygroscopic properties, leading to heterogeneous moisture distribution and localized areas of high water activity that promote accelerated degradation. This phase separation can create microenvironments with dramatically different stability

characteristics within the same powder particle, complicating stability prediction and control strategies (107).

**Process-Induced Stresses and Manufacturing Challenges**

Process-induced stresses during powder manufacture represent critical control points for phage preservation, with each unit operation introducing specific challenges that must be carefully managed. The sudden change of state during processing coupled with the formation of ice crystals during freeze-drying challenges the integrity of the phage capsid and can result in large scale loss of phage viability. Ice crystal formation creates high local pressures and osmotic imbalances that can disrupt capsid structures and damage internal nucleic acids (67, 81).

Atomization shear forces during spray drying can mechanically damage phage particles through high-velocity collisions and turbulent flow patterns in the atomization zone. The pressure drop across spray nozzles creates intense shear fields that can exceed the mechanical strength limits of phage structures, particularly elongated tail regions that experience disproportionate stress in turbulent flow conditions (28).

Air-liquid interface interactions promote protein unfolding and aggregation as phage particles become concentrated at droplet surfaces during the evaporation process. The high surface area of atomized droplets creates extensive interfacial regions where phages can become trapped and subjected to destabilizing surface forces. Protein denaturation at these interfaces can trigger aggregation cascades that propagate throughout the droplet as water evaporates and phage concentration increases (108, 109).

Rapid desiccation, while necessary for powder formation, can induce osmotic stress and vitrification-related damage if not properly controlled. The rate of water removal during spray drying creates transient conditions of extreme osmotic imbalance as the surrounding medium transitions from dilute solution to concentrated syrup to solid glass (78). If this transition occurs

too rapidly, osmotic shock can disrupt phage membranes and capsid structures before protective glass formation is complete.

Temperature gradients during processing create differential thermal expansion that can induce mechanical stress within particles containing phages (67). The coefficient of thermal expansion mismatch between phage particles and surrounding excipient matrix can generate internal stresses during cooling that may compromise structural integrity or create stress concentration points that become failure sites during subsequent handling (67).

Cavitation effects in high-energy processing equipment can generate localized regions of extreme pressure and temperature that are highly damaging to biological structures (110). The collapse of cavitation bubbles creates shock waves and radical species that can cause immediate and irreversible damage to phage particles, making cavitation prevention essential in equipment design and operation (110).

**The Role of Glass Transition Temperature (Tg)**

Glass transition temperature serves as the most critical parameter governing solid-state stability in amorphous phage formulations, representing the temperature at which the amorphous solid transitions from a glassy state to a rubbery state (111). This transition fundamentally alters the molecular mobility within the formulation matrix, directly impacting the stability and viability of encapsulated phage particles (111). The importance of Tg in phage powder formulations stems from its direct relationship to molecular mobility, which governs virtually all degradation processes that can compromise phage infectivity during processing and storage (111).

The concept of ΔT (Tg - storage temperature) provides a practical framework for stability prediction, with the established rule-of-thumb requiring ΔT $\geqslant$46°C for adequate protein

stabilization (78). This thermal buffer ensures that molecular mobility remains sufficiently low to prevent degradative reactions while maintaining acceptable processing characteristics. The 46°C threshold represents the minimum temperature difference necessary to maintain the formulation in a stable glassy state where molecular motion is severely restricted, effectively preventing most chemical and physical degradation pathways that could compromise phage viability (78).

The relationship between Tg and long-term stability enables predictive modeling of shelf-life performance under various storage conditions. Research data (Chapter 3) demonstrating activation energies of approximately 120 kJ $mol^{-1}$ for phage degradation kinetics provide quantitative frameworks for stability modeling using the relationship $\ln k = f(1/T, RH)$. This mathematical relationship allows formulators to predict degradation rates under various temperature and humidity conditions based on the $\Delta T$ maintained in the formulation (98, 112). Humidity plasticization effects on glass transition temperature follow Gordon-Taylor relationships, enabling prediction of Tg depression under various relative humidity conditions (113). Water acts as a plasticizer, effectively lowering the glass transition temperature and reducing the protective $\Delta T$ buffer (114). This plasticization effect can compromise stability even when storage temperatures remain constant, as increasing humidity effectively moves the formulation closer to the glass transition region where molecular mobility increases.

The ability to predict these humidity effects enables formulators to establish appropriate packaging requirements and storage conditions that maintain adequate $\Delta T$ buffers throughout the intended shelf-life. Understanding the quantitative relationship between relative humidity and Tg depression allows for the development of stability models that can predict performance under various distribution and storage scenarios, supporting regulatory submissions and quality assurance programs (114).

Effective phage powder formulation requires strategic manipulation of glass transition temperature through excipient selection and ratio optimization. High-Tg excipients such as trehalose (Tg ≈ 120°C) provide excellent thermal buffers, while lower-Tg materials may be incorporated for specific functional benefits provided the overall formulation Tg meets stability requirements (115). The challenge lies in achieving optimal Tg values while simultaneously meeting aerosol performance requirements, as some high-Tg excipients may compromise powder dispersibility or particle formation characteristics (115).

Multi-component formulations require careful consideration of glass transition behaviour, as the final Tg typically represents a weighted average of individual component contributions modified by molecular interactions. The Gordon-Taylor equation provides a framework for predicting mixture Tg values, though experimental validation remains essential due to potential deviations from ideal mixing behaviour (113).

Advanced formulation strategies may involve the use of Tg-modifying excipients that can fine-tune glass transition properties without compromising other formulation objectives. Polymer excipients with molecular weight-dependent Tg values, such as the PVP K-series, enable precise control over thermal properties while providing additional stabilization mechanisms (116). The selection and optimization of such systems requires understanding both individual component properties and their interactions within the complex formulation matrix (116).

## Research Gap

With antibiotic resistance increasingly limiting treatment options for bacterial infections, bacteriophage therapy has emerged as a promising alternative treatment strategy. However, significant knowledge gaps remain that limit the clinical translation of phage-based

therapeutics. Current research predominantly addresses either therapeutic strategy optimization or pharmaceutical formulation development in isolation, yet these two critical aspects are inherently interconnected and require integrated investigation.

While phage cocktails targeting multiple bacterial receptors demonstrate high efficacy, optimal treatment protocols for minimizing resistance development remain poorly understood. Existing studies have not comprehensively compared sequential versus simultaneous phage application strategies, particularly regarding their impact on resistance emergence patterns and long-term bacterial suppression. Furthermore, the relationship between treatment strategy and bacterial fitness costs associated with resistance mechanisms requires systematic investigation.

From a pharmaceutical perspective, the development of stable, effective delivery systems for bacteriophages presents ongoing challenges. Although progress has been made in understanding glass transition temperature relationships for phage stability, comprehensive long-term studies evaluating different polymeric matrices and their performance under various storage conditions remain limited. Additionally, the development of optimized dry powder formulations for pulmonary delivery requires systematic investigation of excipient combinations and their impact on both phage viability and aerosol performance. The integration of treatment strategy considerations with formulation development approaches has not been adequately addressed in current literature, representing a critical gap in advancing phage therapy toward clinical implementation.

**Research Objectives**

This research aims to develop an integrated approach for optimizing bacteriophage therapy against Pseudomonas aeruginosa through strategic treatment design and advanced

pharmaceutical formulation science, combining resistance minimization strategies with stable dry powder delivery systems to enhance therapeutic efficacy and clinical translation.

The first objective is to evaluate and optimize sequential versus simultaneous phage treatment strategies against Pseudomonas aeruginosa, with specific focus on minimizing resistance development through systematic comparison of treatment protocols using phages targeting different bacterial receptors (lipopolysaccharides and type IV pili). This investigation will assess bacterial population dynamics, resistance emergence patterns, and fitness costs associated with different resistance mechanisms to establish optimal treatment sequencing protocols.

The second objective focuses on developing and characterizing long-term stabilization strategies for bacteriophages using polyvinylpyrrolidone matrices with varying molecular weights. This study will evaluate the relationship between polymer properties, glass transition temperatures, and phage preservation under different storage conditions, establishing design principles for stable phage formulations through accelerated and real-time stability studies.

The third objective involves conducting comprehensive four-year stability studies of spray-dried bacteriophage formulations incorporating lactose and leucine as stabilizing and dispersibility-enhancing excipients. This investigation will assess formulation performance, phage viability retention, particle morphology changes, and aerosol performance characteristics for pulmonary delivery applications under various storage conditions to establish long-term stability profiles.

The fourth objective aims to design and optimize human serum albumin and lactose-based dry powder formulations for pulmonary bacteriophage delivery. This work will evaluate particle engineering parameters, aerosol performance characteristics, and moisture protection

capabilities through systematic formulation optimization and performance assessment, establishing design principles for protein-based phage delivery systems.

The final objective integrates treatment strategy optimization with formulation development by assessing how different pharmaceutical delivery systems affect phage potency, resistance development patterns, and overall therapeutic outcomes. This comprehensive approach will create an integrated framework for phage therapy optimization that addresses both therapeutic strategy and pharmaceutical considerations, providing a foundation for effective clinical translation of bacteriophage therapeutics.

## References

1. Blair, J.M., et al., *Molecular mechanisms of antibiotic resistance.* Nat Rev Microbiol, 2015. **13**(1): p. 42-51.

2. Murray, C.J., et al., *Global burden of bacterial antimicrobial resistance in 2019: a systematic analysis.* The lancet, 2022. **399**(10325): p. 629-655.
3. Tacconelli, E., et al., *Discovery, research, and development of new antibiotics: the WHO priority list of antibiotic-resistant bacteria and tuberculosis.* The Lancet infectious diseases, 2018. **18**(3): p. 318-327.
4. von Wintersdorff, C.J., et al., *Dissemination of Antimicrobial Resistance in Microbial Ecosystems through Horizontal Gene Transfer.* Front Microbiol, 2016. **7**: p. 173.
5. Ventola, C.L., *The antibiotic resistance crisis: part 1: causes and threats.* P T, 2015. **40**(4): p. 277-83.
6. Collignon, P.J. and S.A. McEwen, *One Health-Its Importance in Helping to Better Control Antimicrobial Resistance.* Trop Med Infect Dis, 2019. **4**(1).
7. Flemming, H.-C. and S. Wuertz, *Bacteria and archaea on Earth and their abundance in biofilms.* Nature Reviews Microbiology, 2019. **17**(4): p. 247-260.
8. Theuretzbacher, U., et al., *The global preclinical antibacterial pipeline.* Nat Rev Microbiol, 2020. **18**(5): p. 275-285.
9. Garcia-Vidal, C., A. Stern, and C. Gudiol, *Multidrug-resistant, gram-negative infections in high-risk haematologic patients: an update on epidemiology, diagnosis and treatment.* Curr Opin Infect Dis, 2021. **34**(4): p. 314-322.
10. Pang, Z., et al., *Antibiotic resistance in Pseudomonas aeruginosa: mechanisms and alternative therapeutic strategies.* Biotechnol Adv, 2019. **37**(1): p. 177-192.
11. Ardebili, A., A. Izanloo, and M. Rastegar, *Polymyxin combination therapy for multidrug-resistant, extensively-drug resistant, and difficult-to-treat drug-resistant gram-negative infections: is it superior to polymyxin monotherapy?* Expert review of anti-infective therapy, 2023. **21**(4): p. 387-429.
12. Hareza, D.A., et al., *Clinical outcomes and emergence of resistance of Pseudomonas aeruginosa infections treated with ceftolozane-tazobactam versus ceftazidime-avibactam.* Antimicrobial agents and chemotherapy, 2024. **68**(10): p. e00907-24.
13. Salmond, G.P. and P.C. Fineran, *A century of the phage: past, present and future.* Nat Rev Microbiol, 2015. **13**(12): p. 777-86.
14. Nobrega, F.L., et al., *Revisiting phage therapy: new applications for old resources.* Trends in microbiology, 2015. **23**(4): p. 185-191.
15. Sulakvelidze, A., Z. Alavidze, and J.G. Morris, Jr., *Bacteriophage therapy.* Antimicrob Agents Chemother, 2001. **45**(3): p. 649-59.
16. Kutter, E., et al., *Phage therapy in clinical practice: treatment of human infections.* Curr Pharm Biotechnol, 2010. **11**(1): p. 69-86.
17. Pirnay, J.P., et al., *The Magistral Phage.* Viruses, 2018. **10**(2).
18. Furfaro, L.L., M.S. Payne, and B.J. Chang, *Bacteriophage Therapy: Clinical Trials and Regulatory Hurdles.* Front Cell Infect Microbiol, 2018. **8**: p. 376.
19. Łusiak-Szelachowska, M., et al., *Bacteriophages in the gastrointestinal tract and their implications.* Gut pathogens, 2017. **9**(1): p. 44.
20. Roach, D.R. and D.M. Donovan, *Antimicrobial bacteriophage-derived proteins and therapeutic applications.* Bacteriophage, 2015. **5**(3): p. e1062590.
21. Jault, P., et al., *Efficacy and tolerability of a cocktail of bacteriophages to treat burn wounds infected by Pseudomonas aeruginosa (PhagoBurn): a randomised, controlled, double-blind phase 1/2 trial.* The Lancet Infectious Diseases, 2019. **19**(1): p. 35-45.
22. Topka-Bielecka, G., et al., *Bacteriophage-derived depolymerases against bacterial biofilm.* Antibiotics, 2021. **10**(2): p. 175.

23. Das, T., et al., *Phenazine virulence factor binding to extracellular DNA is important for Pseudomonas aeruginosa biofilm formation.* Scientific Reports, 2015. **5**(1): p. 8398.
24. Lim, E.S., et al., *Early life dynamics of the human gut virome and bacterial microbiome in infants.* Nature medicine, 2015. **21**(10): p. 1228-1234.
25. Onallah, H., R. Hazan, and R. Nir-Paz. *Compassionate use of bacteriophages for failed persistent infections during the first 5 years of the Israeli phage therapy center*. in *Open forum infectious diseases*. 2023. Oxford University Press US.
26. Suh, G.A., et al., *Considerations for the Use of Phage Therapy in Clinical Practice.* Antimicrob Agents Chemother, 2022. **66**(3): p. e0207121.
27. Leung, S.S.Y., et al., *Effects of storage conditions on the stability of spray dried, inhalable bacteriophage powders.* Int J Pharm, 2017. **521**(1-2): p. 141-149.
28. Chang, R.Y., et al., *Production of highly stable spray dried phage formulations for treatment of Pseudomonas aeruginosa lung infection.* Eur J Pharm Biopharm, 2017. **121**: p. 1-13.
29. Regulski, K., P. Champion-Arnaud, and J. Gabard, *Bacteriophage manufacturing: From early twentieth-century processes to current GMP.* Bacteriophages: Biology, Technology, Therapy, 2021: p. 699-729.
30. Yehl, K., et al., *Engineering phage host-range and suppressing bacterial resistance through phage tail fiber mutagenesis.* Cell, 2019. **179**(2): p. 459-469. e9.
31. Bikard, D., et al., *Exploiting CRISPR-Cas nucleases to produce sequence-specific antimicrobials.* Nat Biotechnol, 2014. **32**(11): p. 1146-50.
32. Abedon, S.T., *Phage-antibiotic combination treatments: antagonistic impacts of antibiotics on the pharmacodynamics of phage therapy?* Antibiotics, 2019. **8**(4): p. 182.
33. Schooley, R.T., et al., *Development and Use of Personalized Bacteriophage-Based Therapeutic Cocktails To Treat a Patient with a Disseminated Resistant Acinetobacter baumannii Infection.* Antimicrob Agents Chemother, 2017. **61**(10).
34. Dedrick, R.M., et al., *Engineered bacteriophages for treatment of a patient with a disseminated drug-resistant Mycobacterium abscessus.* Nature medicine, 2019. **25**(5): p. 730-733.
35. Merabishvili, M., J.-P. Pirnay, and D. De Vos, *Guidelines to compose an ideal bacteriophage cocktail.* Bacteriophage Therapy: From Lab to Clinical Practice, 2023: p. 49-66.
36. Le, S., et al., *Mapping the tail fiber as the receptor binding protein responsible for differential host specificity of Pseudomonas aeruginosa bacteriophages PaP1 and JG004.* PloS one, 2013. **8**(7): p. e68562.
37. Bürkle, M., et al., *Phage–phage competition and biofilms affect interactions between two virulent bacteriophages and Pseudomonas aeruginosa.* The ISME Journal, 2025. **19**(1): p. wraf065.
38. Roach, D.R., et al., *Synergy between the host immune system and bacteriophage is essential for successful phage therapy against an acute respiratory pathogen.* Cell host & microbe, 2017. **22**(1): p. 38-47. e4.
39. Weitz, J.S., H. Hartman, and S.A. Levin, *Coevolutionary arms races between bacteria and bacteriophage.* Proceedings of the National Academy of Sciences, 2005. **102**(27): p. 9535-9540.
40. Wright, R.C., et al., *Resistance evolution against phage combinations depends on the timing and order of exposure.* MBio, 2019. **10**(5): p. 10.1128/mbio. 01652-19.
41. Leung, C.Y.J. and J.S. Weitz, *Modeling the synergistic elimination of bacteria by phage and the innate immune system.* J Theor Biol, 2017. **429**: p. 241-252.
42. Pressler, T., et al., *Chronic Pseudomonas aeruginosa infection definition: EuroCareCF Working Group report.* J Cyst Fibros, 2011. **10 Suppl 2**: p. S75-8.
43. Doudakmanis, C. and D. Makris, *Ventilator-Associated Pneumonia in Patients With Increased Intra-abdominal Pressure.* Cureus, 2025. **17**(3): p. e81370.

44. Kwok, W.C., et al., *Risk factors for Pseudomonas aeruginosa colonization in non-cystic fibrosis bronchiectasis and clinical implications.* Respir Res, 2021. **22**(1): p. 132.
45. Pearson, J.P., E.C. Pesci, and B.H. Iglewski, *Roles of Pseudomonas aeruginosa las and rhl quorum-sensing systems in control of elastase and rhamnolipid biosynthesis genes.* J Bacteriol, 1997. **179**(18): p. 5756-67.
46. Wiens, J.R., et al., *Iron-regulated expression of alginate production, mucoid phenotype, and biofilm formation by Pseudomonas aeruginosa.* mBio, 2014. **5**(1): p. e01010-13.
47. Everett, M.J. and D.T. Davies, *Pseudomonas aeruginosa elastase (LasB) as a therapeutic target.* Drug Discovery Today, 2021. **26**(9): p. 2108-2123.
48. Rose, M.C., *Mucins: structure, function, and role in pulmonary diseases.* American Journal of Physiology-Lung Cellular and Molecular Physiology, 1992. **263**(4): p. L413-L429.
49. Giannoni, E., et al., *Surfactant proteins A and D enhance pulmonary clearance of Pseudomonas aeruginosa.* American journal of respiratory cell and molecular biology, 2006. **34**(6): p. 704-710.
50. Giacalone, V.D., et al., *Neutrophil adaptations upon recruitment to the lung: new concepts and implications for homeostasis and disease.* International Journal of Molecular Sciences, 2020. **21**(3): p. 851.
51. Hu, D., et al., *Relief of Biofilm Hypoxia Using an Oxygen Nanocarrier: A New Paradigm for Enhanced Antibiotic Therapy.* Adv Sci (Weinh), 2020. **7**(12): p. 2000398.
52. Eriksson, J., et al., *Pulmonary drug absorption and systemic exposure in human: Predictions using physiologically based biopharmaceutics modeling.* European Journal of Pharmaceutics and Biopharmaceutics, 2020. **156**: p. 191-202.
53. Fowoyo, P.T., *Phage therapy: clinical applications, efficacy, and implementation hurdles.* The Open Microbiology Journal, 2024. **18**(1).
54. Sharma, R., *Plenary Lecture: INHALED DRUG DELIVERY, PAST, PRESENT AND FUTURE: A THERAPEUTIC PERSPECTIVE.* J Aerosol Med, 2000. **13**(1): p. 59-72.
55. Shah, K.A., et al., *Current trends in inhaled pharmaceuticals: challenges and opportunities in respiratory infections treatment.* Journal of Pharmaceutical Investigation, 2025: p. 1-35.
56. Houtmeyers, E., et al., *Regulation of mucociliary clearance in health and disease.* European Respiratory Journal, 1999. **13**(5): p. 1177-1188.
57. Jin, Z., et al., *Harnessing inhaled nanoparticles to overcome the pulmonary barrier for respiratory disease therapy.* Adv Drug Deliv Rev, 2023. **202**: p. 115111.
58. Chow, M.Y.T., et al., *Pharmacokinetics and Time-Kill Study of Inhaled Antipseudomonal Bacteriophage Therapy in Mice.* Antimicrob Agents Chemother, 2020. **65**(1).
59. Lin, Y., et al., *Synergy of nebulized phage PEV20 and ciprofloxacin combination against Pseudomonas aeruginosa.* Int J Pharm, 2018. **551**(1-2): p. 158-165.
60. Guillon, A., et al., *Inhaled bacteriophage therapy in a porcine model of pneumonia caused by Pseudomonas aeruginosa during mechanical ventilation.* British Journal of Pharmacology, 2021. **178**(18): p. 3829-3842.
61. Chan, B., et al., *Personalized inhaled bacteriophage therapy decreases multidrug-resistant Pseudomonas aeruginosa.* MedRxiv, 2023: p. 2023.01. 23.22283996.
62. Lin, Y., et al., *Inhalable combination powder formulations of phage and ciprofloxacin for P. aeruginosa respiratory infections.* Eur J Pharm Biopharm, 2019. **142**: p. 543-552.
63. Zhang, Y., H. Zhang, and D. Ghosh, *The Stabilizing Excipients in Dry State Therapeutic Phage Formulations.* AAPS PharmSciTech, 2020. **21**(4): p. 133.
64. Omidian, H., A. Nokhodchi, and N. Babanejad, *Dry Powder Inhalers for Delivery of Synthetic Biomolecules.* Pharmaceuticals (Basel), 2025. **18**(2).

65. Maloney, S.E., J.B. Mecham, and A.J. Hickey, *Performance testing for dry powder inhaler products: towards clinical relevance.* KONA Powder and Particle Journal, 2023. **40**: p. 172-185.
66. Weiler, C., et al., *Force control and powder dispersibility of spray dried particles for inhalation.* J Pharm Sci, 2010. **99**(1): p. 303-16.
67. Leung, S.S., et al., *Production of Inhalation Phage Powders Using Spray Freeze Drying and Spray Drying Techniques for Treatment of Respiratory Infections.* Pharm Res, 2016. **33**(6): p. 1486-96.
68. Vehring, R., *Pharmaceutical particle engineering via spray drying.* Pharm Res, 2008. **25**(5): p. 999-1022.
69. Merabishvili, M., et al., *Production of phage therapeutics and formulations: Innovative approaches.* Phage therapy: a practical approach, 2019: p. 3-41.
70. Kopp, K.T., et al., *Spray drying for protein stabilization.* Int J Pharm, 2025. **677**: p. 125600.
71. Leung, S.S.Y., et al., *Effect of storage temperature on the stability of spray dried bacteriophage powders.* Eur J Pharm Biopharm, 2018. **127**: p. 213-222.
72. Chang, R.Y.K., et al., *Dry powder pharmaceutical biologics for inhalation therapy.* Adv Drug Deliv Rev, 2021. **172**: p. 64-79.
73. Hoppentocht, M., et al., *Technological and practical challenges of dry powder inhalers and formulations.* Advanced drug delivery reviews, 2014. **75**: p. 18-31.
74. Sutar, A.D., R.K. Verma, and R. Shukla, *Quality by Design in Pulmonary Drug Delivery: A Review on Dry Powder Inhaler Development, Nanotherapy Approaches, and Regulatory Considerations.* AAPS PharmSciTech, 2024. **25**(6): p. 178.
75. Zhang, Y., et al., *Manufacturing Stable Bacteriophage Powders by Including Buffer System in Formulations and Using Thin Film Freeze-drying Technology.* Pharm Res, 2021. **38**(10): p. 1793-1804.
76. Chow, A.H., et al., *Particle engineering for pulmonary drug delivery.* Pharm Res, 2007. **24**(3): p. 411-37.
77. Malik, D.J., et al., *Formulation, stabilisation and encapsulation of bacteriophage for phage therapy.* Adv Colloid Interface Sci, 2017. **249**: p. 100-133.
78. Chang, R.Y.K., et al., *Inhalable bacteriophage powders: Glass transition temperature and bioactivity stabilization.* Bioeng Transl Med, 2020. **5**(2): p. e10159.
79. Simperler, A., et al., *Glass transition temperature of glucose, sucrose, and trehalose: an experimental and in silico study.* The journal of physical chemistry B, 2006. **110**(39): p. 19678-19684.
80. Stojanovska, S., et al., *Maillard reaction and lactose structural changes during milk processing.* Maillard Reaction and Lactose Structural Changes during Milk Processing, 2017. **2**(6): p. 139-145.
81. Merabishvili, M., et al., *Stability of Staphylococcus aureus phage ISP after freeze-drying (lyophilization).* PLoS One, 2013. **8**(7): p. e68797.
82. Walker, S.A., et al., *Sucrose-based cryoprotective storage of extracellular vesicles.* Extracell Vesicle, 2022. **1**.
83. Yu, L., D.S. Mishra, and D.R. Rigsbee, *Determination of the glass properties of D-mannitol using sorbitol as an impurity.* Journal of pharmaceutical sciences, 1998. **87**(6): p. 774-777.
84. Chew, N.Y. and H.K. Chan, *The role of particle properties in pharmaceutical powder inhalation formulations.* J Aerosol Med, 2002. **15**(3): p. 325-30.
85. Li, M., et al., *Phage cocktail powder for Pseudomonas aeruginosa respiratory infections.* International journal of pharmaceutics, 2021. **596**: p. 120200.
86. Allison, S.D., et al., *Hydrogen bonding between sugar and protein is responsible for inhibition of dehydration-induced protein unfolding.* Archives of Biochemistry and Biophysics, 1999. **365**(2): p. 289-298.

87. Mi, Y. and G. Wood, *The application and mechanisms of polyethylene glycol 8000 on stabilizing lactate dehydrogenase during lyophilization.* PDA Journal of Pharmaceutical Science and Technology, 2004. **58**(4): p. 192-202.
88. Li, M., Y. Cao, and H.K. Chan, *Optimizing Performance of Inhalable Bacteriophage Powders using Human Serum Albumin (HSA).* Int J Pharm, 2025. **678**: p. 125709.
89. Maa, Y.-F., P.-A.T. Nguyen, and S.W. Hsu, *Spray-drying of air–liquid interface sensitive recombinant human growth hormone.* Journal of pharmaceutical sciences, 1998. **87**(2): p. 152-159.
90. Mukai, R., et al., *The binding selectivity of quercetin and its structure-related polyphenols to human serum albumin using a fluorescent dye cocktail for multiplex drug-site mapping.* Bioorg Chem, 2024. **145**: p. 107184.
91. Escalante, J., et al., *Human serum albumin (HSA) regulates the expression of histone-like nucleoid structure protein (H-NS) in Acinetobacter baumannii.* Sci Rep, 2022. **12**(1): p. 14644.
92. Xie, Z., et al., *Evaluation of nanoparticle albumin-bound paclitaxel loaded macrophages for glioblastoma treatment based on a microfluidic chip.* Front Bioeng Biotechnol, 2024. **12**: p. 1361682.
93. Fu, M., et al., *Pharmaceutical solid-state kinetic stability investigation by using moisture-modified Arrhenius equation and JMP statistical software.* J Pharm Biomed Anal, 2015. **107**: p. 370-7.
94. Lehmkemper, K., et al., *Long-Term Physical Stability of PVP- and PVPVA-Amorphous Solid Dispersions.* Mol Pharm, 2017. **14**(1): p. 157-171.
95. Khawam, A. and D.R. Flanagan, *Basics and applications of solid-state kinetics: a pharmaceutical perspective.* J Pharm Sci, 2006. **95**(3): p. 472-98.
96. Müller-Merbach, M., T. Rauscher, and J. Hinrichs, *Inactivation of bacteriophages by thermal and high-pressure treatment.* International Dairy Journal, 2005. **15**(6-9): p. 777-784.
97. Ackermann, H.W., *Bacteriophage observations and evolution.* Res Microbiol, 2003. **154**(4): p. 245-51.
98. Delbruck, M., *The Growth of Bacteriophage and Lysis of the Host.* J Gen Physiol, 1940. **23**(5): p. 643-60.
99. Semenyuk, P., V. Orlov, and L. Kurochkina, *Effect of chaperonin encoded by gene 146 on thermal aggregation of lytic proteins of bacteriophage EL Pseudomonas aeruginosa.* Biochemistry (Moscow), 2015. **80**: p. 172-179.
100. Izutsu, K.-i., S. Yoshioka, and T. Terao, *Decreased protein-stabilizing effects of cryoprotectants due to crystallization.* Pharmaceutical research, 1993. **10**: p. 1232-1237.
101. Hancock, B.C. and G. Zografi, *The relationship between the glass transition temperature and the water content of amorphous pharmaceutical solids.* Pharmaceutical research, 1994. **11**: p. 471-477.
102. Andronis, V. and G. Zografi, *The molecular mobility of supercooled amorphous indomethacin as a function of temperature and relative humidity.* Pharm Res, 1998. **15**(6): p. 835-42.
103. Vandenheuvel, D., et al., *Instability of bacteriophages in spray-dried trehalose powders is caused by crystallization of the matrix.* International journal of pharmaceutics, 2014. **472**(1-2): p. 202-205.
104. Airaksinen, S., et al., *Role of water in the physical stability of solid dosage formulations.* J Pharm Sci, 2005. **94**(10): p. 2147-65.
105. Koepf, E., et al., *Notorious but not understood: How liquid-air interfacial stress triggers protein aggregation.* Int J Pharm, 2018. **537**(1-2): p. 202-212.
106. Maa, Y.F. and C.C. Hsu, *Protein denaturation by combined effect of shear and air-liquid interface.* Biotechnol Bioeng, 1997. **54**(6): p. 503-12.

107. Ashokkumar, M., *The characterization of acoustic cavitation bubbles - an overview.* Ultrason Sonochem, 2011. **18**(4): p. 864-72.
108. Hancock, B.C. and G. Zografi, *Characteristics and significance of the amorphous state in pharmaceutical systems.* J Pharm Sci, 1997. **86**(1): p. 1-12.
109. Fan, Z. and L. Zhang, *One- and two-stage Arrhenius models for pharmaceutical shelf life prediction.* J Biopharm Stat, 2015. **25**(2): p. 307-16.
110. Andronis, V. and G. Zografi, *The molecular mobility of supercooled amorphous indomethacin as a function of temperature and relative humidity.* Pharmaceutical research, 1998. **15**: p. 835-842.
111. Airaksinen, S., et al., *Role of water in the physical stability of solid dosage formulations.* Journal of pharmaceutical sciences, 2005. **94**(10): p. 2147-2165.
112. Chang, R.Y., et al., *Production of highly stable spray dried phage formulations for treatment of Pseudomonas aeruginosa lung infection.* European Journal of Pharmaceutics and Biopharmaceutics, 2017. **121**: p. 1-13.
113. Zeng, X.M., G.P. Martin, and C. Marriott, *Effects of molecular weight of polyvinylpyrrolidone on the glass transition and crystallization of co-lyophilized sucrose.* International journal of pharmaceutics, 2001. **218**(1-2): p. 63-73.

# Chapter 2

# Comparing the Efficacy of Sequential Phage Therapy Versus Cocktail Approach in Reducing *Pseudomonas* Virulence

This chapter has been under review in Antimicrobial Agents and Chemotherapy, with the title 'Comparing the Efficacy of Sequential Phage Therapy Versus Cocktail Approach in Reducing Pseudomonas Virulence.' Authors: Mengyu Li, Yue Cao, Rachel Yoon Kyung Chang, Dipesh Khanal, Sandra Morales, Hee-Won Bae, You-Hee Cho, Hak-Kim Chan.

## Introduction

The steady rise of multidrug-resistant *Pseudomonas aeruginosa* has revived interest in bacteriophage therapy. Current practice usually employs lytic phage cocktails that deliver both breadth (coverage of multiple clinical isolates) and depth (two or more phages active against the same strain), thereby reducing the likelihood that a single mutation will confer cross-resistance (117). In *P. aeruginosa*, phages typically target the lipopolysaccharide (LPS) O-antigen/core or type IV pilus (TFP), as exemplified by phages Dobby (LPS-specific) and MPK7 (TFP-specific) (118). Bacterial resistance to these phages most often arises via receptor alteration – for instance, loss or modification of O-antigen and changes in pilus structure (118, 119). Such receptor mutations typically carry fitness trade-offs: mutants resistant to LPS-binding phages often have truncated LPS (e.g., *galU*, *wzy* mutations) with reduced outer-membrane integrity, while TFP-deficient mutants lose twitching motility and biofilm capability (119). These pleiotropic effects can render phage-resistant bacteria less virulent or more antibiotic-sensitive (119). Advanced analytical techniques, particularly atomic force microscopy infrared spectroscopy (AFM-IR), now enable direct characterization of these receptor modifications at the molecular level (120).

Standard phage therapy protocols favour simultaneous administration of multiple phages (cocktails) under the rationale that concurrent targeting of distinct receptors should curb resistance evolution (117, 121). Indeed, experimental and clinical studies report that cocktails often yield the greatest immediate killing. For example, Hall *et al.* found that cocktails gave faster clearance in the short term (e.g., curing lethal infections in insects), though they noted that some sequential schedules were “equally effective” on longer timescales [5]. This success reflects the idea that multi-resistance is harder to evolve in one step if it requires independent mutations (one for each phage) (121, 122). By contrast, sequential phage therapy

(administering different phages in succession) has been relatively little explored but is gaining interest as an alternative way to exploit evolutionary trade-offs. Mathematical models suggest simultaneous administration maximizes immediate killing, but sequential delivery can match efficacy with optimized intervals (123). The theoretical rationale is analogous to antibiotic cycling: by switching selective pressures over time, one may "steer" bacteria into fitness valleys. Importantly, recent studies show that the timing and order of phage exposure can strongly influence resistance. In detailed laboratory evolution, Wright *et al*. reported that simultaneous cocktails led to weaker evolved resistance (since bacteria could not easily evolve dual immunity), whereas sequential regimens produced strong dual resistance at the expense of fitness (122). Ulrich *et al.* observed that a 24-h spaced sequential protocol kept *Pseudomonas* growth suppressed far longer than an equivalent cocktail (124). These results suggest that sequential therapy may exploit "collateral sensitivity": adaptation to the first phage could sensitize bacteria to the second, or vice versa, especially if the phages use different receptors. In line with this idea, a recent clinical review proposed alternating single-phage treatments targeting distinct surface receptors in *P. aeruginosa* (e.g., swapping an LPS-dependent phage for a pili-dependent phage) to impose specific trade-offs in virulence (125).

While simultaneous cocktails excel in immediate bacterial clearance and sequential strategies in sustained suppression, both must consider the multiplicity of infection (MOI), as it significantly affects phage-bacteria dynamics and resistance development. Recent studies demonstrate that bacterial killing kinetics and resistance emergence vary significantly with phage-to-bacteria ratios (126). While high MOIs can achieve rapid initial killing, they may accelerate resistance development by selecting for innate phage resistant mutants. Conversely, lower MOIs might promote sustained bacterial suppression through gradual selective pressure(127) . Both strategies face challenges, as bacteria may eventually develop resistance.

Targeting diverse receptors like LPS and TFP, which impose distinct selection pressures (118, 119), may result on a more tailored therapy. The present study builds on this rationale by directly comparing simultaneous versus sequential use of an LPS-targeting phage (Dobby) and a TFP-targeting phage (MPK7) against *P. aeruginosa*, with the goal of revealing how receptor-specific resistance and fitness trade-offs shape treatment outcomes.

In this proof-of-concept study, we challenge the conventional practice of simultaneous phage application by proposing a sequential dosing strategy targeting distinct bacterial receptors in *P. aeruginosa*. Specifically, we first administer an LPS-targeting phage (Dobby), followed by a TFP-targeting phage (MPK7), and evaluate its effects on bacterial population dynamics and resistance development. We hypothesize that targeting bacterial receptors sequentially rather than simultaneously could enhance bacterial killing efficiency, which we quantify through bacterial growth curves (area under the curve, AUC). Additionally, we assess fitness costs associated with resistance and employ atomic force microscopy infrared spectroscopy (AFM-IR) to gain insights into chemical changes linked to resistance. Ultimately, our findings aim to inform optimal phage dosing strategies, contributing to more effective and sustainable phage-based treatments for bacterial infections.

## Materials and methods

### Materials

The *P. aeruginosa* phage Dobby was kindly provided by Genevieve Johnson in Putonti's Lab (Loyola University Chicago). Nutrient broth (NB) and bacteriological agar (Agar No. 1) were purchased from Oxoid (Basingstoke, UK).

### Time-kill dynamics assay

To investigate the influence of treatment order and MOI on phage efficacy, three treatment conditions were tested at MOIs of 0.01, 1, and 100: (1) simultaneous treatment of phages

Dobby and MPK7 (D + M), (2) sequential treatment with MPK7 followed by Dobby after 24 h (M → D), and (3) Dobby followed by MPK7 after 24 h (D → M).

For each assay, 150 µL of early log-phase *P. aeruginosa* PAO1 (~1 × $10^6$ CFU/mL) was added to 4.7 mL of nutrient broth (NB). Then, 150 µL of phage suspension (prepared at $10^4$, $10^6$, or $10^8$ plaque-forming units (PFU)/mL to achieve MOIs of 0.01, 1, or 100, respectively) was added, making a total volume of 5 mL. For D + M, 75 µL of Dobby and 75 µL of MPK7 were added together at 0 h, each at concentrations such that the total phage particles correspond to the desired MOI. For sequential treatments (e.g., M → D), 150 µL of the first phage (e.g., MPK7) was added at 0 h, and 150 µL of the second phage (e.g., Dobby) was added at 24 h, each at concentrations to achieve the specified MOI based on the initial bacterial count.

Bacterial killing dynamics were tracked over 48 h. Samples (20 µL) were collected at 0, 2, 4, 6, 24, 26, 28, 30, and 48 h, serially diluted in sterile saline, and plated onto nutrient agar. After incubation at 37°C for 24 h, viable bacterial counts were recorded as colony-forming units (CFU)/mL. All experiments were conducted in triplicate.

**Dose impact**

An assay similar to the time-kill study was performed to assess the impact of different phage doses. Early log-phase *P. aeruginosa* PAO1 (150 µL of ~1 × $10^6$ CFU/mL) was added to a 5-mL NB. At 0 h, 150 µL of the first phage (Dobby or MPK7) at $10^4$ PFU/mL was added. After 24 h, 150 µL of the second phage was added at either $10^6$ PFU/mL or $10^8$ PFU/mL. Bacterial counts were measured at 0, 2, 4, 6, 24, 26, 28, 30, and 48 h.

A second assay to measure order of phage impact. Early log-phase *P. aeruginosa* PAO1 (150 µL of ~1 × $10^6$ CFU/mL) was added to a 5-mL NB with 150 µL of phage suspension ($10^6$

PFU/mL) was added, followed by an additional 150 µL of phage suspension ($10^6$ PFU/mL) 24 h later. Bacterial counts were measured at 6 and 30 h, as bacterial regrew just before that time.

**Fitness cost**

To determine whether resistance incurs a fitness cost in the absence of phage selection, resistant mutants were isolated after a single round of phage treatment (either with individual phages or a combination of phages applied simultaneously). For each treatment, three independent resistant mutants were isolated from the time-kill studies. Specifically, 10 µL of the phage-bacteria mixture collected at 24 and 48 h was plated on NB agar and incubated overnight. Ten colonies were randomly selected from the plate and sub-cultured once more on a second NB agar plate. A single resistant mutant was then randomly selected from the second plate and grown in overnight culture to ensure the absence of residual phages. Resistance to phage infection was determined by the absence of bacterial growth inhibition after 24 hours of exposure (128). Fitness was assessed by comparing the growth rates of the resistant mutants to that of the wild type in phage-free NB media. A microplate reader (Victor Multilabel Plate Reader, Perkin Elmer, United States) was used to measure the optical density at 600 nm ($OD_{600}$). $OD_{600}$ measurements were taken at regular intervals over 24 h to monitor the bacterial growth rates.

**Phage adsorption assay**

Phage adsorption rates were determined by mixing bacteria from overnight cultures with phages from pure lysates at a multiplicity of infection (MOI) of 0.01 (bacterial inoculum of $10^8$ CFU/mL) in nutrient broth. The mixture was incubated at 37°C with shaking (150 rpm). At 5, 10, 15, and 20 minutes post-infection, 1-mL samples were transferred into phosphate-buffered saline (PBS), vortexed vigorously for 30 seconds, and centrifuged at 4,500 × g for 5 minutes at 4°C to pellet cellular debris. The supernatant was collected and serially diluted in PBS for

enumeration by the soft agar overlay method. Adsorption efficiency was calculated as the percentage reduction in free phage titer compared to the initial phage concentration. All assays were performed in triplicate.

**Swimming mobility**

Swimming motility was assessed for both 24 h wild-type and 24 h phage-resistant bacterial isolates. Swimming assay plates (NB plates containing 0.3% agar) were inoculated using a sterile 200-µL pipette tip from overnight-grown single colonies on NB agar plates. The plates were incubated at 37°C overnight, and bacterial motility was assessed by measuring the diameter of the circular turbid zone, which indicated the migration of bacterial cells away from the point of inoculation. Swimming diameters were measured in two perpendicular directions and averaged for both wild-type and phage-resistant isolates. The experiment was repeated three times.

**Morphology of bacteria**

A 1 mL of bacterial suspension was centrifuged at 4500 × *g* for 5 minutes to pellet the cells. The supernatant was discarded, and the pellet resuspended in 1 mL of phosphate-buffered saline (PBS). This resuspension was then centrifuged again at 4500 × *g* for 5 minutes. The washing process (resuspension in PBS followed by centrifugation) was repeated two additional times, for a total of three washes. After the final wash, the bacterial pellet was resuspended in 1 mL of PBS. A 20 µL droplet of this washed bacterial suspension was then placed onto clean glass coverslips. The coverslips were allowed to settle for 5 min, followed by gentle washing with PBS. The coverslips were then incubated in 2% glutaraldehyde in PBS for 1 h, washed with deionized water, and air-dried in an oven at 60 °C for 10 min. The samples were dehydrated by immersing them in increasing concentrations of ethanol, with each immersion performed three times. Residual ethanol was removed using a critical-point dryer (CPD 030,

BAL-TEC). The dehydrated samples were mounted on standard metal SEM stubs and coated with a ~5 nm-thick gold layer using a K550X sputter coater (Quorum Emitech, Kent, UK). The coated samples were examined under high vacuum using a scanning electron microscope (SEM) (Zeiss Ultra Plus, Carl Zeiss NTS GmbH, Oberkochen, Germany) with a working distance of 5 mm.

**Genome sequence analysis**

Genomic DNA was extracted from overnight cultures of wild-type and phage-resistant bacterial isolates using the GenElute Bacterial Genomic DNA Kit (Sigma-Aldrich, St. Louis, MO) according to the manufacturer's instructions. DNA quality and concentration were assessed using a NanoDrop 2000 spectrophotometer (Thermo Fisher Scientific) and Qubit 4.0 fluorometer (Invitrogen), with DNA integrity verified by agarose gel electrophoresis. Only samples with $A_{260}/A_{280}$ ratios between 1.8-2.0 and concentrations ≥ 50 ng/μL were used for sequencing.

Paired-end sequencing libraries were prepared using the Nextera XT DNA Library Preparation Kit (Illumina) and sequenced on the NovaSeq 6000 platform (Illumina) at the Australian Genome Research Facility (Melbourne, Australia) to generate 150-bp paired-end reads with a target coverage of 100×. Sequencing quality was monitored in real-time using NovaSeq Control Software (NCS v1.6) and Real-Time Analysis (RTA v3.4.4) software.

Raw sequencing reads were quality-filtered using Trimmomatic v0.39 with parameters LEADING:3 TRAILING:3 SLIDINGWINDOW:4:15 MINLEN:36. Genome assembly was performed using SPAdes v3.15.3 with default parameters for bacterial genomes. Assembly

quality was assessed using QUAST v5.0.2, and genomes with N50 values >50 kb and <200 contigs were retained for analysis.

Genome annotation was conducted using Prokka v1.14.6 with default settings. Comparative genomic analysis was performed by aligning assembled genomes against the reference *P. aeruginosa* PAO1 genome (RefSeq accession NC_002516.2) using progressive Mauve v2.4.0. Single nucleotide polymorphisms (SNPs) and insertions/deletions (indels) were identified using Snippy v4.6.0 with a minimum coverage threshold of 10× and minimum variant frequency of 0.9. Functional annotation of identified variants was performed using SnpEff v5.0 against the PAO1 reference annotation.

Large structural variations, including insertions, deletions, and rearrangements >1 kb, were detected using Mauve alignment and verified by manual inspection. Acquired resistance genes and mobile genetic elements were identified using ResFinder v4.1 and ISfinder databases, respectively. All bioinformatics analyses were performed using default parameters unless otherwise specified.

**AFM-IR Measurements**

One mL of bacterial samples were pelleted by centrifugation at 4000 × *g* at 4°C for 5 minutes and then washed with 1 mL of sterile ultrapure water. This washing process was repeated twice, resulting in a total of three washes, to effectively remove residual media. Ten microliters of the cell suspension were transferred onto a zinc selenide prism and allowed to settle for 3 minutes. After removing the remaining liquid, the sample was dried on the prism for 10 minutes and stored in a glass petri dish to prevent contamination prior to AFM-IR measurements.

Nanoscale infrared spectroscopy was conducted using an AFM-IR instrument (nanoIR, Anasys Instruments) according to our previously published protocol (129). Four IR background spectra were acquired over the range of 1000 to 1800 $cm^{-1}$, averaged, and normalized for signal

intensity as a function of wavenumber. The cantilever oscillation mode was employed to optimize the cantilever ringdown signal, centred at a frequency of 185 kHz with a 20 kHz frequency window. To achieve the best signal-to-noise ratio during spectral acquisition, the infrared laser focus was fine-tuned at specific wavenumbers—1080, 1250, 1450, 1550, 1650, and 1720 $cm^{-1}$—using 256 co-averaged scans for optimization. The laser power was adjusted to create a distinct "IR-hotspot" at the image centre, aligning with the point of contact between the AFM tip and the sample. AFM-IR spectra were collected across the 1000 to 1800 $cm^{-1}$ range at 1 $cm^{-1}$ intervals, with 256 co-averaged cantilever ringdown signals recorded at each wavenumber. A minimum of ten spectra were obtained from each sample. IR images and maps were generated in contact mode at a scan rate of 0.1 Hz with a co-average of 16, utilizing a silicon nitride cantilever with a nominal spring constant of 0.5 N $m^{-1}$ (PR-EX-C450-10 tips, AppNano, Mountain View, CA).

The AFM data files were processed using Gwyddion software for roughness analyses. The root mean square roughness was measured for each individual bacteria cell, with a minimum of 10 cells analyzed per sample. Data analysis of the IR spectra was performed using Vektor Direktor software (KAX Group, Australia). The AFM-IR spectra were normalized using the Standard Normal Variate (SNV) method and smoothed using the Savitzky-Golay algorithm with 11 smoothing points. Second derivatives were then computed using the Savitzky-Golay algorithm with 17 smoothing points. Finally, Principal Component Analysis (PCA) was applied to the full set of spectra acquired from both phages across the 1000 to 1800 $cm^{-1}$ range.

**Statistical analysis**

One-way analysis for variance (ANOVA) and unpaired two-sample t test at a confidence level of 95% were employed to identify any statistically significant differences in surface roughness in bacteria cells after exposing to different phage treatments. A $p$ value of less than 0.05 ($p <$

0.05) was considered statistically significant.

## Results

### Sequential LPS-first dosing (D → M) achieves sustained bacterial suppression

We examined bacterial dynamics following simultaneous and sequential treatments with two phages (Dobby targeting LPS and MPK7 targeting TFP) at various theoretical multiplicities of infection (MOI: 0.01, 1, and 100) over 48 h.

In simultaneous treatments, bacterial populations initially decreased but regrew after 6 h, stabilizing until 48 h. At MOI 100, bacterial concentrations reached approximately $10^9$ CFU/mL, while at MOIs 1 and 0.01, growth plateaued at about $10^8$ CFU/mL (Fig. 1A–C).

In the sequential treatment, bacterial concentrations initially regrew after 24 h but then either decreased or suppressed growth following the addition of the second phage. At an MOI of 100, bacterial regrowth occurred as early as 2 h post-treatment, reaching $10^8$ CFU/mL. Adding MPK7 after this initial regrowth temporarily decreased bacterial concentrations to $10^3$ CFU/mL for 4 h, but they eventually increased to $10^6$ CFU/mL (Fig. 1A). At an MOI of 1, Dobby initially reduced bacterial levels below the limit of detection within 6 h, but levels then stabilized at $10^3$ CFU/mL for 30 h before increasing to $10^6$ CFU/mL at 48 h (Fig. 1B). Sequential treatment with Dobby at an MOI of 0.01 resulted in CFU counts below the limit of detection for the first 6 h, but by the 24 h time point the bacteria had regrown to $10^5$ CFU/mL (Fig. 1C). Subsequent

treatment with MPK7 reduced the bacterial concentrations to $10^4$ CFU/mL, which were sustained for 48 h (Fig. 1C).

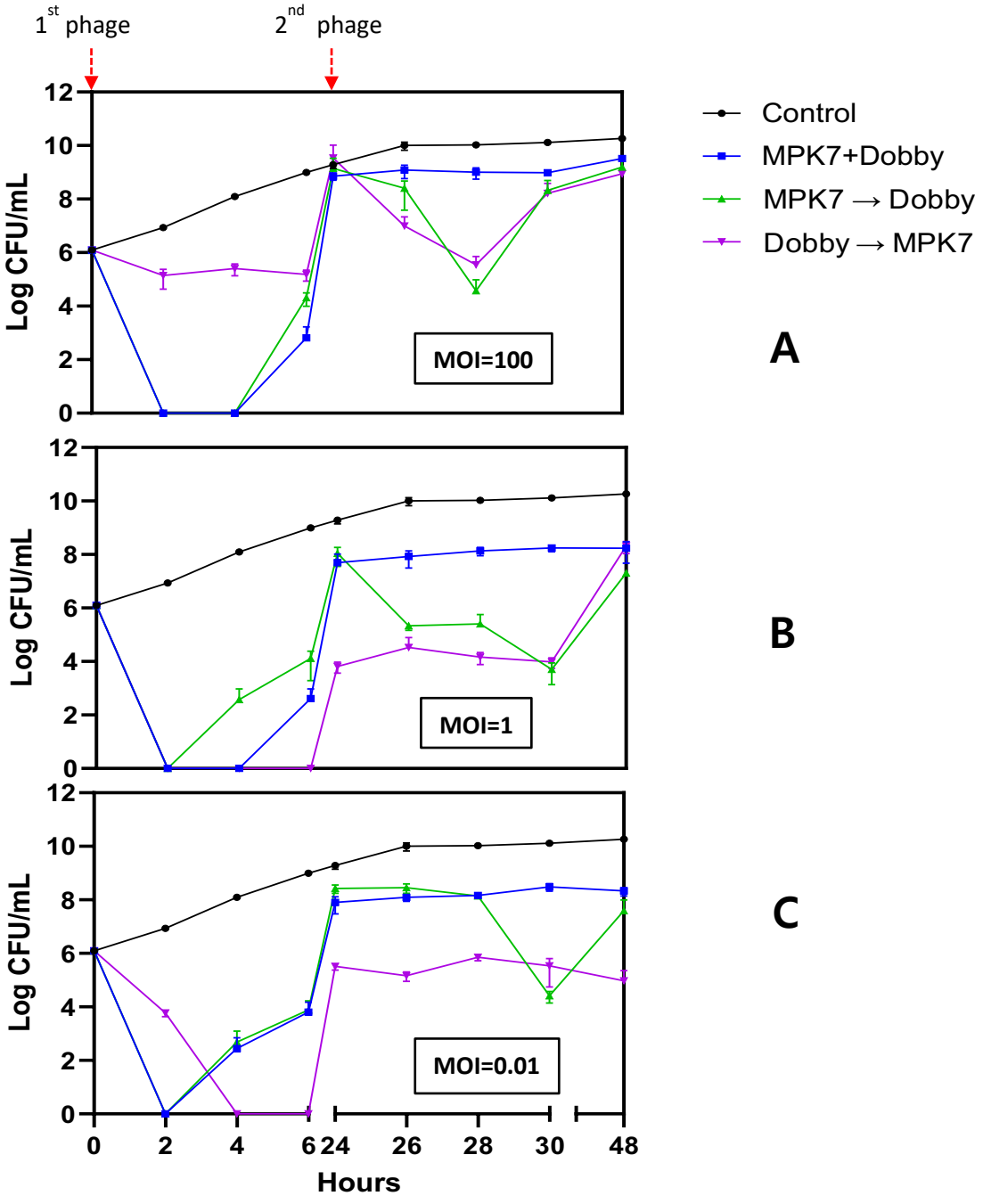

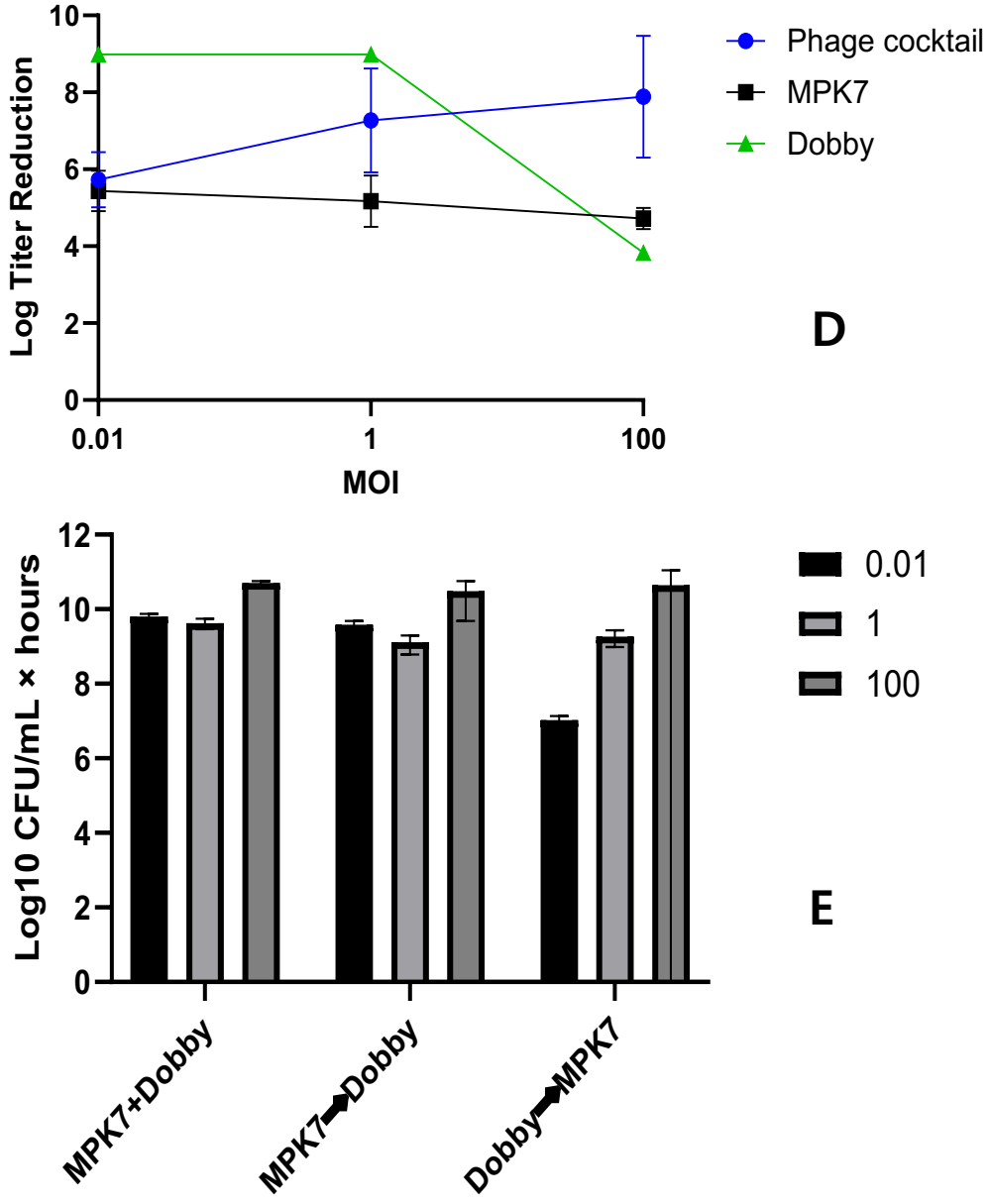


Fig.1. Time-kill studies for simultaneous and sequential phage treatments. Bacterial growth over time was assessed for 48 h. Representative interactions between MPK7 and Dobby on wild-type PAO1 (the ratio of phages to bacteria): (A) MOI=100; (B) MOI=1; (C) MOI=0.01. (D) Dose-response assays with phage cocktail MPK7 +Dobby, MPK7, and Dobby were determined at 6 h. (E) Area under the curve. Data are presented as mean ± SEM (n = 3). Statistical significance was assessed using two-way ANOVA. *n.s.*, not significant.

To determine the minimum effective concentration of the phage *in vitro*, we calculated the dose-response for each treatment after 6 h. Dobby at an MOI of 0.01 resulted in the highest bacterial reduction, achieving an 8.9 $\log_{10}$ decrease (Fig. 1D). Increasing the MOI from 0.01 to 100 for the phage cocktail increased bacterial reduction from 5.7 $\log_{10}$ to 7.9 $\log_{10}$ (Fig. 1D). To quantify the overall bacterial burden during the 48-h treatment period, we calculated the area under the curve (AUC) for bacterial concentrations over time, expressed in $\log_{10}$ CFU/mL × h. Sequential treatment (D → M) at an MOI of 0.01 resulted in the lowest AUC of 7.0 $\log_{10}$ CFU/mL × h, indicating a substantial reduction in bacterial burden compared to the other treatment regimens (Fig. 1E). The AUC for the phage cocktail treatment at an MOI of 100 was 9.6 $\log_{10}$ CFU/mL × h, while sequential treatment (M → D) at the same MOI reduced the AUC to 9.1 $\log_{10}$ CFU/mL × h, demonstrating greater suppression of bacterial growth (Fig. 1E). Overall, the AUC values indicate that sequential phage treatments were more effective in suppressing bacterial growth than simultaneous treatments, particularly at lower MOI levels.

**Low initial MOI is sufficient; minimal additional benefit from second treatment with an increased MOI**

To further examine the importance of phage order in bacterial clearance, we conducted a follow-up experiment using the same phage sequentially (MOI = 1) for both initial and subsequent treatments. Bacterial concentrations were measured at 6 and 30 h, corresponding to peak phage activity observed in previous experiments. Sequential application of the same phage (Dobby → Dobby or MPK7 → MPK7) reduced bacterial levels to ~$10^7$ and ~$10^9$ CFU/mL, respectively, at 30 h (Fig. 2C). In contrast, sequential application of different phages (Dobby → MPK7 or MPK7 → Dobby) was more effective, reducing bacterial concentrations

to ~$10^3$ CFU/mL at 30 h (Fig. 2C). Sequential use of different phages led to a greater reduction in bacterial levels compared to the same phage.

We then investigated whether controlling the initial MOI and subsequently increasing the MOI of the second phage treatment could enhance bacterial killing efficacy. The experiments began with an initial MOI of 0.01 for the first phage, followed by a second phage treatment at increased theoretical MOIs of 1 and 100 (by increasing the phage concentration from ~$10^4$ PFU/mL to ~$10^6$ PFU/mL or ~$10^8$ PFU/mL).

In all treatments, the second phage dose produced comparable profiles of bacterial count reduction (Fig. 2A & B). When MPK7 was applied first, bacterial levels decreased from ~$10^7$ to ~$10^4$ CFU/mL between 24 and 30 h, before rebounding to ~$10^7$ CFU/mL by 48 h at both MOIs (Fig. 2B). Conversely, when Dobby was used first, bacterial concentrations decreased from ~$10^6$ to ~$10^4$ CFU/mL between 24 and 48 h, maintaining this lower level over time (Fig. 2A).

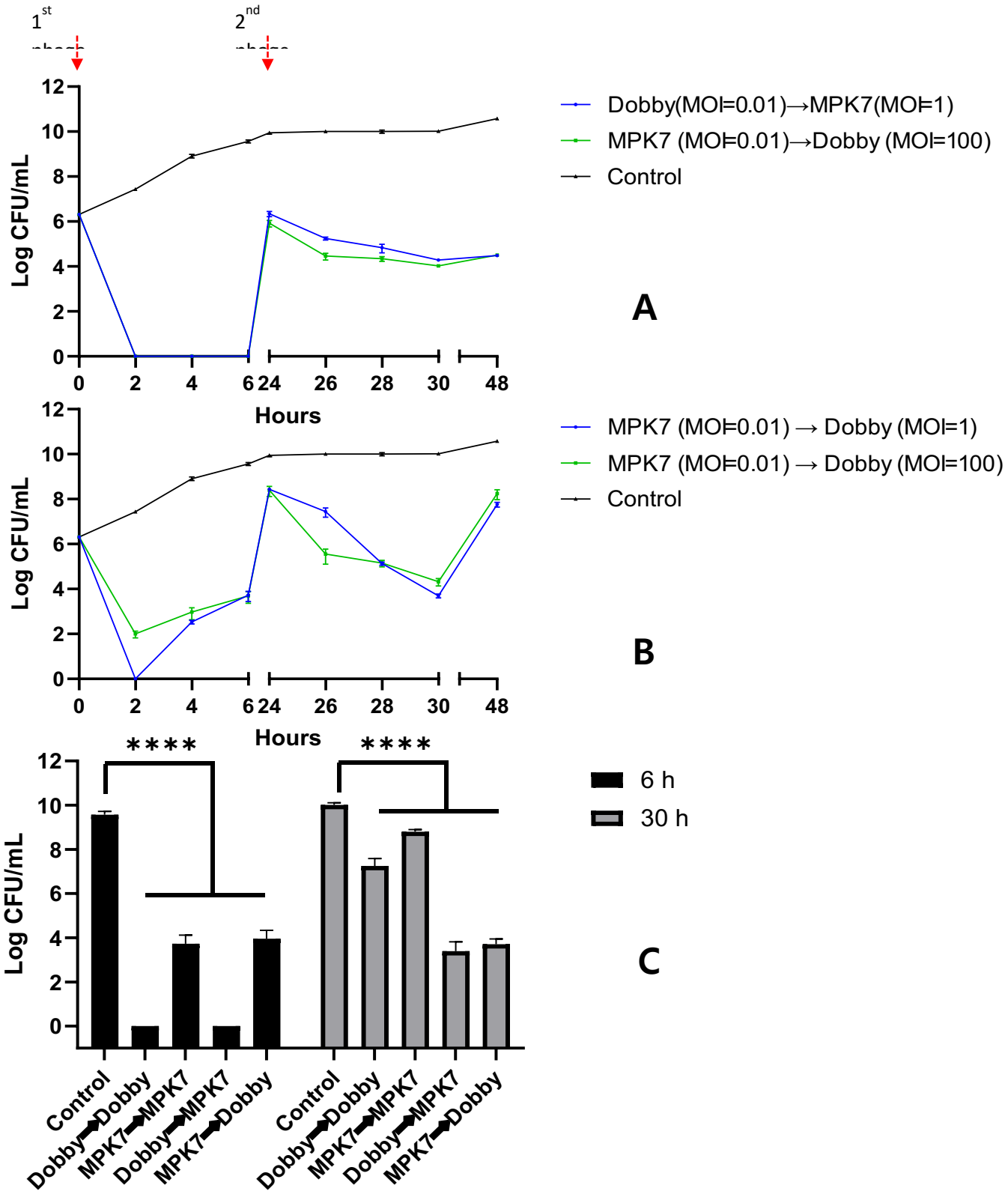


Fig.2. Impact of sequential phage treatments on bacteria growth. (A) and (B) show 48-h bacterial growth dynamics at 37 °C following sequential treatment with MPK7 and Dobby phages at varying MOIs. In (A), phage Dobby was added first, followed by MPK7. The blue line represents treatment with Dobby at MOI 0.01 followed by MPK7 at MOI 1, while the green line represents Dobby at MOI 0.01 followed by MPK7 at MOI 100. In (B), the treatment order was reversed, with MPK7 added first and Dobby second. (C) compares the effects of using the same versus different phage combinations on bacterial regrowth at 6 and 30 h of incubation, with an MOI of 1. Data are presented as mean ± SEM (n=3). Statistical significance was assessed using two-way ANOVA. ****, $p$< 0.0001; *n.s.*, not significant.

**Resistance trade-offs in phage-selected mutants: fitness costs and reduced phage adsorption**

Resistance profiles and phenotypic characteristics of bacteria reisolated at 24 and 48 h post-treatment was assessed. At the 24-h time point, three mutants isolated from sequential phage treatments were resistant to a single phage, either MPK7 or Dobby. At the 48-h time point, following exposure to the second phage in the treatment sequence, all isolated bacteria exhibited resistance to both MPK7 and Dobby.

Growth of the reisolated bacteria was measured using optical density at 600 nm ($OD_{600}$). At the 24-hour time point, Dobby-resistant isolates had an $OD_{600}$ of 0.5, which was significantly lower than the wild-type control ($p < 0.001$) (Fig. 3A). At the 48-hour time point, Dobby-resistant isolates showed an $OD_{600}$ of 1.0. Phage-resistant isolates from the 48-hour time point, including those from the phage cocktail treatment, displayed higher $OD_{600}$ values compared to the 24-hour isolates across all treatments (Fig. 3A). Resistant isolates from the 48-hour phage cocktail treatment exhibited the highest $OD_{600}$ among the groups tested.

SEM images of ten resistant bacteria showed that approximately 50% of the resistant cells smaller than that of the wild-type PAO1 strain. Additionally, flagella were detected in only 2 out of the 10 cells (Fig. S1).

Phage adsorption assays revealed that Dobby-resistant isolates from the 24-hour time point had reduced adsorption rates, with a 70% reduction for MPK7 (Fig. 3B) and a 30% reduction for Dobby (Fig. 3C) compared to the wild-type strain. Dobby-resistant isolates exhibited reduced swimming motility compared to MPK7-resistant isolates (Fig. S2).

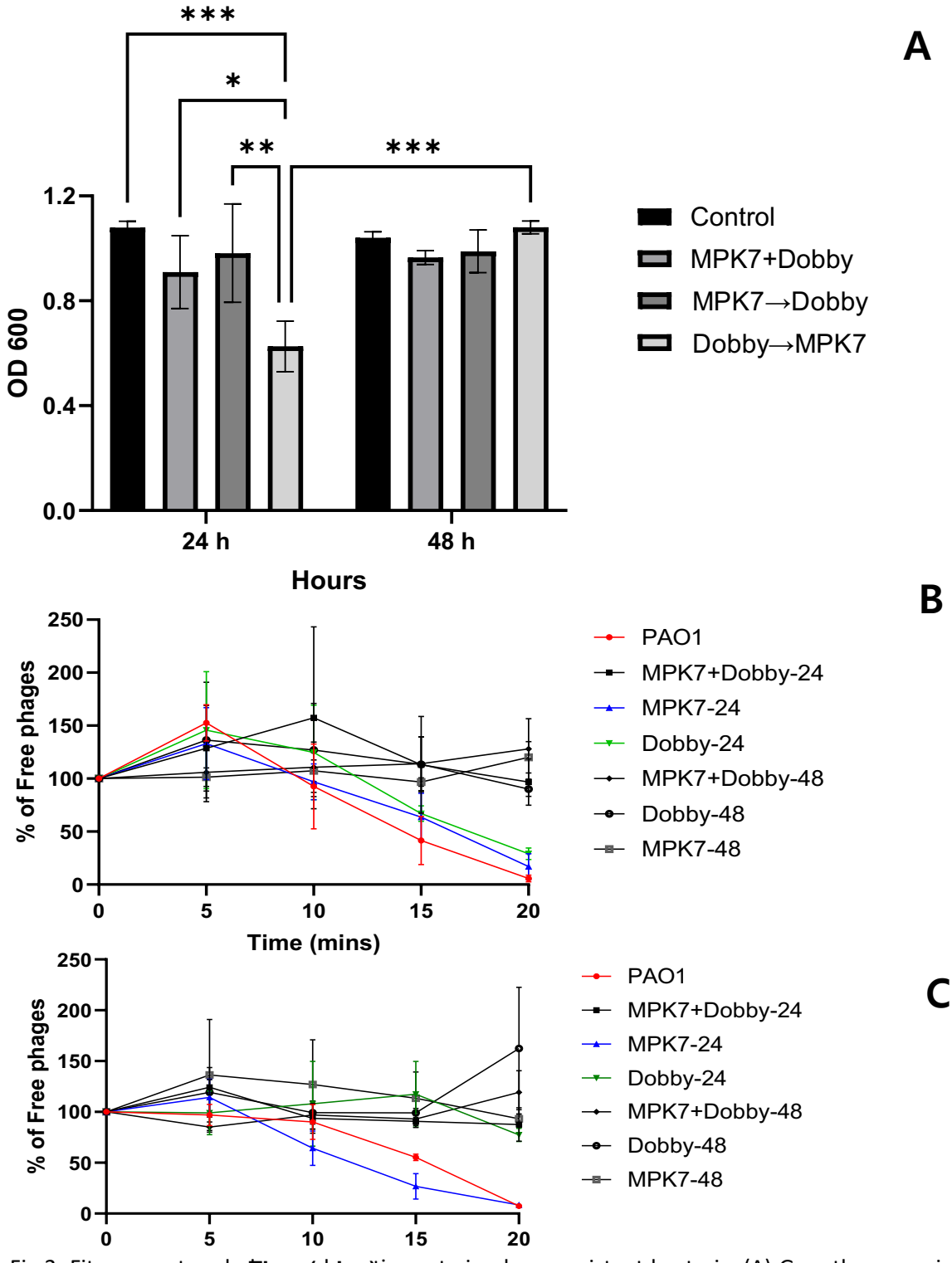


Fig.3. Fitness cost and phage adsorption rate in phage-resistant bacteria. (A) Growth comparison of mutants vs. wild-type after phage treatments. Statistical significance was assessed using two-way ANOVA. *, $p < 0.05$; **, $p < 0.01$; ***, $p < 0.001$; *n.s.*, not significant. Phage adsorption efficiency of resistant bacterial isolates exposed to phages (B) MPK7 and (C) Dobby. Data are presented as mean ± SEM (n = 3).

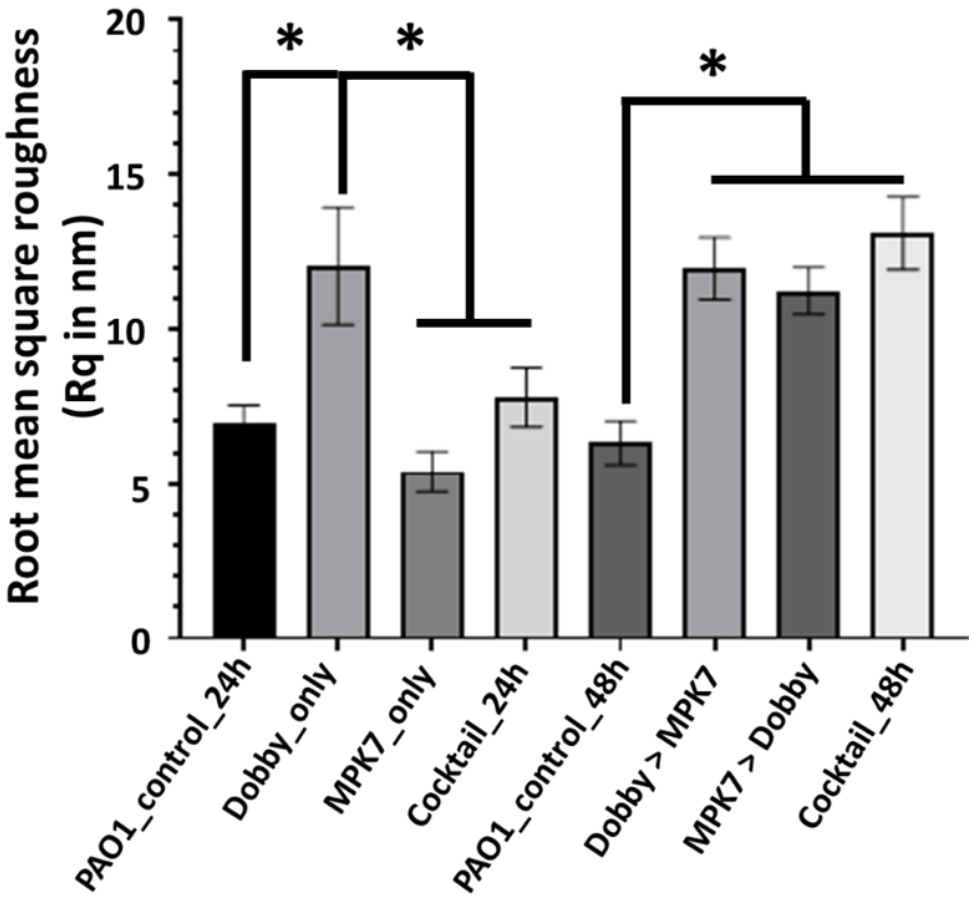


Figure 4. AFM surface roughness analysis of the bacteria cell after various treatments. Statistical significance was assessed using two-way ANOVA. *, $p < 0.05$; *n.s.*, not significant. Data are presented as mean ± SEM (n = 3).

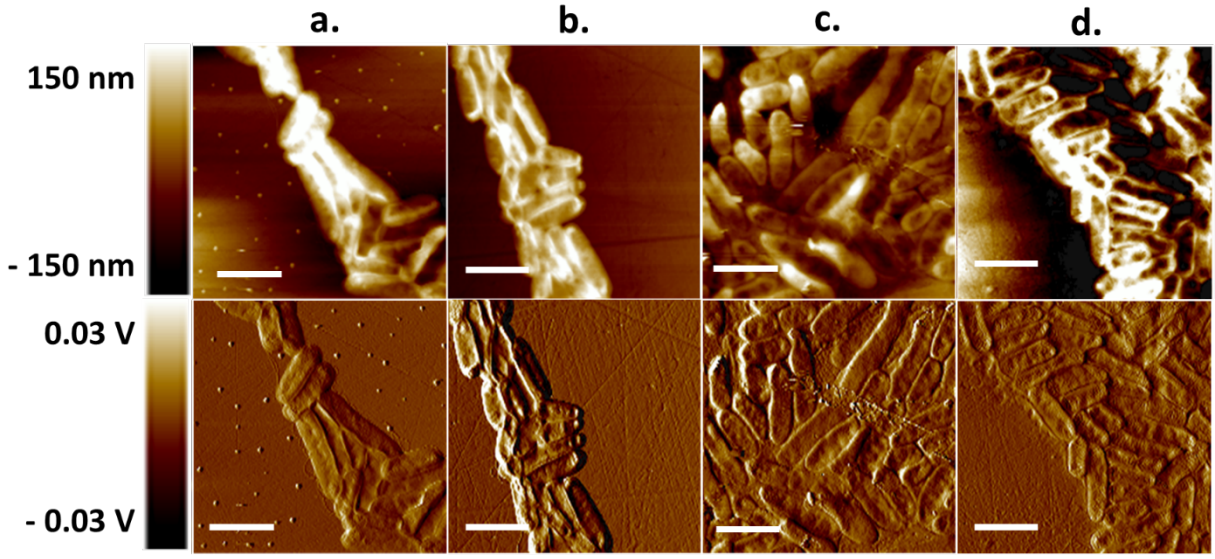


Figure 5. Atomic Force Microscopy (AFM) images of bacterial cells at 24 hours. Top: Height image showing surface topography. Bottom: Phase image indicating material and compositional differences. Subfigures represent: (a) PAO1 control (untreated cells); (b) cells treated with a phage cocktail for 24 hours; (c) cells exposed to Dobby phage only for 24 hours; (d) cells exposed to MPK7 phage only for 24 hours. (Scale bar = 5 µm)

**AFM-IR reveals distinct LPS- vs TFP-based chemical adaptations linked to resistance**

The root mean square roughness (Rq), expressed in nanometers (nm), was quantified from atomic force microscopy (AFM) images (Fig. 5 & 7) of individual bacterial cells to assess surface morphological changes in response to phage treatments (Fig. 4). At both the 24-hour and 48-hour time points, PAO1 control samples exhibited consistent Rq values (~ 6 and 7 nm, respectively), indicating stable surface roughness in the absence of phage exposure. At the 24-hour time point, Dobby-resistant isolates displayed significantly different Rq values (~ 12 nm) compared to the PAO1 control samples, MPK-resistant isolates, and cocktail-treated bacteria. By the 48-hour time point, all phage-treated samples—regardless of treatment type—showed significant differences in Rq relative to the PAO1 control samples. However, no significant difference in Rq was observed between sequentially treated samples (Dobby followed by MPK7, denoted Dobby → MPK7 (~ 12 nm), or vice versa, denoted MPK7 → Dobby (~ 11 nm)) and cocktail-treated samples (~ 13 nm) at 48 h.

At 24 h (Fig. 6a & b), the control *P. aeruginosa* PAO1 strain exhibited distinct infrared (IR) absorption peaks: 1650 $cm^{-1}$ (amide I, proteins), 1550 $cm^{-1}$ (amide II, proteins), ~1240 $cm^{-1}$ (asymmetric phosphodiester stretching), and minor peaks between 1400–1450 $cm^{-1}$ (C-H bending modes of end ethyl groups of proteins) and at approximately 1080 $cm^{-1}$ (carbohydrates, such as peptidoglycan or LPS). Dobby-resistant isolates exhibited a shifted amide I peak at 1660 $cm^{-1}$, a peak at 1550 $cm^{-1}$ and ~1240 $cm^{-1}$. The intensity at ~1240 $cm^{-1}$ was markedly higher than in the control, while the signal at 1080 $cm^{-1}$ was reduced, and signals between 1400–1450 $cm^{-1}$ were absent. Bacteria treated with the cocktail phage (Dobby and MPK7) displayed an amide I peak at 1660 $cm^{-1}$, alongside peaks at 1550 $cm^{-1}$ and ~1240 $cm^{-1}$. The signal at 1080 $cm^{-1}$ matched the control in intensity, with no detectable peaks between 1400–1450 $cm^{-1}$. MPK7-resistant isolates presented peaks at 1660 $cm^{-1}$, 1550 $cm^{-1}$, and an elevated

~1240 $cm^{-1}$ peak relative to the control. A faint signal at 1390 $cm^{-1}$ (C=O symmetric stretching of COO−) (130) was observed, along with the strongest intensity at 1080 $cm^{-1}$ among the 24-hour samples. Principal Component Analysis (PCA) at 24 h (Fig. 6 c & d) showed the first principal component (PC1) explaining 38.23% of the variance, driven by the amide I band, peaks near 1250 $cm^{-1}$, and ~1050 $cm^{-1}$. The second principal component (PC2) accounted for 25.7% of the variance, influenced by peaks at ~1660 $cm^{-1}$, 1460 $cm^{-1}$, and 1100 $cm^{-1}$. This analysis effectively separated Dobby-resistant isolates from the control and other resistant groups.

At 48 h (Fig. 8a & b), the control PAO1 sample exhibited a spectral profile with peaks at 1650 $cm^{-1}$, 1550 $cm^{-1}$ (highest intensity), ~1420 $cm^{-1}$ (C-H bending), ~1240 $cm^{-1}$, and 1080 $cm^{-1}$. MPK7-resistant isolates, evaluated at 24 h and then treated with Dobby phage for analysis at 48 h, showed peaks similar to the control, with a slightly increased intensity at 1080 $cm^{-1}$ and no signals between 1400–1450 $cm^{-1}$. Dobby-resistant isolates from 24 h, treated with MPK7 phage and assessed at 48 h, displayed heightened intensities at 1080 $cm^{-1}$ and ~1240 $cm^{-1}$ compared to the control and other treatment groups. Bacteria exposed to the cocktail phage for 48 h presented a spectral profile with peaks at 1650 $cm^{-1}$, 1550 $cm^{-1}$ (lowest intensity among 48-hour samples), ~1240 $cm^{-1}$, and 1080 $cm^{-1}$, though with reduced intensities relative to sequentially treated bacteria. PCA at 48 h (Fig. 8 c & d) indicated that PC1 captured 32.06% of the variance, influenced by peaks at 1720 $cm^{-1}$ (possibly carbonyl stretching), ~1640 $cm^{-1}$, 1560 $cm^{-1}$, 1420 $cm^{-1}$, ~1240 $cm^{-1}$, and 1100 $cm^{-1}$. PC2 and PC3 explained 25.01% and 17.79% of the variance, respectively, with PC2 driven by peaks at 1640 $cm^{-1}$, 1560 $cm^{-1}$, and 1050 $cm^{-1}$, and PC3 by peaks at 1710 $cm^{-1}$, 1500 $cm^{-1}$, and 1050 $cm^{-1}$. This analysis distinguished isolates

from sequential phage treatments, particularly those involving Dobby followed by MPK7 phage.

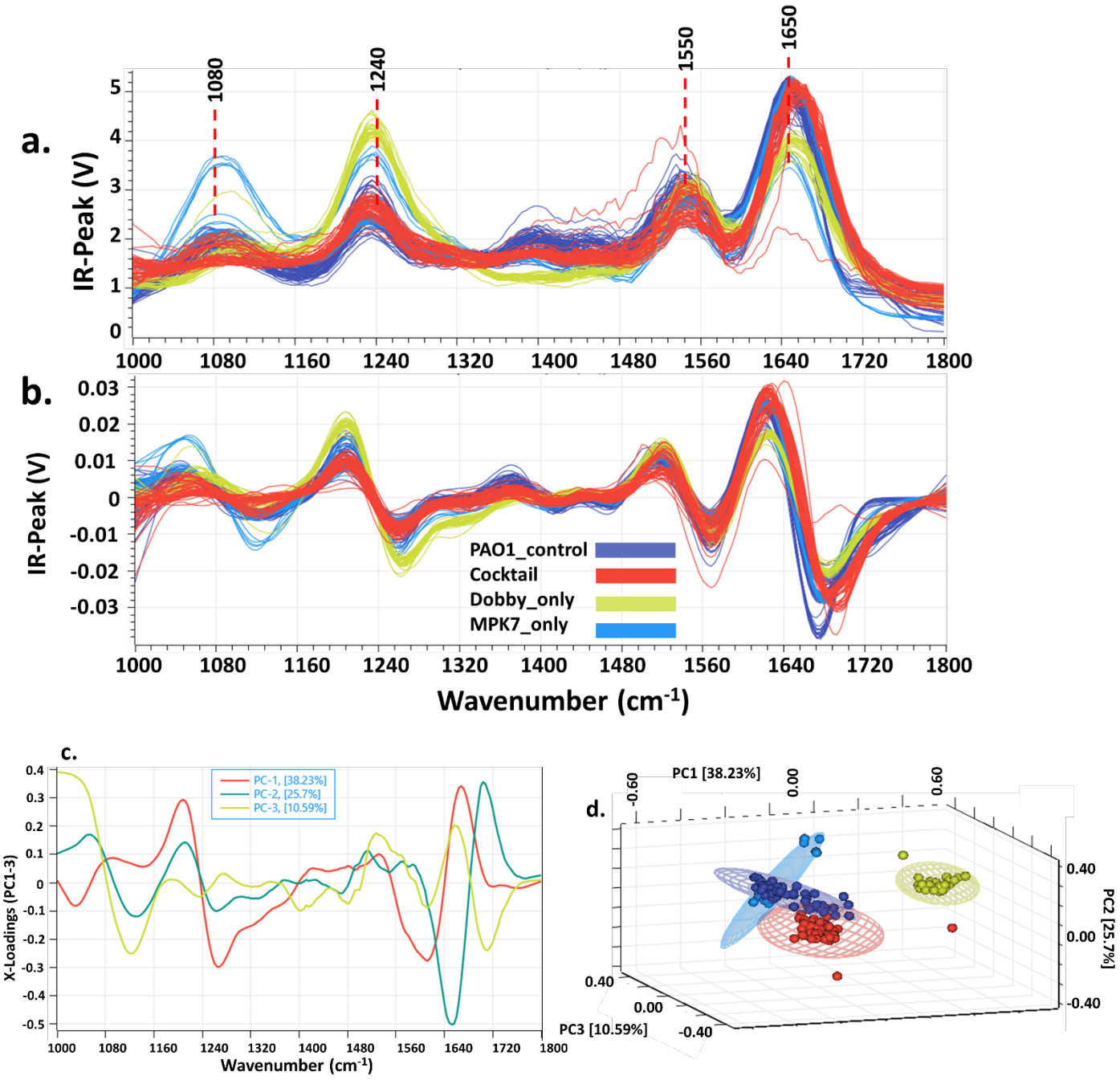


Figure 6. Spectral analysis of bacterial cells after various treatments at 24 hours. (a) Original infrared spectra of bacterial cells. (b) Second derivative spectra, sharpening overlapping bands and revealing key spectral features. (c) X-variable loadings from the second derivative spectra, pinpointing spectral regions driving observed differences. (d) Three-dimensional scatter plot showing spectral separation of samples (color-coded as in (a)).

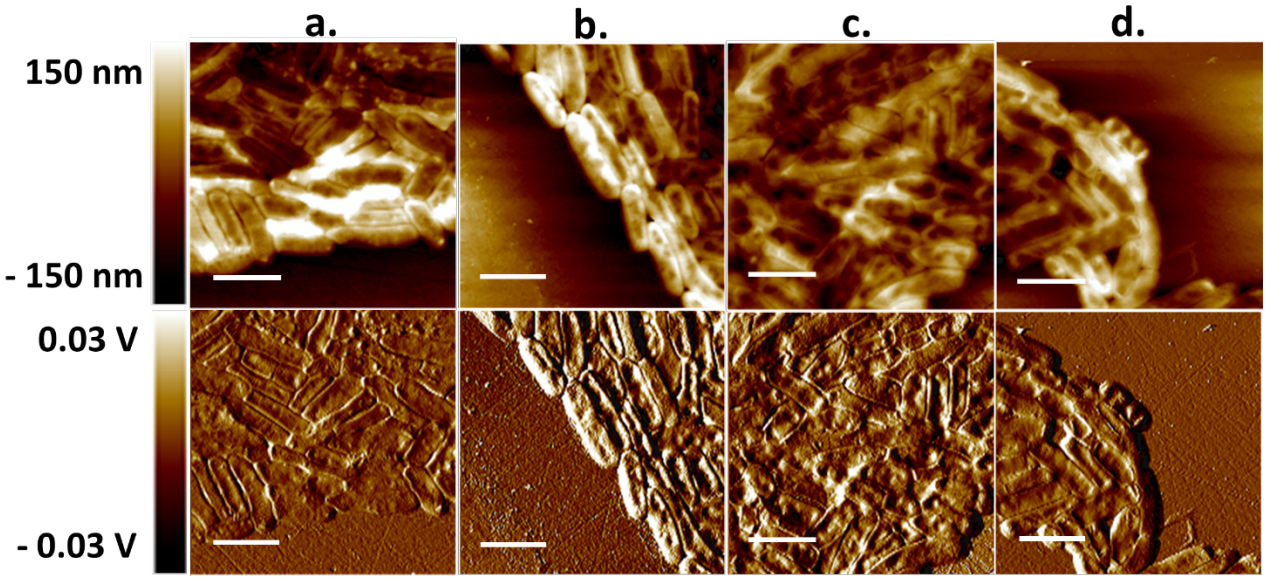


Figure 7. Atomic Force Microscopy (AFM) images of bacterial cells after 48 hours. The upper panel presents the height image the lower panel depicts the phase image. Subfigures include:(a) PAO1 control (untreated cells); (b) cells treated with a phage cocktail over 48 hours; (c) cells subjected to Dobby phage for 24 hours, then MPK7 phage for 24 hours; (d) cells exposed to MPK7 phage for 24 hours, followed by Dobby phage for 24 hours. (Scale bar = 5 µm)

## Discussion

In this study, we introduce a novel approach for improving phage therapy against *P. aeruginosa* by employing a sequential dosing regimen that targets distinct bacterial receptors. Our findings demonstrate that sequentially administering an LPS-targeting phage (Dobby) followed by a TFP-targeting phage (MPK7) reduces bacterial concentrations compared to simultaneous treatments. This outcome contrasts with prior a report looking at sequential and simultaneous phage administration of multiple phages (121), emphasizing the need to better understand specific bacteria-phage pairs and the potential advantages of receptor-specific sequencing to maximize therapeutic effectiveness. Additionally, we observed that a low initial MOI (0.01) was sufficient to achieve substantial bacterial suppression, with little additional benefit derived from increasing the concentration in the second-dose of the different phage. Analysis of resistant mutants highlighted significant fitness costs and reduced phage adsorption rates, consistent with receptor-specific modifications.

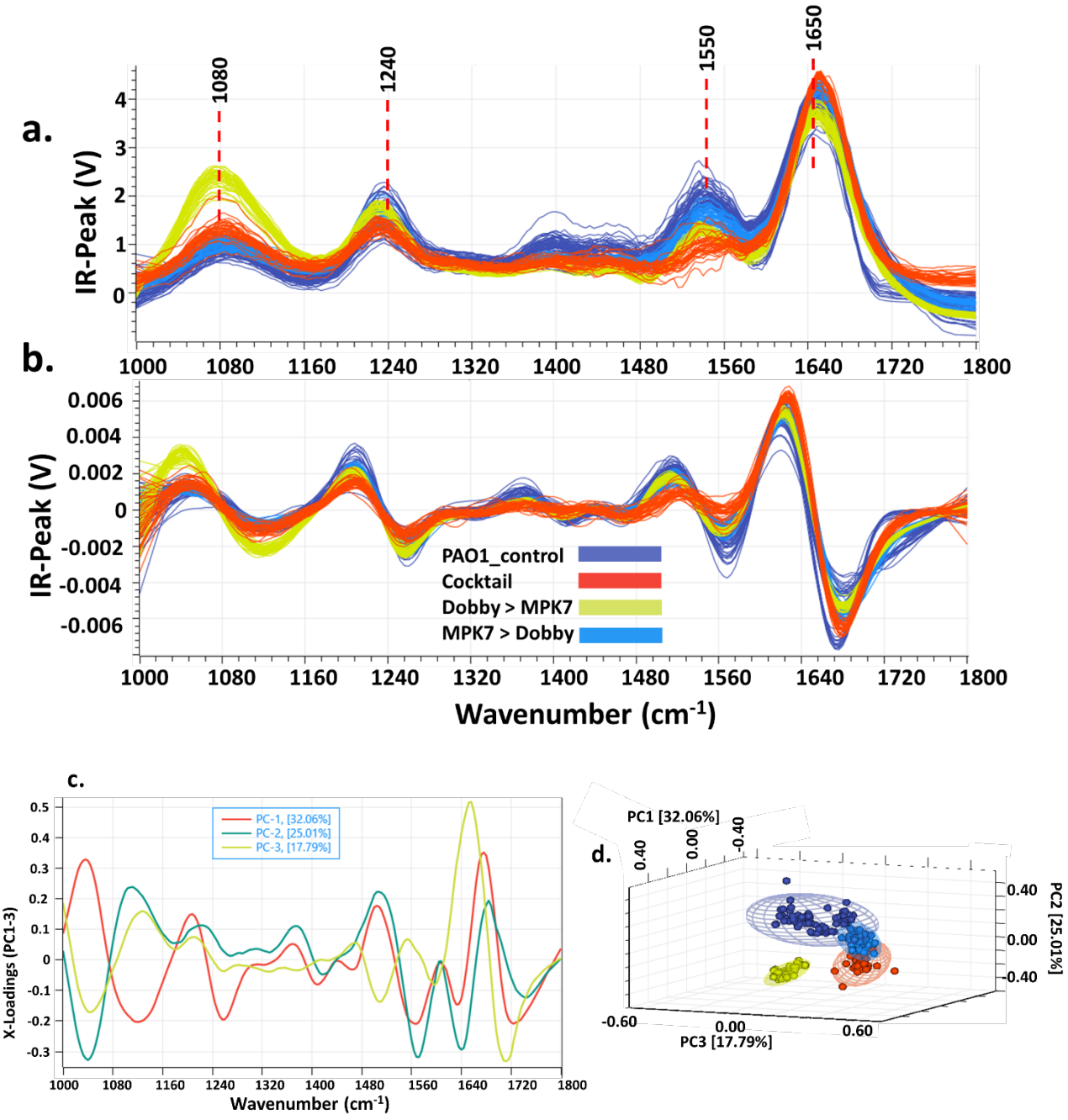


Figure 8. Infrared spectral analysis of bacterial cells at 48 hours, following initial treatment at 24 hours. (a) Original infrared spectra of bacterial cells. (b) Second derivative spectra, sharpening overlapping bands and revealing key spectral features. (c) X-variable loadings from the second derivative spectra, pinpointing spectral regions driving observed differences. (d) Three-dimensional scatter plot showing spectral separation of samples (color-coded as in (a)).

AFM-IR spectroscopy revealed distinct chemical signatures associated with resistance mechanisms targeting either LPS or TFP, suggesting divergent molecular pathways in response to phage pressure. Our results demonstrate that the order of phage administration profoundly influences treatment outcomes at both bacteria population and molecular levels. The D → M regimen proved most effective, particularly at MOI 0.01, where Dobby nearly eradicated bacteria within 6 h, reducing counts to below the limit of detection. Although regrowth to $10^5$ CFU/mL occurred by 24 h, the addition of MPK7 maintained suppression, resulting in the lowest AUC of 7.0 $\log_{10}$ CFU/mL × h (Fig. 1C & E). This sustained control indicates that resistance to Dobby does not impair MPK7's ability to target TFP. A follow-up experiment confirmed the importance of using different phages sequentially, as D → M reduced bacterial counts to ~$10^3$ CFU/mL at 30 h, compared to ~$10^7$ and ~$10^9$ CFU/mL for sequential application of the same phage (D → D or M → M; Fig. 2C). The molecular basis for this enhanced efficacy is revealed by AFM-IR analysis. In Dobby-resistant isolates, AFM-IR showed significantly reduced intensity of the carbohydrate band at ~1080 $cm^{-1}$ alongside increased intensity at ~1240 $cm^{-1}$ (Fig. 6a). The diminished 1080 $cm^{-1}$ signal indicates loss or alteration of surface polysaccharides, consistent with LPS truncation—a common adaptation that disrupts primary phage adsorption sites (131, 132). Bacteria typically escape LPS-targeting phages through mutational inactivation of LPS, yielding shortened LPS that blocks phage attachment [2]. Concurrently, the increased ~1240 $cm^{-1}$ intensity may reflect elevated phosphodiester content, possibly due to membrane remodeling under phage pressure [27]. Importantly, Dobby-resistant isolates exhibited significantly lower fitness ($OD_{600}$ of 0.5, $p < 0.001$; Fig. 3A), suggesting that LPS modifications impose substantial metabolic costs. Phage adsorption assays confirm this adaptation pattern, showing that Dobby-resistant isolates at 24 h had only a 30% reduction in adsorption compared to a 70% reduction for MPK7 (Fig. 3B), indicating retained MPK7

binding capacity. These LPS modifications, while conferring resistance to the Dobby phage, may destabilize the outer membrane, potentially increasing susceptibility to the MPK7 phage in sequential treatments [3]. The disruption of LPS, a critical outer membrane component, likely compromises bacterial membrane integrity, enhancing TFP accessibility for MPK7 [23]. By 48 h, sequential D → M treatment produced greater spectral complexity, with intensified peaks at 1080 $cm^{-1}$ and 1240 $cm^{-1}$ (Fig. 8a), indicating stepwise resistance development where initial LPS modifications prime bacteria for TFP glycosylation upon MPK7 exposure. In contrast, the reverse sequence (M → D) was less effective. In this regimen, bacterial regrowth occurred as early as 2 h post-MPK7 treatment at MOI 100, reaching ~$10^8$ CFU/mL by 24 h. The addition of Dobby temporarily reduced counts to ~$10^3$ CFU/mL for 4 h, but regrowth resumed, reaching ~$10^6$ CFU/mL by 48 h (Fig. 1A). The AUC for M → D at MOI 100 was 9.1 $\log_{10}$ CFU/mL × h, indicating lesser suppression compared to simultaneous treatment (9.6 $\log_{10}$ CFU/mL × h; Fig. 1E). M → D treatment yielded AFM-IR spectra resembling untreated bacteria, suggesting fewer adaptive changes when TFP resistance precedes LPS-targeted phage exposure (Fig. 8a). MPK7-resistant isolates show a different molecular signature. AFM-IR revealed a prominent ~1080 $cm^{-1}$ carbohydrate peak alongside shifts in protein and phosphodiester-related peaks (Fig. 6a). The preserved 1080 $cm^{-1}$ signal, coupled with a new 1390 $cm^{-1}$ peak (C=O symmetric stretching in carbohydrate), indicates resistance centered on TFP modification rather than LPS alteration. This pattern suggests TFP glycosylation—where O-antigen units or D-arabinofuranose mask phage binding sites (133). While this protects against TFP-targeting phages like MPK7, it imposes costs, including reduced swimming motility (Fig. 7d) and potentially decreased virulence [21]. Simultaneous treatments (D + M) initially reduced bacterial concentrations across all MOIs, but regrowth began after 6 h, reaching ~$10^9$ CFU/mL at MOI 100 and ~$10^8$ CFU/mL at MOIs 1 and 0.01 by 48 h (Fig. 1A–

C). Isolates from this treatment exhibited the highest fitness (highest $OD_{600}$ values; Fig. 3A), suggesting optimization for dual resistance. AFM-IR analysis revealed spectral profiles similar to control PAO1, with reduced intensities at 1550 and 1240 $cm^{-1}$, consistent with either suppressed bacterial biomass or emergence of a generalist resistance phenotype (134, 135). This likely reflects selective pressure favoring genetic mutations, such as pilus-related gene changes, over phenotypic adaptations(136). These findings underscore an important consideration for the specific phage-bacteria system studied here: the sequence of Dobby and MPK7 administration against *P. aeruginosa* PAO1 impacts bacterial suppression under the experimental conditions tested. In this system, initiating treatment with the LPS-targeting phage Dobby forced bacterial adaptations that, while conferring Dobby resistance through LPS modifications, imposed fitness costs and inadvertently increased bacterial susceptibility to the subsequent TFP-targeting phage MPK7, suggesting that receptor-specific sequential targeting may optimize treatment outcomes for these particular phage-bacteria pairs.

Our investigation into phage-bacteria ratios revealed that low multiplicity of infection (MOI) can be sufficient for effective bacterial control. Dose-response studies showed that Dobby at MOI 0.01 achieved an 8.9 $log_{10}$ reduction in bacterial counts at 6 h, the highest among treatments (Fig. 1D). Remarkably, increasing the second dose of MPK7 to MOI 1 or 100 in sequential treatments did not significantly enhance bacterial clearance beyond the low-dose regimen (Fig. 2A & B). This phenomenon appears independent of treatment sequence and instead reflects the self-replicating nature of phages, which can amplify from low initial doses, making higher concentrations unnecessary, at least in *vitro* where there are no other factors affecting phage concentration (137). When examining phage-ratio effects specifically, we observed that bacterial counts decreased from ~$10^6$ to ~$10^4$ CFU/mL between 24 and 48 h across both low and high MOI conditions when using the effective D→M sequence. The phage

amplification dynamics explain this dose-independent effect: once the initial bacterial density (~$10^6$ CFU/mL) exceeds the phage proliferation threshold (~$10^4$ CFU/mL), phages can replicate efficiently even at low MOI. High phage concentrations may actually be counterproductive, potentially triggering bacterial stress responses such as the SOS response, which can accelerate resistance development (138). The molecular basis for this dosage phenomenon appears distinct from sequence-dependent effects. While treatment sequence influences which surface receptors are modified (LPS versus TFP), dosage primarily affects the rate and extent of phage replication within the bacterial population. In low-density infections, higher initial doses may be needed to exceed the inundation threshold, but this comes with an increased risk of resistance (139). This threshold-dependent behavior suggests that phage therapy protocols should be tailored to bacterial density rather than maximizing phage concentration. These findings support the efficacy of low-dose (MOI <1) phage therapy for bacterial control through in situ amplification, offering several advantages: reduced production costs, minimized side effects including immune responses and endotoxin release, and potentially delayed resistance development (26). However, practically, the determination of bacterial densities in vivo, particularly in the presence of biofilms, is not an easily achievable goal. While timing must be optimized to ensure phage replication outpaces bacterial growth, our results demonstrate that the lower MOI (0.01) provided more effective control of the target population, with excess phage providing no additional benefit once bacteria were overwhelmed (26). Indeed, unnecessarily high doses may drive resistance without enhancing clearance. It should be noted that the theoretical MOI values reported in this study (0.01, 1, and 100) represent calculated ratios at the time of inoculation. As highlighted in recent discussions of phage therapy dosing, the practical MOI at any given timepoint may differ from theoretical calculations due to factors such as phage decay, bacterial growth kinetics, adsorption dynamics,

and spatial distribution within the culture system (121). These considerations should be factored into the interpretation of our MOI-dependent results and emphasize the need for real-time monitoring in future dose optimization studies.

Despite the efficacy of sequential phage treatment, a subset of bacteria persisted through resistance to one or both phages. Analysis of these resistant mutants revealed significant evolutionary trade-offs, with molecular and phenotypic evidence that resistance adaptations frequently compromised bacterial fitness in critical aspects of pathogenicity and survival. Distinct resistance mechanisms emerged depending on treatment regimen, with each carrying specific fitness penalties. Dobby-resistant mutants at 24 h exhibited significantly lower fitness ($OD_{600}$ of 0.5, $p < 0.001$; Fig. 3A), suggesting a high metabolic cost associated with LPS modifications (140). AFM-IR analysis of these isolates revealed a diminished 1080 $cm^{-1}$ carbohydrate signal, consistent with LPS truncation that likely weakens the cell surface. Principal Component Analysis (PCA) at 24 h distinguished these Dobby-resistant isolates based on characteristic spectral patterns in amide I, ~1250 $cm^{-1}$, and ~1050 $cm^{-1}$ peaks (Fig. 6d), providing a molecular signature of LPS-targeting phage resistance. Phage adsorption assays (Fig. 3B and 3C) confirmed reduced phage attachment, reflecting alterations at the phage-binding interface. These bacteria likely modified their LPS by shortening the O-polysaccharide chain (141), similar to documented cases involving mutations in LPS biosynthesis genes (e.g., *galU*, *wapR*) [33]. MPK7-resistant mutants showed different adaptations, with AFM-IR analysis indicating TFP modifications rather than LPS alterations. These isolates exhibited reduced swimming motility (Fig. S2), potentially decreasing virulence by impairing tissue colonization [26]. Their resistance likely stemmed from altered or eliminated pili (142), aligning with known mutations in pilus assembly genes (142) prevent phage binding. The functional consequences of these adaptations—impaired motility and

potentially reduced biofilm formation—represent virulence costs. Simultaneous treatment mutants at 48 h exhibited the highest fitness (highest $OD_{600}$ =1.1; Fig. 3A) and harbored a mutation in the *PilU* gene involved in TFP retraction (Table S1), likely conferring MPK7 resistance by altering TFP function. Despite their relatively high fitness in laboratory conditions, morphological examination showed these mutants were approximately 50% smaller than wild-type PAO1, with rare flagella (Fig. S1), suggesting potential virulence deficits through impaired motility and biofilm formation (143). Intriguingly, sequential treatment isolates lacked mutations in six analyzed genes (*lpxA, lpxC, lpxD, PilT, PilU, PilA*) (Table S1), while AFM-IR detected significant chemical shifts. This discrepancy suggests that resistance in these mutants likely stems from alternative genetic or epigenetic mechanisms that are potentially less stable and more costly (134). PCA at 48 h highlighted sequential D → M treatments based on their spectral profiles (Fig. 8d), emphasizing treatment order's role in shaping bacterial chemical adaptations that contribute to resistance. These surface structure modifications carry significant implications for bacterial pathogenicity. LPS and TFP are vital for bacterial physiology and virulence (10), and their disruption can attenuate pathogenicity while increasing susceptibility to host immune responses or antibiotics (144, 145). Even when resistance emerged, compromised growth of mutants delayed regrowth, as noted in post-treatment incubations. This delay provides a therapeutic window for combining phage therapy with antibiotics, to which resistant mutants may have regained sensitivity (146), or immune-based interventions to achieve complete clearance.

Beyond chemical adaptations detected by AFM-IR, our study revealed significant physical alterations in bacterial cell surfaces in response to phage pressure. Quantitative analysis of root mean square roughness (Rq) derived from AFM images (Fig. 5 & 7) provided nanoscale insights into how phage resistance manifests as topographical modifications. At 24 h, Dobby-

resistant isolates exhibited distinctive surface roughness patterns that differed significantly from PAO1 control, MPK7-resistant isolates, and cocktail-treated bacteria (Fig. 4). This receptor-specific topographical signature corresponds to molecular changes in LPS structure observed via AFM-IR. The altered surface roughness likely results from LPS truncation, particularly the loss of O-antigen or core polysaccharides that normally extend from the cell surface. This interpretation aligns with previous work on *P. aeruginosa* strain AK1401 lacking B-band O-antigen, which demonstrated that LPS truncation produces shorter surface polymers and modified surface interactions(147). The physical manifestation of these changes—increased surface roughness—provides complementary evidence of LPS modifications that disrupt phage binding sites. MPK7-resistant isolates presented a contrasting physical adaptation pattern. AFM-IR spectra indicating TFP glycosylation (Fig. 6) corresponded with decreased surface roughness compared to control PAO1 (Fig. 4). This seemingly paradoxical smoothing effect can be explained by the biophysical properties of glycosylated pili. TFP, directly observable via atomic force microscopy (148), influence bacterial surface morphology and interaction dynamics. Native TFP are inherently hydrophobic, potentially causing irregular clustering or uneven protrusion that increases surface roughness. Glycosylation—the addition of hydrophilic sugar groups to pili—fundamentally alters these properties, promoting more uniform distribution and potentially flatter conformation across the cell surface. This structural reorganization minimizes surface irregularities, resulting in the observed smoother surface (149). The correlation between molecular evidence of glycosylation and physical measurements of decreased roughness provides compelling validation of this resistance mechanism. By 48 h, a convergence phenomenon emerged in surface topography. All phage-treated samples—sequential treatments (D → M or M → D) and cocktail treatment alike—exhibited significant differences in surface roughness compared to the untreated control.

Notably, no significant differences in Rq values were observed between sequential and cocktail treatments, suggesting that while chemical adaptations may differ based on treatment regimen, the physical surface modifications ultimately converge toward similar topographical outcomes. This physical convergence despite distinct molecular pathways indicates potential constraints in how bacteria can physically reorganize their surfaces while maintaining viability. These nanoscale physical adaptations provide critical insights into resistance mechanisms that complement molecular analyses. While chemical signatures reveal specific biochemical modifications, physical measurements capture the structural reorganization of the bacterial surface that directly affects phage-host interactions. The integration of these complementary approaches strengthens our understanding of how bacteria physically evade phage predation through receptor modifications that alter surface topology.

While our study demonstrates the efficacy of sequential phage dosing in reducing *P. aeruginosa* load in *vitro*, several limitations warrant consideration. The use of a single bacterial strain and specific phages may limit the generalizability of our findings to other strains or phage combinations. Additionally, the molecular mechanisms underlying resistance were inferred from AFM-IR data but require genetic validation; notably, no mutations were detected in key genes related to LPS and TFP in some resistant isolates, suggesting alternative mechanisms at play. The 48-hour experimental timeframe may not fully capture long-term bacterial dynamics and resistance evolution. To advance this research, future studies should validate the sequential dosing strategy in *vivo* and across diverse bacterial isolates. Investigating a broader array of phages and their combinations will help optimize therapeutic regimens. Comprehensive genetic analyses, including whole-genome sequencing and transcriptomics, are essential to elucidate the full spectrum of resistance mechanisms. Extending observation periods will provide insights into long-term efficacy and resistance development. Furthermore, exploring

the synergy between sequential phage therapy and conventional antibiotics could enhance treatment outcomes. Integrating AFM-IR with complementary techniques such as Raman spectroscopy or mass spectrometry would further elucidate the precise molecular drivers of these nanoscale topographical changes (150). Additionally, real-time monitoring of surface modifications during phage challenge could reveal the dynamics of these adaptations and potentially identify transient states vulnerable to therapeutic intervention. Such multi-dimensional analyses would advance our understanding of bacterial resistance mechanisms and inform the development of more effective phage therapy strategies that target bacteria during periods of physical adaptation.

## Conclusions

Sequential administration of phages targeting distinct receptors—initiating with an LPS-targeting phage followed by a TFP-targeting phage— enhances *P. aeruginosa* suppression compared to simultaneous treatment. This approach achieves substantial bacterial reductions (→3-log10 within 48 h) at low MOI (0.01) and minimizes resistance by exploiting fitness costs in resistant mutants. AFM-IR analysis elucidated molecular adaptations, such as LPS truncation and TFP glycosylation, guiding therapy optimization. These findings support sequential phage therapy as a promising strategy against antibiotic-resistant infection.

## References


1. Abedon, S.T., K.M. Danis-Wlodarczyk, and D.J. Wozniak, *Phage Cocktail Development for Bacteriophage Therapy: Toward Improving Spectrum of Activity Breadth and Depth.* Pharmaceuticals (Basel), 2021. **14**(10).
2. Yang, Y., et al., *Development of a Bacteriophage Cocktail to Constrain the Emergence of Phage-Resistant Pseudomonas aeruginosa.* Front Microbiol, 2020. **11**: p. 327.
3. Li, N., et al., *Characterization of phage resistance and their impacts on bacterial fitness in Pseudomonas aeruginosa.* Microbiology Spectrum, 2022. **10**(5): p. e02072-22.
4. Kochan, K., et al., *Detection of Antimicrobial Resistance-Related Changes in Biochemical Composition of Staphylococcus aureus by Means of Atomic Force Microscopy-Infrared Spectroscopy.* Anal Chem, 2019. **91**(24): p. 15397-15403.
5. Hall, A.R., et al., *Effects of sequential and simultaneous applications of bacteriophages on populations of Pseudomonas aeruginosa in vitro and in wax moth larvae.* Appl Environ Microbiol, 2012. **78**(16): p. 5646-52.
6. Wright, R.C.T., et al., *Resistance Evolution against Phage Combinations Depends on the Timing and Order of Exposure.* mBio, 2019. **10**(5).
7. Yu, Z., et al., *Leveraging mathematical modeling framework to guide regimen strategy for phage therapy.* PLOS Complex Systems, 2024. **1**(3): p. e0000015.
8. Ulrich, L., et al., *Optimizing bacteriophage treatment of resistant Pseudomonas.* mSphere, 2024. **9**(7): p. e0070723.
9. Chan, B.K., et al., *Personalized inhaled bacteriophage therapy for treatment of multidrug-resistant Pseudomonas aeruginosa in cystic fibrosis.* Nat Med, 2025.
10. Abedon, S.T., *Bacteriophage clinical use as antibacterial "drugs": utility and precedent.* Bugs as Drugs: Therapeutic Microbes for the Prevention and Treatment of Disease, 2018: p. 417-451.
11. Casey, E., D. Van Sinderen, and J. Mahony, *In vitro characteristics of phages to guide 'real life'phage therapy suitability.* Viruses, 2018. **10**(4): p. 163.
12. Brockhurst, M.A., et al., *Experimental coevolution with bacteria and phage. The Pseudomonas fluorescens--Phi2 model system.* Infect Genet Evol, 2007. **7**(4): p. 547-52.
13. Khanal, D., et al., *Biospectroscopy of Nanodiamond-Induced Alterations in Conformation of Intra- and Extracellular Proteins: A Nanoscale IR Study.* Anal Chem, 2016. **88**(15): p. 7530-8.
14. Erukhimovitch, V., et al., *FTIR microscopy as a method for identification of bacterial and fungal infections.* Journal of pharmaceutical and biomedical analysis, 2005. **37**(5): p. 1105-1108.
15. Vaitekenas, A., et al., *Pseudomonas aeruginosa Resistance to Bacteriophages and Its Prevention by Strategic Therapeutic Cocktail Formulation.* Antibiotics (Basel), 2021. **10**(2).
16. Li, G., et al., *Adaptation of Pseudomonas aeruginosa to Phage PaP1 Predation via O-Antigen Polymerase Mutation.* Front Microbiol, 2018. **9**: p. 1170.
17. Labrie, S.J., J.E. Samson, and S. Moineau, *Bacteriophage resistance mechanisms.* Nat Rev Microbiol, 2010. **8**(5): p. 317-27.
18. Hoyland-Kroghsbo, N.M., et al., *Quorum sensing controls the Pseudomonas aeruginosa CRISPR-Cas adaptive immune system.* Proc Natl Acad Sci U S A, 2017. **114**(1): p. 131-135.

19. Kunisch, F., et al., *Targeting Pseudomonas aeruginosa biofilm with an evolutionary trained bacteriophage cocktail exploiting phage resistance trade-offs.* Nat Commun, 2024. **15**(1): p. 8572.
20. Oechslin, F., *Resistance Development to Bacteriophages Occurring during Bacteriophage Therapy.* Viruses, 2018. **10**(7).
21. Abedon, S.T., *Phage therapy dosing: The problem(s) with multiplicity of infection (MOI).* Bacteriophage, 2016. **6**(3): p. e1220348.
22. Campoy, S., et al., *Induction of the SOS response by bacteriophage lytic development in Salmonella enterica.* Virology, 2006. **351**(2): p. 360-367.
23. Cairns, B.J., et al., *Quantitative models of in vitro bacteriophage–host dynamics and their application to phage therapy.* PLoS Pathogens, 2009. **5**(1): p. e1000253.
24. Suh, G.A., et al., *Considerations for the Use of Phage Therapy in Clinical Practice.* Antimicrob Agents Chemother, 2022. **66**(3): p. e0207121.
25. Maldonado, R.F., I. Sá-Correia, and M.A. Valvano, *Lipopolysaccharide modification in Gram-negative bacteria during chronic infection.* FEMS microbiology reviews, 2016. **40**(4): p. 480-493.
26. Jarrell, K.F. and A. Kropinski, *Isolation and characterization of a bacteriophage specific for the lipopolysaccharide of rough derivatives of Pseudomonas aeruginosa strain PAO.* Journal of Virology, 1981. **38**(2): p. 529-538.
27. Li, P., et al., *Phages adapt to recognize an O-antigen polysaccharide site by mutating the 'backup'tail protein ORF59, enabling reinfection of phage-resistant Klebsiella pneumoniae.* Emerging Microbes & Infections, 2025(just-accepted): p. 2455592.
28. Tala, L., et al., *Pseudomonas aeruginosa orchestrates twitching motility by sequential control of type IV pili movements.* Nat Microbiol, 2019. **4**(5): p. 774-780.
29. Pang, Z., et al., *Antibiotic resistance in Pseudomonas aeruginosa: mechanisms and alternative therapeutic strategies.* Biotechnol Adv, 2019. **37**(1): p. 177-192.
30. Sadikot, R.T., et al., *Pathogen-host interactions in Pseudomonas aeruginosa pneumonia.* Am J Respir Crit Care Med, 2005. **171**(11): p. 1209-23.
31. Pelicic, V., *Type IV pili: e pluribus unum?* Mol Microbiol, 2008. **68**(4): p. 827-37.
32. Chan, B.K., et al., *Phage selection restores antibiotic sensitivity in MDR Pseudomonas aeruginosa.* Sci Rep, 2016. **6**: p. 26717.
33. Atabek, A. and T.A. Camesano, *Atomic force microscopy study of the effect of lipopolysaccharides and extracellular polymers on adhesion of Pseudomonas aeruginosa.* J Bacteriol, 2007. **189**(23): p. 8503-9.
34. Smedley III, J.G., et al., *Influence of pilin glycosylation on Pseudomonas aeruginosa 1244 pilus function.* Infection and immunity, 2005. **73**(12): p. 7922-7931.
35. Kinnari, T.J., et al., *Effect of surface roughness and sterilization on bacterial adherence to ultra-high molecular weight polyethylene.* Clin Microbiol Infect, 2010. **16**(7): p. 1036-41.
36. Kassem, A., et al., *Applications of Fourier Transform-Infrared spectroscopy in microbial cell biology and environmental microbiology: advances, challenges, and future perspectives.* Frontiers in microbiology, 2023. **14**: p. 1304081.

# Chapter 3

# Stability of Bacteriophages in Spray-Dried Polymeric Formulations: Effect of Excipient Polyvinylpyrrolidone (PVP) Glass Transition Temperature and Molecular Weight

This chapter has been submitted in Bioengineering & Translational Medicine, with the title 'Stability of Bacteriophages in Spray-Dried Polymeric Formulations: Effect of Excipient Polyvinylpyrrolidone (PVP) Glass Transition Temperature and Molecular Weight.' Authors: Mengyu Li, Yue Cao, Hak-Kim Chan.

## Introduction

Recent advances in bacteriophage therapy for antibiotic-resistant bacterial infections have driven development of phage powder formulations (91, 151). Spray-drying has emerged as a viable approach for producing phage powders, with demonstrated feasibility both in *vitro* and in *vivo* (152, 153). The critical challenge in phage powder development lies in preserving biological activity during processing and storage. Spray-drying process exposes phages to thermal, osmotic, and shear stresses that can cause structural damage and viability loss (28). Protective excipients are essential to maintain phage infectivity in the dry state. While disaccharides such as lactose have shown promise in phage formulations (154), alternative polymeric stabilizers like polyvinylpyrrolidone (PVP) offer unique advantages including superior processing characteristics and matrix-forming properties (97, 155).

The mechanisms of biologic stabilization in solid formulations are generally explained by two established hypotheses: water replacement and vitrification (156, 157). In the water replacement hypothesis, excipient molecules form hydrogen bonds with proteins to replace water interactions lost during dehydration, maintaining native protein structure (89). This mechanism requires the excipient to remain in an amorphous state, as crystallization reduces molecular interactions between excipient and protein, leading to structural damage (103, 158). The vitrification hypothesis proposes that biologics are immobilized within a rigid, glassy matrix formed by the excipient. The protective capacity of this glassy state is characterized by the glass transition temperature (Tg), above which the matrix transitions from rigid glass to mobile rubber, potentially compromising stability (156). Studies on protein formulations have established that maintaining storage temperature at least 50°C below glass transition temperature (Tg) ensures adequate protection through reduced molecular mobility (159, 160).

Environmental factors, particularly humidity, can significantly affect matrix properties through plasticization effects. Increased humidity reduces Tg values, potentially compromising the protective glassy state even when storage temperature remains constant (104). This humidity dependence has been demonstrated in protein formulations, where moisture-induced Tg depression correlates with increased degradation rates (161). Despite the success of using glass state in protein stabilization, its systematic application to phage formulations remains largely unexplored. Phages are complex biological entities containing both protein components and nucleic acids, potentially requiring different stabilization approaches compared to individual proteins (162). The larger size and structural complexity of phages may necessitate higher thermal offsets or different excipient properties for adequate protection.

Limited studies have investigated the relationship between Tg and phage stability in powder formulations. Vandenheuvel *et al.* demonstrated that recrystallization of trehalose-based phage powders at elevated humidity resulted in up to 3 $\log_{10}$ titre reduction, highlighting the importance of maintaining amorphous matrices (163). More recently, our previous work on bacteriophage powder stabilization established the fundamental relationship between glass transition temperature and phage bioactivity of lactose-leucine formulations (164). This study demonstrated that maintaining storage temperature below Tg was critical for phage stability, with optimal protection achieved when thermal offsets $\Delta T$ exceeded 50 °C. However, the investigation focused on sugar-based excipient systems only.

Building upon these foundational findings, the present study extends the glass transition approach to polymer-based formulations to explore the influence of polymer molecular weight on phage stabilization. Polyvinylpyrrolidone (PVP) offers advantages for phage formulation due to its ability to form stable amorphous matrices across a range of molecular weights.

Different PVP molecular weights (K15, K25, K40, K100) exhibit varying Tg values and matrix properties, potentially providing tenable stabilization characteristics (165). The hydrogen-bonding capacity of PVP may contribute to both water replacement and vitrification mechanisms (166), though the relative importance of these effects in phage stabilization remains unclear.

The present study investigated the stability of PEV1 bacteriophages in spray-dried formulations containing PVP excipients of varying molecular weights. We systematically evaluated the validity of established ΔT thresholds for phage stability while characterizing molecular weight-dependent effects on matrix properties and long-term stability. The research integrated thermodynamic analysis of glass transition behaviour with kinetic evaluation of degradation processes to establish design principles for phage powder formulations. Our approach examined whether the ~50°C thermal offset proven effective for phage stabilization in sugar-based formulation applies to polymeric systems, while identifying critical humidity thresholds and molecular weight effects that govern formulation performance. The findings provided insights into phage-polymer relationships and establish a framework for developing stable phage therapeutics with extended shelf-life suitable for clinical applications.

## Materials and methods

### Materials

Polyvinylpyrrolidone excipients of varying molecular weights (PVP K15, K25, K40, and K100) were purchased from Sigma-Aldrich (St. Louis, MO, USA). Agar and nutrient broth were supplied by Amyl Media Pty Ltd. The lytic bacteriophage PEV1, specific against *Pseudomonas aeruginosa*, was sourced from AmpliPhi Biosciences AU (Australia) with an initial concentration of approximately $10^{10}$ PFU/mL.

**Phage powders**

Spray-dried phage powders were prepared following the methodology described in our previous work. Briefly, the liquid feed consisted of 0.5 mL of a bacteriophage suspension (approximately $10^{10}$ PFU/mL) combined with 50 mL of the excipient solution containing either 100% w/w PVP K15, PVP K25, PVP K40, or PVP K100 (pH adjusted to 7.4), yielding a total solid concentration of 25 mg/mL. The phage titre of the suspension was determined prior to spray drying using a standard plaque assay. The mixture was then spray-dried using a Büchi Mini Spray Dryer B-290 (Buchi Labortechnik AG, Flawil, Switzerland) equipped with a standard two-fluid atomizing nozzle. The spray drying parameters were: liquid feed rate, 1.9 mL/min; atomizing airflow, 742 L/h; aspiration rate, 35 $m^3$/h; inlet temperature, 60 °C; and outlet temperature maintained between 40–41 °C. The resulting powders were collected and aliquoted into scintillation vials for storage. To determine the phage titre in the powders, samples were reconstituted in phosphate-buffered saline (PBS), and phage titres were quantified by plaque assay.

**Phage stability**

Phage stability was assessed using a standard double-layer agar method. Briefly, 0.2 mL of an overnight culture of *Pseudomonas aeruginosa* strain PAV237 (~2 × $10^8$ CFU/mL) was combined with 5 mL of molten nutrient broth top agar (0.4% w/v) and poured onto nutrient agar plates (1.5% w/v). After solidification, aliquots (10 µL) of serially diluted phage suspensions were spotted onto the surface of the agar overlay, allowed to air-dry for approximately 15 min, and incubated at 37 °C for 18 h. Each assay was performed independently in triplicate. Phages were classified as stable if the observed titre loss was below

1 $\log 10_{10}$. Statistical significance of the observed differences was evaluated by two-way ANOVA, with results considered statistically significant at $p < 0.05$.

**Storage conditions**

The phage powders were stored following the methodology describe in our previous work. Aliquoted phage powders (200 mg per vial) were stored uncapped at controlled temperatures (4, 22, or 40°C) and relative humidity (RH) conditions (15%, 33%, 43%, or 53% RH) for 7 days to allow equilibration of the powders. Following equilibration, the powders continued to be stored under these conditions for up to 180 days, except for conditions at 40°C combined with either 43% or 53% RH, which were excluded from extended studies due to significant titre loss observed within 7 days. To avoid unintended moisture uptake during handling, powders were managed within humidity-controlled acrylic boxes at either 15% or 33% RH. The chosen storage conditions intentionally deviated from standard ICH guidelines (167), reflecting the study's specific aim to explore the mechanistic basis of phage stability by inducing differential changes in Tg across formulations. Specific humidity environments were established using various saturated salt solutions: silica beads provided 15% RH, saturated magnesium chloride solution 33% RH, potassium carbonate 43% RH, and magnesium nitrate 53% RH. These saturated salt solutions were prepared by dissolving excess magnesium chloride, potassium carbonate, or magnesium nitrate in distilled water at 40°C under continuous stirring until saturation. Solutions were subsequently cooled to ambient temperature and sealed in airtight containers for 24 hours to equilibrate. Saturated solutions were then placed into vacuum-sealed containers equipped with humidity sensors for 7 days to confirm stable humidity levels. Once the target RH was consistently achieved, phage powders were

prepared and placed into the humidity-controlled boxes containing the respective saturated solutions.

**X-ray Diffraction (XRD) Analysis**

The crystallinity of the powder formulations was analysed using X-ray powder diffraction (XRPD) with an X'Pert PRO diffractometer (PANalytical, Almelo, The Netherlands) under ambient conditions. Samples were packed into glass capillary tubes (internal diameter: 1.0 mm; WJM-Glas, Berlin, Germany). The diffraction patterns were obtained using Cu Kα radiation (45 kV, 40 mA), recording scattered intensities over a 2θ range of 3° to 50° with an angular increment of 0.028° 2θ per second.

**Scanning Electron Microscopy (SEM)**

The morphology of spray-dried particles was characterized using scanning electron microscopy (SEM; Zeiss Ultra Plus, Carl Zeiss NTS GmbH, Oberkochen, Germany). Samples were fixed onto aluminum stubs using adhesive carbon tape and subsequently sputter-coated with gold (approximately 15 nm thickness) utilizing a K550X sputter coater (Quorum Emitech, UK).

**Differential Scanning Calorimeter (DSC)**

Tg of different grades of PVP were determined using modulated Differential Scanning Calorimetry (MDSC) with a DSC 823e instrument (Mettler Toledo, Greifensee, Switzerland). All formulations underwent 7-day equilibration periods under their respective storage conditions to permit complete Tg adjustment according to environmental temperature and humidity parameters. For each grade, samples weighing 5 ± 1 mg were prepared in sealed aluminium pans. Samples were heated from 30 °C to 200 °C at a heating rate of 2 °C/min,

employing a modulation amplitude of ±0.5 °C and a modulation period of 60 s. Each sample was analysed independently in duplicate.

## Results

### Solid-state and morphological characterization

XRD analysis of spray-dried PEV1 phage powder formulations containing PVP of varying molecular weights (K15, K25, K40, K100) showed no crystalline peaks after 7 days at 4- 40°C with 15-53% RH (Figure 1).

SEM analysis showed molecular weight-dependent morphological changes under various storage conditions following 7-day equilibration (Figure 2). PVP K15 formulations exhibited dimpled, irregular surfaces at mild storage conditions (≤ 22°C, ≤ 33% RH). At 40°C/33% RH, K15 particles displayed smooth, spherical morphologies. At 40°C/53% RH, extensive particle fusion was observed. PVP K25 formulations maintained smooth, spherical particle shapes under most storage conditions, with particle fusion occurring only at 40°C/53% RH. PVP K40 and K100 formulations consistently displayed discrete, spherical particle morphologies across all tested storage conditions, including 40°C/53% RH.

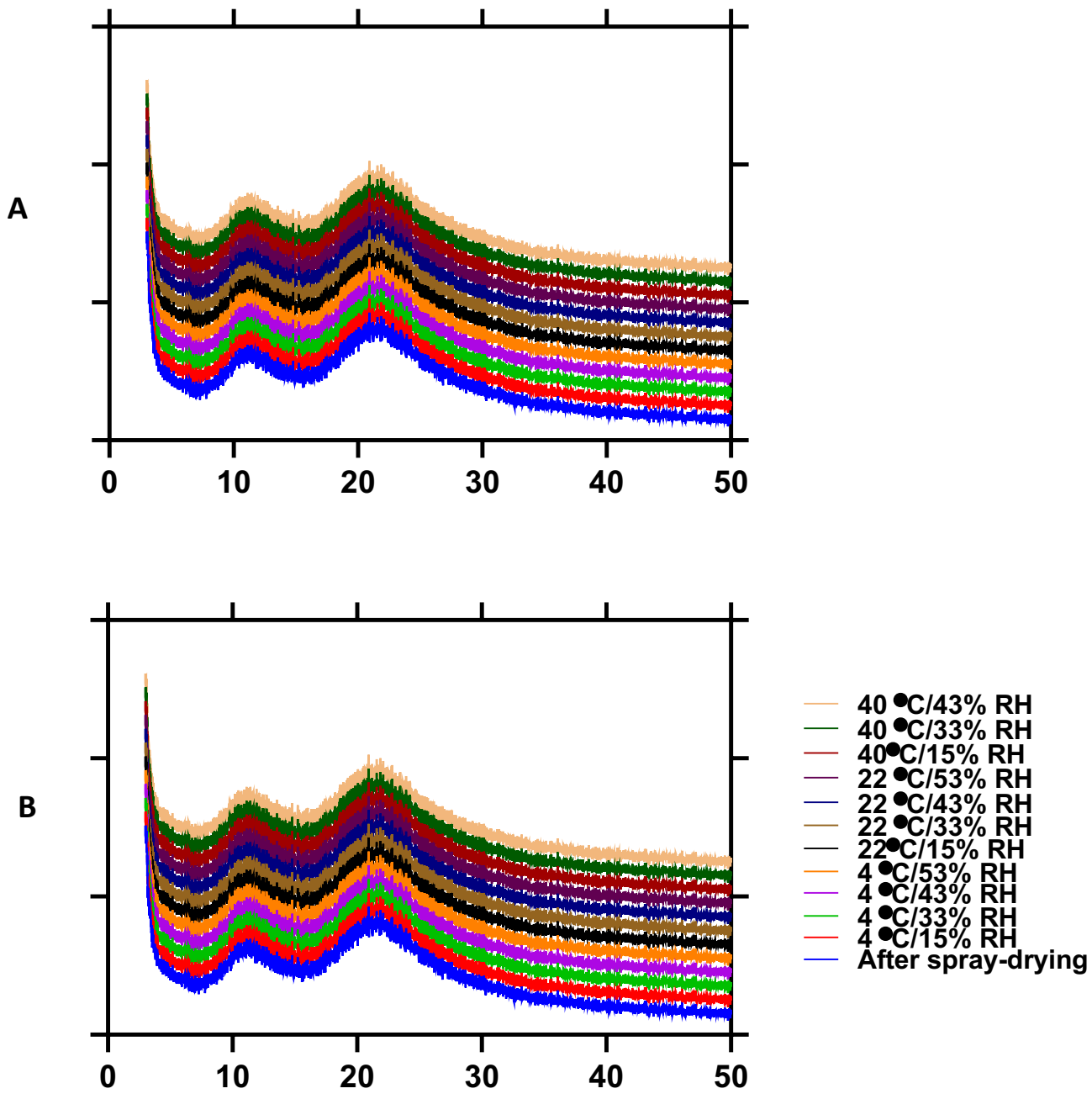
A
B
0
10
20
30
40
50
40 ●C/43% RH
40 ●C/33% RH
40●C/15% RH
22 ●C/53% RH
22 ●C/43% RH
22 ●C/33% RH
22●C/15% RH
4 ●C/53% RH
4 ●C/43% RH
4 ●C/33% RH
4 ●C/15% RH
After spray-drying

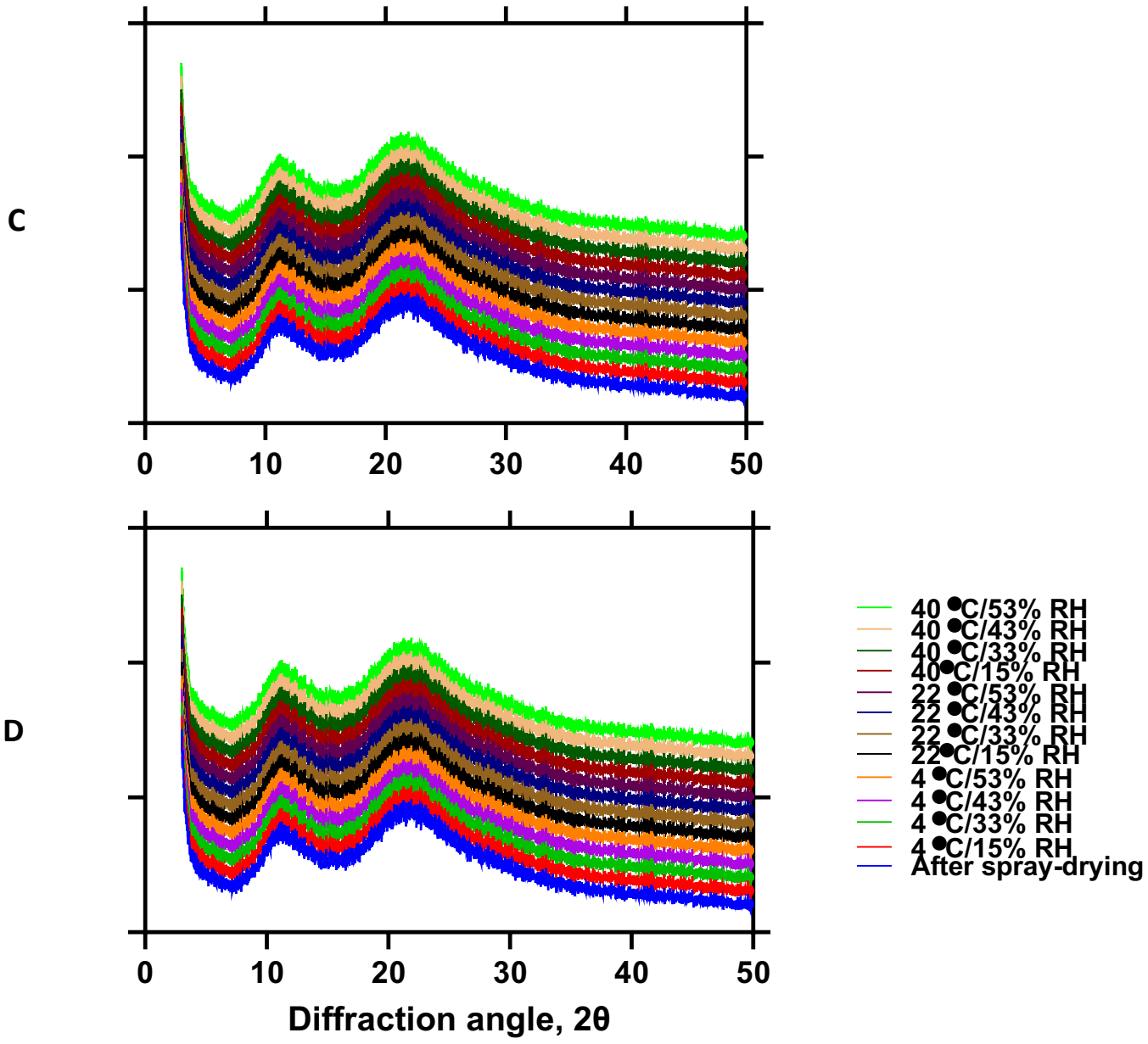


Figure 1. X-ray diffraction (XRD) patterns of spray-dried phage formulations with PVP K15 (A), PVP K25 (B), PVP K40 (C), and PVP K100 (D) after 7-day storage at various temperatures and relative humidities.

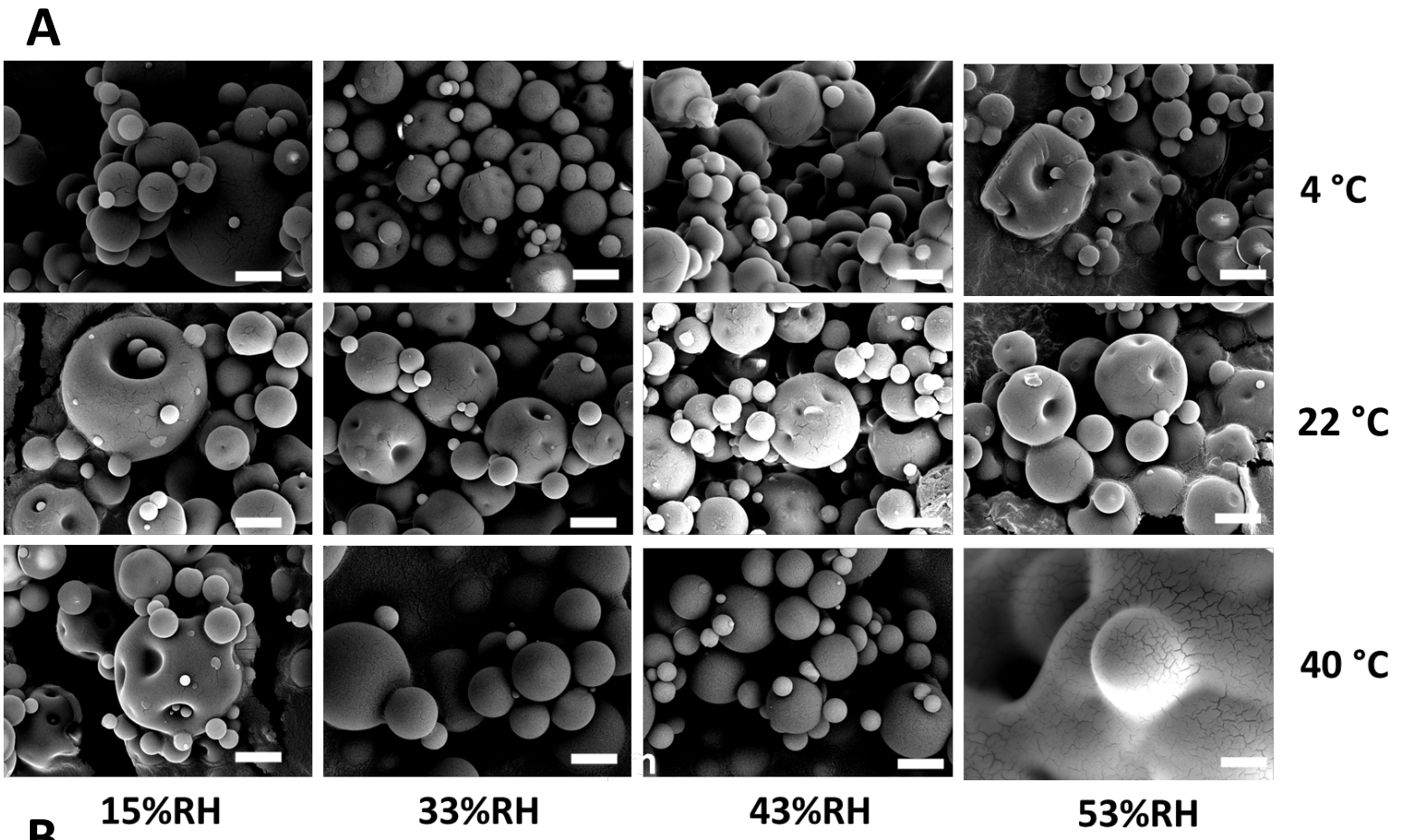
A
4 °C
22 °C
40 °C
15%RH
33%RH
43%RH
53%RH

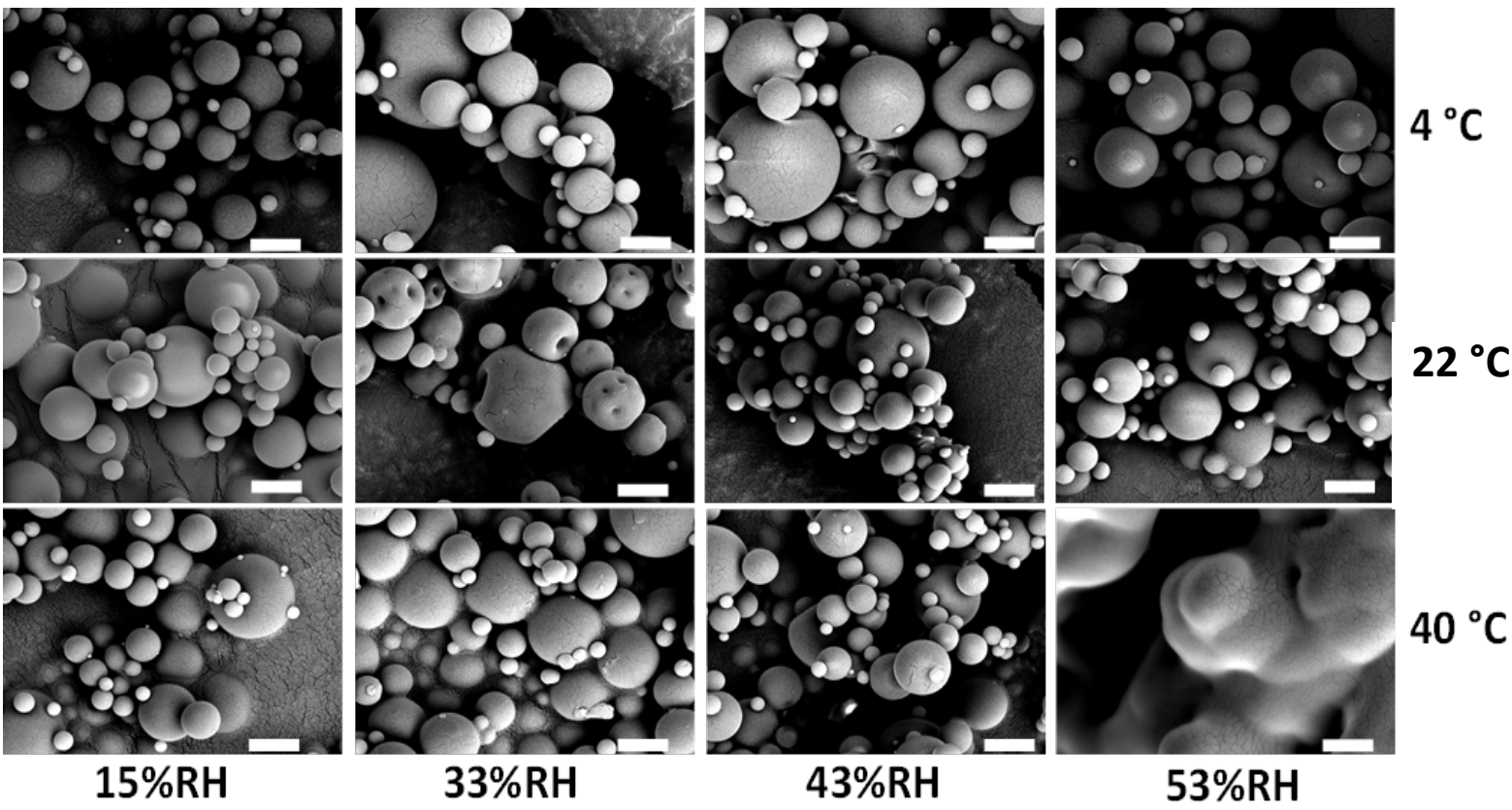
B
4 °C
22 °C
40 °C
15%RH
33%RH
43%RH
53%RH

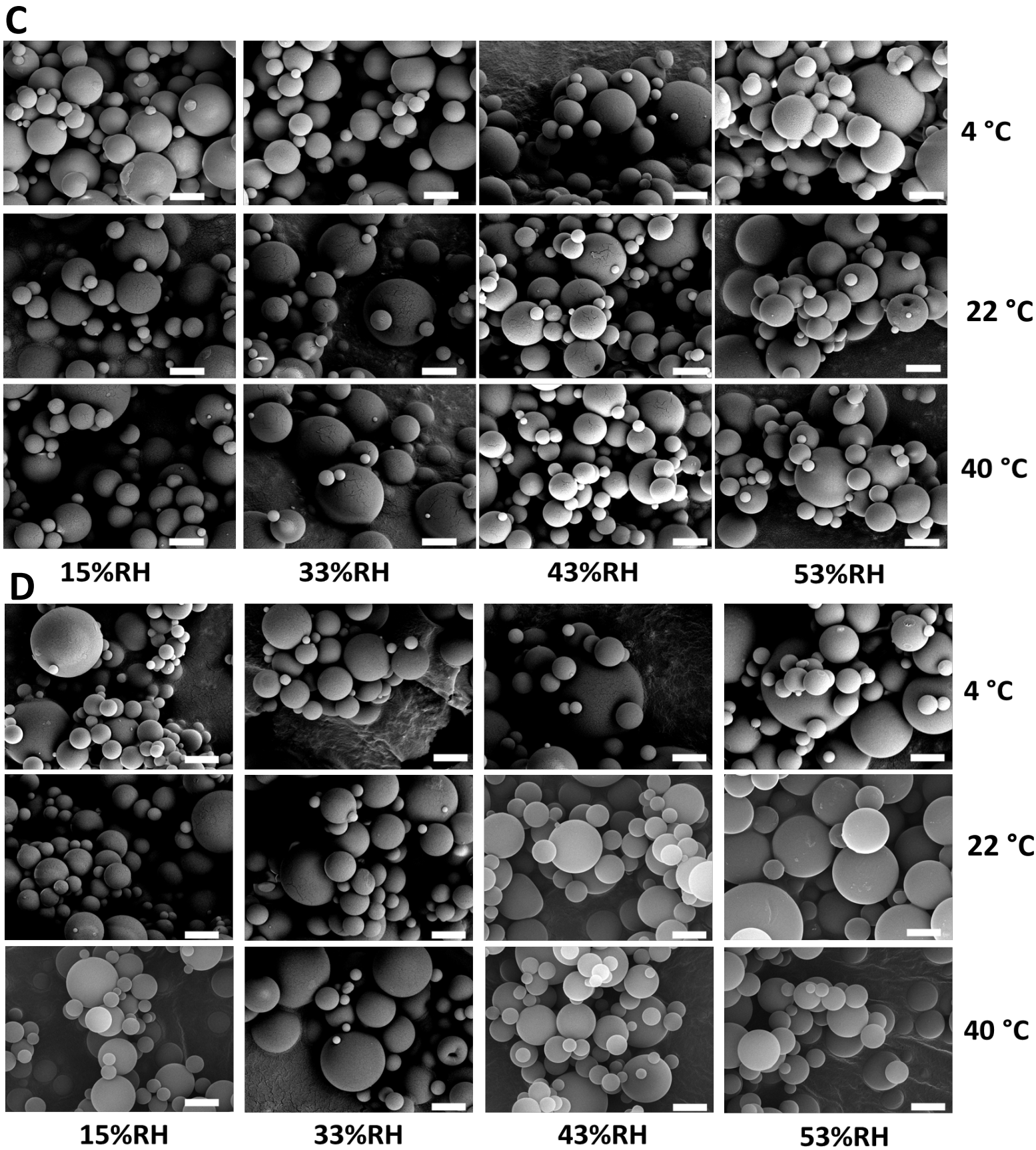


Figure 2. Scanning electron microscopy (SEM) images of spray-dried phage formulations with PVP K15 (A), PVP K25 (B), PVP K40 (C), and PVP K100 (D) after 7-day storage at various temperatures and relative humidities.

**DSC thermograms**

Differential scanning calorimetry following 7-day equilibration showed Tg variations with PVP molecular weight and storage humidity. Under dry conditions (4°C/15% RH), Tg values ranged from 124°C for PVP K15 to 171°C for PVP K100. At 33% RH, Tg decreased by approximately 40°C across all molecular weight grades. Further increase in humidity to 43% RH produced an additional 25-30°C depression.

This pattern was consistent across all storage temperatures (4- 40°C). At each temperature, PVP K100 maintained Tg values approximately 45°C higher than K15. Each 20% increase in relative humidity resulted in 30-50°C reduction in Tg across the molecular weight series.

Table 1. Tg of phage powders after 7 days under various storage conditions

| Excipient | Storage RH (%) | Tg at 4°C (°C) | Tg at 22°C (°C) | Tg at 40°C (°C) |
|---|---|---|---|---|
| PVP K15 | 15 | 128 ± 0.2 | 131 ± 0.6 | 147 ± 0.8 |
| | 33 | 88 ± 0.5 | 98 ± 0.2 | 109 ± 0.2 |
| | 43 | 58 ± 0.2 | N/A | N/A |
| | 53 | N/A | N/A | N/A |
| PVP K25 | 15 | 142 ± 0.2 | 164 ± 0.2 | 173 ± 0.7 |
| | 33 | 102 ± 0.1 | 112 ± 0.3 | 123 ± 0.2 |
| | 43 | 70 ± 0.2 | 82 ± 0.2 | N/A |
| | 53 | N/A | N/A | N/A |
| PVP K40 | 15 | 167 ± 0.2 | 176 ± 2.7 | 187 ± 0.2 |
| | 33 | 127 ± 0.7 | 136 ± 0.2 | 155 ± 0.8 |
| | 43 | 97 ± 0.2 | 103 ± 0.5 | N/A |
| | 53 | 47 ± 0.2 | N/A | N/A |
| PVP K120 | 15 | 175 ± 0.9 | 182 ± 0.8 | 192 ± 0.8 |
| | 33 | 135 ± 0.2 | 145 ± 0.2 | 160 ± 1.1 |
| | 43 | 106 ± 0.2 | 111 ± 0.2 | N/A |
| | 53 | 54 ± 0.3 | N/A | N/A |

N/A – not applicable

**Processing stability (immediately post spray-drying)**

Phage viability measurements immediately following spray-drying showed $log_{10}$ titre losses of 0.20 (K15), 0.45 (K25), 0.38 (K40), and 0.58 (K100) (Figure 3). All formulations retained viable phage concentrations with losses below 1 $log_{10}$.

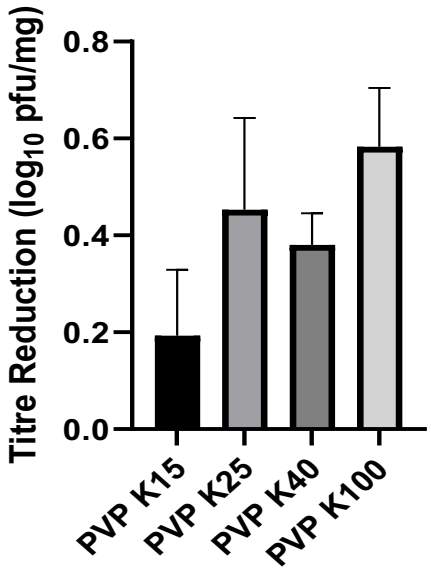


Figure 3. Titre loss of PEV1 after spray-drying process (n=3).

**Baseline stability following 7-day equilibration**

Phage titre losses following 7-day equilibration varied with storage temperature, relative humidity, and PVP molecular weight (Figure 4, Table 1). Under mild storage conditions (4°C and 22°C at 15% RH), all formulations-maintained titre losses below 1 $log_{10}$. At 40°C with 15% RH, K100 showed 0.95 $log_{10}$ loss while K15, K25, and K40 showed 2.1-2.23 $log_{10}$ losses.

At elevated humidity levels, titre losses increased substantially. At 33% RH and 4°C, titre losses ranged from 0.5 $log_{10}$ (K100) to 1.2-1.6 $log_{10}$ (K15-K40). At 40°C/33% RH, losses were 2.3 $log_{10}$ (K100) and up to 3.8 $log_{10}$ (K15).

At higher humidity conditions (43% and 53% RH), titre losses increased further. At 53% RH and 4°C, titre losses increased with decreasing molecular weight: 1.76 $\log_{10}$ (K100), 2.50 $\log_{10}$ (K40), 6.55 $\log_{10}$ (K25), and 9.45 $\log_{10}$ (K15). At 40°C with ≥43% RH, all formulations exceeded 9 $\log_{10}$ losses.

**Thermal offsets (ΔT) analysis**

Thermal offset ΔT and corresponding phage titre losses after 7-day equilibration are presented in Table 2 and Figure 5. Under dry conditions (15% RH), titre losses at high ΔT values were: 0.36 $\log_{10}$ at ΔT = 124°C (K15), 0.80 $\log_{10}$ at ΔT = 138°C (K25), 0.99-2.23 $\log_{10}$ at ΔT = 127-152°C (K40), and 0.49-0.95 $\log_{10}$ at ΔT = 102-171°C (K100).

At 33% RH, ΔT values decreased to 69-131°C with corresponding titre losses of 0.50-3.79 $\log_{10}$. K100 showed 0.50 $\log_{10}$ loss at ΔT = 131°C, while other grades showed 3.18-3.79 $\log_{10}$ losses at similar or higher ΔT values.

Table 2. Difference Between Tg - Ts of phage powders after 7 days under various storage conditions

| Excipient | Storage RH (%) | Tg – Ts at 4°C (°C) | Tg – Ts at 22°C (°C) | Tg – Ts at 40°C (°C) |
|---|---|---|---|---|
| PVP K15 | 15 | 124 | 109 | 107 |
| | 33 | 84 | 76 | 69 |
| | 43 | 54 | N/A | N/A |
| | 53 | N/A | N/A | N/A |
| PVP K25 | 15 | 138 | 142 | 133 |
| | 33 | 98 | 90 | 83 |
| | 43 | 66 | 60 | N/A |
| | 53 | N/A | N/A | N/A |
| PVP K40 | 15 | 163 | 154 | 147 |
| | 33 | 123 | 114 | 115 |
| | 43 | 93 | 81 | N/A |
| | 53 | 43 | N/A | N/A |
| PVP K120 | 15 | 171 | 160 | 152 |
| | 33 | 131 | 123 | 120 |
| | 43 | 102 | 89 | N/A |
| | 53 | 50 | N/A | N/A |

N/A – not applicable

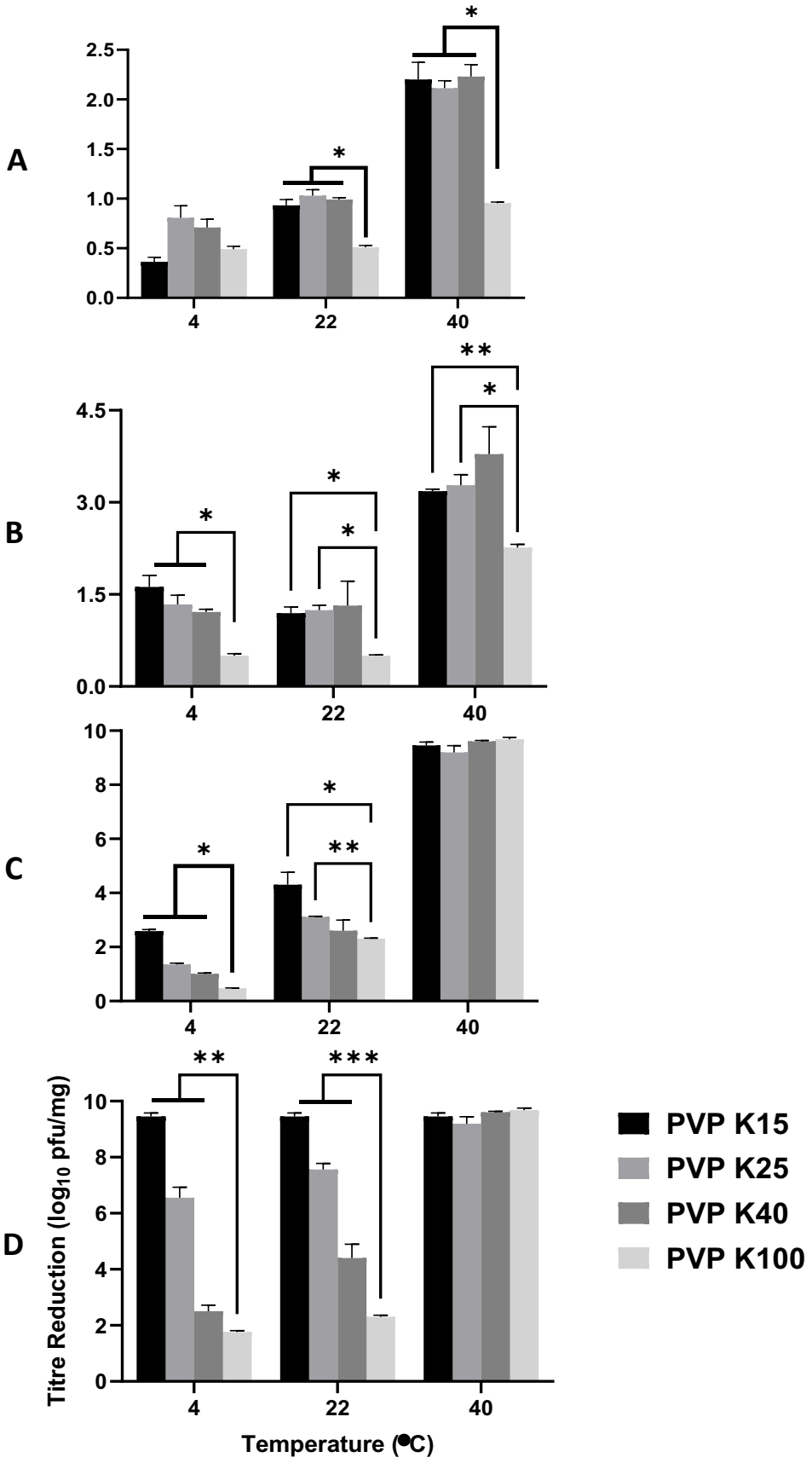


Figure 4. Titre loss of PEV1 powders with PVP K15, K25, K40, and K100 after 7-day storage at 4, 22, or 40°C and 15% RH (A), 33% RH (B), 43% RH (C), or 53% RH (D), presented as mean ± SD (n=3). Statistical significance was assessed using two-way ANOVA. *, $p < 0.05$; **, $p < 0.01$; ***, $p < 0.001$; n.s., not significant.

**Extended storage stability (180 Days)**

Extended storage stability varied with formulation and storage conditions (Figure 6).

For PVP K15, titres remained at ~$10^8$ pfu/mg at 4°C/15% and 33% RH after 180 days. At 4°C/43% RH, titres dropped from $2.9 \times 10^9$ to <1 pfu/mg. At 22°C/15% RH, titres decreased to $3.4 \times 10^6$ pfu/mg; at 22°C/33% RH, to $6.3 \times 10^5$ pfu/mg.

For PVP K25, titres remained at ~$10^8$ pfu/mg at 4°C and 22°C with 15% RH after 180 days. At 4°C/43% RH, titres fell to $4.0 \times 10^5$ pfu/mg by 90 days, then <1 pfu/mg by 180 days. At 4°C/53% RH, titres dropped to $2.1 \times 10^3$ pfu/mg after 30 days, then became undetectable.

For PVP K40, titres were ~$10^9$ pfu/mg at 4°C and 22°C with 15% RH, and ~$10^8$ pfu/mg at 33% RH after 180 days. At 4°C/43% RH, titres fell to $2.3 \times 10^6$ pfu/mg by 90 days, then <1 pfu/mg. At 4°C/53% RH, titres dropped to $2.5 \times 10^3$ pfu/mg by 90 days, then <1 pfu/mg. At 40°C/15% RH, titres fell to $2.4 \times 10^5$ pfu/mg after 30 days, then became undetectable.

For PVP K100, titres remained at ~$10^9$ pfu/mg after 30 days and ~$10^8$ pfu/mg after 180 days at 4°C/15%, 33% RH, and 22°C/15%, 33% RH. At 4°C/53% RH, titres decreased to $5.3 \times 10^5$ pfu/mg by 90 days, then 110 pfu/mg by 180 days. At 22°C/43% RH, titres fell to 1400 pfu/mg by 180 days. At 40°C/15% RH, titres dropped to $6.0 \times 10^5$ pfu/mg by 90 days, then <1 pfu/mg.

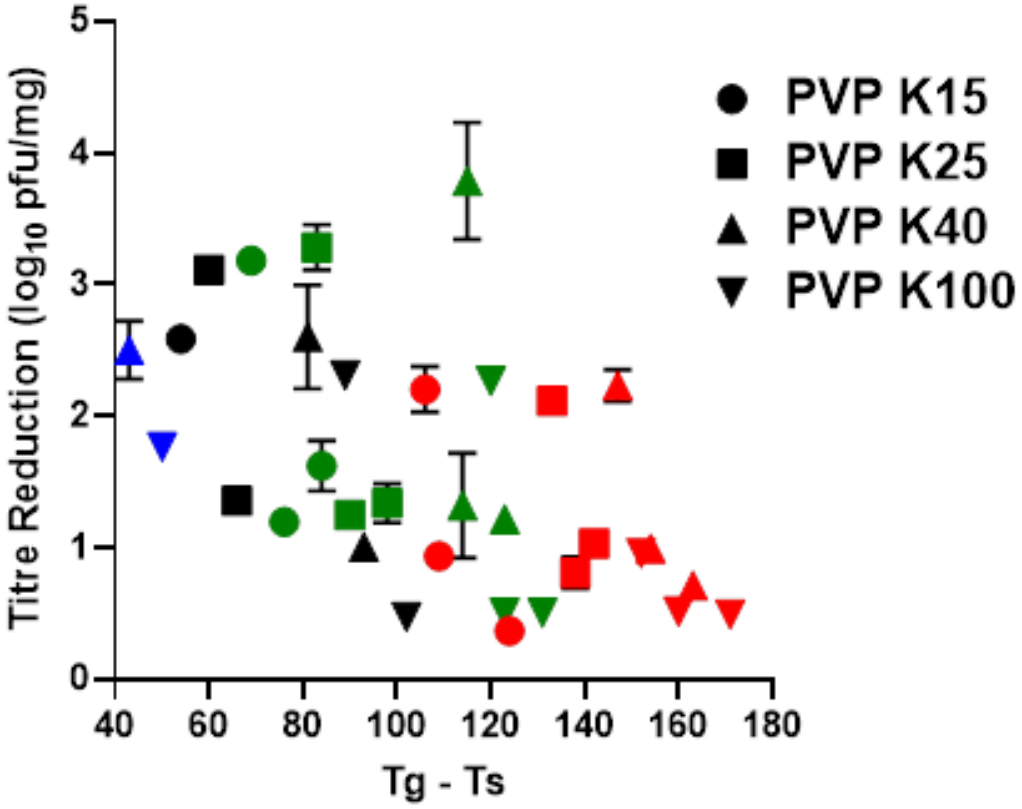


Figure 5. Scatterplot of glass transition temperature (Tg) minus storage temperature (Ts) versus $log_{10}$ titre loss of PEV1, with 15% RH (red), 33% RH (green), 43% RH (black), and 53% RH (blue).

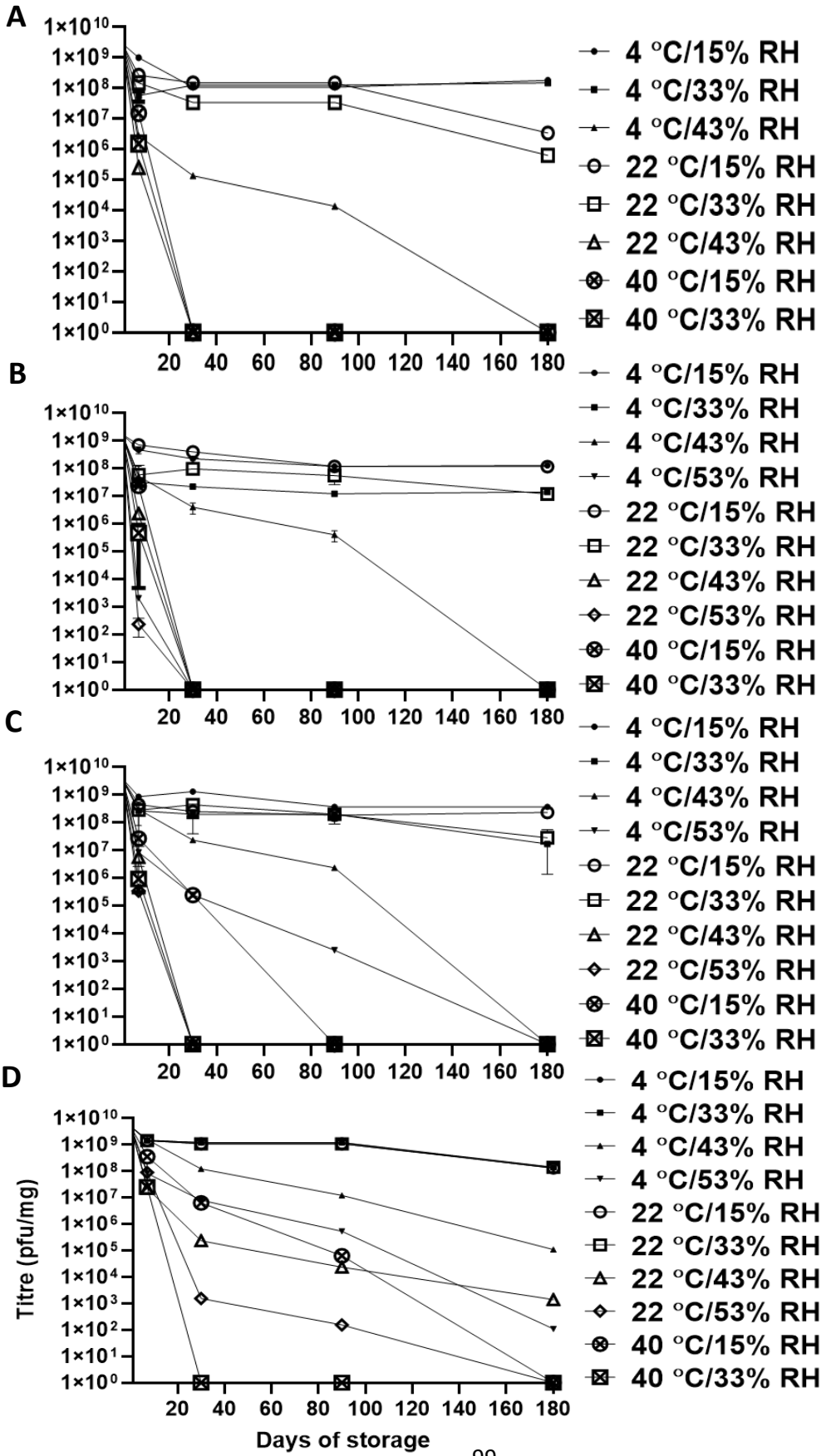




Figure 6. Titre of PEV1 powders with PVP K15 (A), PVP K25 (B), PVP K40 (C), and PVP K100 (D) after storage at various temperatures and relative humidities, presented as mean ± SD (n=3).

**Degradation kinetics analysis**

The Arrhenius equation was applied to describe the temperature-dependent degradation kinetics of phage formulations. The plots of ln k versus 1000/T for spray-dried PEV1 powders formulated with PVP grades K15, K25, K40 and K100 produced linear relationships across the 4 – 40 °C range at both 15 and 33 % RH (Fig. 7A–D). The goodness-of-fit coefficients ($R^2$ = 0.60–0.99) confirmed the suitability of an apparent first-order model. Figure 8 showed that increasing water activity from 0.15 to 0.33 produced only a modest change in the degradation constant (ln k ≤ –2.7 for all PVP formulations). However, elevating the water activity further to 0.43 elicited a marked rise, with ln k values approximating –1.1 for K15–K40 and –1.9 for K100. At *aw* 0.53 the degradation rate remained elevated, yielding ln k of –1.1 for K25–K40 and –1.6 for K100.

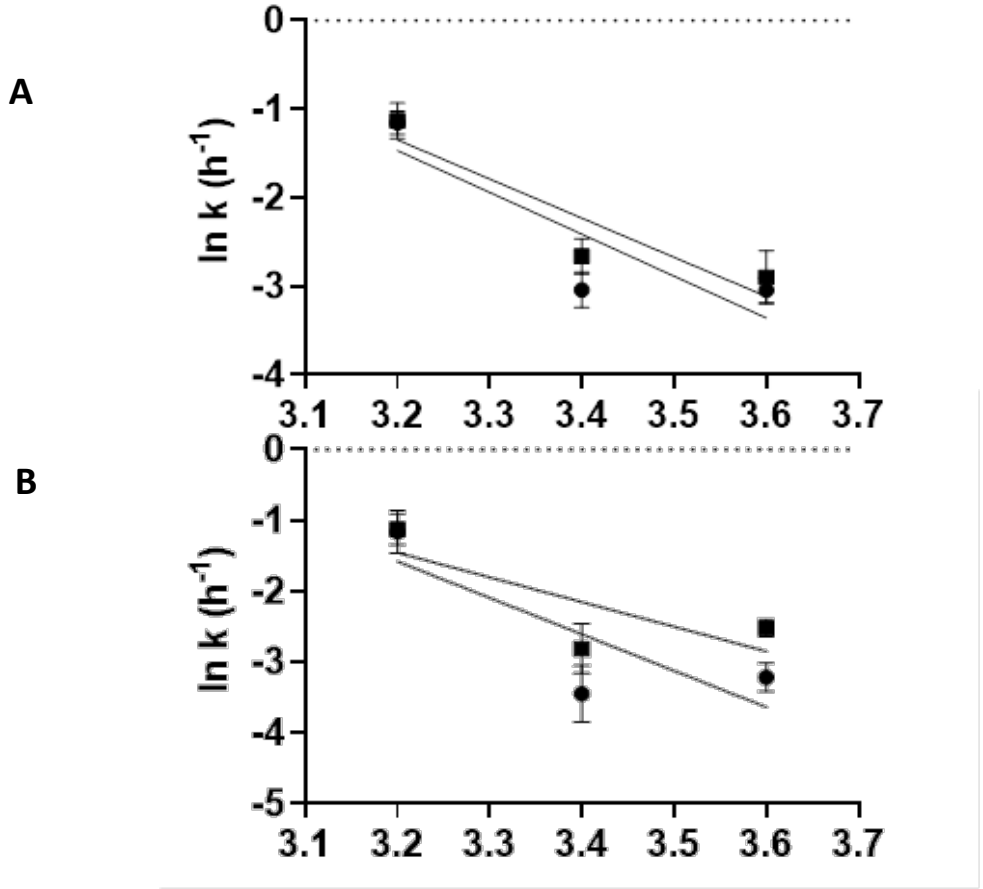

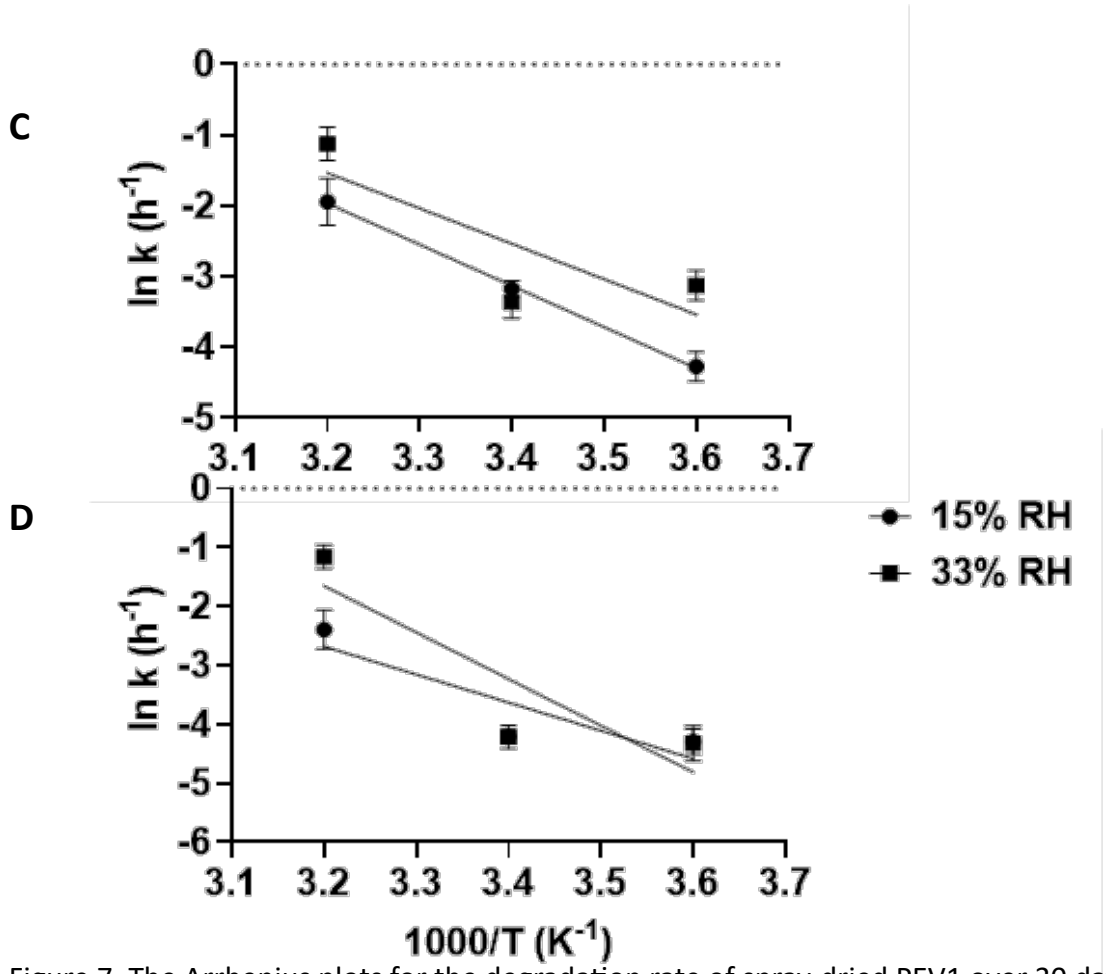


Figure 7. The Arrhenius plots for the degradation rate of spray-dried PEV1 over 30 days stored 15% and 33% RH for each formulation: PVP K15 (A), PVP K25 (B), PVP K40 (C), and

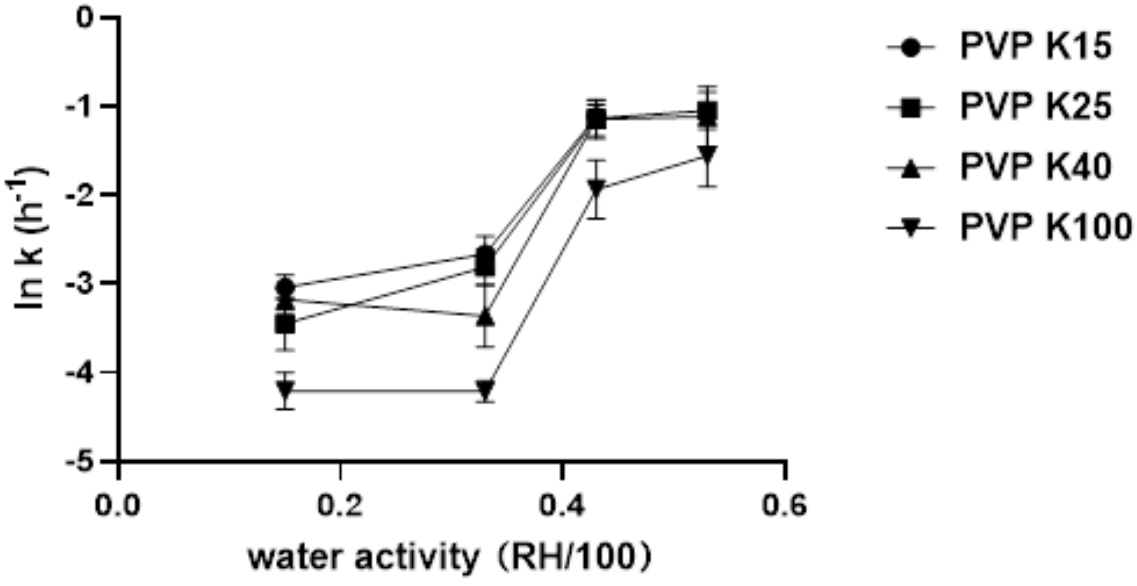


Figure 8. The effect of water activity on the degradation rate of spray-dried phage formulations at 22 °C.

## Discussion

In this study, we aimed to investigate PVP-based polymeric matrices for stabilization of spray-dried bacteriophage formulations, as a suitable alternative to conventional saccharide systems across various storage conditions. Building upon previous findings from Chang *et al* (2020), which demonstrated that having a ΔT of approximately 50°C using saccharide-based excipients maintained phage stability for up to 250 days under controlled conditions (164), we sought to evaluate whether polymer-based systems could offer enhanced storage stability, particularly under elevated humidity conditions that typically compromise saccharide formulations. Our systematic evaluation focused on glass transition temperature, humidity-dependent degradation kinetics, and the effects of polymer molecular weight (K15, K25, K40, K100) across storage temperatures ranging from 4°C to 40°C and RH values of 15% to 53% over a 180-day period. Our analysis revealed that while all PVP formulations achieved equivalent stability at 4-22°C and low (15%) RH, phage preservation under elevated humidity (33% RH) required substantially higher thermal offsets ($\Delta T \geqslant 100°C$), which is achievable only with the high-molecular-weight variants (K40, K100). These findings establish that PVP-based systems offer the distinct advantage of reduced cold-chain dependency at $aw \leqslant 0.33$, but to fully realize this potential would require the use of high molecular weight PVP in the formulation.

PVP has proven stabilizing properties for biologics in pharmaceutical formulations (168). During spray-drying, the process may impose the phages to thermal stresses, desiccation, and mechanical shear (67), particularly at the air-liquid interface where phages can undergo structural damage. PVP having both hydrophilic and hydrophobic components may counteract this by adsorbing at the interface, reducing surface tension, and preventing phage adsorption, thus protecting them within the droplet core (169). Additionally, PVP in the dry state could

stabilize phages through vitrification, forming a glassy matrix that limits molecular mobility and prevents capsid unfolding (170). Its ability to form hydrogen bonds with phage proteins could potentially compensate for water loss during drying, preserving structural integrity (171). In our study, all PVP variants effectively preserved PEV1 phage viability immediately posts spray-drying, with the titre losses all below 1 log10, ranging from 0.20 (K15) to 0.58 (K100) (Figure 3). The differences in titre losses between formulations, spanning less than 0.5 $\log_{10}$, are within the typical variability of plaque assays, indicating that these minor variations are not significant and do not suggest a meaningful trend among the PVP variants. These low losses demonstrate PVP's suitability as a stabilizer for phage formulations.

The thermal offset ΔT emerged as a decisive factor maintaining bacteriophage stability in dry formulations containing saccharides as an excipient. The identification of $\Delta T \geqslant 50°C$ as the critical threshold for stabilizing phage in these formulations represents the minimum thermal offset required to preserve the rigid glassy state that restricts degradative molecular processes (172). This threshold provides baseline protection through reduced molecular mobility as predicted by Adam-Gibbs theory, which establishes the fundamental relationship between cooperative motion and thermodynamic properties in glass-forming systems (172). Molecular relaxation processes become increasingly constrained as temperature decreases below Tg, which improves the likelihood for biological macromolecules to maintain their structural integrity (173). These findings align with established principles for stabilization of protein formulation, where maintaining storage temperature at least 50°C below Tg ensures adequate protection through reduced molecular mobility (174). In the present study, the short-term stability assessment after 7 days demonstrated that PVP formulations with ΔT significantly above 100 °C exhibited low titre losses, indicating effective preservation of phage bioactivity.

For instance, at 4°C and 15% RH, where ΔT ranged from 120°C to 167°C across PVP variants, losses were minimal, with values below 1 log10 for all formulations (Figure 4). Similarly, at 22°C and 15% RH, with ΔT between 87°C and 138°C, all variants-maintained losses below 1 $log_{10}$, confirming the protective capacity of the glassy state. However, the data revealed that ΔT alone does not fully account for stability differences observed across the PVP formulations. At elevated temperature storage conditions (40°C/15% RH), only K100 maintained titre reduction within 1 $log_{10}$ (0.95 $log_{10}$), while K15, K25, and K40 exhibited significantly higher losses (2.1-2.23 $log_{10}$; $p < 0.05$ for all comparisons) despite ΔT values having been maintained above the generally accepted critical threshold of 50°C for saccharide systems. This disparity indicates that additional factors beyond the bulk thermal properties may influence the local microenvironment surrounding individual phages in the PVP formulation.

Long-term storage stability is a critical consideration in the development of biopharmaceuticals for commercial application, as the need for frequent replenishment of phage products may lead to increased production and distribution costs. Formulations stored at conditions where ΔT was substantially above 50 °C, particularly at lower temperatures (4°C and 22°C) with low RH (15% and 33%), retained high phage titres, consistent with short-term (7 days) observations. For example, K100 at 4°C/15% RH (ΔT= 167°C) and 22°C/33% RH (ΔT= 101°C) maintained titres around 108 pfu/mg after 180 days, mirroring the low losses observed after 7 days (Figure 6). However, the long-term stability data also highlight limitations of relying solely on ΔT, particularly at elevated storage temperatures. At 40°C and 15% RH, despite a ΔT of 112°C for K100, phage titres dropped below 1 pfu/mg by 180 days, a stark contrast to the short-term loss of 0.95 log10 after 7 days (Figure 6). This suggests that temperature-dependent degradation processes, such as thermal denaturation of phage proteins, accelerate over time, even within a

glassy matrix. Studies on phage thermal stability indicate that some phages lose infectivity at temperatures above 40°C, even in stabilized forms, due to structural damage (175). Analysis of Arrhenius degradation kinetics across the 4-40°C temperature range demonstrated linear relationships for all PVP formulations over the initial 30 days, with goodness-of-fit coefficients ($R^2$ = 0.60-0.99) confirming the applicability of apparent first-order kinetics (Figure 7). This temperature dependence validates that phage inactivation follows predictable thermodynamic principles, allowing quantitative prediction of degradation rate under different environmental conditions (96, 112).

The impact of humidity on glass transition temperature is an important factor governing phage stability in the PVP formulations. DSC analysis revealed substantial Tg decreases with increasing humidity across all molecular weight PVP samples. Under the dry condition (15% RH) at 4°C, Tg values ranged from 124°C for PVP K15 to 171°C for PVP K100 (Table 1). At 33% RH, Tg was decreased by approximately 40°C in all PVP samples, while further humidity increased to 43% RH produced an additional 25-30°C depression (Table 1). Each 20% increase in relative humidity resulted in 30-50°C reduction in Tg across this PVP molecular weight series, demonstrating the pronounced plasticization effect of moisture on polymer matrices. High humidity posed challenges for long-term phage stability, even with a $\Delta T > 100$ °C. At 4° C and 53% RH, PVP K100 exhibited a titre reduction to 110 pfu/mg (~7 $\log_{10}$ loss) by 180 days, with an $\Delta T$ of ~80°C (Table 2 and Figure 6). Similarly, at 22°C and 43% RH (estimated $\Delta T \approx 70$ °C), titres dropped to 1400 pfu/mg (~6 $\log_{10}$ loss). The *aw* dependence of degradation kinetics provides mechanistic insight into humidity-mediated destabilization of phage formulations (114). Kinetic analysis (Figure 8) revealed that increasing *aw* from 0.15 to 0.33 produced only modest changes in the degradation constant ($\ln k \leqslant -2.7$ for all PVP

formulations), indicating that the glassy matrix maintains reasonable protective capacity under low to mild humidity conditions. However, a critical threshold emerges at *aw* 0.43, where the degradation kinetics was increased by an order-of-magnitude, as reflected by the ln k values of approximately of -1.1 for K15-K40 and -1.9 for K100 (Figure 8). At *aw* 0.53, the degradation rate remained elevated, yielding ln k values of -1.1 for K25-K40 and -1.6 for K100 (Figure 8). The increased *aw* likely plasticizes the polymeric matrix, enhancing molecular mobility of PVP and facilitating degradation of phages, as commonly observed in studies where water acts as a plasticizer in amorphous solids of small molecule drugs and biologics (104, 176).

Polymeric molecular weight impacts Tg and, consequently, bacteriophage stability in formulations. Our results demonstrated a clear correlation between increasing molecular weight of PVP and higher Tg values (Table 1), due to enhanced polymer chain entanglement and reduced molecular mobility (172, 177). The elevated Tg associated with higher molecular weight PVPs translated directly into improved bacteriophage stability. At 53% RH and 4°C, titre losses increased significantly with decreasing molecular weight after 7-day storage: 1.76 $\log_{10}$ (K100), 2.50 $\log_{10}$ (K40), 6.55 $\log_{10}$ (K25), and 9.45 $\log_{10}$ (K15) ($p < 0.01$) (Figure 4). At 40°C and 15% RH, PVP K100, with a ΔT of 112°C, showed a loss of 0.95 log10, compared with > 2 log10 in K15, K25, and K40, indicating that higher molecular weight PVPs enhance stability even at elevated temperatures (Table 2 and Figure 4). PVP K100 maintained titres of approximately $10^9$ pfu/mg at 4°C and 22°C with 15% and 33% RH after 180 days (Figure 6). At the more humid conditions of 53% RH at 4°C, a detectable titre (110 pfu/mg) after 180 days was still retained in the K100 sample, but not in the lower molecular weight PVP (K15, K25, K40). We proposed that in the higher molecular weight K100, extended polymer chains provide more extensive hydrogen bonding opportunities with phage surface proteins, creating

stabilizing networks of intermolecular interactions that facilitate maintenance of protein tertiary structure (171). Higher molecular weight PVP matrices exhibit increased entanglement density, which generates more tortuous diffusion pathways (178). This structural complexity acts as a barrier to the ingress of mobile species such as water molecules, thereby offering enhanced protection against moisture-induced degradation and preserving phage integrity (178).

In the earlier study by Chang *et al* on lactose-based powders (164), phages remained stable for 250 days at 5 °C/15% RH with negligible titre loss (<1 $\log_{10}$), but showed ~3 $\log_{10}$ titre reductions at 33% RH as water uptake plasticized the matrix (lowering Tg by ~30 °C and shrinking the ΔT margin to ~19–28 °C). This insufficient ΔT led to increased molecular mobility and phage inactivation, indicating a threshold ΔT > 50 °C is required for stability of phages in the lactose-leucine system. The PVP-based formulations exhibited a comparable short-term stability (7 days) under a range of temperatures, and over 180 days they too upheld phage viability when stored under conditions that maintained a large ΔT gap (on the order of tens of degrees). PVP's inherently high Tg (in dry state) afforded a generous initial ΔT, but its hygroscopic nature meant that ambient humidity could markedly depress Tg and soften the amorphous matrix, mirroring the destabilizing effect of moisture seen in the lactose–leucine system. Mechanistically, the disaccharide lactose provides numerous hydroxyl groups for hydrogen bonding to phage capsid proteins (water-replacement) and creates a rigid amorphous glass, while leucine's crystalline phase at particle surfaces limits water absorption and preserves matrix integrity (28). By contrast, PVP (a non-reducing, non-saccharide polymer) stabilizes phages primarily via the vitrification mechanism, entrapping phages in a high-Tg glassy matrix; this can be effective for immobilization but also necessitates appropriate

polymer molecular weight and moisture control, as improper formulation with polymers has previously led to phage inactivation (63, 84). Building on this, our results demonstrate that higher molecular-weight PVPs are more effective at maintaining phage viability, as they form more rigid matrices with elevated Tg and reduced susceptibility to moisture-induced destabilization.

This study provides valuable insights into phage stabilization but has several limitations that warrant further investigation. First, the findings are specific to PEV1 phages, and generalizability to other phage types is uncertain due to variations in structure and stability requirements. Testing a broader range of phages would clarify whether higher molecular weight PVPs universally enhance stability. Second, while the 180-day study is substantial, pharmaceutical products often require multi-year shelf lives; longer-term studies (e.g., 1–2 years) are needed to assess clinical suitability. Third, anomalies in stability data, such as the high titre loss in PVP K40 at 22°C/33% RH despite $\Delta T = 115°C$, suggest unidentified factors influencing stability, possibly phage-polymer interactions or moisture-induced degradation pathways. Furthermore, the similar Tg values observed among different PVP molecular weights under certain humidity conditions may limit the ability to distinguish polymer-specific stabilization effects, warranting investigation of excipients with more distinct thermal properties. Additionally, this study did not include dynamic vapor sorption (DVS) or thermogravimetric analysis (TGA) to characterize the hygroscopicity of PVP-based formulations. Further investigation is warranted to understand how variations in ambient humidity and water content influence the moisture uptake behaviour of PVP and its impact on phage formulation stability. Finally, even when formulations met the $\Delta T > 100\,°C$ criterion, phage viability deteriorated under the most extreme condition tested (40 °C/43–53 % RH),

indicating that additional thermal effect—beyond bulk glass transition effects—contribute to instability at high temperature-humidity stress. Future research should address these limitations by testing diverse phages, conducting extended stability studies, investigating anomalies to optimize phage powder formulations.

## Conclusions

This study presents the first systematic investigation of PVP-based polymer matrices for bacteriophage stabilization, establishing novel formulation principles distinct from saccharide-based systems. All PVP formulations preserved phage viability within 1 $\log_{10}$ loss over 180 days at 4–22 °C and 15% RH. At higher humidity (33% RH), long-term stability was successfully achieved at ambient temperatures ($\leqslant$ 22°C) using high-molecular-weight PVPs (K40, K100), which provided the necessary thermal offsets ($\Delta T \geq 100$ °C) to maintain a protective glassy state. These findings introduce humidity-tolerant design parameters for phage formulation in PVP that allow long-term phage stability storage and reducing cold-chain dependency.

**Acknowledgements**

Authors do not have any conflict of interest to declare.

## References


1. Chang, R.Y.K., et al., *Inhalable bacteriophage powders: Glass transition temperature and bioactivity stabilization.* Bioengineering & Translational Medicine, 2020. **5**(2): p. e10159.
2. Leung, S.S., et al., *Production of inhalation phage powders using spray freeze drying and spray drying techniques for treatment of respiratory infections.* Pharmaceutical research, 2016. **33**(6): p. 1486-1496.
3. Li, M., Y. Cao, and H.K. Chan, *Optimizing Performance of Inhalable Bacteriophage Powders using Human Serum Albumin (HSA).* Int J Pharm, 2025. **678**: p. 125709.
4. Lin, Y., et al., *Synergistic activity of phage PEV20-ciprofloxacin combination powder formulation-A proof-of-principle study in a P. aeruginosa lung infection model.* Eur J Pharm Biopharm, 2021. **158**: p. 166-171.
5. Li, M., et al., *Phage cocktail powder for Pseudomonas aeruginosa respiratory infections.* Int J Pharm, 2021. **596**: p. 120200.
6. Chang, R.Y., et al., *Production of highly stable spray dried phage formulations for treatment of Pseudomonas aeruginosa lung infection.* Eur J Pharm Biopharm, 2017. **121**: p. 1-13.
7. Wang, Y., et al., *Bacteriophage endolysin powders for inhaled delivery against pulmonary infections.* Int J Pharm, 2023. **635**: p. 122679.
8. Luo, Y., et al., *Multifunctional Role of Polyvinylpyrrolidone in Pharmaceutical Formulations.* AAPS PharmSciTech, 2021. **22**(1): p. 34.
9. Lehmkemper, K., et al., *Long-Term Physical Stability of PVP- and PVPVA-Amorphous Solid Dispersions.* Mol Pharm, 2017. **14**(1): p. 157-171.
10. Chang, L.L. and M.J. Pikal, *Mechanisms of protein stabilization in the solid state.* J Pharm Sci, 2009. **98**(9): p. 2886-908.
11. Grasmeijer, N., et al., *Unraveling protein stabilization mechanisms: vitrification and water replacement in a glass transition temperature controlled system.* Biochim Biophys Acta, 2013. **1834**(4): p. 763-9.
12. Allison, S.D., et al., *Hydrogen bonding between sugar and protein is responsible for inhibition of dehydration-induced protein unfolding.* Archives of Biochemistry and Biophysics, 1999. **365**(2): p. 289-298.
13. Izutsu, K.-i., S. Yoshioka, and T. Terao, *Decreased protein-stabilizing effects of cryoprotectants due to crystallization.* Pharmaceutical research, 1993. **10**: p. 1232-1237.
14. Pyne, A., K. Chatterjee, and R. Suryanarayanan, *Solute crystallization in mannitol-glycine systems--implications on protein stabilization in freeze-dried formulations.* J Pharm Sci, 2003. **92**(11): p. 2272-83.
15. Roughton, B.C., E.M. Topp, and K.V. Camarda, *Use of glass transitions in carbohydrate excipient design for lyophilized protein formulations.* Comput Chem Eng, 2012. **36**(10).
16. Chang, B.S., et al., *Physical factors affecting the storage stability of freeze-dried interleukin-1 receptor antagonist: glass transition and protein conformation.* Arch Biochem Biophys, 1996. **331**(2): p. 249-58.
17. Hancock, B.C. and G. Zografi, *The relationship between the glass transition temperature and the water content of amorphous pharmaceutical solids.* Pharmaceutical research, 1994. **11**: p. 471-477.
18. Rao, Q., A. Klaassen Kamdar, and T.P. Labuza, *Storage Stability of Food Protein Hydrolysates-A Review.* Crit Rev Food Sci Nutr, 2016. **56**(7): p. 1169-92.
19. Haq, I.U., et al., *Bacteriophages and their implications on future biotechnology: a review.* Virol J, 2012. **9**: p. 9.

20. Vandenheuvel, D., et al., *Instability of bacteriophages in spray-dried trehalose powders is caused by crystallization of the matrix.* Int J Pharm, 2014. **472**(1-2): p. 202-5.
21. Zeng, X.M., G.P. Martin, and C. Marriott, *Effects of molecular weight of polyvinylpyrrolidone on the glass transition and crystallization of co-lyophilized sucrose.* Int J Pharm, 2001. **218**(1-2): p. 63-73.
22. Yuan, X., et al., *Hydrogen Bonding Interactions in Amorphous Indomethacin and Its Amorphous Solid Dispersions with Poly(vinylpyrrolidone) and Poly(vinylpyrrolidone-co-vinyl acetate) Studied Using (13)C Solid-State NMR.* Mol Pharm, 2015. **12**(12): p. 4518-28.
23. Guideline, I., *Stability testing of new drug substances and products.* Q1A (R2), current step, 2003. **4**(1-24).
24. Mikayilov, E., et al., *Exploring the Role of Poly (N-vinyl pyrrolidone) in Drug Delivery.* Chemical and Biochemical Engineering Quarterly, 2024. **38**(3): p. 185-196.
25. Leung, S.S., et al., *Production of Inhalation Phage Powders Using Spray Freeze Drying and Spray Drying Techniques for Treatment of Respiratory Infections.* Pharm Res, 2016. **33**(6): p. 1486-96.
26. Águila-Hernández, J., A. Trejo, and B.E. García-Flores, *Volumetric and surface tension behavior of aqueous solutions of polyvinylpyrrolidone in the range (288 to 303) K.* Journal of Chemical & Engineering Data, 2011. **56**(5): p. 2371-2378.
27. Wdowiak, M., J. Paczesny, and S. Raza, *Enhancing the stability of bacteriophages using physical, chemical, and nano-based approaches: A review.* Pharmaceutics, 2022. **14**(9): p. 1936.
28. Sivasankaran, R.P., et al., *Polymer-mediated protein/peptide therapeutic stabilization: current progress and future directions.* Progress in Polymer Science, 2024: p. 101867.
29. Asgreen, C., et al., *Influence of the Polymer Glass Transition Temperature and Molecular Weight on Drug Amorphization Kinetics Using Ball Milling.* Pharmaceutics, 2020. **12**(6).
30. Cangialosi, D., A. Alegria, and J. Colmenero, *Route to calculate the length scale for the glass transition in polymers.* Phys Rev E Stat Nonlin Soft Matter Phys, 2007. **76**(1 Pt 1): p. 011514.
31. Patel, N.G., S. Banella, and A.T.M. Serajuddin, *Moisture Sorption by Polymeric Excipients Commonly Used in Amorphous Solid Dispersions and its Effect on Glass Transition Temperature: II. Cellulosic Polymers.* J Pharm Sci, 2022. **111**(11): p. 3114-3129.
32. Gonzalez-Menendez, E., et al., *Comparative analysis of different preservation techniques for the storage of Staphylococcus phages aimed for the industrial development of phage-based antimicrobial products.* PLoS One, 2018. **13**(10): p. e0205728.
33. Fu, M., et al., *Pharmaceutical solid-state kinetic stability investigation by using moisture-modified Arrhenius equation and JMP statistical software.* J Pharm Biomed Anal, 2015. **107**: p. 370-7.
34. Fan, Z. and L. Zhang, *One- and two-stage Arrhenius models for pharmaceutical shelf life prediction.* J Biopharm Stat, 2015. **25**(2): p. 307-16.
35. Airaksinen, S., et al., *Role of water in the physical stability of solid dosage formulations.* Journal of pharmaceutical sciences, 2005. **94**(10): p. 2147-2165.
36. Fitzpatrick, S., et al., *Effect of moisture on polyvinylpyrrolidone in accelerated stability testing.* Int J Pharm, 2002. **246**(1-2): p. 143-51.
37. Turner, D. and A. Schwartz, *The glass transition temperature of poly (N-vinyl pyrrolidone) by differential scanning calorimetry.* Polymer, 1985. **26**(5): p. 757-762.
38. Reimschuessel, H., *On the glass transition temperature of comblike polymers: Effects of side chain length and backbone chain structure.* Journal of Polymer Science: Polymer Chemistry Edition, 1979. **17**(8): p. 2447-2457.
39. Zhang, Y., H. Zhang, and D. Ghosh, *The Stabilizing Excipients in Dry State Therapeutic Phage Formulations.* AAPS PharmSciTech, 2020. **21**(4): p. 133.

40. Merabishvili, M., et al., *Stability of Staphylococcus aureus phage ISP after freeze-drying (lyophilization).* PLoS One, 2013. **8**(7): p. e68797.

# Chapter 4

# Long-term Storage Stability of Inhalable Phage Powder Formulations: A Four-Year Study

This chapter has been accepted in Journal of the American Association of Pharmaceutical Scientists, with the title 'Long-term Storage Stability of Inhalable Phage Powder Formulations: A Four-Year Study'. Authors: Mengyu Li, Wei-Ren Keb, Rachel Yoon Kyung Chang, Hak-Kim Chan.

## Introduction

Pulmonary infections pose a significant global health threat, particularly affecting individuals with chronic respiratory diseases such as cystic fibrosis (CF). These infections are often caused by pathogens like *Pseudomonas aeruginosa*, leading to extensive inflammation, lung damage, and increased mortality. The presence of multidrug-resistant (MDR) bacteria further complicates treatment due to their intrinsic and acquired resistance mechanisms against various antibiotics, contributing to higher mortality and complication rates (179). The World Health Organization reports that bacterial resistance is outpacing the development of new antibiotics, underscoring the urgent need for alternative therapies (180). Bacteriophage (phage) therapy has re-emerged as a promising option, showing success in treating respiratory infections where antibiotics have failed (181). This therapy exploits the lytic cycle of phages, where phages specifically infect bacterial cells, replicate, and cause bacteriolysis, releasing progeny that continue to target nearby bacteria (182). This approach offers advantages over conventional antibiotics, including natural antibacterial activity, self-amplification in the host, and high specificity that minimizes harm to non-target microbiota (183, 184). The efficacy of phages against MDR bacteria has been confirmed in *in vitro* studies (185), as well as in animal and human models (186, 187). Recent studies have highlighted the ability of phages to reduce bacterial load and inflammatory responses in infection models, particularly in cases of *Pseudomonas aeruginosa* lung infections (182). Additionally, phages exhibit an intrinsic capability to penetrate and disrupt bacterial biofilms, further enhancing their therapeutic potential (188). Importantly, phages can naturally adapt to bacterial resistance, making them a versatile tool for managing persistent infections. These unique properties position phages as a promising alternative in addressing the growing challenge of antibiotic resistance.

Significant efforts have been dedicated to developing inhalation phage formulations for the treatment of respiratory infections, with a focus on ensuring the viability of phages during production and delivery (189, 190). Nebulization has been used for delivering liquid phage formulations to the lower airways. Recent studies have shown that phages can remain viable throughout the nebulization process (191). However, nebulized liquid formulations often encounter challenges such as limited shelf-life and biologics stability, depending on both the phages and solvent types (192-194), thus requiring cold chain during transport and storage. To address these issues, inhalable phage powder formulations have been developed, offering longer shelf-life and greater stability under various storage conditions (195). Studies have demonstrated that spray-dried phage powders retain their viability more effectively than liquid formulations, even after extended storage periods (88). Sugars, such as lactose and trehalose, are often employed as stabilizers to protect phages from thermal, drying, and shear stresses during spray drying (196). Vandenheuvel et al. evaluated the impact of adding dextran, lactose, and trehalose on phage titer reduction during the spray drying of two phages (LUZ19 and Romulus) and identified trehalose as an effective stabilizer (197). However, high humidity (54% RH) caused the recrystallization of the spray-dried trehalose matrix, deteriorating the viability of the embedded phages (198). Leung et al. explored a formulation combining trehalose, mannitol, and leucine at varying concentrations to stabilize two *Pseudomonas* phages (PEV2 and PEV40). They revealed that phages in spray-dried powder comprising 80% trehalose and 20% leucine remained viable at 4°C with 0% and 22% RH for 12 months, with a titer reduction of approximately 0.5 $\log_{10}$ (199).

Our group previously identified key excipients necessary for the biological and physical stabilization and aerosolization of spray-dried PEV phage powders (PEV1, PEV20, and

PEV61). Eight formulations containing lactose and leucine successfully preserved phage viability in spray-dried powders, achieving low titer loss (< 1 $\log_{10}$) and a fine particle fraction (FPF) exceeding 50%. Compared to trehalose, lactose revealed better protective effects for phages. Additionally, the use of lactose, an FDA-approved excipient for inhalation products, enhances the commercial viability of these inhalable phage formulations (115). After formulation development, we conducted a one-year stability test by storing the powders at 20°C and 15% RH. Overall, for PEV20 and PEV61, formulations with lower lactose content exhibited greater reductions in phage titer. However, even in the most affected formulation (PEV61 with 55% lactose and 45% leucine) in terms of titer loss, the titer and FPF reduction was only around 1.8 $\log_{10}$ and 5%, respectively. This demonstrates encouraging one-year stability results of the phage formulations in both biological activity and aerosol performance (200).

Given the critical importance of establishing clear performance benchmarks for inhalable phage therapeutics, we propose quality target product profile (QTPP) criteria based on the unique characteristics of phage therapy. For biological activity, we consider an acceptable titre loss of ≤ 2 $\log_{10}$ reduction over 24 months storage as appropriate for phage therapeutics, with final titers maintained at $\geq 10^7$pfu to ensure therapeutic efficacy. This criterion is based on our previous in *vivo* studies which demonstrated therapeutic efficacy with initial doses as low as $10^7$ pfu/mouse, with phage auto-amplification compensating for reduced initial titre during treatment (201). Regarding aerosol performance, the formulations should achieve a fine particle fraction (FPF) of ≥30%, which is comparable to commercial DPI products currently available (202). The volume median diameter should remain between 1-5 μm for optimal lung deposition, with a geometric standard deviation of ≤3.0 to ensure consistent delivery across

doses (203). For physical stability parameters, the powders should maintain moisture content ≤5% w/w and exhibit a glass transition temperature ≥50°C above the intended storage temperature (164). Additionally, formulations should show no visible crystallization or agglomeration during the storage period (204, 205). These criteria reflect the unique self-amplifying nature of phage therapeutics, distinguishing them from conventional dose-dependent drugs where linear dose-response relationships apply (206).

The initial success in preserving phage viability and maintaining aerosol performance led us to further explore the longer term stability of these formulations. The objective of the present study was to evaluate the stability over four years, including biological and physicochemical aspects, of eight phage formulations stored under controlled conditions of 20°C/15% RH and 4°C/15% RH. This is the first study which explored storage stability of phage powder formulations over such an extended period.

## Methods and materials

### Materials

Three bacteriophages targeting *Pseudomonas*, namely PEV1, PEV20, and PEV61, were *myovirus* sourced from a wastewater treatment facility in Olympia, Washington, USA, by the Kutter laboratory (Evergreen Phage Lab). These phages were preserved at a concentration of $10^{10}$ pfu/ml in phosphate-buffered saline (PBS) composed of 0.01M phosphate buffer, 0.0027M potassium chloride, and 0.137M sodium chloride, with the pH adjusted to 7.4. The *Pseudomonas aeruginosa* strain PAV237 was used for the propagation of these phages. The composition of eight different formulations developed in this study is detailed in Table 1.

### Phage powder preparation

Phage powders were produced via spray drying, following the methods outlined in our prior research (115). The process began with preparing a liquid feed comprising 198 mL of an excipient solution (25 mg/mL) in ultra-pure water, combined with 2 mL of a phage suspension at a concentration of $10^{10}$ pfu/mL. Based on a solid yield of 4.95 g per batch and an input of $2 \times 10^{10}$ pfu, the resultant powder contained $4.0 \times 10^{6}$ pfu/mg. Phage viability within the phage-excipient solution was assessed using a plaque assay. The solutions were then processed using a Büchi 290 spray dryer (Büchi Labortechnik AG, Flawil, Switzerland), which employs a conventional two-fluid nozzle for atomization in an open-loop configuration. The spray drying conditions were set as follows: an aspiration rate of 35 $m^3$/h, a feed rate of 2 mL/min, atomizing airflow at 742 L/h, an inlet temperature of 60 °C, and an outlet temperature ranging between 40-41 °C. Following drying, the powders were placed into scintillation vials, sealed within aluminum pouches, followed by stored either at 4 °C / 15% RH or 20 °C / 15% RH for four years.

Table 1. Spray-dried phage formulation compositions

| Formulation name | Phage | Contents % (w/w) | |
|---|---|---|---|
| | | Lactose | Leucine |
| PEV20 80%LT 20%LC | PEV20 | 80 | 20 |
| PEV20 70%LT 30%LC | PEV20 | 70 | 30 |

| | | | |
|---|---|---|---|
| PEV20 55%LT 45%LC | PEV20 | 55 | 45 |
| PEV1 70%LT 30% LC | PEV1 | 70 | 30 |
| PEV61 90%LT 10%LC | PEV61 | 90 | 10 |
| PEV61 80%LT 20%LC | PEV61 | 80 | 20 |
| PEV61 70%LT 30%LC | PEV61 | 70 | 30 |
| PEV61 55%LT 45%LC | PEV61 | 55 | 45 |

**Plaque assay**

The viability of the phages was assessed using a plaque assay method described previously (115). In brief, nutrient agar plates were first overlaid with soft agar that had been mixed with 200 µL of an overnight culture of *P. aeruginosa* strain PAV237, which is particularly suitable for counting the phages PEV1, PEV20, and PEV61. For each type of phage, 10 µL of serially diluted samples were applied to the designated soft agar surface, allowed to air dry, and then incubated at 37 °C for 24 hours before the number of plaques was quantified. Only plates with 30-300 plaques were counted for statistical reliability. Phage titers were calculated as plaque-forming units per milliliter (pfu/mL) using the formula: titer = (number of plaques × dilution

factor × 100)/volume plated (μL). For powder formulations, titers were also expressed as plaque-forming units per milligram of powder (pfu/mg) based on the reconstitution volume and powder mass. Each sample was assayed in triplicate, and results were expressed as mean ± standard deviation with a detection limit of $10^2$ pfu/mL.

Based on our laboratory validation, the method demonstrated intra-assay precision of RSD ≤12% (n=3 replicates), inter-assay precision of RSD ≤18% (3 separate days), and linear range of $10^2$-$10^9$ pfu/mL.

Based on this precision profile and established microbiological guidelines (207), we consider changes >0.5 $\log_{10}$ as statistically significant (28), accounting for inherent method variability while detecting meaningful biological changes. This threshold ensures that reported stability changes reflect true formulation performance rather than analytical noise.

**Particle morphology**

The morphology of the spray-dried powders was analyzed using scanning electron microscopy (SEM, Zeiss Ultra Plus HD, Oberkochen, Germany). Samples were affixed to carbon tapes and sputter-coated with a 15 nm layer of gold using a K550X sputter coater (Quorum Emitech, Kent, UK) prior to imaging.

**Particle size distribution**

The particle size distribution of the phage powders was determined using laser diffraction (Mastersizer 2000, Malvern Instruments Ltd., UK). For analysis, the powders were introduced into a Scirocco 2000 dry powder module (Malvern Instruments, UK) and dispersed across the measurement window using compressed air at 4.0 bar. The size distribution was presented as

volumetric diameters ($D_{10}$, $D_{50}$, and $D_{90}$) along with the span, calculated as $(D_{90}-D_{10})/D_{50}$. All measurements were conducted in triplicate.

**Differential scanning calorimetry**

Each of the samples (5 ± 1 mg) was enclosed in a perforated-lid aluminum crucible and analyzed using differential scanning calorimetry (DSC, Mettler Toledo, Greifensee, Switzerland). The sample was heated from 22 to 150 °C at 10 °C/min under nitrogen flow. The measurements were performed twice.

**Powder dispersion**

The aerosol performance of each phage powder was assessed using a multi-stage liquid impinger (MSLI) connected to a mouthpiece adapter and a USP throat. A powder dose (25 ± 5 mg) in a size 3 hydroxypropyl methylcellulose capsule was aerosolized using an Osmohaler™. The MSLI test, performed at a flow rate of 100 L/min over 2.4 seconds, utilized stage cut-off diameters of 13, 6.8, 3.1, 1.7 and <1.7 μm, and a filter. Powder deposited on each of the MSLI stages was dissolved in ultra-pure water for analysis by high-performance liquid chromatography (HPLC). The fine particle fraction (FPF), defined as the mass of particles ≤ 5.0 μm relative to the initial loaded dose, was interpolated from cumulative fraction plots versus MSLI cut-off diameters, adhering to British Pharmacopeia standards. All tests were conducted in triplicate.

**High-performance liquid chromatography**

The deposition of lactose across the inhaler, capsule, adaptor, throat, and each MSLI component was analyzed using a HPLC system equipped with refractive index detection (Model LC-20; Shimadzu, Japan). For the analysis, 50 μL of the samples were filtered and

introduced into a dual ion-exchange and ligand-exchange column (Agilent Hi-Plex Ca column, 7.7 × 50 mm, 8 µm; Agilent Technologies), which was maintained at 75 °C. The mobile phase, consisting of ultrapure water, was flowed at 0.6 ml/min.

## Results

### Phage stability

Phage viability declined over four years, with titer reduction ranging from 0.97 to 2.49 $\log_{10}$ (Figure 1). PEV61 phage powder containing 90% lactose remained biologically stable with no further titer loss at 12 months and maintained stability within a 1.5 $\log_{10}$ titer loss after 48 months. On the other hand, powders containing 80% and 70% lactose experienced titer losses of 1.5 and 2.0 $\log_{10}$, respectively, after 48 months. Phage powder with 55% lactose showed a titer loss of 2.5 $\log_{10}$ after 48 months. Similar trends were observed for phages PEV1 and PEV20. PEV1 powder containing 70% lactose showed a 2.0 $\log_{10}$ titer loss across both storage temperatures, while PEV20 powder containing 55% lactose showed a titer loss of 2.5 $\log_{10}$. No significant difference in titer reduction was observed across storage temperatures or phage families.

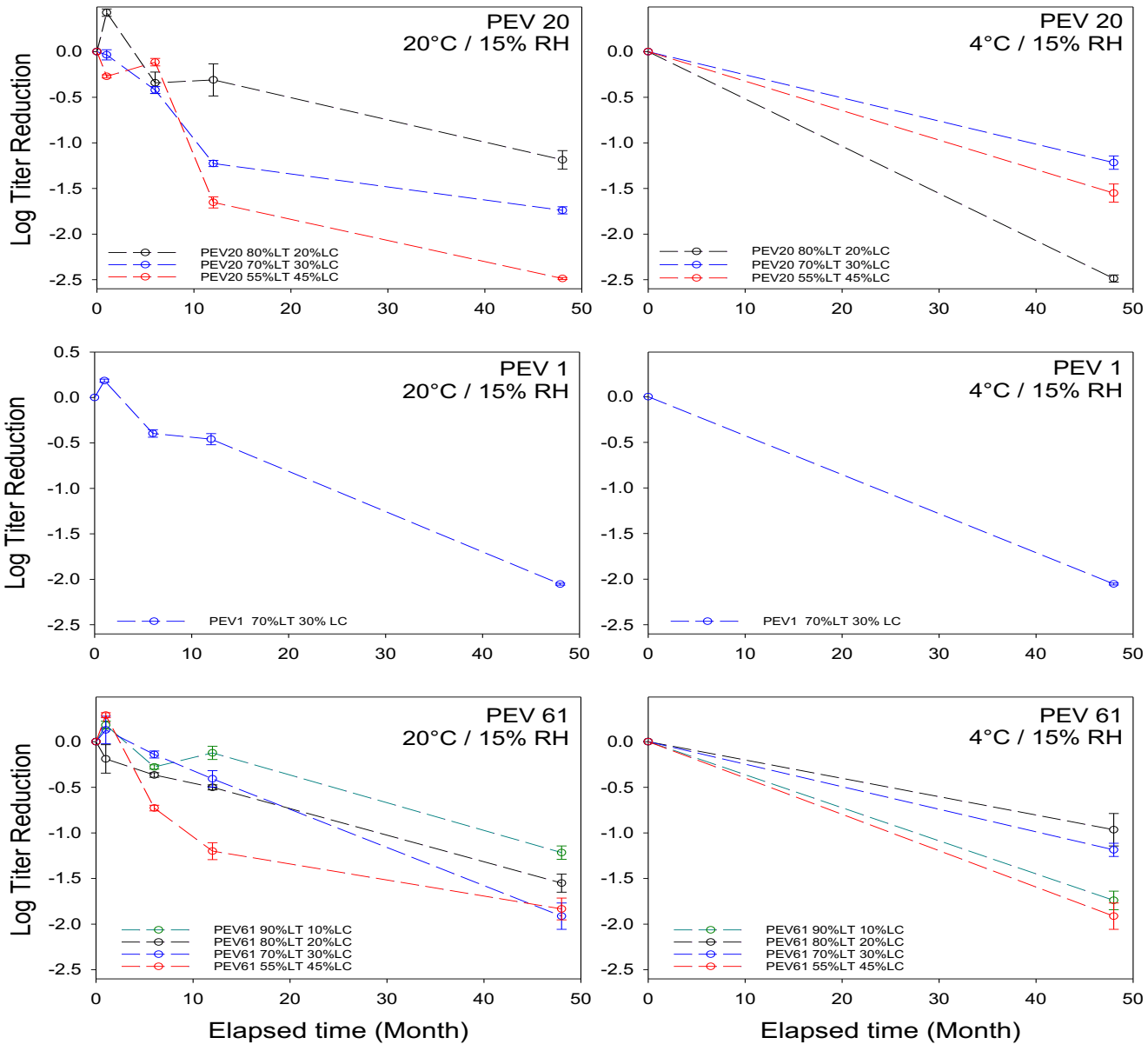


Figure 1. Phage titer reduction in spray-dried powders after 4-year storage at 20 °C/15% RH and 4 °C/15% RH.

## Particle morphology

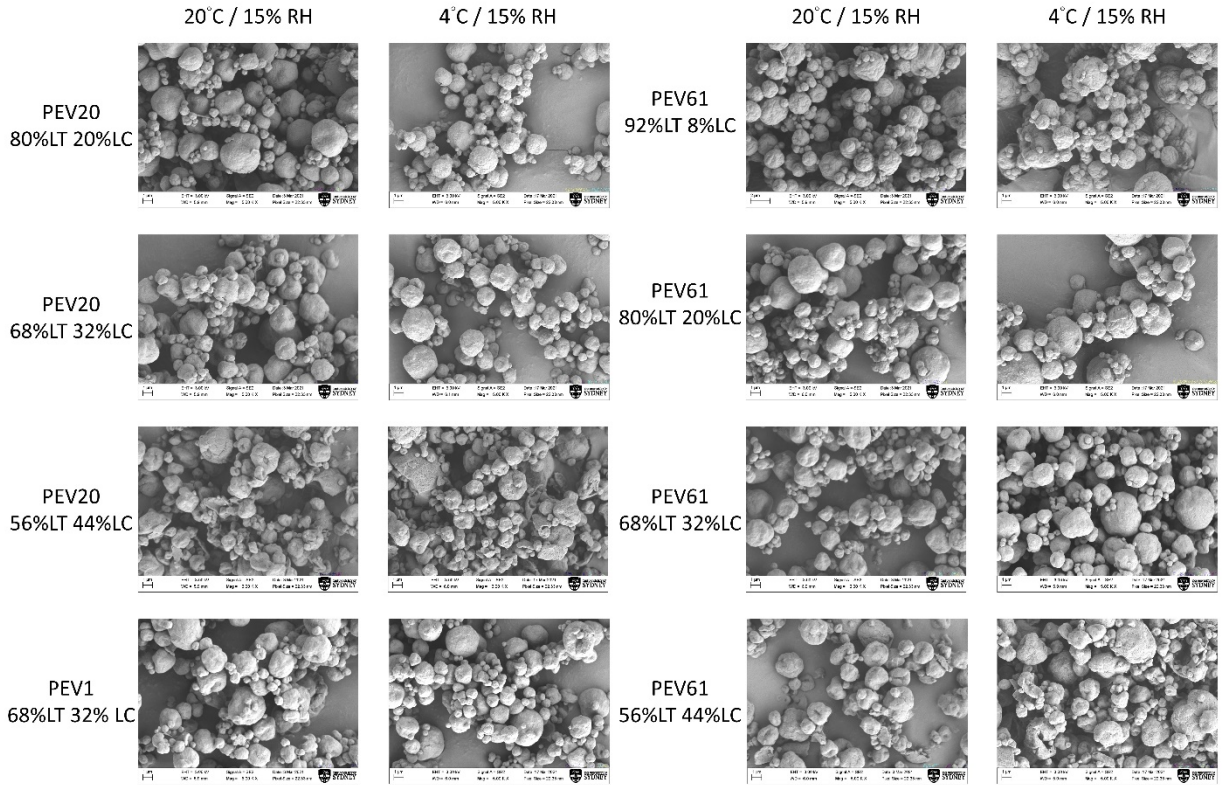


Figure 2. SEM images of spray-dried phage powders stored at 20°C / 15% RH and 4°C / 15% RH for 4 years.

**Figure 2** presents SEM images of the phage powder formulations after 4 years of storage, including Phage PEV20 with 80%, 70%, and 55% lactose, Phage PEV61 with 90%, 80%, 70%, and 55% lactose, and Phage PEV1 with 70% lactose.

In general, the phage powders exhibited a spherical shape with a rough surface morphology. After 4 years of storage at 4°C, the particle morphology of the phage powders remained largely unchanged. However, during storage at 20°C, a subtle yet noticeable change was observed, with some thread-like elongated features emerging from the particle surfaces. The prominence

of these elongated features increased with higher lactose content. Interestingly, formulations sharing the same excipient composition (20% leucine) displayed identical particle morphology, regardless of the specific phage used.

**Particle size distribution**

The volume median diameters and span values of the spray-dried phage powders were 1.8 - 2.2 μm and 1.5 - 6.4, separately (**Table 2**). The size distribution did not vary notably with excipient content nor the phage type. Similar to our previous study, the size was not practically changed for all formulations after 4-year storage.

Table 2. Particle size distributions of phage powders spray dried after 4-year storage at 20 °C/15% RH. Data are presented as mean ± standard deviation, with changes from the initial fresh powder values shown in parentheses (positive values indicate an increase).

| Formulation Name | $D_{10}$ (μm) | $D_{50}$ (μm) | $D_{90}$ (μm) | Span |
|---|---|---|---|---|
| PEV20 80%LT 20%LC | 0.89 ± 0.04 (+0.1) | 1.89 ± 0.19 (-0.1) | 3.67 ± 0.52 (-0.4) | 1.43 ± 0.17 (-0.3) |
| PEV20 70%LT 30%LC | 0.85 ± 0.02 (+0.2) | 2.09 ± 0.05 (+0.3) | 4.08 ±0.16 (+0.4) | 1.54 ± 0.07 (-0.1) |
| PEV20 55%LT 45%LC | 0.92 ± 0.01 (+0.1) | 2.02 ± 0.02 (+0.1) | 3.99 ± 0.02 (+0.2) | 1.53 ± 0.02 (+0.0) |
| PEV1 70%LT 30% LC | 0.83 ± 0.01 (+0.0) | 2.11 ± 0.03 (+0.3) | 4.09 ± 0.04 (+0.4) | 1.55 ± 0.02 (+0.0) |
| PEV61 90%LT 10%LC | 0.74 ± 0.07 (+0.0) | 1.88 ± 0.09 (+0.0) | 4.19 ± 0.34 (+0.3) | 1.84 ± 0.24 (+0.2) |
| PEV61 80%LT 20%LC | 0.83 ± 0.05 (+0.1) | 1.90 ± 0.05 (+0.0) | 3.81 ± 0.04 (+0.0) | 1.58 ± 0.05 (-0.1) |
| PEV61 70%LT 30%LC | 0.91 ± 0.04 (+0.1) | 2.05 ± 0.05 (+0.2) | 4.19 ± 0.28 (+0.4) | 1.60 ± 0.16 (-0.2) |
| PEV61 55%LT 45%LC | 0.86 ± 0.10 (+0.1) | 2.01 ±0.16 (+0.0) | 4.67 ± 0.84 (+0.4) | 1.90 ± 0.36 (+0.2) |

**Thermal analysis**

After four years of storage, the glass transition temperatures ($T_g$) of the phage powder formulations increased by 3 – 11°C (4 °C/15% RH samples) and 13 – 18°C (20 °C/15% samples), compared to fresh powders (Table 3).

Table 3. Glass transition temperature ($T_g$) of phage powders spray dried after 4-year storage at 4 °C/15% RH and 20 °C/15% RH. Data are presented as individual measurements (*n*=2), with changes from the initial fresh powder values shown in parentheses (positive values indicate an increase).

| Formulation Name | Storage temperature | |
|---|---|---|
| | 4 °C / 15% RH | 20 °C / 15% RH |
| PEV20 80%LT 20%LC | 69.0, 69.2 (+6.8) | 74.3, 75.6 (+12.7) |
| PEV20 70%LT 30%LC | 66.8, 70.7 (+6.1) | 78.9, 75.8 (+14.6) |
| PEV20 55%LT 45%LC | 63.7, 68.0 (+2.6) | 75.2, 77.3 (+13.1) |
| PEV1 70%LT 30% LC | 62.5, 70.9 (+5.2) | 79.0, 77.3 (+16.6) |
| PEV61 90%LT 10%LC | 67.9, 71.5 (+9.7) | 77.6, 78.1 (+17.9) |
| PEV61 80%LT 20%LC | 69.3, 77.3 (+11.3) | 78.0, 78.1 (+16.0) |
| PEV61 70%LT 30%LC | 71.1, 71.0 (+10.6) | 75.1, 75.1 (+14.6) |
| PEV61 55%LT 45%LC | 69.0, 73.4 (+9.6) | 78.5, 77.2 (+16.3) |

**In *vitro* aerosol performance**

Figure 3 and Table 4 present the changes in powder dispersion performance and fine particle fraction (FPF, defined as the percentage of particles smaller than 5 μm) of the phage formulations after four years of storage under two conditions. Formulations with higher leucine content (45% w/w) showed a smaller reduction in FPF (Table 4). This trend was particularly evident in PEV61 stored at both temperatures, where FPF was reduced by less than 10%. Similarly, for PEV20 stored at 4 °C and 20 °C, FPF declined by 10.0 ± 0.9% and 12.2 ± 0.9%, respectively. For formulations with lower leucine content (<45% w/w), FPF decreased by more

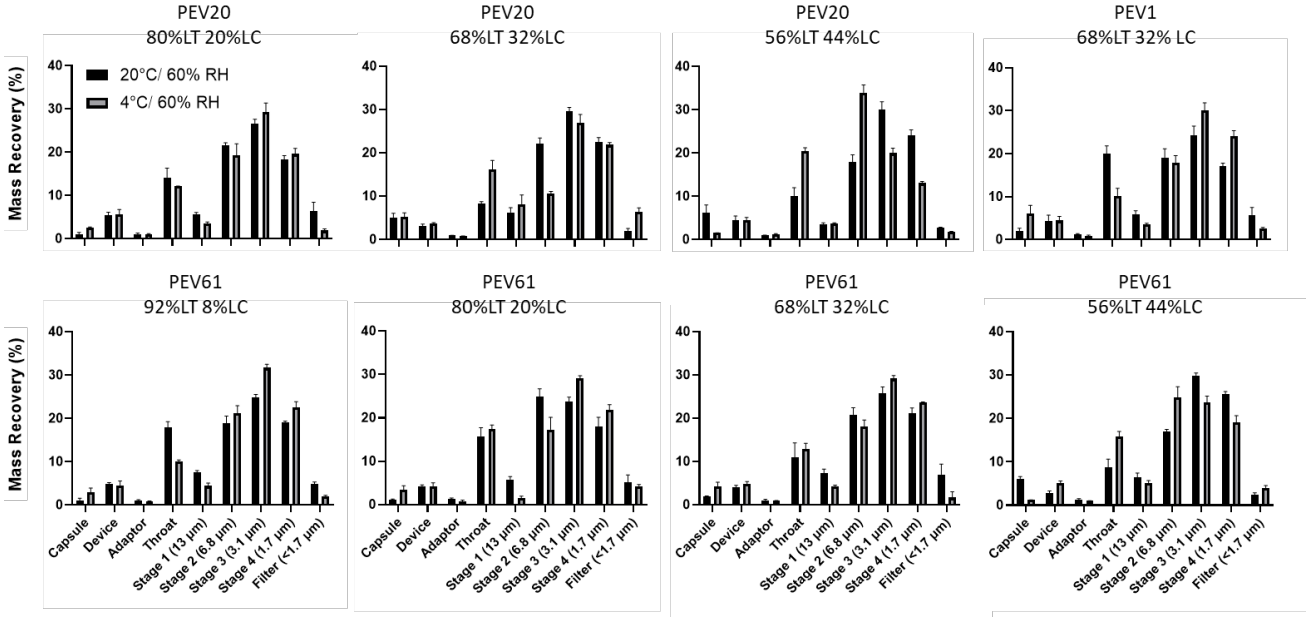


Figure 3. Powder dispersion performances of aerosolized phage formulations stored at 20 °C / 15% RH and 4 °C / 15% RH stored for 4 years. All formulations were dispersed using an Osmohaler at 100 L/min for 2.4 s. Data presented as mean ± standard deviation (n = 3).

than 10%. In particular, FPF for formulations containing PEV20 (< 30% w/w leucine) and PEV1 (30% w/w leucine) dropped by more than 15% and 35%, respectively.

**Table 4.** Fine particle fraction (FPF) of phage powders spray dried after 4-year storage at 4 °C/15% RH and 20 °C/15% RH. Data are presented as mean ± standard deviation, with decreases from the initial fresh powder values shown in parentheses.

| Formulation Name | Storage temperature | |
|---|---|---|
| | 4 °C / 15% RH | 20 °C / 15% RH |
| PEV20 80%LT 20%LC | 36.3 ± 0.9 (-21.4) | 37.0 ± 2.8 (-20.7) |
| PEV20 70%LT 30%LC | 40.5 ± 1.7 (-17.7) | 42.1 ± 3.3 (-16.1) |
| PEV20 55%LT 45%LC | 41.8 ± 0.9 (-10.4) | 39.5 ± 1.8 (-12.2) |
| PEV1 70%LT 30% LC | 26.7 ± 1.0 (-36.1) | 26.7 ± 0.6 (-36.1) |
| PEV61 90%LT 10%LC | 39.9 ± 1.3 (-12.6) | 33.8 ± 0.5 (-18.7) |
| PEV61 80%LT 20%LC | 39.6 ± 0.4 (-15.6) | 34.6 ± 3.6 (-20.6) |
| PEV61 70%LT 30%LC | 40.7 ± 1.0 (-16.0) | 39.9 ± 2.4 (-16.8) |
| PEV61 55%LT 45%LC | 41.5 ± 2.5 (-7.2) | 43.9 ± 1.4 (-4.8) |

**Discussion**

To the best of our knowledge, this is the first study to demonstrate the long-term stability of inhalable phage powder formulations stored under controlled conditions over a four-year period. Unlike chemically synthesized small-molecule drugs, biopharmaceuticals generally exhibit limited stability, as their structural integrity is essential for maintaining biological activity and potency. This makes it challenging to develop formulations with a shelf life

exceeding 2-3 years while also keeping manufacturing costs manageable (208). Given these concerns, we conducted a four-year stability study to assess the feasibility of long-term storage for inhalable phage powders.

Since lower storage temperatures are well known to better preserve biological activity (209), we initially conducted a one-month stability test and observed changes in the physicochemical properties and biological activity of some phage powders stored at 20°C/15% RH. However, due to limited availability of same-batch powders, the remaining fresh powders were stored only under a lower-stress condition (4°C/15% RH) to maximize the chance of bioactivity preservation. Characterization of these powders was conducted only at the final time point (48 months) to conserve samples for a meaningful assessment of long-term stability. As a result, powders stored at 20°C/15% RH were analyzed at multiple time points in the study, whereas those stored at 4°C/15% RH were evaluated only at the last time point.

With these conditions established, we evaluated the stability of spray-dried phage powders over the storage period by assessing their biological viability and physicochemical properties. Our findings revealed that the long-term phage stability was influenced by both the specific phage type and the formulation composition. Notably, formulations with optimized lactose-to-leucine ratios exhibited the highest stability. In particular, the PEV61 formulation (80% w/w of lactose) maintained viability with titer reductions of less than 1 $\log_{10}$ over four years of storage at 4°C /15% RH. For PEV20, the most significant decline in viability occurred during the first year of storage at 20°C/15% RH, after which the rate of decline slowed between years one and four. Overall, both PEV20 and PEV61 formulations with higher lactose content exhibited better phage stability over the storage period, suggesting that lactose concentration is crucial for preserving phage viability over extended periods. Lactose less than 70% w/w in the formulation

caused large titer loss more than 2 $\log_{10}$. The protective role of lactose, a well-established excipient in dry powder formulations, is probably due to its ability to form a stable glassy matrix, limiting mobility of phages and thereby protecting them from degradation (210). To ensure that this glassy matrix was preserved during manufacturing, we selected gentle dehydration parameters that minimize thermal and moisture stress. Spray drying at an outlet temperature of 40–41 °C followed by storage at ≤20 °C, together with residual water contents maintained at ≤2.5 % w/w after one-year storage (211) creates a low-temperature, low-humidity environment that suppresses the initial Schiff-base formation required for Maillard chemistry (212). Consistent with this, DSC scans of all formulations showed no emergence of additional thermal events, while bioactivity remained high ($\geq 4 \times 10^8$ pfu/ mg) across lactose-rich powders. Taken together, these observations indicate that the formation of lactose-derived Amadori or advanced glycation products is highly improbable under the processing and storage conditions employed in this study. Moreover, there were slight differences in stability between the three tested phages, despite the identical excipients used. Compared to PEV20 and PEV61 phages, PEV1 was most susceptible to inactivation over extended storage when the lactose content in the formulation was 70% w/w. PEV1 exhibited a more linear decline in viability over the entire storage period, indicating that different phages had varying stability profiles. This variability underscores the importance of capsid-specific structural features in governing long-term infectivity retention. Hardy *et al.* demonstrated that flagellotropic phages employ dual chainmail-like stabilization systems: an internal network of extended N-arms creating "inner chainmail" and external clamping loops with trimeric auxiliaries forming "outer chainmail" that collectively reinforce capsid integrity under environmental stress (213). This dual stabilization prevents the gradual structural deterioration that leads to titer loss, as the outer chainmail locks down critical capsomer interfaces while the

inner network provides core stability. Complementing this, Cardarelli *et al.* revealed that phages have adapted conserved protein folds—particularly HK97-like folds—to fulfill multiple stabilizing functions in virion assembly, where the same structural motif can serve as both a scaffolding element and a stabilizing component (214). These architectural adaptations create redundant stabilization pathways that maintain particle integrity and preserve infectivity titer even when individual structural elements experience stress-induced changes. Tape measure protein (TMP) architecture represents a critical but complex determinant of phage stability, with structural modifications directly influencing titer retention patterns. Mahony *et al.* provided detailed structural analysis of lactococcal phage TP901-1's TMP, revealing a modular architecture of 11-amino acid repeats with conserved tryptophan and phenylalanine residues that serve as structural anchors within the tail tube (215). These suggest that phage-specific factors, possibly related to protein constituents, may also play a role in their long-term stability (190). Although the PEV1 formulation experienced a titer loss of more than 2 $\log_{10}$, the potential for phage self-replication (auto-dosing) may help mitigate dosing challenges.

Leucine was added to the formulation to provide moisture protection and to prevent the recrystallization of amorphous lactose during storage. Our previous study confirmed that incorporating 10% leucine in the formulation delayed the recrystallization of amorphous lactose, increasing the recrystallization RH from 40% to 50% at 25°C. However, increasing the leucine content further (to 20-45%) did not yield additional improvements in delaying the recrystallization RH (115). Typically, the recrystallization of amorphous powders occurs when the environment provides sufficient driving force, either through increased temperature or humidity (216, 217). To minimize changes in amorphous lactose, we conducted the physical

stability studies of these phage powder formulations using scintillation vials sealed in aluminum pouches with desiccant. While samples were conditioned at 15% RH before sealing, the sealed system limited moisture exchange with the external environment during storage, representing a controlled but not continuously humidity-controlled storage condition. This allowed us to focus primarily on the biological stability of the phages. However, after four years of storage, most formulations exhibited subtle but noticeable changes, with some thread-like elongated features appearing on the surfaces of the particles. A study by Lin et al. produced phage-ciprofloxacin combination powders with ciprofloxacin, lactose, and leucine in a 1:1:1 mass ratio. Their results also reported thread-like particles after one year of storage (218). These physical changes were more pronounced in formulations stored at room temperature compared to refrigerated samples. Storage conditions also influenced $T_g$ of the powders. After 4 years, powders stored at 4 °C/15% RH exhibited a $T_g$ increase by 3 – 11°C , whereas those stored at 20 °C/15% RH showed a $T_g$ increase by 13 – 18°C. This increase in $T_g$ can be attributed to two main factors. First, residual moisture redistribution where initial moisture (~2-3% w/w) may redistribute within the sealed system or be absorbed by packaging materials. Since water acts as a plasticizer by enhancing molecular mobility, its removal results in a decrease in mobility and, consequently, an elevated $T_g$ (219). Second, amorphous materials inherently undergo physical aging—a process during which the material relaxes toward a more thermodynamically stable state. This relaxation leads to densification, reduced free volume, and an increased energy barrier for molecular motion, all contributing to the upward shift in $T_g$ (220). Our previous study also observed this phenomenon and demonstrated phage stability under <25 °C/15% RH storage conditions, with a significant $T_g$–storage temperature difference ($T_g - T_s > 46$ °C) reinforcing formulation stability (195). Despite these minor morphological changes and shifts in Tg, the overall stability and crystallinity of the powders remained largely

intact. This preservation of structural integrity is reflected in the minimal titer loss observed (ranging from 0.97 to 2.49 logs), ensuring sustained phage viability over extended storage periods.

Although morphological changes were observed in the phage powders after four-year storage, these alterations had only a subtle impact on the particle size distribution. This could be attributed to the relatively small amount of the thread-like elongated features which were fragile and breaking apart during the high-pressure dispersion used in particle size measurements, resulting in sizes comparable to the original particle size. On the contrary, these physicochemical changes were found to greatly reduce the FPF, which is critical for effective lung delivery. The reduction in FPF suggests that the powders became less dispersible over time, potentially due to increased inter-particle cohesion or changes in surface properties caused by recrystallization (221). It is worth noting that phage therapy does not follow the traditional dose-response relationship seen with small molecule antibiotics. When encountering bacteria, phages initiate bacterial killing through phage-mediated lysis, accompanied by phage replication. While initial differences in administered phage titer primarily affect the growth rate of phages, they do not necessarily influence the final phage titer reached in the targeted organ. Our team previously evaluated the effects of various doses ($7.5\times10^4$, $5\times10^6$, and $5\times10^8$ PFU/mouse) of inhaled PEV31 phage in treating mice with *Pseudomonas aeruginosa* pulmonary infection. At 24 hours post-infection, phage titers in all three groups exceeded $10^8$ PFU in the lungs (222). Therefore, even if the FPF of phage powders gradually deteriorates over time and some reduction in phage titer occurs, these powders are still expected to retain their efficacy in bacterial killing. Despite the deterioration in FPF after four years of storage,

the overall FPF still reached approximately 40%, which is comparable to most commercial dry powder inhaler (DPI) products (223), demonstrating the formulations' capability for bacterial killing by pulmonary delivery. Notably, formulations with higher leucine content exhibited less reduction in FPF over the storage period. Leucine is known for its dispersibility-enhancing properties, primarily by migrating to the particle surface during spray drying and forming a hydrophobic layer (224). This surface layer reduces inter-particle cohesive forces, improving powder flowability and aerosolization efficiency (225). The higher leucine content likely maintained this hydrophobic surface coating more effectively over time, mitigating the decrease in dispersion performance observed in formulations stored at both 4°C and 20°C. This highlights the essential role of leucine in preserving the aerosol performance of the phage powders by minimizing FPF deterioration, thereby ensuring efficient pulmonary delivery.

These findings are particularly significant as this study is the first to demonstrate the long-term stability of phage powder formulations over a four-year period. By demonstrating the feasibility of storing phage powders for extended durations while retaining an acceptable level of biological viability and aerosol performance, which are crucial for practical applications in treating respiratory infections, this study provides a strong foundation for future development of phage therapies. The use of lactose and leucine as excipients not only supports phage viability but also enhances the powder physical properties, making them suitable for long-term storage without the need for a cold chain. With the growing interest in phage therapy as an alternative to traditional antibiotics, especially for treating MDR infections, these formulations offer a robust solution that could facilitate wider adoption of phage-based pulmonary treatments (226). Overall, this study highlights the importance of the formulation (lactose-to-leucine ratio) and storage conditions in stabilizing the phage over long term storage. The

findings may be applicable also to non-inhalation formulations and to storage of phages in powders for improved stability over liquid storage. Due to sample availability, a limitation of the present study is the absence of longitudinal stability data over the entire 4 years, which is necessary for the approval of phage therapeutic products. For inhalation products, it may be sufficient to show storage stability over 2 to 3 years during which the decrease in the aerosol performance could potentially be less. Future investigations could explore additional excipient combinations to further enhance the stability and delivery efficiency of these powder formulations. Two non-reducing, high-Tg polysaccharides—inulin and pullulan—show particular promise as alternative stabilizers. Inulin offers a glass-transition temperature above 100°C, proven phage-stabilizing capacity, and prebiotic properties that may be beneficial for pulmonary delivery (227, 228). Pullulan, by contrast, forms robust, low-hygroscopic films and has been shown to protect phages in prior studies (229). The ongoing design of experiments (DoE) approach will systematically evaluate these excipients in combination with lactose-leucine systems, focusing on: (1) spray drying process optimization, (2) biological stability enhancement, and (3) aerosol performance maintenance. Additionally, our sealed storage system (scintillation vials in aluminum pouches with desiccant) may not fully represent true controlled humidity storage conditions, as moisture exchange with the external environment was limited. Future studies should employ open storage systems with continuous humidity control to better represent real-world storage conditions and enable more accurate assessment of humidity effects on long-term stability. Eventually, clinical studies are necessary to validate their efficacy and safety in human subjects, paving the way for their potential use in managing chronic respiratory infections.

## Conclusions

In conclusion, this study is the first to show that phage powder formulations can be stored for four years while retaining acceptable biological activity. Critical to this stability is the careful selection of excipients—formulations with ≥70% lactose provide a robust glassy matrix that protects phage viability, while leucine enhances moisture resistance and dispersibility. Although some formulations experienced higher titer losses exceeding 2 $\log_{10}$, and the aerosol performance also decreased, the FPF of most of the formulations remained around 40%, and the auto-dosing potential of phages may compensate for these reductions to attain effective therapeutic concentrations. Additionally, while storage at 20 °C/15% RH resulted in a greater $T_g$ increase than refrigerated conditions, the overall structural integrity of the powders was maintained. These findings support the long-term storage of phages in dry powder at room temperature for the development and use of phage-based therapies against infections, including those caused by multidrug-resistant bacteria.

**References**


1. Pang, Z., et al., *Antibiotic resistance in Pseudomonas aeruginosa: mechanisms and alternative therapeutic strategies.* Biotechnology Advances, 2019. **37**(1): p. 177-192.
2. Tacconelli, E., et al., *Discovery, research, and development of new antibiotics: the WHO priority list of antibiotic-resistant bacteria and tuberculosis.* Lancet Infectious Diseases, 2018. **18**(3): p. 318-327.
3. Kingwell, K., *Bacteriophage therapies re-enter clinical trials.* Nature Reviews Drug Discovery, 2015. **14**(8): p. 515-516.
4. Chang, R.Y.K., et al., *Phage therapy for respiratory infections.* Advanced Drug Delivery Reviews, 2018. **133**: p. 76-86.
5. Liu, C., et al., *Phage–Antibiotic Therapy as a Promising Strategy to Combat Multidrug-Resistant Infections and to Enhance Antimicrobial Efficiency.* Antibiotics, 2022. **11**(5): p. 570.
6. Pathak, V., H.-K. Chan, and Q.T. Zhou, *Formulation of Bacteriophage for Inhalation to Treat Multidrug-Resistant Pulmonary Infections.* KONA Powder and Particle Journal, 2024.
7. Chang, R.Y.K., et al., *Proof-of-Principle Study in a Murine Lung Infection Model of Antipseudomonal Activity of Phage PEV20 in a Dry-Powder Formulation.* Antimicrobial Agents and Chemotherapy, 2018. **62**(2): p. 01714-17.
8. Wang, S.-y., et al., *Pharmacokinetics and safety evaluation of intravenously administered Pseudomonas phage PA_LZ7 in a mouse model.* Microbiology Spectrum, 2023. **12**(1): p. e01882-23.
9. Chow, M.Y.T., et al., *Pharmacokinetics and Time-Kill Study of Inhaled Antipseudomonal Bacteriophage Therapy in Mice.* Antimicrobial Agents and Chemotherapy, 2020. **65**(1): p. 01470-20.
10. Chang, R.Y.K., et al., *Bacteriophage PEV20 and Ciprofloxacin Combination Treatment Enhances Removal of Pseudomonas aeruginosa Biofilm Isolated from Cystic Fibrosis and Wound Patients.* The AAPS Journal, 2019. **21**(3): p. 49.
11. Khanal, D., et al., *High Resolution Nanoscale Probing of Bacteriophages in an Inhalable Dry Powder Formulation for Pulmonary Infections.* Analytical Chemistry, 2019. **91**(20): p. 12760-12767.
12. Chan, H.-K. and R.Y.K. Chang, *Inhaled Delivery of Anti-Pseudomonal Phages to Tackle Respiratory Infections Caused by Superbugs.* Journal of Aerosol Medicine and Pulmonary Drug Delivery, 2021. **35**(2): p. 73-82.
13. Lin, Y., et al., *Synergy of nebulized phage PEV20 and ciprofloxacin combination against Pseudomonas aeruginosa.* International Journal of Pharmaceutics, 2018. **551**(1): p. 158-165.

14. Cao, Y., et al., *Stability of bacteriophages in organic solvents for formulations.* International Journal of Pharmaceutics, 2023. **646**: p. 123505.

15. Leung, S.S.Y., et al., *Jet nebulization of bacteriophages with different tail morphologies – Structural effects.* International Journal of Pharmaceutics, 2019. **554**: p. 322-326.

16. Flint, R., et al., *Stability Considerations for Bacteriophages in Liquid Formulations Designed for Nebulization.* Cells, 2023. **12**(16).

17. Chang, R.Y.K., et al., *Inhalable bacteriophage powders: Glass transition temperature and bioactivity stabilization.* Bioengineering & Translational Medicine, 2020. **5**(2): p. e10159.

18. Li, M., et al., *Phage cocktail powder for Pseudomonas aeruginosa respiratory infections.* International Journal of Pharmaceutics, 2021. **596**: p. 120200.

19. Ke, W.-R., R.Y.K. Chang, and H.-K. Chan, *Engineering the right formulation for enhanced drug delivery.* Advanced Drug Delivery Reviews, 2022. **191**: p. 114561.

20. Vandenheuvel, D., et al., *Feasibility of spray drying bacteriophages into respirable powders to combat pulmonary bacterial infections.* European Journal of Pharmaceutics and Biopharmaceutics, 2013. **84**(3): p. 578-582.

21. Vandenheuvel, D., et al., *Instability of bacteriophages in spray-dried trehalose powders is caused by crystallization of the matrix.* International Journal of Pharmaceutics, 2014. **472**(1): p. 202-205.

22. Leung, S.S.Y., et al., *Effects of storage conditions on the stability of spray dried, inhalable bacteriophage powders.* International Journal of Pharmaceutics, 2017. **521**(1): p. 141-149.

23. Chang, R.Y., et al., *Production of highly stable spray dried phage formulations for treatment of Pseudomonas aeruginosa lung infection.* European Journal of Pharmaceutics and Biopharmaceutics, 2017. **121**: p. 1-13.

24. Chang, R.Y.K., et al., *Storage stability of inhalable phage powders containing lactose at ambient conditions.* International Journal of Pharmaceutics, 2019. **560**: p. 11-18.

25. Chang, R.Y.K., et al., *Proof-of-principle study in a murine lung infection model of antipseudomonal activity of phage PEV20 in a dry-powder formulation.* Antimicrobial Agents and Chemotherapy, 2018. **62**(2): p. 10.1128/aac. 01714-17.

26. Steckel, H. and B.W. Müller, *In vitro evaluation of dry powder inhalers I: drug deposition of commonly used devices.* International Journal of Pharmaceutics, 1997. **154**(1): p. 19-29.

27. Patton, J.S. and P.R. Byron, *Inhaling medicines: delivering drugs to the body through the lungs.* Nature reviews Drug discovery, 2007. **6**(1): p. 67-74.

28. Chang, R.Y.K., et al., *Inhalable bacteriophage powders: Glass transition temperature and bioactivity stabilization.* Bioengineering & translational medicine, 2020. **5**(2): p. e10159.

29. Costantino, H.R., R. Langer, and A.M. Klibanov, *Solid-phase aggregation of proteins under pharmaceutically relevant conditions.* Journal of pharmaceutical sciences, 1994. **83**(12): p. 1662-1669.

30. Hancock, B.C. and G. Zografi, *Characteristics and significance of the amorphous state in pharmaceutical systems.* Journal of pharmaceutical sciences, 1997. **86**(1): p. 1-12.

31. Abedon, S.T., et al., *Phage treatment of human infections.* Bacteriophage, 2011. **1**(2): p. 66-85.

32. Coelho, J.M., et al., *Microbiological Quality and Stability of Pharmaceutical Products in Europe: Discrepancies, Regulatory Perspectives and Challenges.* 2025.

33. Chang, R.Y., et al., *Production of highly stable spray dried phage formulations for treatment of Pseudomonas aeruginosa lung infection.* Eur J Pharm Biopharm, 2017. **121**: p. 1-13.

34. Muralidhara, B.K. and M. Wong, *Critical considerations in the formulation development of parenteral biologic drugs.* Drug Discovery Today, 2020. **25**(3): p. 574-581.

35. Leung, S.S.Y., et al., *Effect of storage temperature on the stability of spray dried bacteriophage powders.* European Journal of Pharmaceutics and Biopharmaceutics, 2018. **127**: p. 213-222.

36. Chang, R.Y.K. and H.-K. Chan, *Advancements in Particle Engineering for Inhalation Delivery of Small Molecules and Biotherapeutics.* Pharmaceutical Research, 2022. **39**(12): p. 3047-3061.

37. Chang, R.Y.K., et al., *Storage stability of inhalable phage powders containing lactose at ambient conditions.* Int J Pharm, 2019. **560**: p. 11-18.

38. Qiu, Z., et al., *Kinetic study of the Maillard reaction between metoclopramide hydrochloride and lactose.* International journal of pharmaceutics, 2005. **303**(1-2): p. 20-30.

39. Hardy, J.M., et al., *The architecture and stabilisation of flagellotropic tailed bacteriophages.* Nature Communications, 2020. **11**(1): p. 3748.

40. Cardarelli, L., et al., *Phages have adapted the same protein fold to fulfill multiple functions in virion assembly.* Proceedings of the National Academy of Sciences of the United States of America, 2010. **107**(32): p. 14384-14389.

41. Mahony, J., et al., *Functional and structural dissection of the tape measure protein of lactococcal phage TP901-1.* Scientific Reports, 2016. **6**(1): p. 36667.

42. Ke, W.-R., et al., *Co-spray dried hydrophobic drug formulations with crystalline lactose for inhalation aerosol delivery.* International Journal of Pharmaceutics, 2021. **602**: p. 120608.

43. Ke, W.-R., et al., *Spray drying lactose from organic solvent suspensions for aerosol delivery to the lungs.* International Journal of Pharmaceutics, 2020. **591**: p. 119984.

44. Lin, Y., et al., *Storage stability of phage-ciprofloxacin combination powders against Pseudomonas aeruginosa respiratory infections.* International Journal of Pharmaceutics, 2020. **591**: p. 119952.

45. Heljo, V.P., et al., *The Effect of Water Plasticization on the Molecular Mobility and Crystallization Tendency of Amorphous Disaccharides.* Pharmaceutical Research, 2012. **29**(10): p. 2684-2697.

46. Surana, R., A. Pyne, and R. Suryanarayanan, *Effect of Aging on the Physical Properties of Amorphous Trehalose.* Pharmaceutical Research, 2004. **21**(5): p. 867-874.

47. Chen, L., et al., *Amorphous powders for inhalation drug delivery.* Advanced Drug Delivery Reviews, 2016. **100**: p. 102-115.

48. Chang, R.Y.K., et al., *The effects of different doses of inhaled bacteriophage therapy for Pseudomonas aeruginosa pulmonary infections in mice.* Clinical Microbiology and Infection, 2022. **28**(7): p. 983-989.

49. Newman, S. and H.-K. Chan, *In Vitro / In Vivo Comparisons in Pulmonary Drug Delivery.* Journal of aerosol medicine and pulmonary drug delivery, 2008. **21**: p. 77-84.

50. Alhajj, N., N.J. O'Reilly, and H. Cathcart, *Leucine as an excipient in spray dried powder for inhalation.* Drug Discovery Today, 2021. **26**(10): p. 2384-2396.

51. Chang, R.Y.K., et al., *Overcoming challenges for development of amorphous powders for inhalation.* Expert Opinion on Drug Delivery, 2020. **17**(11): p. 1583-1595.

52. Leung, S.S.Y. and H.-K. Chan, *Emerging antibiotic alternatives: From antimicrobial peptides to bacteriophage therapies.* Advanced Drug Delivery Reviews, 2022. **191**: p. 114594.

53. Mensink, M.A., et al., *Inulin, a flexible oligosaccharide I: Review of its physicochemical characteristics.* Carbohydrate polymers, 2015. **130**: p. 405-419.

54. Ergin, F., *Effect of freeze drying, spray drying and electrospraying on the morphological, thermal, and structural properties of powders containing phage Felix O1 and activity of phage Felix O1 during storage.* Powder Technology, 2022. **404**: p. 117516.

55. Carrigy, N.B., et al., *Trileucine and pullulan improve anti-campylobacter bacteriophage stability in engineered spray-dried microparticles.* Annals of biomedical engineering, 2020. **48**(4): p. 1169-1180.

# Chapter 5

# Optimizing Performance of Inhalable Bacteriophage Powders using Human Serum Albumin (HSA)

This chapter has been accepted in International Journal of Pharmaceutics, with the title 'Optimizing Performance of Inhalable Bacteriophage Powders using Human Serum Albumin (HSA).' Authors: Mengyu Li, Yue Cao, Hak-Kim Chan.

## Introduction

The rise of multidrug-resistant (MDR) bacteria HSA posed significant challenges in treating respiratory infections, particularly in cystic fibrosis (CF) patients, where *Pseudomonas aeruginosa* is a leading cause of morbidity and mortality (10, 230, 231). Many of these bacteria are either inherently resistant or have developed resistance to current antibiotics (232). In response, bacteriophage (phage) therapy HSA gained renewed attention as a potential alternative for eradicating MDR bacteria. Phages, the most abundant organisms on Earth, offer a relatively rapid and simpler approach compared to the discovery of new antibiotic classes (233). The advantages of phage therapy over conventional antibiotics include its natural occurrence, low toxicity, self-amplifying nature, and high specificity, which minimizes the impact on non-target bacteria (234). Phage efficacy against MDR bacteria has been demonstrated in vitro (235), as well as in animal (236, 237) and human studies (238, 239).

As foreign biological entities, bacteriophages have the potential to elicit immune responses or cause toxicity when introduced into the human body. However, extensive research on phage therapy, including inhaled formulations, suggests that phages are generally safe and well-tolerated. Systematic reviews of clinical trials have concluded that phage therapy is safe, with no phage-related adverse effects reported in modern trials involving various administration routes, including oral, topical, and intranasal (240). Specifically for inhaled phage therapy, in vitro studies have demonstrated that human lung epithelial (A549, HEK249) and alveolar macrophage (THP-1) cells exhibit high survival rates (>94%) after 24-hour exposure to phage powders at concentrations of 10, 100, and 1000 mg/L (211). In *vivo* studies in mice have shown that inhaled phage powders, such as those containing anti-pseudomonal phage PEV31, do not cause significant local toxicity in the lungs and can even alleviate lung damage in neutropenic

mice with *P. aeruginosa* infections (241). Pharmacokinetic investigations further indicated that inhaled phages primarily remained in the lungs, with minimal systemic distribution; less than 0.01% of the administered dose was detected in organs such as the kidney, liver, blood, and spleen, although a slight accumulation in the liver was observed over 24 hours at higher doses (109 PFU) (58). This localization reduces the likelihood of systemic immune responses or toxicity compared to intravenous administration, which results in greater systemic exposure. The low immunogenicity of phages is supported by their natural presence in the human body, such as in the gut and cerebrospinal fluid, suggesting co-adaptation with humans that minimizes adverse immunological effects (240). However, high-purity phage preparations are essential to avoid immune responses triggered by bacterial debris, as observed in historical trials with impure formulations (240). A recent study on personalized inhaled bacteriophage therapy for multidrug-resistant P. aeruginosa in cystic fibrosis patients demonstrated that nebulized phage therapy was well-tolerated, with no adverse events reported, and led to a significant reduction in sputum Pseudomonas density and an improvement in lung function (242). While preclinical studies indicate that inhaled phages primarily remain in the lungs with minimal systemic exposure and no significant toxicity, further clinical validation is necessary to confirm these findings in diverse patient populations.

Traditional methods for treating bacterial infections, such as oral or parenteral administration, often encounter significant limitations in delivering effective concentrations to the lower respiratory tract, leading to reduced bioavailability (243). For instance, Semler *et al.* demonstrated that aerosolized phages delivered via a jet nebulizer attached to a Nose-Only Inhalation Device resulted in substantial bacterial reduction in the lungs of mice infected with *Burkholderia cepacia* complex (BCC) (244). In contrast, intraperitoneal administration of

phages did not produce a significant antibacterial effect (244). This discrepancy can be attributed to varying systemic clearance rates, where intraperitoneal treatments are less efficient at maintaining therapeutic concentrations at the infection site. Direct lung delivery emerges as a more effective alternative, enabling higher drug concentrations directly at the site of infection with minimal systemic exposure (243). This targeted approach enhances the therapeutic efficacy of phage therapy for pulmonary infections. Supporting this, Debarbieux and co-workers reported a 100% survival rate in *Pseudomonas aeruginosa*-infected mice following intranasal phage administration at a phage-to-bacteria ratio of 10:1 (245, 246). These findings underscore that the most effective route for phage delivery is one that provides direct access to the infection site, ensuring that phages can reach and sustain therapeutic concentrations near the target bacteria. Aerosol delivery, therefore, offers superior targeting efficiency compared to traditional systemic routes. By facilitating the deposition of phages directly into the lungs, aerosolized formulations maximize antibacterial activity where it is most needed, enhancing overall treatment outcomes for respiratory infections.

A critical factor in the success of inhalable therapies is the formulation of aerosols, which can be prepared as liquids (solutions, suspensions, emulsions) or dry powders. Currently, phage preparations for therapeutic use are primarily limited to liquid formulations, typically stored at 4°C with a shelf life of about 126 days (247). As a result, much of the phage research for respiratory infections HSA focused on liquid aerosols administered via intranasal instillation (248, 249). However, many phage strains can be stabilized in powder form for extended periods, making dry powder formulations particularly attractive due to their convenience, long shelf life, and ease of use, all of which enhance patient compliance. Additionally, dry powder inhalers are more user-friendly compared to nebulizers. Techniques such as spray drying (197), and spray

freeze-drying are commonly used to prepare phage powders for inhalation. For instance, Leung et al. compared spray drying and spray freeze-drying for the production of stable anti-Pseudomonal phage powders using trehalose, mannitol, and leucine, finding that spray drying offered better phage protection (67). Our group demonstrated that a combination of the antibiotic ciprofloxacin and phage can be formulated as an inhalable powder with less than 1 $\log_{10}$ loss (62).

Our previous work successfully developed inhalable phage powders by combining lactose as an excipient with leucine as a dispersion enhancer, achieving minimal phage viability loss (below 1.3 $\log_{10}$) (88, 115). Despite this successful combination, lactose itself has inherent limitations; its reducing functional groups can negatively affect phage stability, especially in the absence of additional stabilizers (197). To overcome this drawback and broaden the choice of viable excipients, we propose exploring human serum albumin (HSA) (250). HSA is widely recognized for its protein-stabilizing properties and capacity to enhance powder dispersion. As a native human protein, HSA in the formulation is unlikely to elicit an immune response in humans, unlike foreign proteins or modified proteins that may trigger antibody formation. It is the most abundant protein in human plasma and is naturally present in the lung environment, contributing to fluid balance and transport (251). Its presence in the lungs suggests high biocompatibility and low immunogenicity when administered via inhalation (252). As a native human protein, HSA is unlikely to elicit an immune response in humans, unlike foreign proteins or modified proteins that may trigger antibody formation. Studies on inhaled albumin-based nanoparticles provide further support for its safety. For instance, a study evaluating inhaled tacrolimus-bound albumin nanoparticles in a mouse model of pulmonary fibrosis reported no inflammation or adverse effects attributable to the albumin component (253), indicating that

HSA is well-tolerated in the pulmonary environment. Additionally, HSA's use in other pharmaceutical applications, such as drug delivery (254), underscores its favorable safety profile, with no significant reports of immunogenicity when used as an excipient . However, rare cases of hypersensitivity to HSA have been reported in intravenous administration, such as an IgE-mediated anaphylactic reaction during plasmapheresis (255, 256). These reactions are likely route-specific and may not apply to inhalation, where systemic exposure is minimal. The spray-drying process used in this study is a standard pharmaceutical technique and is not expected to introduce toxic residues or alter HSA in a way that increases immunogenicity, provided good manufacturing practices are followed. Therefore, the natural presence of HSA in the lung environment suggests improved biocompatibility and potentially lower immunogenicity, positioning it as a promising alternative for inhalable phage formulations.

Building on this foundation, the current study evaluates novel inhalable phage powder formulations using combination of HSA and lactose. We selected PEV2, a fragile short-tail *podovirus* targeting *Pseudomonas aeruginosa*, as our model phage because of its heightened sensitivity to formulation and processing stresses. This characteristic makes PEV2 particularly suitable for assessing HSA's protective effects. To our knowledge, this is the first study to incorporate HSA into dry powder inhalable phage formulations, combining it with lactose to enhance both phage stability and aerosol performance, without using leucine as an additional excipient. This novel approach leverages HSA's protein-stabilizing properties and its role in optimizing aerosol performance through improved dispersibility, offering a promising alternative for treating respiratory infections caused by MDR bacteria.

## Materials and methods

### *Materials*

Lactose monohydrate (DFE Pharma, Goch, Germany) and human serum HSA (Merck Life Science) were used as excipients. Agar and nutrient broth were obtained from Amyl Media Pty Ltd. Pseudomonas lytic phage PEV2, with a high titer of $10^{10}$ PFU/mL, was sourced from AmpliPhi Biosciences AU.

***Experimental design***

A three-factor, two-level Box-Behnken (BB) design with three replicated center points was employed to optimize the antibacterial activity of phage PEV2 in HSA/lactose formulations. Statistical analyses were performed using Minitab® 18.1 (Minitab LLC, State College, PA, USA). Table 1 outlines the experimental factors and their corresponding levels, while Table 2 details each experimental run.

The study investigated three critical factors affecting the spray-drying process: HSA concentration, total solute concentration of the feed solution, and inlet temperature. Based on preliminary data indicating minimal titer loss in formulations containing 80% w/w lactose, the HSA concentration was systematically varied from 20% w/w to 100% w/w. This variation resulted in a corresponding decrease in lactose concentration from 80% w/w to 0% w/w, thereby enabling a detailed assessment of HSA substitution effects on phage stability. Additionally, the total solute concentration of the feed solution was varied from 10 mg/mL to 40 mg/mL. This parameter is critical for determining the solid mass per droplet during spray drying, which in turn influences particle size distribution. The selected range extends beyond the 25 mg/mL concentration used in earlier investigations, providing an expanded parameter space for optimization. Furthermore, inlet temperature, recognized as a pivotal factor for maintaining phage viability during spray drying, was varied between 50°C and 80°C, with a center point set at 65°C based on prior findings. This systematic and statistically guided

approach facilitated a comprehensive evaluation of the process parameters, ultimately contributing to the optimization of the spray-drying process for enhanced phage stability and antibacterial efficacy.

Interactions between factors were included in the Box-Behnken design to evaluate their combined influence on formulation outcomes. Specifically, interactions between HSA concentration and total solute concentration could affect particle morphology and glass matrix rigidity, influencing phage stability and aerosol performance. HSA concentration interacting with inlet temperature potentially modulates the protective effect against thermal stress on phages. The interplay between total solute concentration and inlet temperature may also impact droplet drying kinetics and thus particle size distribution (hence aerosol performance) and phage exposure time and stability. Evaluating these interactions through the response surface model provides comprehensive insights for formulation optimization.

Table 1. Factors and factor levels investigated in the BB experimental design.

| Factor | Unit | Factor Level | | |
|---|---|---|---|---|
| | | -1 | 0 | 1 |
| HSA concentration | %w/w | 20 | 60 | 100 |
| Inlet temperature | °C | 50 | 65 | 80 |
| Solute concentration | mg/mL | 10 | 25 | 40 |

Table 2. BB experimental design of 15 experiments (F1 – F15).

| Experiment (run) | Factor and factor level | | |
|---|---|---|---|
| | HSA concentration (w/w%) | Inlet temperature (°C) | Solute concentration (mg/mL) |
| F1 | 20 | 50 | 25 |
| F2 | 100 | 50 | 25 |
| F3 | 60 | 80 | 10 |
| F4 | 20 | 65 | 10 |
| F5 | 60 | 65 | 25 |
| F6 | 60 | 50 | 40 |
| F7 | 20 | 65 | 40 |
| F8 | 60 | 50 | 25 |
| F9 | 100 | 80 | 25 |
| F10 | 20 | 80 | 25 |

| | | | |
|---|---|---|---|
| F11 | 60 | 65 | 25 |
| F12 | 100 | 65 | 40 |
| F13 | 60 | 80 | 40 |
| F14 | 60 | 50 | 10 |
| F15 | 100 | 65 | 10 |

***Spray drying method***

The phage PEV2 liquid formulation was mixed with an HSA/lactose solution at a 1:100 ratio in deionized water. This mixture was stirred continuously and fed into a B-290 mini spray-dryer (Büchi, Flawil, Switzerland). Process parameters, such as feed rate (1.8 mL/min), atomizing airflow (742 L/h), and aspirator setting (35 $m^3$/h), were kept constant. The HSA/lactose ratio, solute concentration, and inlet temperature were adjusted based on Table 1 and Table 2 specifications. After drying, the powder was collected and stored in dry glass containers (relative humidity <15%).

***Phage viability***

The phage titer in the powder formulations was determined using the soft-agar overlay method (257). Reconstituted phage powders were diluted in phosphate-buffered saline (PBS). Serial dilutions were prepared by adding 20 µL of the sample to 180 µL of PBS. The diluted phage suspension (10 µL) was spotted onto nutrient agar overlaid with *Pseudomonas aeruginosa* PAV237 ($2 \times 10^8$ CFU) in 0.4% nutrient broth top agar. Plates were incubated at 37°C for 18 h, and plaque formation was used to assess phage viability. The assay was performed in triplicate for accuracy.

***Particle size distribution***

Particle size distribution was measured using laser diffraction (Mastersizer 3000, Malvern Instruments Ltd., UK) with the Scirocco 3000 dry powder module. Compressed air (4.0 bars)

was used for particle dispersion. Size distribution was reported as D10, D50, and D90, with the span calculated as (D90-D10)/D50. All measurements were conducted in triplicate.

***X-ray Diffraction (XRD) Analysis***

X-ray diffraction (XRD) patterns of the samples were recorded using a Siemens D5000 X-ray diffractometer (Munich, Germany) under ambient conditions. The samples were evenly spread on glass slides and exposed to Cu Kα radiation at 30 mA and 40 kV. The scattered intensity was measured by a detector over a 2θ range of 5–50°, with an angular increment rate of 0.04° 2θ per second.

***Thermal gravimetric analysis (TGA)***

Thermal properties were analyzed using a thermal gravimetric analyzer (Mettler Toledo, Greifensee, Switzerland). Samples (5 ± 1 mg) were heated from 30°C to 200°C at a rate of 10°C/min under nitrogen flow. Data were processed using STARe software (V.9.0x; Mettler Toledo). The assay was conducted in duplicate.

***Differential scanning calorimetry (DSC)***

Samples (5 ± 1 mg) were sealed in aluminum crucibles with perforated lids and heated from 30°C to 200°C at 10°C/min under nitrogen flow using a DSC instrument (Mettler Toledo). Each assay was performed independently in duplicate.

***Scanning electron microscopy (SEM)***

Particle morphology was examined using scanning electron microscopy (SEM) (Zeiss Ultra Plus, Carl Zeiss NTS GmbH, Oberkochen, Germany). Samples were mounted on carbon tape

and coated with a 15 nm layer of gold using a K550X sputter coater (Quorum Emitech, UK) before imaging.

***Dynamic vapor sorption (DVS)***

The moisture sorption profile was assessed using a dynamic vapor sorption system (DVS-Intrinsic, Surface Measurement Systems, UK). Approximately 10 mg of powder underwent one moisture ramping cycle from 0% to 90% relative humidity (RH) in 10% increments. Equilibrium moisture content was defined by a dm/dt value of <0.02% per minute.

***In vitro aerosol performance***

A Next Generation Impactor (NGI, Copley, UK) equipped with a mouthpiece adapter and USP induction port was used to assess aerosol performance. Each formulation (25 ± 1 mg) was placed into size 3 hydroxypropyl methylcellulose (HPMC) capsules and loaded into an Osmohaler® inhaler. Airflow (100 L/min) was drawn through the device for 2.4 seconds, creating a pressure drop of 4 kPa. The total recovered mass was determined by washing the device components with deionized water. Fine particle fraction (FPF) was defined as the mass fraction of particles ≤5.0 μm relative to the loaded dose. Emitted fraction (EF) was defined as the mass fraction of aerosolized powder relative to the total loaded dose. Experiments were performed in triplicate.

***High-performance liquid chromatography chemical assay***

HPLC was performed using a Shimadzu system with a Luna 5 μm C18(2) column (Phenomenex, CA, USA). Detection was at 220 nm, with the mobile phase consisting of 0.05% trifluoroacetic acid in water and acetonitrile (40:60, v/v). The flow rate was 0.5 mL/min.

Calibration curves for HSA (0.01–1 mg/mL) were linear ($r^2 > 0.999$) within the required concentration range.

## Results

### Response surface analysis and Factorial Design Analysis

Response surface analysis evaluated the individual and combined effects of three independent variables: solute concentration, HSA concentration, and inlet temperature on key formulation parameters. Three-dimensional (3D) response surface plots were generated by varying two factors simultaneously while keeping the third constant, resulting in a total of nine response surface diagrams for each protective excipient. Aerosol performance measured as FPF is depicted in Figures 1a–c, particle size ($D_{50}$) is illustrated in Figures 2a–c, and phage viability is shown in Figures 3a–c.

For FPF, the analysis revealed distinct trends across the response surface plots: as HSA concentration increased from 20% to 100%, FPF rose sharply (Figure 1a); conversely, FPF declined steeply as solute concentration increased from 10 mg/ml to 40 mg/ml, with inlet temperature showing a non-linear relationship marked by a valley (Figure 1b); and the highest FPF was achieved at the lowest solute concentration (10 mg/ml) paired with the highest HSA concentration (100%) (Figure 1c).

Regarding particle size ($D_{50}$), the plots demonstrated specific patterns: a ridge at 60% HSA concentration suggested an optimal point with inlet temperature having little influence, indicated by a flat slope (Figure 2a), while a sharp increase in $D_{50}$ occurred as solute concentration rose from 10 mg/ml to 40 mg/ml, highlighting its strong impact (Figures 2b and 2c).

For phage viability as assessed in terms of titer loss, the plots showed a steep increase in titer loss as HSA concentration rose from 20% to 100% with inlet temperature having a negligible effect (Figure 3a), a minimal impact from solute concentration reflected by a flat slope (Figure 3b), and a slight increase in titer loss (from 0.5 to 1.0 log) with higher inlet temperatures alongside a gradual decrease as solute concentration increased (Figure 3c).

Pareto charts of the standardized effects were included to compare the relative magnitude and the statistical significance (at the $\alpha = 0.05$ significance level) of main, square, and interaction effects. The results identified that the solute concentration alone significantly influenced (Figure 4a), HSA concentration significantly affected FPF (Figure 4b) and phage viability (Figure 4c), and no interactions between variables reached statistical significance, indicating that main effects predominantly drove the outcomes.

**a**

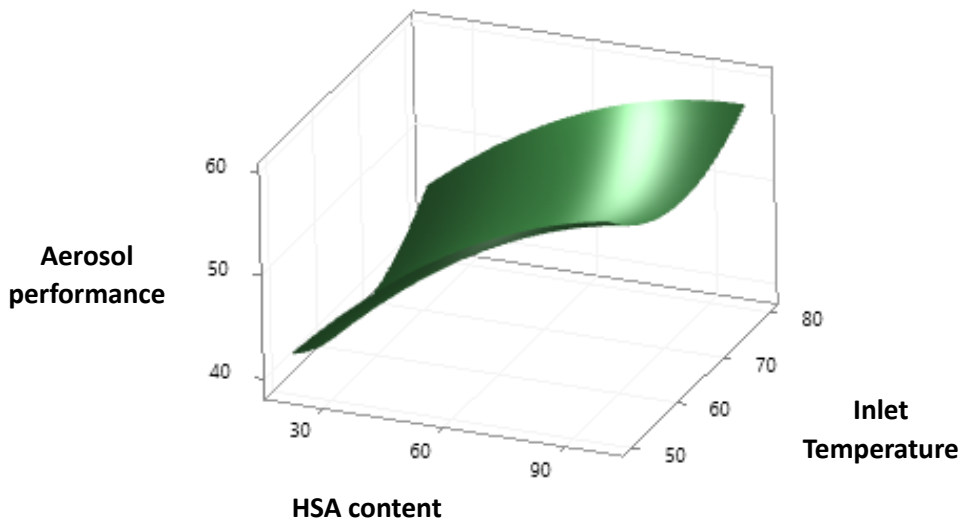
Aerosol performance
60
50
40
30
60
90
HSA content
80
70
60
50
Inlet Temperature

**b**

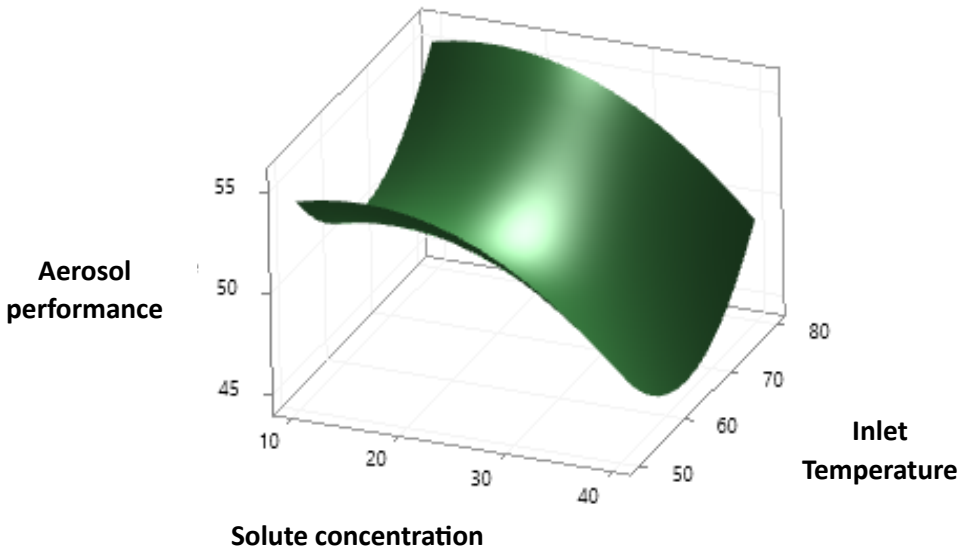
Aerosol performance
55
50
45
10
20
30
40
Solute concentration
80
70
60
50
Inlet Temperature

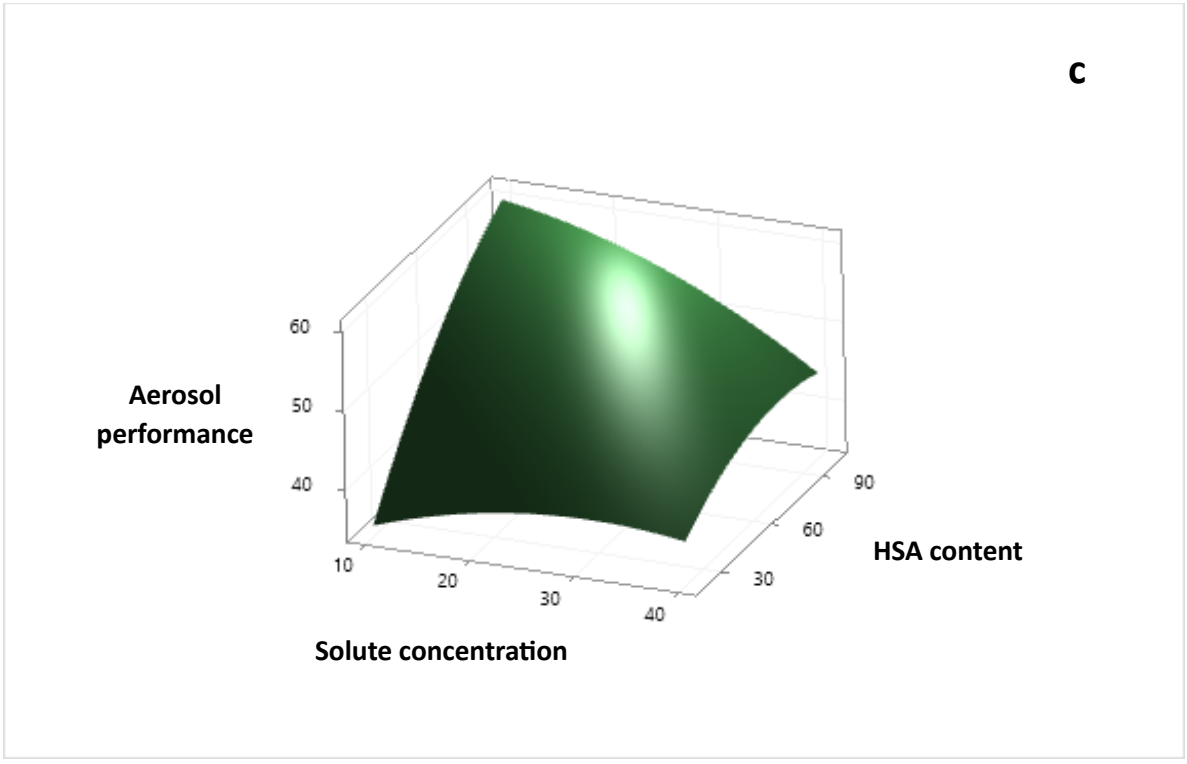


Fig.1. Response surface plots showing the effect of HSA content, inlet temperature and solute concentration on aerosol performance.

**a**

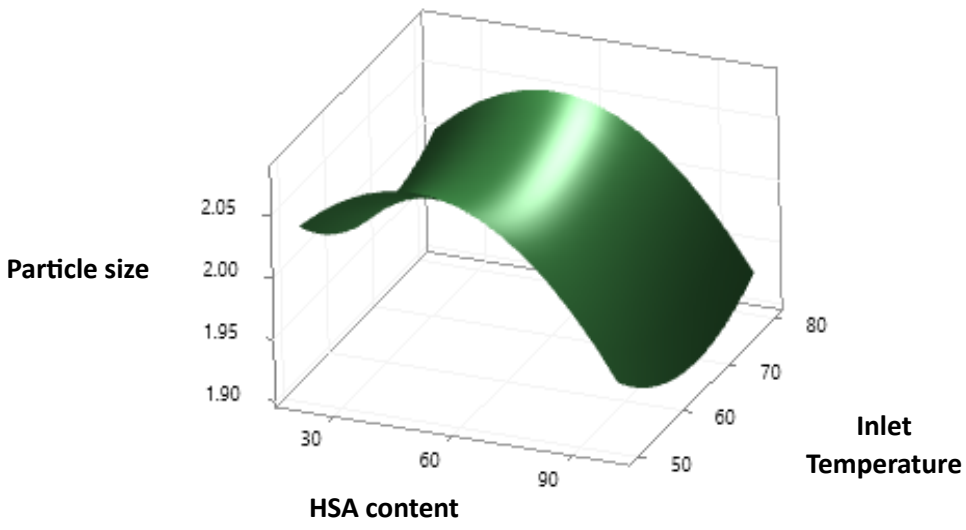
Particle size
2.05
2.00
1.95
1.90
30
60
90
HSA content
50
60
70
80
Inlet
Temperature

**b**

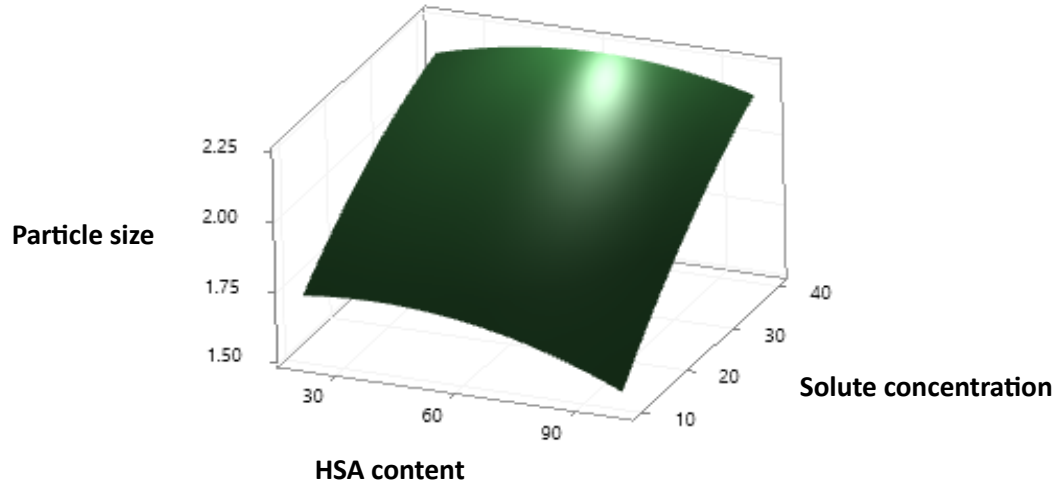
Particle size
2.25
2.00
1.75
1.50
30
60
90
HSA content
10
20
30
40
Solute concentration

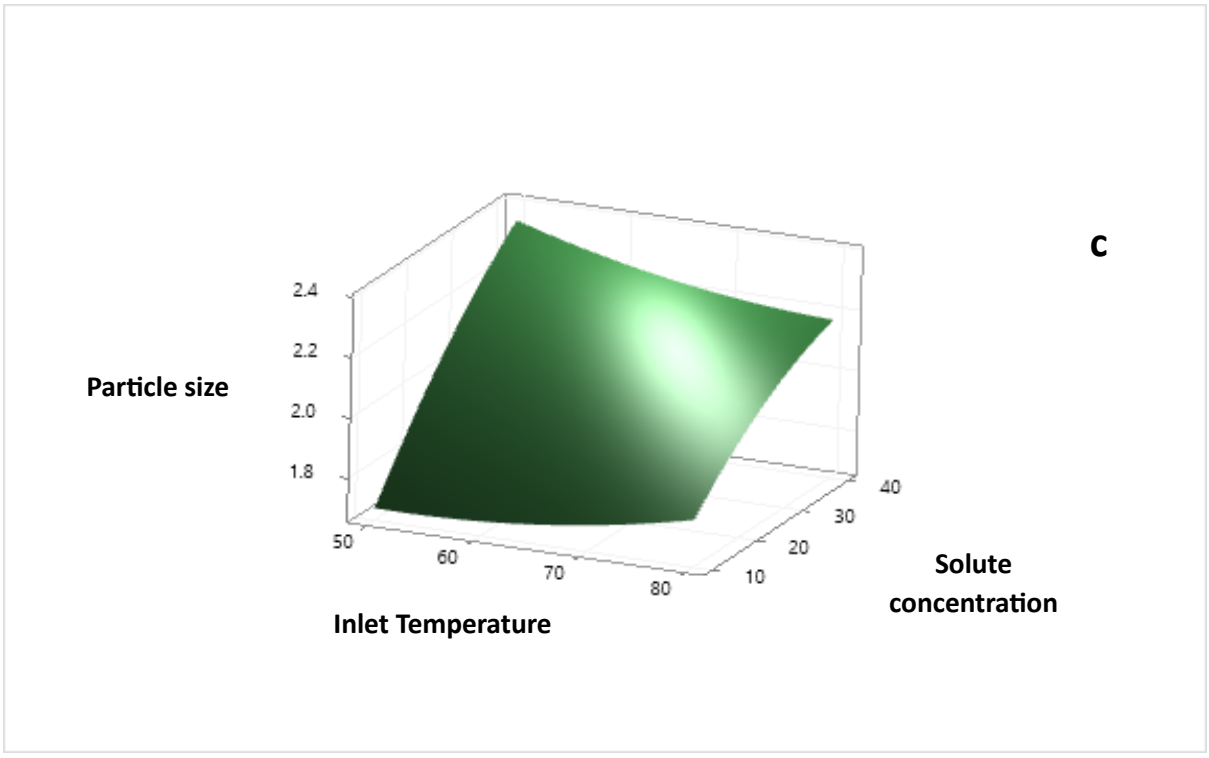


Fig.2. Response surface plots showing the effect of HSA content, inlet temperature and solute concentration on particle size.

**a**

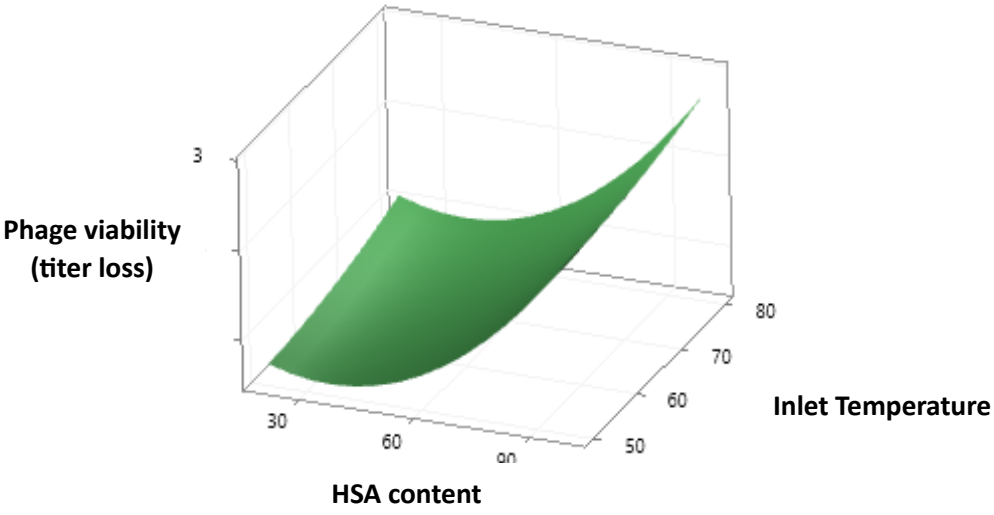
Phage viability
(titer loss)
3
30
60
90
HSA content
50
60
70
80
Inlet Temperature

**b**

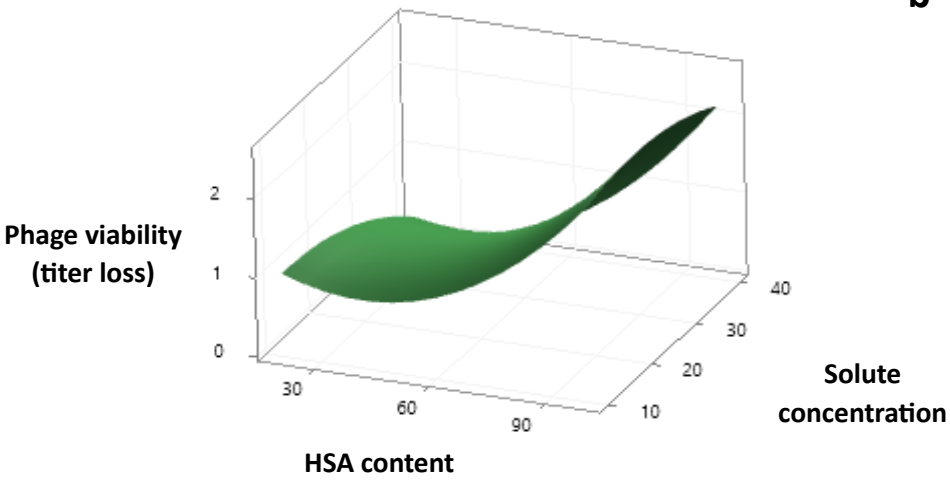
Phage viability
(titer loss)
0
1
2
30
60
90
HSA content
10
20
30
40
Solute
concentration

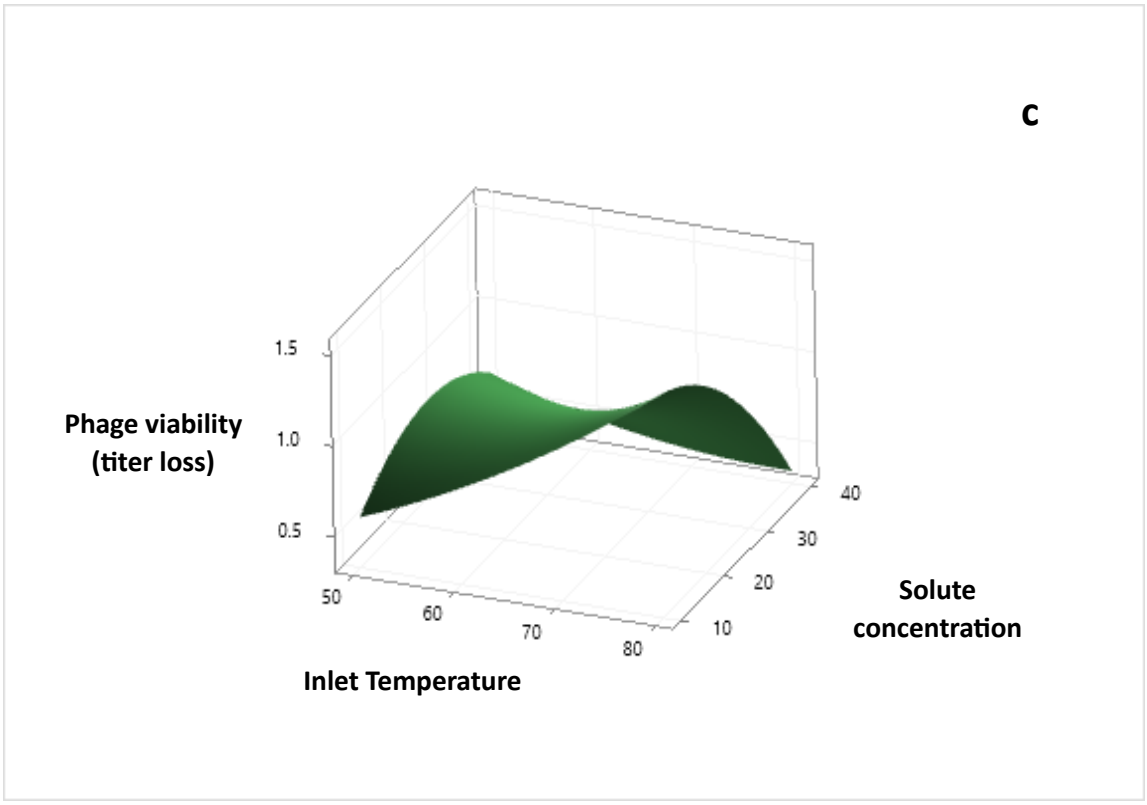


Fig.3. Response surface plots showing the effect of HSA content, inlet temperature and solute concentration on phage viability.

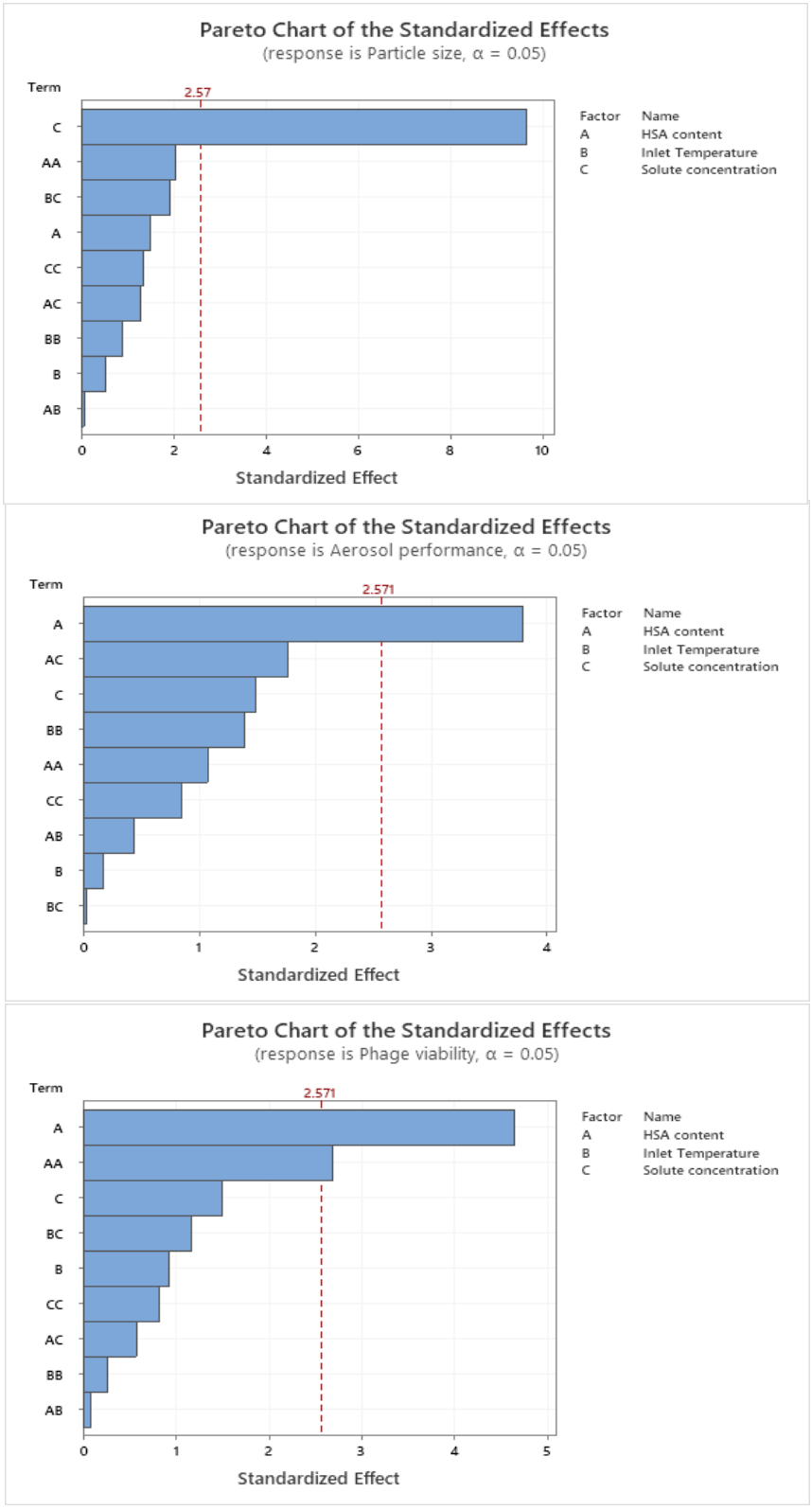


**A**

**B**

**C**

Fig.4. Pareto charts show the standardized impact of independent variables and their interactions on (a) particle size, (b) aerosol performance, and (c) phage viability. Factors that exceed the vertical line are considered statistically significant.

**Particle size distribution**

All spray-dried powders exhibited $D_{90}$ values below 5 µm (Table 3). The center point formulations (F5, F8 and F11) had average $D_{10}$, $D_{50}$, and $D_{90}$ values of 1.0 ± 0.05 µm, 2.03 ± 0.07 µm, and 4.0 ± 0.19 µm, respectively. Span values ranged from 1.2 to 4.1 across all formulations.

Table 3. Particle size distribution and moisture content of all formulations

| Formulation | $D_{10}$ (µm) | $D_{50}$ (µm) | $D_{90}$ (µm) | Span | Moisture content (wt%) | Tg (˚C) |
|---|---|---|---|---|---|---|
| F1 | 0.48 ± 0.02 | 2.00 ± 0.00 | 4.42 ± 0.08 | 1.97 ± 0.05 | 1.20 ± 0.02 | 73 |
| F2 | 0.60 ± 0.35 | 1.97 ± 0.16 | 3.74 ± 0.18 | 1.61 ± 0.21 | 4.10 ± 0.71 | ND |
| F3 | 1.01 ± 0.01 | 1.83 ± 0.05 | 4.30 ± 0.25 | 1.80 ± 0.17 | 2.73 ± 0.15 | ND |
| F4 | 0.90 ± 0.09 | 1.73 ± 0.04 | 4.06 ± 0.22 | 1.83 ± 0.20 | 1.56 ± 0.62 | 68 |
| F5 | 0.97 ± 0.01 | 2.02 ± 0.09 | 4.20 ± 0.54 | 1.59 ± 0.22 | 3.35 ± 0.82 | ND |
| F6 | 1.11 ± 0.06 | 2.33 ± 0.18 | 4.46 ± 0.71 | 1.42 ± 0.23 | 2.79 ± 0.13 | 68 |
| F7 | 1.07 ± 0.04 | 2.19 ± 0.12 | 4.35 ± 0.60 | 1.48 ± 0.20 | 1.94 ± 0.12 | 70 |
| F8 | 0.95 ± 0.08 | 1.94 ± 0.06 | 3.74 ± 0.48 | 1.44 ±0.16 | 2.16 ± 0.28 | 70 |
| F9 | 0.89 ± 0.14 | 1.96 ± 0.06 | 3.49 ± 0.20 | 1.32 ± 0.13 | 2.17 ± 0.52 | ND |
| F10 | 0.57 ± 0.09 | 1.98 ± 0.02 | 4.00 ± 0.16 | 1.73 ± 0.05 | 4.00 ± 0.34 | 66 |
| F11 | 1.07 ± 0.04 | 2.12 ± 0.04 | 4.03 ± 0.22 | 1.39 ± 0.13 | 1.67 ± 0.22 | ND |
| F12 | 1.06 ± 0.06 | 2.15 ± 0.05 | 4.09 ± 0.13 | 1.41 ± 0.07 | 3.10 ± 0.18 | ND |
| F13 | 1.04 ± 0.01 | 2.15 ± 0.04 | 4.14 ± 0.27 | 1.44 ± 0.10 | 1.55 ± 0.12 | ND |
| F14 | 0.68 ± 0.04 | 1.72 ± 0.09 | 3.29 ± 0.21 | 1.52 ± 0.09 | 3.12 ± 0.11 | ND |
| F15 | 0.86 ± 0.01 | 1.50 ± 0.01 | 2.42 ± 0.00 | 1.04 ± 0.01 | 3.24 ± 0.14 | ND |

ND- not discernible

**Particle morphology**

At 20% w/w HSA (F1, F4, F7, and F10), the spray-dried phage particles displayed spherical morphology, with only minor surface grooves observed on some larger particles (Fig. 5). In contrast, when the HSA concentration increased to 100% (F2, F9, F12, and F15), the particles generally remained spherical but exhibited deep wrinkles on their surfaces.

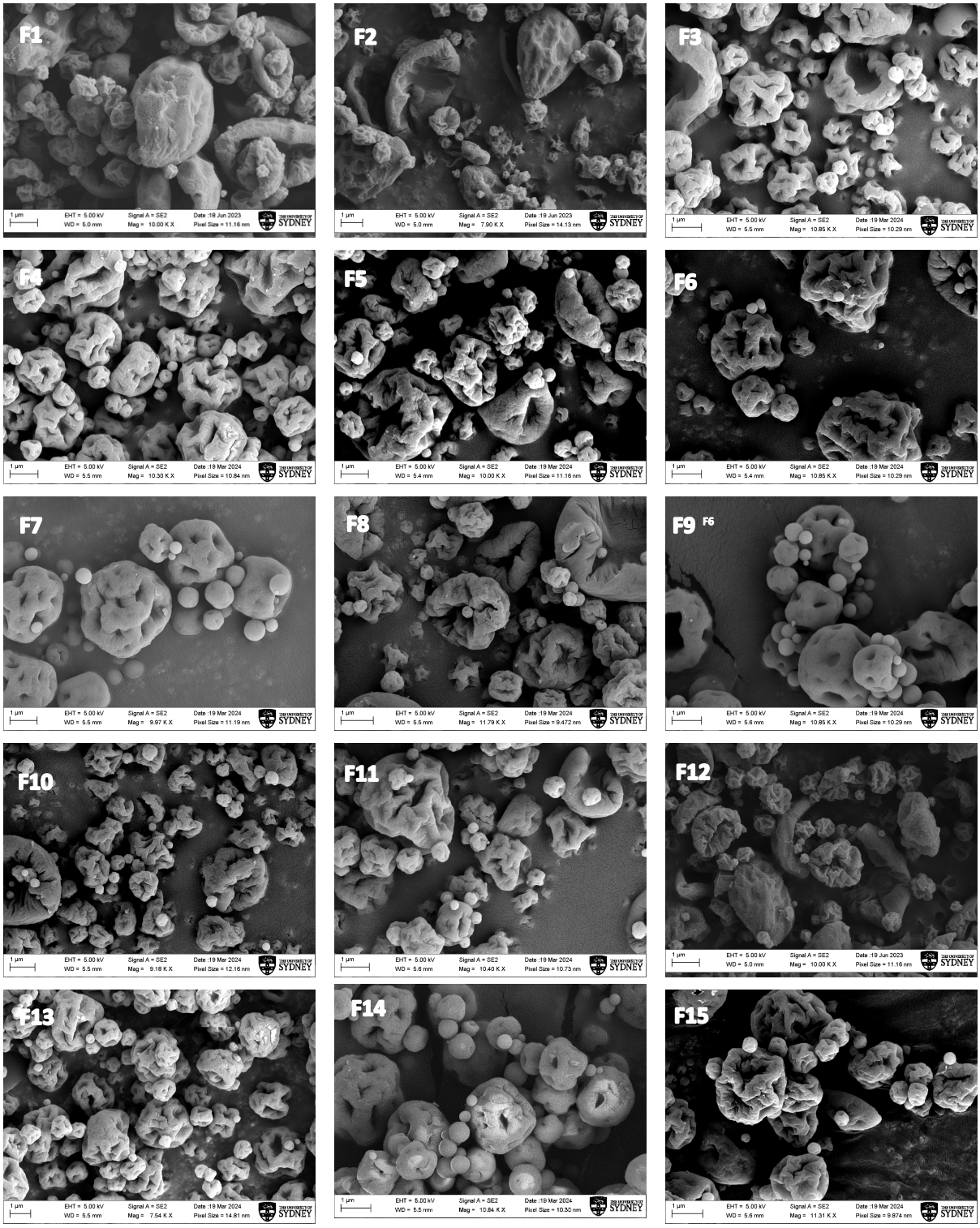

Fig. 5. Scanning electron microscopy (SEM) images of phage formulations F1 to F15.

**Aerosol performance**

FPF was increased with higher HSA concentrations. Formulation F15, which contained the highest HSA concentration, achieved an FPF of 63%, while formulation F7, with the lowest HSA concentration, had an FPF of 36.1% (Fig. 6a). The FPF for formulations containing 60% w/w HSA was 51.7 ± 4.3%.

All formulations demonstrated EF above 60% (Fig. 6b). Formulations with HSA concentrations exceeding 60% w/w consistently achieved EF values above 80%. Notably, formulation F15, with the highest HSA content, attained an EF of 87%, whereas formulation F7, with only 20% w/w HSA, exhibited the lowest EF of 61%. The EF for 60% w/w HSA formulations was 81.9 ± 7.0%.

At the lowest inlet temperature of 50°C, formulations F1, F2, and F6 displayed a wide range of titre losses, from 2.5 to 0.2 $\log_{10}$. When the inlet temperature was increased to the highest level of 80°C, F9 (with 100% w/w HSA) lost more than 2 $\log_{10}$. In contrast, F10 (with 80% w/w lactose) exhibited losses of approximately 1 $\log_{10}$.

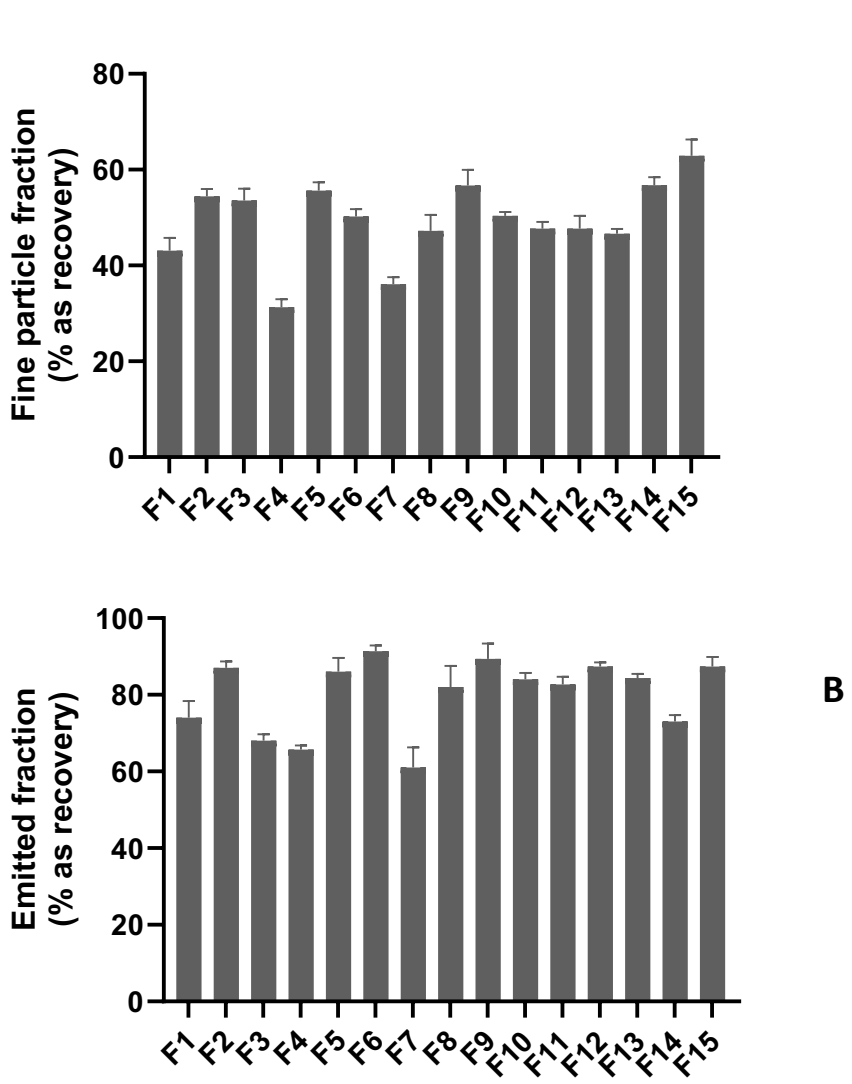


Fig.6. Aerosol performance of 15 spray-dried phage formulations: (a) Fine particle fraction (FPF) and (b) Emitted fraction (EF).

**Phage viability**

Phage bioactivity was evaluated by measuring the $\log_{10}$ titre loss under various formulation conditions (Fig. 7). At the highest HSA concentration of 100% (F2, F9, F12, and F15), bioactivity was compromised, with losses exceeding 2 $\log_{10}$. In contrast, reducing HSA to the lowest level of 20% (F1, F4, and F7) improved bioactivity retention, with titre losses remaining below 1 $\log_{10}$.

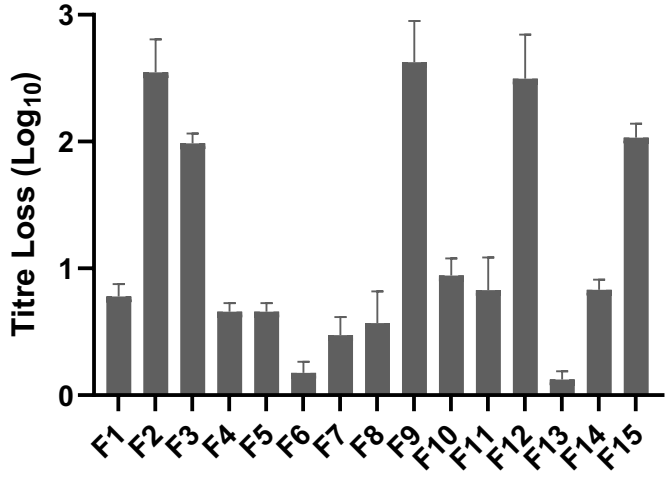


Fig.7. Titre loss of PEV2 after spray-drying process (n=3).

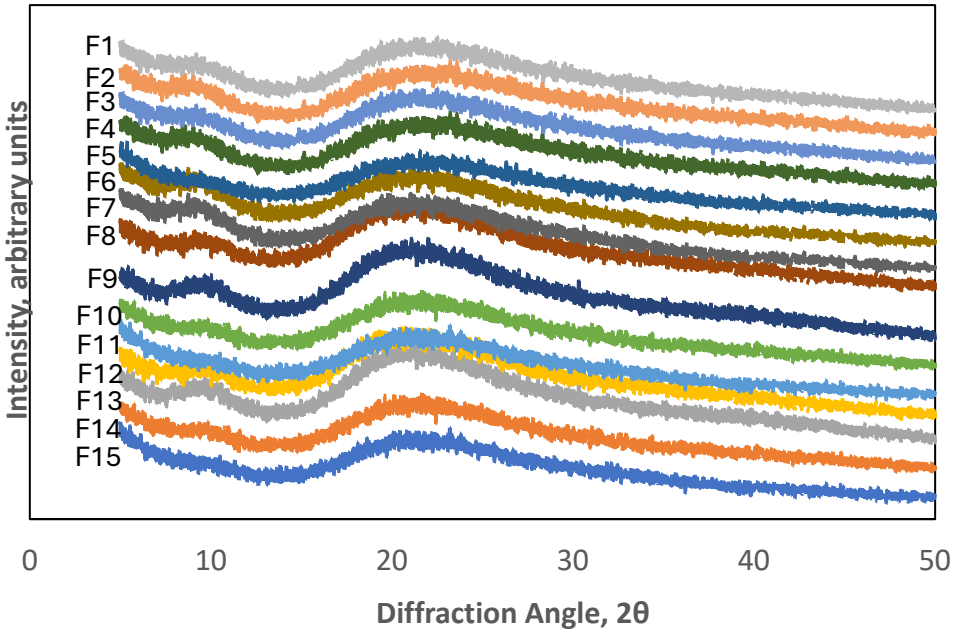


Fig. 8. Powder X-ray diffractograms of spray-dried phage powder formulations from 2θ values of 5° to 50°.

**Solid state characterization**

The solid-state properties of the spray-dried powders were characterized using XRD, DSC, TGA and moisture sorption. XRD analysis revealed the absence of crystalline peaks for all formulations (Fig. 8).TGA analysis indicated that the water content of all formulations ranged from 1.2% to 4.1% w/w (Table 3). (Table.3).

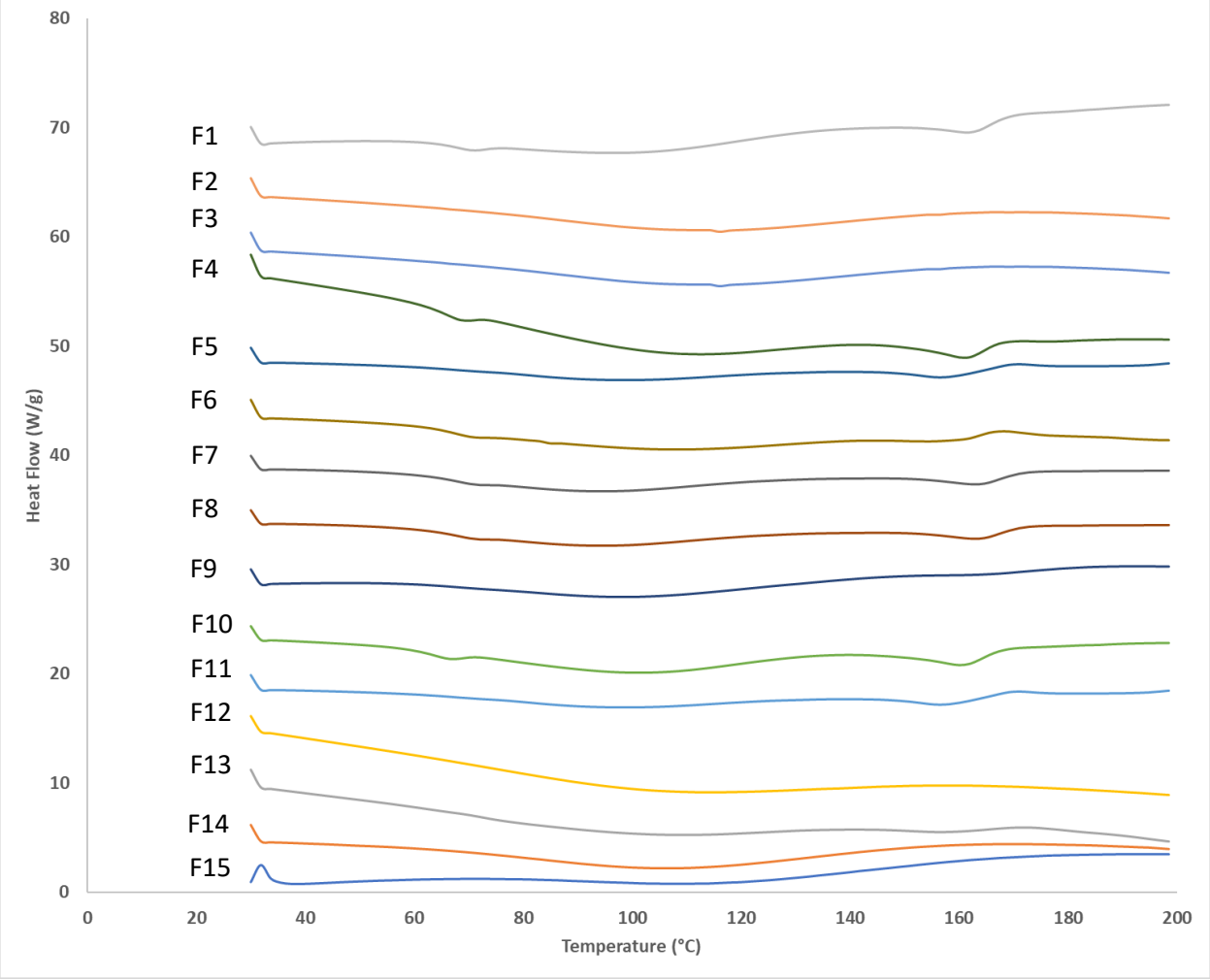


Fig.9. Differential scanning calorimetry (DSC) thermograms of spray-dried powder samples, measured from 30°C to 200°C. The negative peaks indicate endothermic events.

DSC analysis did not detect a glass transition temperature (Tg) for the 100% w/w HSA powders (F2, F9, F12, F15) (Fig. 9). The moisture content, as determined by TGA, decreased with increasing inlet temperature: 4.10 ± 0.71% at 50°C (F2), 3.10 ± 0.18% at 65°C (F9), 3.24 ± 0.14% at 65°C (F12), and 2.17 ± 0.52% at 80°C (F15).

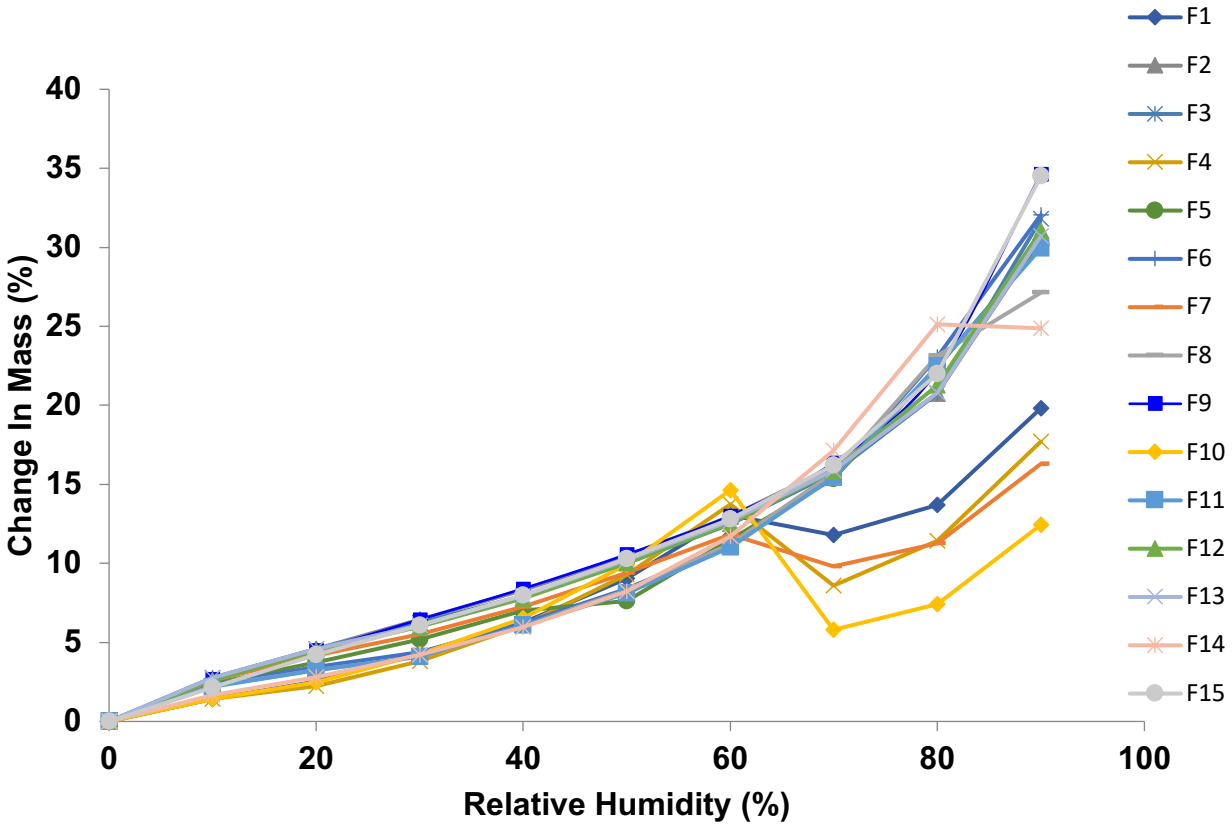


Fig.10. Vapor sorption profiles of formulations F1–F15 under ramped RH from 0 to 90%.

For the 80% lactose/20% HSA formulations (F1, F4, F7, F10), DSC analysis demonstrated that Tg inversely correlated with moisture content: F1 (1.20% moisture, Tg 72°C), F4 (1.56%, 68°C), F7 (1.94%, 70°C), and F10 (4.00%, 66°C).

DSC analysis did not detect Tg for the 60% lactose/40% HSA formulations (F3, F5, F11, F13, F14), except F6 and F8 which showed Tg values of 68°C and 70°C, with moisture content of 2.79 ± 0.13% and 2.16 ± 0.28%, respectively.

Formulations F1, F4, F7, and F10 (20% w/w HSA) exhibited a mass increase as RH rose from 0% to 60%, followed by a reduction in mass between 60% and 70% RH (Fig.10). Formulation F14 (60% w/w HSA) showed a similar initial trend, with mass increasing from 0% to 80% RH before declining between 80% and 90% RH. In contrast, formulations F3, F5, F6, F8, F11, and F33 (60% w/w HSA) demonstrated progressive mass gain across the entire RH range (0% to 90%). Formulations F2, F9, F12, and F15 (100% w/w HSA) displayed consistent mass accumulation from 0% to 90% RH. Notably, F15 exhibited the highest moisture uptake, with a maximum absorption of 14.6% w/w.

## Discussion

In this study, we developed an inhalable dry powder formulation for pulmonary delivery of the *P. aeruginos*a–specific phage PEV2. We found that combining human serum albumin (HSA) with lactose would enhance phage stability and aerosol performance, offering an improved platform for inhalable phage therapies. To further investigate this approach, we used a Box–Behnken experimental design to examine how the HSA/lactose ratio, the solute concentration of the feed solution, and the spray-drying inlet temperature affect phage viability and aerosol properties.

The response surface analysis revealed that the ratio of HSA and lactose is the key factor affecting both the powder aerosolization efficiency and the maintenance of phage viability. Within the studied range of 50°-80°C, changes in inlet temperature had little direct effect on phage viability, indicating that the formulations are thermally robust under the conditions applied. Higher HSA concentrations led to a significant improvement in FPF, underscoring the importance of HSA in promoting effective powder dispersion. Although the solute concentration (HSA and lactose) was not a major contributor overall, formulations with lower

solute concentrations yielded particles that were more porous and less dense, which further enhanced aerosol performance. Therefore, carefully balancing HSA concentration with appropriate solute levels and inlet temperature is critical to achieving both efficient aerosolization and sustained phage viability.

HSA plays a critical role in enhancing the aerosol performance of dry powder inhaler formulations. The spray-dried powders exhibited optimal volume median diameters ($D_{50}$) below 2.5 μm (Table 3). SEM analyses showed that the particle morphology was influenced by HSA content. Formulations with 20% w/w HSA produced predominantly spherical particles, while those with 100% w/w HSA yielded highly wrinkled particles (Fig. 1). This morphological shift is primarily due to rapid solvent evaporation during spray drying, characterized by high Péclet numbers (Pe ~$10^3$), which drives protein enrichment at the particle surface (258). As Chow et al. have noted, this enrichment occurs during the drying process of HSA (259). The resulting rigid shell undergoes inward buckling due to surface tension gradients, reducing interparticle contact area by approximately 40% (260), (261). We observed that increasing HSA content from 20% w/w to 100% w/w significantly improved the FPF from 31% to 63%, far exceeding the typical 20–40% range observed in commercial inhalers (262). This enhanced FPF, coupled with a $D_{50}$ below 2.5 μm, underscores the formulation's potential for effective deep lung delivery. Such characteristics are especially pertinent for the treatment of respiratory infections in cystic fibrosis (CF) patients, where the pathogen *P. aeruginosa* predominantly colonizes the lower airways. However, CF lungs present challenges like thick mucus, narrowed airways, and uneven airflow, which can cause the particles to deposit unevenly—favoring well-ventilated areas and leaving blocked regions undertreated. This approach is similar to inhaled antibiotics, which improve lung function and reduce flare-ups in CF patients (263). Effective

delivery is key at all disease stages, from early infection to chronic biofilms. However, in *vivo* studies are needed to confirm how well it works in the complex, mucus-filled, and inflamed CF lung environment. Furthermore, formulations with HSA levels above 60% w/w consistently achieved an EF greater than 80%, indicating a marked reduction in not just the powder cohesiveness, but also powder adhesion to the inhaler interior surfaces and together, a corresponding improvement in dispersion efficiency. These findings align with previous research using bovine serum albumin (BSA), which demonstrated that spray drying produces particles with a highly corrugated surface morphology, enhancing aerosol performance by reducing interparticle contact and cohesive forces (264, 265). The benefits of HSA-based formulations are further enhanced by the protein's intrinsic surfactant-like properties, superior biocompatibility, and lower propensity to trigger allergic reactions, making them advantageous for clinical applications (254).

The stabilization mechanisms of HSA in phage powder formulations are critical for maintaining phage viability. The results demonstrate that HSA at 20%–40% w/w significantly reduces titer losses (<1 $\log_{10}$), whereas 100% w/w HSA compromises phage bioactivity (>2 $\log_{10}$ losses). HSA likely mitigates interfacial stresses to phages during spray drying by adsorbing to the air-liquid interface, preventing phage denaturation at droplet surfaces, as observed in protein stabilization studies (266). By acting as ‘sacrificial’ protein molecules at the interface, HSA undergoes unfolding instead of the phage structural proteins, thereby sparing the phages from deactivation. Additionally, HSA’s thiol groups, particularly the free cysteine residue (Cys-34), act as antioxidants, scavenging reactive oxygen species to protect phage capsid proteins from potential oxidative damage (267). Notably, the protection of phage stability offered by HSA is achievable at a concentration of 20% w/w, with no further benefits

observed at 40% w/w, suggesting a threshold beyond which further increases in HSA concentration yields diminishing returns. In fact, paradoxically formulations with HSA alone (100% w/w) reveal the opposite effect with significant titer loss. The pure HSA matrix has a very low glass transition temperature (Tg) below 0°C (268). Consequently, at room temperature, it remains in a rubbery state with increased molecular mobility, facilitating degradation processes in the phage and explaining the observed titer loss of more than 2 $\log_{10}$. This highlights the importance of optimizing HSA concentrations to balance stabilization and minimize adverse degradation.

The co-stabilization of phages by HSA and lactose is fundamental to preserving their viability, as evidenced by formulations with 80% w/w lactose and 20% w/w HSA (e.g., F1, F4, F7, F10), which achieve titer losses <1 $\log_{10}$. Each component contributes a distinct protective mechanism, together ensuring robust stability during drying and storage. Lactose is a suitable excipient for pulmonary applications due to its FDA approval for inhalation products. It can form an amorphous, glassy matrix that enables vitrification of biologics (269), and in the present case, phages and HSA within a rigid structure, preserving their integrity. This is consistent with previous reports that phages can be sufficiently stabilized by immobilization inside a rigid glassy sugar matrix (78). Under thermal stress at 80°C during spray drying, high-lactose formulation like F10 (Tg 72°C) show titer losses of approximately 1 $\log_{10}$, compared to more than 2 $\log_{10}$ for non-lactose formulations like F2, highlighting lactose's role in vitrification. At the molecular level, HSA interacts with lactose through hydrogen bonds between its polar residues (e.g., lysine, arginine) and lactose's hydroxyl groups, stabilizing the matrix and enhancing phage embedding, as supported by studies on protein-sugar interactions (89). Additionally, HSA delays lactose recrystallization under high humidity, maintaining the

protective glassy state of lactose. While high Tg of 80% w/w lactose ensures phage stability in dry conditions, recrystallization at 60% RH will disrupt the glassy matrix. Formulations with 60% w/w HSA content resist recrystallization of lactose at 80% RH and remain amorphous, owing to HSA's stabilizing interactions with lactose. Conversely, 100% w/w HSA formulations lacking a measurable Tg absorb higher moisture and fail to protect phages, emphasizing the need for the presence of both HSA and lactose for stabilization. The experimental results from this study reveal a significant interplay between moisture content and the Tg in spray-dried formulations containing HSA and lactose, corroborating the plasticizing role of residual water. Specifically, for the formulation of 80% w/w lactose and 20% w/w HSA, as the inlet temperature increased from 50°C to 80°C the moisture content increased from 1.2% to 4.0%, accompanied by a decrease in Tg from 72°C to 66°C. These results indicate that higher moisture content corresponds to a lower Tg in these formulations. However, a slight anomaly is observed between F4 and F7, where F7, with a higher moisture content (1.94%) compared to F4 (1.56%), exhibited a marginally higher Tg (70°C vs. 68°C). This minor discrepancy may be attributed to experimental variability, potentially arising from the large standard deviation in F4's moisture content (±0.62%) or subtle differences in sample preparation. Despite this, the overall pattern across F1, F4, F7, and F10 supports the inverse relationship between moisture content and Tg. This behavior aligns with the well-established plasticizing effect of water in amorphous systems, where residual moisture enhances molecular mobility within the matrix, thereby reducing Tg (104). Additionally, HSA's high moisture uptake allows residual water to act as a plasticizer, further lowering its effective Tg (104). The elevated moisture retention attributed to HSA is evident when comparing formulations: the 100% w/w HSA powders exhibited moisture contents ranging from 2.17% to 4.1%, notably higher than those with lower HSA proportions, although Tg values were not observed for these samples. Further evidence

emerges from the 60% w/w HSA formulation processed at 50°C, where moisture contents of 2.79 ± 0.13% and 2.16 ± 0.28% corresponded to Tg values of 68°C and 70°C, respectively, indicating that even modest differences in moisture can measurably affect Tg. These observations highlight HSA's role in amplifying moisture-related effects, consistent with the principles outlined by Hancock and Zografi (1994), who emphasized water's plasticizing impact on amorphous solids. Consequently, these findings suggest that careful control of moisture levels during processing and storage of HSA-containing formulations is critical to maintaining desirable Tg values, which in turn will influence physical stability and shelf-life. Thus, HSA and lactose comprehensively address phage inactivation pathways: lactose ensures structural rigidity of phages and HSA via vitrification while HSA mitigates spray drying process-induced stresses (interfacial stress and oxidation) and bolsters amorphous stability of the lactose glassy matrix.

From a manufacturing standpoint, the HSA–lactose phage powder platform is readily translatable to industrial scale spray-drying. Both HSA and lactose are available at bulk, pharmaceutical-grade quality and are compatible with continuous-feed spray dryers (e.g., GEA Niro). Key scale-up parameters—such as feed-solution solute concentration, atomizer type (two-fluid nozzle or rotary atomizer), inlet/outlet temperatures, and spray-gas flow—can be maintained to preserve particle morphology and phage viability. The industrial scalability of spray drying for inhalable pharmaceuticals is well-established, as demonstrated by the successful commercialization of products like Aridol, Bronchitol, Exubera, Afrezza, and TOBI Podhaler. These examples illustrate the technology's ability to produce consistent, high-quality dry powders at large scales, with precise control over particle characteristics critical for inhalation therapy. The adaptability of spray drying to various active ingredients—ranging

from small molecules to proteins —further supports its suitability for the HSA–lactose phage platform, where maintaining phage viability and aerosol performance is paramount. Leveraging this proven manufacturing process, the platform can seamlessly transition from laboratory to industrial production, ensuring both scalability and therapeutic efficacy.

While this study provides valuable insights into the formulation of inhalable phage powders, several limitations remain. First, the precise molecular mechanisms by which HSA confers protection during spray drying, including possibly the effects of macromolecular crowding and finite interfacial adsorption, require further elucidation under various drying conditions. Secondly, long-term stability, especially under different humidity and storage environments, warrants comprehensive evaluation, as moisture-induced changes could significantly impact phage viability and aerosol performance. Interestingly, formulation F10, processed at the highest inlet temperature of 80°C, retained a moisture content of 4.0%. The mechanism underlying the increase in moisture content with elevated inlet temperatures remains unclear and requires further investigation. Additionally, the generalizability of our findings beyond the PEV2 phage is unclear; phages vary in structural robustness, potentially influencing their stability and viability under spray-drying stresses. Future research should address these gaps by examining detailed protein-phage interactions, systematically assessing storage stability across diverse environmental conditions, and validating formulation strategies for multiple phage types. By clarifying these critical aspects, the clinical potential and applicability of inhalable phage therapies can be fully realized.

## Conclusions

This work represents the first study incorporating HSA as a performance-enhancing excipient into inhalable phage dry powders, optimized by a Box–Behnken design to achieve both high

powder dispersibility and minimal phage titer loss. The optimized powders (60% w/w HSA / 40% w/w lactose) demonstrated favorable aerosol performance, achieving a FPF exceeding 50% and minimizing phage titer loss to less than 1 $\log_{10}$.While the combination of HSA and lactose effectively protected phages during spray drying, HSA notably enhanced powder dispersion and mitigated lactose recrystallization. Although further research is needed to elucidate the protective mechanisms of HSA, this formulation strategy represents a promising platform for phage delivery.

## References


1. Blair JM, Webber MA, Baylay AJ, Ogbolu DO, Piddock LJ. Molecular mechanisms of antibiotic resistance. Nat Rev Microbiol. 2015;13(1):42-51.
2. Murray CJ, Ikuta KS, Sharara F, Swetschinski L, Aguilar GR, Gray A, Han C, Bisignano C, Rao P, Wool E. Global burden of bacterial antimicrobial resistance in 2019: a systematic analysis. The lancet. 2022;399(10325):629-55.
3. Tacconelli E, Carrara E, Savoldi A, Harbarth S, Mendelson M, Monnet DL, Pulcini C, Kahlmeter G, Kluytmans J, Carmeli Y. Discovery, research, and development of new antibiotics: the WHO priority list of antibiotic-resistant bacteria and tuberculosis. The Lancet infectious diseases. 2018;18(3):318-27.
4. von Wintersdorff CJ, Penders J, van Niekerk JM, Mills ND, Majumder S, van Alphen LB, Savelkoul PH, Wolffs PF. Dissemination of Antimicrobial Resistance in Microbial Ecosystems through Horizontal Gene Transfer. Front Microbiol. 2016;7:173.
5. Ventola CL. The antibiotic resistance crisis: part 1: causes and threats. P T. 2015;40(4):277-83.
6. Collignon PJ, McEwen SA. One Health-Its Importance in Helping to Better Control Antimicrobial Resistance. Trop Med Infect Dis. 2019;4(1).
7. Flemming H-C, Wuertz S. Bacteria and archaea on Earth and their abundance in biofilms. Nature Reviews Microbiology. 2019;17(4):247-60.
8. Theuretzbacher U, Outterson K, Engel A, Karlen A. The global preclinical antibacterial pipeline. Nat Rev Microbiol. 2020;18(5):275-85.
9. Garcia-Vidal C, Stern A, Gudiol C. Multidrug-resistant, gram-negative infections in high-risk haematologic patients: an update on epidemiology, diagnosis and treatment. Curr Opin Infect Dis. 2021;34(4):314-22.
10. Pang Z, Raudonis R, Glick BR, Lin TJ, Cheng Z. Antibiotic resistance in Pseudomonas aeruginosa: mechanisms and alternative therapeutic strategies. Biotechnol Adv. 2019;37(1):177-92.
11. Ardebili A, Izanloo A, Rastegar M. Polymyxin combination therapy for multidrug-resistant, extensively-drug resistant, and difficult-to-treat drug-resistant gram-negative infections: is it superior to polymyxin monotherapy? Expert review of anti-infective therapy. 2023;21(4):387-429.
12. Hareza DA, Cosgrove SE, Bonomo RA, Dzintars K, Karaba SM, Hawes AM, Tekle T, Simner PJ, Tamma PD. Clinical outcomes and emergence of resistance of Pseudomonas aeruginosa infections treated with ceftolozane-tazobactam versus ceftazidime-avibactam. Antimicrobial agents and chemotherapy. 2024;68(10):e00907-24.
13. Salmond GP, Fineran PC. A century of the phage: past, present and future. Nat Rev Microbiol. 2015;13(12):777-86.
14. Nobrega FL, Costa AR, Kluskens LD, Azeredo J. Revisiting phage therapy: new applications for old resources. Trends in microbiology. 2015;23(4):185-91.
15. Sulakvelidze A, Alavidze Z, Morris JG, Jr. Bacteriophage therapy. Antimicrob Agents Chemother. 2001;45(3):649-59.
16. Kutter E, De Vos D, Gvasalia G, Alavidze Z, Gogokhia L, Kuhl S, Abedon ST. Phage therapy in clinical practice: treatment of human infections. Curr Pharm Biotechnol. 2010;11(1):69-86.
17. Pirnay JP, Verbeken G, Ceyssens PJ, Huys I, De Vos D, Ameloot C, Fauconnier A. The Magistral Phage. Viruses. 2018;10(2).
18. Furfaro LL, Payne MS, Chang BJ. Bacteriophage Therapy: Clinical Trials and Regulatory Hurdles. Front Cell Infect Microbiol. 2018;8:376.
19. Łusiak-Szelachowska M, Weber-Dąbrowska B, Jończyk-Matysiak E, Wojciechowska R, Górski A. Bacteriophages in the gastrointestinal tract and their implications. Gut pathogens. 2017;9(1):44.

20. Roach DR, Donovan DM. Antimicrobial bacteriophage-derived proteins and therapeutic applications. Bacteriophage. 2015;5(3):e1062590.
21. Jault P, Leclerc T, Jennes S, Pirnay JP, Que Y-A, Resch G, Rousseau AF, Ravat F, Carsin H, Le Floch R. Efficacy and tolerability of a cocktail of bacteriophages to treat burn wounds infected by Pseudomonas aeruginosa (PhagoBurn): a randomised, controlled, double-blind phase 1/2 trial. The Lancet Infectious Diseases. 2019;19(1):35-45.
22. Topka-Bielecka G, Dydecka A, Necel A, Bloch S, Nejman-Faleńczyk B, Węgrzyn G, Węgrzyn A. Bacteriophage-derived depolymerases against bacterial biofilm. Antibiotics. 2021;10(2):175.
23. Das T, Kutty SK, Tavallaie R, Ibugo AI, Panchompoo J, Sehar S, Aldous L, Yeung AW, Thomas SR, Kumar N. Phenazine virulence factor binding to extracellular DNA is important for Pseudomonas aeruginosa biofilm formation. Scientific Reports. 2015;5(1):8398.
24. Lim ES, Zhou Y, Zhao G, Bauer IK, Droit L, Ndao IM, Warner BB, Tarr PI, Wang D, Holtz LR. Early life dynamics of the human gut virome and bacterial microbiome in infants. Nature medicine. 2015;21(10):1228-34.
25. Onallah H, Hazan R, Nir-Paz R, editors. Compassionate use of bacteriophages for failed persistent infections during the first 5 years of the Israeli phage therapy center. Open forum infectious diseases; 2023: Oxford University Press US.
26. Suh GA, Lodise TP, Tamma PD, Knisely JM, Alexander J, Aslam S, Barton KD, Bizzell E, Totten KMC, Campbell JL, Chan BK, Cunningham SA, Goodman KE, Greenwood-Quaintance KE, Harris AD, Hesse S, Maresso A, Nussenblatt V, Pride D, Rybak MJ, Sund Z, van Duin D, Van Tyne D, Patel R, Antibacterial Resistance Leadership G. Considerations for the Use of Phage Therapy in Clinical Practice. Antimicrob Agents Chemother. 2022;66(3):e0207121.
27. Leung SSY, Parumasivam T, Gao FG, Carter EA, Carrigy NB, Vehring R, Finlay WH, Morales S, Britton WJ, Kutter E, Chan HK. Effects of storage conditions on the stability of spray dried, inhalable bacteriophage powders. Int J Pharm. 2017;521(1-2):141-9.
28. Chang RY, Wong J, Mathai A, Morales S, Kutter E, Britton W, Li J, Chan HK. Production of highly stable spray dried phage formulations for treatment of Pseudomonas aeruginosa lung infection. Eur J Pharm Biopharm. 2017;121:1-13.
29. Regulski K, Champion-Arnaud P, Gabard J. Bacteriophage manufacturing: From early twentieth-century processes to current GMP. Bacteriophages: Biology, Technology, Therapy. 2021:699-729.
30. Yehl K, Lemire S, Yang AC, Ando H, Mimee M, Torres MDT, de la Fuente-Nunez C, Lu TK. Engineering phage host-range and suppressing bacterial resistance through phage tail fiber mutagenesis. Cell. 2019;179(2):459-69. e9.
31. Bikard D, Euler CW, Jiang W, Nussenzweig PM, Goldberg GW, Duportet X, Fischetti VA, Marraffini LA. Exploiting CRISPR-Cas nucleases to produce sequence-specific antimicrobials. Nat Biotechnol. 2014;32(11):1146-50.
32. Abedon ST. Phage-antibiotic combination treatments: antagonistic impacts of antibiotics on the pharmacodynamics of phage therapy? Antibiotics. 2019;8(4):182.
33. Schooley RT, Biswas B, Gill JJ, Hernandez-Morales A, Lancaster J, Lessor L, Barr JJ, Reed SL, Rohwer F, Benler S, Segall AM, Taplitz R, Smith DM, Kerr K, Kumaraswamy M, Nizet V, Lin L, McCauley MD, Strathdee SA, Benson CA, Pope RK, Leroux BM, Picel AC, Mateczun AJ, Cilwa KE, Regeimbal JM, Estrella LA, Wolfe DM, Henry MS, Quinones J, Salka S, Bishop-Lilly KA, Young R, Hamilton T. Development and Use of Personalized Bacteriophage-Based Therapeutic Cocktails To Treat a Patient with a Disseminated Resistant Acinetobacter baumannii Infection. Antimicrob Agents Chemother. 2017;61(10).

34. Dedrick RM, Guerrero-Bustamante CA, Garlena RA, Russell DA, Ford K, Harris K, Gilmour KC, Soothill J, Jacobs-Sera D, Schooley RT. Engineered bacteriophages for treatment of a patient with a disseminated drug-resistant Mycobacterium abscessus. Nature medicine. 2019;25(5):730-3.
35. Merabishvili M, Pirnay J-P, De Vos D. Guidelines to compose an ideal bacteriophage cocktail. Bacteriophage Therapy: From Lab to Clinical Practice. 2023:49-66.
36. Le S, He X, Tan Y, Huang G, Zhang L, Lux R, Shi W, Hu F. Mapping the tail fiber as the receptor binding protein responsible for differential host specificity of Pseudomonas aeruginosa bacteriophages PaP1 and JG004. PloS one. 2013;8(7):e68562.
37. Bürkle M, Korf IH, Lippegaus A, Krautwurst S, Rohde C, Weissfuss C, Nouailles G, Tene XM, Gaborieau B, Ghigo J-M. Phage–phage competition and biofilms affect interactions between two virulent bacteriophages and Pseudomonas aeruginosa. The ISME Journal. 2025;19(1):wraf065.
38. Roach DR, Leung CY, Henry M, Morello E, Singh D, Di Santo JP, Weitz JS, Debarbieux L. Synergy between the host immune system and bacteriophage is essential for successful phage therapy against an acute respiratory pathogen. Cell host & microbe. 2017;22(1):38-47. e4.
39. Weitz JS, Hartman H, Levin SA. Coevolutionary arms races between bacteria and bacteriophage. Proceedings of the National Academy of Sciences. 2005;102(27):9535-40.
40. Wright RC, Friman V-P, Smith MC, Brockhurst MA. Resistance evolution against phage combinations depends on the timing and order of exposure. MBio. 2019;10(5):10.1128/mbio. 01652-19.
41. Leung CYJ, Weitz JS. Modeling the synergistic elimination of bacteria by phage and the innate immune system. J Theor Biol. 2017;429:241-52.
42. Pressler T, Bohmova C, Conway S, Dumcius S, Hjelte L, Hoiby N, Kollberg H, Tummler B, Vavrova V. Chronic Pseudomonas aeruginosa infection definition: EuroCareCF Working Group report. J Cyst Fibros. 2011;10 Suppl 2:S75-8.
43. Doudakmanis C, Makris D. Ventilator-Associated Pneumonia in Patients With Increased Intra-abdominal Pressure. Cureus. 2025;17(3):e81370.
44. Kwok WC, Ho JCM, Tam TCC, Ip MSM, Lam DCL. Risk factors for Pseudomonas aeruginosa colonization in non-cystic fibrosis bronchiectasis and clinical implications. Respir Res. 2021;22(1):132.
45. Pearson JP, Pesci EC, Iglewski BH. Roles of Pseudomonas aeruginosa las and rhl quorum-sensing systems in control of elastase and rhamnolipid biosynthesis genes. J Bacteriol. 1997;179(18):5756-67.
46. Wiens JR, Vasil AI, Schurr MJ, Vasil ML. Iron-regulated expression of alginate production, mucoid phenotype, and biofilm formation by Pseudomonas aeruginosa. mBio. 2014;5(1):e01010-13.
47. Everett MJ, Davies DT. Pseudomonas aeruginosa elastase (LasB) as a therapeutic target. Drug Discovery Today. 2021;26(9):2108-23.
48. Rose MC. Mucins: structure, function, and role in pulmonary diseases. American Journal of Physiology-Lung Cellular and Molecular Physiology. 1992;263(4):L413-L29.
49. Giannoni E, Sawa T, Allen L, Wiener-Kronish J, Hawgood S. Surfactant proteins A and D enhance pulmonary clearance of Pseudomonas aeruginosa. American journal of respiratory cell and molecular biology. 2006;34(6):704-10.
50. Giacalone VD, Margaroli C, Mall MA, Tirouvanziam R. Neutrophil adaptations upon recruitment to the lung: new concepts and implications for homeostasis and disease. International Journal of Molecular Sciences. 2020;21(3):851.
51. Hu D, Zou L, Yu W, Jia F, Han H, Yao K, Jin Q, Ji J. Relief of Biofilm Hypoxia Using an Oxygen Nanocarrier: A New Paradigm for Enhanced Antibiotic Therapy. Adv Sci (Weinh). 2020;7(12):2000398.
52. Eriksson J, Thörn H, Lennernäs H, Sjögren E. Pulmonary drug absorption and systemic exposure in human: Predictions using physiologically based biopharmaceutics modeling. European Journal of Pharmaceutics and Biopharmaceutics. 2020;156:191-202.

53. Fowoyo PT. Phage therapy: clinical applications, efficacy, and implementation hurdles. The Open Microbiology Journal. 2024;18(1).
54. Sharma R. Plenary Lecture: INHALED DRUG DELIVERY, PAST, PRESENT AND FUTURE: A THERAPEUTIC PERSPECTIVE. J Aerosol Med. 2000;13(1):59-72.
55. Shah KA, Razzaq A, Dormocara A, You B, Elbehairi SEI, Shati AA, Alfaifi MY, Iqbal H, Cui J-H. Current trends in inhaled pharmaceuticals: challenges and opportunities in respiratory infections treatment. Journal of Pharmaceutical Investigation. 2025:1-35.
56. Houtmeyers E, Gosselink R, Gayan-Ramirez G, Decramer M. Regulation of mucociliary clearance in health and disease. European Respiratory Journal. 1999;13(5):1177-88.
57. Jin Z, Gao Q, Wu K, Ouyang J, Guo W, Liang XJ. Harnessing inhaled nanoparticles to overcome the pulmonary barrier for respiratory disease therapy. Adv Drug Deliv Rev. 2023;202:115111.
58. Chow MYT, Chang RYK, Li M, Wang Y, Lin Y, Morales S, McLachlan AJ, Kutter E, Li J, Chan HK. Pharmacokinetics and Time-Kill Study of Inhaled Antipseudomonal Bacteriophage Therapy in Mice. Antimicrob Agents Chemother. 2020;65(1).
59. Lin Y, Chang RYK, Britton WJ, Morales S, Kutter E, Chan HK. Synergy of nebulized phage PEV20 and ciprofloxacin combination against Pseudomonas aeruginosa. Int J Pharm. 2018;551(1-2):158-65.
60. Guillon A, Pardessus J, L'Hostis G, Fevre C, Barc C, Dalloneau E, Jouan Y, Bodier-Montagutelli E, Perez Y, Thorey C. Inhaled bacteriophage therapy in a porcine model of pneumonia caused by Pseudomonas aeruginosa during mechanical ventilation. British Journal of Pharmacology. 2021;178(18):3829-42.
61. Chan B, Stanley G, Kortright K, Modak M, Ott I, Sun Y, Würstle S, Grun C, Kazmierczak B, Rajagopalan G. Personalized inhaled bacteriophage therapy decreases multidrug-resistant Pseudomonas aeruginosa. MedRxiv. 2023:2023.01. 23.22283996.
62. Lin Y, Chang RYK, Britton WJ, Morales S, Kutter E, Li J, Chan HK. Inhalable combination powder formulations of phage and ciprofloxacin for P. aeruginosa respiratory infections. Eur J Pharm Biopharm. 2019;142:543-52.
63. Zhang Y, Zhang H, Ghosh D. The Stabilizing Excipients in Dry State Therapeutic Phage Formulations. AAPS PharmSciTech. 2020;21(4):133.
64. Omidian H, Nokhodchi A, Babanejad N. Dry Powder Inhalers for Delivery of Synthetic Biomolecules. Pharmaceuticals (Basel). 2025;18(2).
65. Maloney SE, Mecham JB, Hickey AJ. Performance testing for dry powder inhaler products: towards clinical relevance. KONA Powder and Particle Journal. 2023;40:172-85.
66. Weiler C, Egen M, Trunk M, Langguth P. Force control and powder dispersibility of spray dried particles for inhalation. J Pharm Sci. 2010;99(1):303-16.
67. Leung SS, Parumasivam T, Gao FG, Carrigy NB, Vehring R, Finlay WH, Morales S, Britton WJ, Kutter E, Chan HK. Production of Inhalation Phage Powders Using Spray Freeze Drying and Spray Drying Techniques for Treatment of Respiratory Infections. Pharm Res. 2016;33(6):1486-96.
68. Vehring R. Pharmaceutical particle engineering via spray drying. Pharm Res. 2008;25(5):999-1022.
69. Merabishvili M, Pirnay J-P, Vogele K, Malik DJ. Production of phage therapeutics and formulations: Innovative approaches. Phage therapy: a practical approach. 2019:3-41.
70. Kopp KT, Beer M, Voorspoels J, Lysebetten DV, den Mooter GV. Spray drying for protein stabilization. Int J Pharm. 2025;677:125600.
71. Leung SSY, Parumasivam T, Nguyen A, Gengenbach T, Carter EA, Carrigy NB, Wang H, Vehring R, Finlay WH, Morales S, Britton WJ, Kutter E, Chan HK. Effect of storage temperature on the stability of spray dried bacteriophage powders. Eur J Pharm Biopharm. 2018;127:213-22.
72. Chang RYK, Chow MYT, Khanal D, Chen D, Chan HK. Dry powder pharmaceutical biologics for inhalation therapy. Adv Drug Deliv Rev. 2021;172:64-79.

73. Hoppentocht M, Hagedoorn P, Frijlink H, De Boer A. Technological and practical challenges of dry powder inhalers and formulations. Advanced drug delivery reviews. 2014;75:18-31.
74. Sutar AD, Verma RK, Shukla R. Quality by Design in Pulmonary Drug Delivery: A Review on Dry Powder Inhaler Development, Nanotherapy Approaches, and Regulatory Considerations. AAPS PharmSciTech. 2024;25(6):178.
75. Zhang Y, Soto M, Ghosh D, Williams RO, 3rd. Manufacturing Stable Bacteriophage Powders by Including Buffer System in Formulations and Using Thin Film Freeze-drying Technology. Pharm Res. 2021;38(10):1793-804.
76. Chow AH, Tong HH, Chattopadhyay P, Shekunov BY. Particle engineering for pulmonary drug delivery. Pharm Res. 2007;24(3):411-37.
77. Roberts DL, Chambers F, Copley M, Mitchell JP. Internal Volumes of Pharmaceutical Compendial Induction Port, Next-Generation Impactor With and Without Its Pre-separator, and Several Configurations of the Andersen Cascade Impactor With and Without Pre-separator. J Aerosol Med Pulm Drug Deliv. 2020;33(4):214-29.
78. Chang RYK, Kwok PCL, Khanal D, Morales S, Kutter E, Li J, Chan HK. Inhalable bacteriophage powders: Glass transition temperature and bioactivity stabilization. Bioeng Transl Med. 2020;5(2):e10159.
79. Dolovich MB, Ahrens RC, Hess DR, Anderson P, Dhand R, Rau JL, Smaldone GC, Guyatt G, American College of Chest P, American College of Asthma A, Immunology. Device selection and outcomes of aerosol therapy: Evidence-based guidelines: American College of Chest Physicians/American College of Asthma, Allergy, and Immunology. Chest. 2005;127(1):335-71.
80. Longest W, Spence B, Hindle M. Devices for Improved Delivery of Nebulized Pharmaceutical Aerosols to the Lungs. J Aerosol Med Pulm Drug Deliv. 2019;32(5):317-39.
81. Malik DJ, Sokolov IJ, Vinner GK, Mancuso F, Cinquerrui S, Vladisavljevic GT, Clokie MRJ, Garton NJ, Stapley AGF, Kirpichnikova A. Formulation, stabilisation and encapsulation of bacteriophage for phage therapy. Adv Colloid Interface Sci. 2017;249:100-33.
82. Simperler A, Kornherr A, Chopra R, Bonnet PA, Jones W, Motherwell WS, Zifferer G. Glass transition temperature of glucose, sucrose, and trehalose: an experimental and in silico study. The journal of physical chemistry B. 2006;110(39):19678-84.
83. Stojanovska S, Gruevska N, Tomovska J, Tasevska J. Maillard reaction and lactose structural changes during milk processing. Maillard Reaction and Lactose Structural Changes during Milk Processing. 2017;2(6):139-45.
84. Merabishvili M, Vervaet C, Pirnay JP, De Vos D, Verbeken G, Mast J, Chanishvili N, Vaneechoutte M. Stability of Staphylococcus aureus phage ISP after freeze-drying (lyophilization). PLoS One. 2013;8(7):e68797.
85. Walker SA, Davidovich I, Yang Y, Lai A, Goncalves JP, Deliwala V, Busatto S, Shapiro S, Koifman N, Salomon C, Talmon Y, Wolfram J. Sucrose-based cryoprotective storage of extracellular vesicles. Extracell Vesicle. 2022;1.
86. Yu L, Mishra DS, Rigsbee DR. Determination of the glass properties of D-mannitol using sorbitol as an impurity. Journal of pharmaceutical sciences. 1998;87(6):774-7.
87. Chew NY, Chan HK. The role of particle properties in pharmaceutical powder inhalation formulations. J Aerosol Med. 2002;15(3):325-30.
88. Li M, Chang RYK, Lin Y, Morales S, Kutter E, Chan H-K. Phage cocktail powder for Pseudomonas aeruginosa respiratory infections. International journal of pharmaceutics. 2021;596:120200.
89. Allison SD, Chang B, Randolph TW, Carpenter JF. Hydrogen bonding between sugar and protein is responsible for inhibition of dehydration-induced protein unfolding. Archives of Biochemistry and Biophysics. 1999;365(2):289-98.

90. Mi Y, Wood G. The application and mechanisms of polyethylene glycol 8000 on stabilizing lactate dehydrogenase during lyophilization. PDA Journal of Pharmaceutical Science and Technology. 2004;58(4):192-202.
91. Li M, Cao Y, Chan HK. Optimizing Performance of Inhalable Bacteriophage Powders using Human Serum Albumin (HSA). Int J Pharm. 2025;678:125709.
92. Maa Y-F, Nguyen P-AT, Hsu SW. Spray-drying of air–liquid interface sensitive recombinant human growth hormone. Journal of pharmaceutical sciences. 1998;87(2):152-9.
93. Mukai R, Okuyama H, Uchimura M, Sakao K, Matsuhiro M, Ikeda-Imafuku M, Ishima Y, Nishikawa M, Ikushiro S, Tai A. The binding selectivity of quercetin and its structure-related polyphenols to human serum albumin using a fluorescent dye cocktail for multiplex drug-site mapping. Bioorg Chem. 2024;145:107184.
94. Escalante J, Nishimura B, Tuttobene MR, Subils T, Pimentel C, Georgeos N, Sieira R, Bonomo RA, Tolmasky ME, Ramirez MS. Human serum albumin (HSA) regulates the expression of histone-like nucleoid structure protein (H-NS) in Acinetobacter baumannii. Sci Rep. 2022;12(1):14644.
95. Xie Z, Ye J, Gao X, Chen H, Chen M, Lian J, Ma J, Wang H. Evaluation of nanoparticle albumin-bound paclitaxel loaded macrophages for glioblastoma treatment based on a microfluidic chip. Front Bioeng Biotechnol. 2024;12:1361682.
96. Fu M, Perlman M, Lu Q, Varga C. Pharmaceutical solid-state kinetic stability investigation by using moisture-modified Arrhenius equation and JMP statistical software. J Pharm Biomed Anal. 2015;107:370-7.
97. Lehmkemper K, Kyerematen SO, Heinzerling O, Degenhardt M, Sadowski G. Long-Term Physical Stability of PVP- and PVPVA-Amorphous Solid Dispersions. Mol Pharm. 2017;14(1):157-71.
98. Khawam A, Flanagan DR. Basics and applications of solid-state kinetics: a pharmaceutical perspective. J Pharm Sci. 2006;95(3):472-98.
99. Müller-Merbach M, Rauscher T, Hinrichs J. Inactivation of bacteriophages by thermal and high-pressure treatment. International Dairy Journal. 2005;15(6-9):777-84.
100. Ackermann HW. Bacteriophage observations and evolution. Res Microbiol. 2003;154(4):245-51.
101. Delbruck M. The Growth of Bacteriophage and Lysis of the Host. J Gen Physiol. 1940;23(5):643-60.
102. Semenyuk P, Orlov V, Kurochkina L. Effect of chaperonin encoded by gene 146 on thermal aggregation of lytic proteins of bacteriophage EL Pseudomonas aeruginosa. Biochemistry (Moscow). 2015;80:172-9.
103. Izutsu K-i, Yoshioka S, Terao T. Decreased protein-stabilizing effects of cryoprotectants due to crystallization. Pharmaceutical research. 1993;10:1232-7.
104. Hancock BC, Zografi G. The relationship between the glass transition temperature and the water content of amorphous pharmaceutical solids. Pharmaceutical research. 1994;11:471-7.
105. Andronis V, Zografi G. The molecular mobility of supercooled amorphous indomethacin as a function of temperature and relative humidity. Pharm Res. 1998;15(6):835-42.
106. Vandenheuvel D, Meeus J, Lavigne R, Van den Mooter G. Instability of bacteriophages in spray-dried trehalose powders is caused by crystallization of the matrix. International journal of pharmaceutics. 2014;472(1-2):202-5.
107. Airaksinen S, Karjalainen M, Shevchenko A, Westermarck S, Leppanen E, Rantanen J, Yliruusi J. Role of water in the physical stability of solid dosage formulations. J Pharm Sci. 2005;94(10):2147-65.
108. Koepf E, Eisele S, Schroeder R, Brezesinski G, Friess W. Notorious but not understood: How liquid-air interfacial stress triggers protein aggregation. Int J Pharm. 2018;537(1-2):202-12.

109. Maa YF, Hsu CC. Protein denaturation by combined effect of shear and air-liquid interface. Biotechnol Bioeng. 1997;54(6):503-12.
110. Ashokkumar M. The characterization of acoustic cavitation bubbles - an overview. Ultrason Sonochem. 2011;18(4):864-72.
111. Hancock BC, Zografi G. Characteristics and significance of the amorphous state in pharmaceutical systems. J Pharm Sci. 1997;86(1):1-12.
112. Fan Z, Zhang L. One- and two-stage Arrhenius models for pharmaceutical shelf life prediction. J Biopharm Stat. 2015;25(2):307-16.
113. Andronis V, Zografi G. The molecular mobility of supercooled amorphous indomethacin as a function of temperature and relative humidity. Pharmaceutical research. 1998;15:835-42.
114. Airaksinen S, Karjalainen M, Shevchenko A, Westermarck S, Leppänen E, Rantanen J, Yliruusi J. Role of water in the physical stability of solid dosage formulations. Journal of pharmaceutical sciences. 2005;94(10):2147-65.
115. Chang RY, Wong J, Mathai A, Morales S, Kutter E, Britton W, Li J, Chan H-K. Production of highly stable spray dried phage formulations for treatment of Pseudomonas aeruginosa lung infection. European Journal of Pharmaceutics and Biopharmaceutics. 2017;121:1-13.
116. Zeng XM, Martin GP, Marriott C. Effects of molecular weight of polyvinylpyrrolidone on the glass transition and crystallization of co-lyophilized sucrose. International journal of pharmaceutics. 2001;218(1-2):63-73.
117. Abedon ST, Danis-Wlodarczyk KM, Wozniak DJ. Phage Cocktail Development for Bacteriophage Therapy: Toward Improving Spectrum of Activity Breadth and Depth. Pharmaceuticals (Basel). 2021;14(10).
118. Yang Y, Shen W, Zhong Q, Chen Q, He X, Baker JL, Xiong K, Jin X, Wang J, Hu F, Le S. Development of a Bacteriophage Cocktail to Constrain the Emergence of Phage-Resistant Pseudomonas aeruginosa. Front Microbiol. 2020;11:327.
119. Li N, Zeng Y, Wang M, Bao R, Chen Y, Li X, Pan J, Zhu T, Hu B, Tan D. Characterization of phage resistance and their impacts on bacterial fitness in Pseudomonas aeruginosa. Microbiology Spectrum. 2022;10(5):e02072-22.
120. Kochan K, Nethercott C, Perez Guaita D, Jiang JH, Peleg AY, Wood BR, Heraud P. Detection of Antimicrobial Resistance-Related Changes in Biochemical Composition of Staphylococcus aureus by Means of Atomic Force Microscopy-Infrared Spectroscopy. Anal Chem. 2019;91(24):15397-403.
121. Hall AR, De Vos D, Friman VP, Pirnay JP, Buckling A. Effects of sequential and simultaneous applications of bacteriophages on populations of Pseudomonas aeruginosa in vitro and in wax moth larvae. Appl Environ Microbiol. 2012;78(16):5646-52.
122. Wright RCT, Friman VP, Smith MCM, Brockhurst MA. Resistance Evolution against Phage Combinations Depends on the Timing and Order of Exposure. mBio. 2019;10(5).
123. Yu Z, Luong T, Banuelos S, Sue A, Ryu H, Segal R, Roach DR, Huang Q. Leveraging mathematical modeling framework to guide regimen strategy for phage therapy. PLOS Complex Systems. 2024;1(3):e0000015.
124. Ulrich L, Steiner LX, Giez C, Lachnit T. Optimizing bacteriophage treatment of resistant Pseudomonas. mSphere. 2024;9(7):e0070723.
125. Chan BK, Stanley GL, Kortright KE, Vill AC, Modak M, Ott IM, Sun Y, Wurstle S, Grun CN, Kazmierczak BI, Rajagopalan G, Harris ZM, Britto CJ, Stewart J, Talwalkar JS, Appell CR, Chaudary N, Jagpal SK, Jain R, Kanu A, Quon BS, Reynolds JM, Teneback CC, Mai QA, Shabanova V, Turner PE, Koff JL. Personalized inhaled bacteriophage therapy for treatment of multidrug-resistant Pseudomonas aeruginosa in cystic fibrosis. Nat Med. 2025.
126. Abedon ST. Bacteriophage clinical use as antibacterial “drugs”: utility and precedent. Bugs as Drugs: Therapeutic Microbes for the Prevention and Treatment of Disease. 2018:417-51.

127. Casey E, Van Sinderen D, Mahony J. In vitro characteristics of phages to guide 'real life'phage therapy suitability. Viruses. 2018;10(4):163.
128. Brockhurst MA, Morgan AD, Fenton A, Buckling A. Experimental coevolution with bacteria and phage. The Pseudomonas fluorescens--Phi2 model system. Infect Genet Evol. 2007;7(4):547-52.
129. Khanal D, Kondyurin A, Hau H, Knowles JC, Levinson O, Ramzan I, Fu D, Marcott C, Chrzanowski W. Biospectroscopy of Nanodiamond-Induced Alterations in Conformation of Intra- and Extracellular Proteins: A Nanoscale IR Study. Anal Chem. 2016;88(15):7530-8.
130. Erukhimovitch V, Pavlov V, Talyshinsky M, Souprun Y, Huleihel M. FTIR microscopy as a method for identification of bacterial and fungal infections. Journal of pharmaceutical and biomedical analysis. 2005;37(5):1105-8.
131. Vaitekenas A, Tai AS, Ramsay JP, Stick SM, Kicic A. Pseudomonas aeruginosa Resistance to Bacteriophages and Its Prevention by Strategic Therapeutic Cocktail Formulation. Antibiotics (Basel). 2021;10(2).
132. Li G, Shen M, Yang Y, Le S, Li M, Wang J, Zhao Y, Tan Y, Hu F, Lu S. Adaptation of Pseudomonas aeruginosa to Phage PaP1 Predation via O-Antigen Polymerase Mutation. Front Microbiol. 2018;9:1170.
133. Labrie SJ, Samson JE, Moineau S. Bacteriophage resistance mechanisms. Nat Rev Microbiol. 2010;8(5):317-27.
134. Hoyland-Kroghsbo NM, Paczkowski J, Mukherjee S, Broniewski J, Westra E, Bondy-Denomy J, Bassler BL. Quorum sensing controls the Pseudomonas aeruginosa CRISPR-Cas adaptive immune system. Proc Natl Acad Sci U S A. 2017;114(1):131-5.
135. Kunisch F, Campobasso C, Wagemans J, Yildirim S, Chan BK, Schaudinn C, Lavigne R, Turner PE, Raschke MJ, Trampuz A, Gonzalez Moreno M. Targeting Pseudomonas aeruginosa biofilm with an evolutionary trained bacteriophage cocktail exploiting phage resistance trade-offs. Nat Commun. 2024;15(1):8572.
136. Oechslin F. Resistance Development to Bacteriophages Occurring during Bacteriophage Therapy. Viruses. 2018;10(7).
137. Abedon ST. Phage therapy dosing: The problem(s) with multiplicity of infection (MOI). Bacteriophage. 2016;6(3):e1220348.
138. Campoy S, Hervàs A, Busquets N, Erill I, Teixidó L, Barbé J. Induction of the SOS response by bacteriophage lytic development in Salmonella enterica. Virology. 2006;351(2):360-7.
139. Cairns BJ, Timms AR, Jansen VA, Connerton IF, Payne RJ. Quantitative models of in vitro bacteriophage–host dynamics and their application to phage therapy. PLoS Pathogens. 2009;5(1):e1000253.
140. Maldonado RF, Sá-Correia I, Valvano MA. Lipopolysaccharide modification in Gram-negative bacteria during chronic infection. FEMS microbiology reviews. 2016;40(4):480-93.
141. Jarrell KF, Kropinski A. Isolation and characterization of a bacteriophage specific for the lipopolysaccharide of rough derivatives of Pseudomonas aeruginosa strain PAO. Journal of Virology. 1981;38(2):529-38.
142. Li P, Ma W, Cheng J, Zhan C, Lu H, Shen J, Zhou X. Phages adapt to recognize an O-antigen polysaccharide site by mutating the 'backup'tail protein ORF59, enabling reinfection of phage-resistant Klebsiella pneumoniae. Emerging Microbes & Infections. 2025(just-accepted):2455592.
143. Tala L, Fineberg A, Kukura P, Persat A. Pseudomonas aeruginosa orchestrates twitching motility by sequential control of type IV pili movements. Nat Microbiol. 2019;4(5):774-80.
144. Sadikot RT, Blackwell TS, Christman JW, Prince AS. Pathogen-host interactions in Pseudomonas aeruginosa pneumonia. Am J Respir Crit Care Med. 2005;171(11):1209-23.
145. Pelicic V. Type IV pili: e pluribus unum? Mol Microbiol. 2008;68(4):827-37.

146. Chan BK, Sistrom M, Wertz JE, Kortright KE, Narayan D, Turner PE. Phage selection restores antibiotic sensitivity in MDR Pseudomonas aeruginosa. Sci Rep. 2016;6:26717.
147. Atabek A, Camesano TA. Atomic force microscopy study of the effect of lipopolysaccharides and extracellular polymers on adhesion of Pseudomonas aeruginosa. J Bacteriol. 2007;189(23):8503-9.
148. Smedley III JG, Jewell E, Roguskie J, Horzempa J, Syboldt A, Stolz DB, Castric P. Influence of pilin glycosylation on Pseudomonas aeruginosa 1244 pilus function. Infection and immunity. 2005;73(12):7922-31.
149. Kinnari TJ, Esteban J, Zamora N, Fernandez R, Lopez-Santos C, Yubero F, Mariscal D, Puertolas JA, Gomez-Barrena E. Effect of surface roughness and sterilization on bacterial adherence to ultra-high molecular weight polyethylene. Clin Microbiol Infect. 2010;16(7):1036-41.
150. Kassem A, Abbas L, Coutinho O, Opara S, Najaf H, Kasperek D, Pokhrel K, Li X, Tiquia-Arashiro S. Applications of Fourier Transform-Infrared spectroscopy in microbial cell biology and environmental microbiology: advances, challenges, and future perspectives. Frontiers in microbiology. 2023;14:1304081.
151. Leung SS, Parumasivam T, Gao FG, Carrigy NB, Vehring R, Finlay WH, Morales S, Britton WJ, Kutter E, Chan H-K. Production of inhalation phage powders using spray freeze drying and spray drying techniques for treatment of respiratory infections. Pharm Res. 2016;33(6):1486-96.
152. Lin Y, Quan D, Chang RYK, Chow MYT, Wang Y, Li M, Morales S, Britton WJ, Kutter E, Li J, Chan HK. Synergistic activity of phage PEV20-ciprofloxacin combination powder formulation-A proof-of-principle study in a P. aeruginosa lung infection model. Eur J Pharm Biopharm. 2021;158:166-71.
153. Li M, Chang RYK, Lin Y, Morales S, Kutter E, Chan HK. Phage cocktail powder for Pseudomonas aeruginosa respiratory infections. Int J Pharm. 2021;596:120200.
154. Wang Y, Khanal D, Alreja AB, Yang H, Yk Chang R, Tai W, Li M, Nelson DC, Britton WJ, Chan HK. Bacteriophage endolysin powders for inhaled delivery against pulmonary infections. Int J Pharm. 2023;635:122679.
155. Luo Y, Hong Y, Shen L, Wu F, Lin X. Multifunctional Role of Polyvinylpyrrolidone in Pharmaceutical Formulations. AAPS PharmSciTech. 2021;22(1):34.
156. Chang LL, Pikal MJ. Mechanisms of protein stabilization in the solid state. J Pharm Sci. 2009;98(9):2886-908.
157. Grasmeijer N, Stankovic M, de Waard H, Frijlink HW, Hinrichs WL. Unraveling protein stabilization mechanisms: vitrification and water replacement in a glass transition temperature controlled system. Biochim Biophys Acta. 2013;1834(4):763-9.
158. Pyne A, Chatterjee K, Suryanarayanan R. Solute crystallization in mannitol-glycine systems--implications on protein stabilization in freeze-dried formulations. J Pharm Sci. 2003;92(11):2272-83.
159. Roughton BC, Topp EM, Camarda KV. Use of glass transitions in carbohydrate excipient design for lyophilized protein formulations. Comput Chem Eng. 2012;36(10).
160. Chang BS, Beauvais RM, Dong A, Carpenter JF. Physical factors affecting the storage stability of freeze-dried interleukin-1 receptor antagonist: glass transition and protein conformation. Arch Biochem Biophys. 1996;331(2):249-58.
161. Rao Q, Klaassen Kamdar A, Labuza TP. Storage Stability of Food Protein Hydrolysates-A Review. Crit Rev Food Sci Nutr. 2016;56(7):1169-92.
162. Haq IU, Chaudhry WN, Akhtar MN, Andleeb S, Qadri I. Bacteriophages and their implications on future biotechnology: a review. Virol J. 2012;9:9.
163. Vandenheuvel D, Meeus J, Lavigne R, Van den Mooter G. Instability of bacteriophages in spray-dried trehalose powders is caused by crystallization of the matrix. Int J Pharm. 2014;472(1-2):202-5.

164. Chang RYK, Kwok PCL, Khanal D, Morales S, Kutter E, Li J, Chan HK. Inhalable bacteriophage powders: Glass transition temperature and bioactivity stabilization. Bioengineering& Transla Med. 2020;5(2):e10159.
165. Zeng XM, Martin GP, Marriott C. Effects of molecular weight of polyvinylpyrrolidone on the glass transition and crystallization of co-lyophilized sucrose. Int J Pharm. 2001;218(1-2):63-73.
166. Yuan X, Xiang TX, Anderson BD, Munson EJ. Hydrogen Bonding Interactions in Amorphous Indomethacin and Its Amorphous Solid Dispersions with Poly(vinylpyrrolidone) and Poly(vinylpyrrolidone-co-vinyl acetate) Studied Using (13)C Solid-State NMR. Mol Pharm. 2015;12(12):4518-28.
167. Guideline I. Stability testing of new drug substances and products. Q1A (R2), current step. 2003;4(1-24).
168. Mikayilov E, Tagiyev D, Zeynalov N, Tagiyev S. Exploring the Role of Poly (N-vinyl pyrrolidone) in Drug Delivery. Chemical and Biochemical Engineering Quarterly. 2024;38(3):185-96.
169. Águila-Hernández J, Trejo A, García-Flores BE. Volumetric and surface tension behavior of aqueous solutions of polyvinylpyrrolidone in the range (288 to 303) K. Journal of Chemical & Engineering Data. 2011;56(5):2371-8.
170. Wdowiak M, Paczesny J, Raza S. Enhancing the stability of bacteriophages using physical, chemical, and nano-based approaches: A review. Pharmaceutics. 2022;14(9):1936.
171. Sivasankaran RP, Snell K, Kunkel G, Georgiou P, Puente EG, Maynard HD. Polymer-mediated protein/peptide therapeutic stabilization: current progress and future directions. Prog Polym Sci. 2024:101867.
172. Asgreen C, Knopp MM, Skytte J, Lobmann K. Influence of the Polymer Glass Transition Temperature and Molecular Weight on Drug Amorphization Kinetics Using Ball Milling. Pharmaceutics. 2020;12(6).
173. Cangialosi D, Alegria A, Colmenero J. Route to calculate the length scale for the glass transition in polymers. Phys Rev E Stat Nonlin Soft Matter Phys. 2007;76(1 Pt 1):011514.
174. Patel NG, Banella S, Serajuddin ATM. Moisture Sorption by Polymeric Excipients Commonly Used in Amorphous Solid Dispersions and its Effect on Glass Transition Temperature: II. Cellulosic Polymers. J Pharm Sci. 2022;111(11):3114-29.
175. Gonzalez-Menendez E, Fernandez L, Gutierrez D, Rodriguez A, Martinez B, Garcia P. Comparative analysis of different preservation techniques for the storage of Staphylococcus phages aimed for the industrial development of phage-based antimicrobial products. PLoS One. 2018;13(10):e0205728.
176. Fitzpatrick S, McCabe JF, Petts CR, Booth SW. Effect of moisture on polyvinylpyrrolidone in accelerated stability testing. Int J Pharm. 2002;246(1-2):143-51.
177. Turner D, Schwartz A. The glass transition temperature of poly (N-vinyl pyrrolidone) by differential scanning calorimetry. Polymer. 1985;26(5):757-62.
178. Reimschuessel H. On the glass transition temperature of comblike polymers: Effects of side chain length and backbone chain structure. Journal of Polymer Science: Polymer Chemistry Edition. 1979;17(8):2447-57.
179. Pang Z, Raudonis R, Glick BR, Lin T-J, Cheng Z. Antibiotic resistance in Pseudomonas aeruginosa: mechanisms and alternative therapeutic strategies. Biotechnol Adv. 2019;37(1):177-92.
180. Tacconelli E, Carrara E, Savoldi A, Harbarth S, Mendelson M, Monnet DL, Pulcini C, Kahlmeter G, Kluytmans J, Carmeli Y, Ouellette M, Outterson K, Patel J, Cavaleri M, Cox EM, Houchens CR, Grayson ML, Hansen P, Singh N, Theuretzbacher U, Magrini N, Aboderin AO, Al-Abri SS, Awang Jalil N, Benzonana N, Bhattacharya S, Brink AJ, Burkert FR, Cars O, Cornaglia G, Dyar OJ, Friedrich AW, Gales AC, Gandra S, Giske CG, Goff DA, Goossens H, Gottlieb T, Guzman Blanco M, Hryniewicz W, Kattula D, Jinks T, Kanj SS, Kerr L, Kieny M-P, Kim YS, Kozlov RS, Labarca J, Laxminarayan R, Leder K, Leibovici L,

Levy-Hara G, Littman J, Malhotra-Kumar S, Manchanda V, Moja L, Ndoye B, Pan A, Paterson DL, Paul M, Qiu H, Ramon-Pardo P, Rodríguez-Baño J, Sanguinetti M, Sengupta S, Sharland M, Si-Mehand M, Silver LL, Song W, Steinbakk M, Thomsen J, Thwaites GE, van der Meer JWM, Van Kinh N, Vega S, Villegas MV, Wechsler-Fördös A, Wertheim HFL, Wesangula E, Woodford N, Yilmaz FO, Zorzet A. Discovery, research, and development of new antibiotics: the WHO priority list of antibiotic-resistant bacteria and tuberculosis. Lancet Infect Dis. 2018;18(3):318-27.
181. Kingwell K. Bacteriophage therapies re-enter clinical trials. Nature Reviews Drug Discovery. 2015;14(8):515-6.
182. Chang RYK, Wallin M, Lin Y, Leung SSY, Wang H, Morales S, Chan H-K. Phage therapy for respiratory infections. Adv Drug Del Rev. 2018;133:76-86.
183. Liu C, Hong Q, Chang RY, Kwok PC, Chan H-K. Phage–Antibiotic Therapy as a Promising Strategy to Combat Multidrug-Resistant Infections and to Enhance Antimicrobial Efficiency. Antibiotics. 2022;11(5):570.
184. Pathak V, Chan H-K, Zhou QT. Formulation of Bacteriophage for Inhalation to Treat Multidrug-Resistant Pulmonary Infections. KONA Powder Part J. 2024.
185. Chang RYK, Chen K, Wang J, Wallin M, Britton W, Morales S, Kutter E, Li J, Chan H-K. Proof-of-Principle Study in a Murine Lung Infection Model of Antipseudomonal Activity of Phage PEV20 in a Dry-Powder Formulation. Antimicrob Agents Chemother. 2018;62(2):01714-17.
186. Wang S-y, Tan X, Liu Z-q, Ma H, Liu T-b, Yang Y-q, Ying Y, Gao R-y, Zhang D-z, Ma Y-f, Chen K, Lin L, Jiang Z-h, Yu J-l. Pharmacokinetics and safety evaluation of intravenously administered Pseudomonas phage PA_LZ7 in a mouse model. Microbiol Spectr. 2023;12(1):e01882-23.
187. Chow MYT, Chang RYK, Li M, Wang Y, Lin Y, Morales S, McLachlan Andrew J, Kutter E, Li J, Chan H-K. Pharmacokinetics and Time-Kill Study of Inhaled Antipseudomonal Bacteriophage Therapy in Mice. Antimicrob Agents Chemother. 2020;65(1):01470-20.
188. Chang RYK, Das T, Manos J, Kutter E, Morales S, Chan H-K. Bacteriophage PEV20 and Ciprofloxacin Combination Treatment Enhances Removal of Pseudomonas aeruginosa Biofilm Isolated from Cystic Fibrosis and Wound Patients. AAPS J. 2019;21(3):49.
189. Khanal D, Chang RYK, Morales S, Chan H-K, Chrzanowski W. High Resolution Nanoscale Probing of Bacteriophages in an Inhalable Dry Powder Formulation for Pulmonary Infections. Anal Chem. 2019;91(20):12760-7.
190. Chan H-K, Chang RYK. Inhaled Delivery of Anti-Pseudomonal Phages to Tackle Respiratory Infections Caused by Superbugs. J Aerosol Med Pulm Drug Deliv. 2021;35(2):73-82.
191. Lin Y, Chang RYK, Britton WJ, Morales S, Kutter E, Chan H-K. Synergy of nebulized phage PEV20 and ciprofloxacin combination against Pseudomonas aeruginosa. Int J Pharm. 2018;551(1):158-65.
192. Cao Y, Khanal D, Kim J, Chang RYK, Byun AS, Morales S, Banaszak Holl MM, Chan H-K. Stability of bacteriophages in organic solvents for formulations. Int J Pharm. 2023;646:123505.
193. Leung SSY, Carrigy NB, Vehring R, Finlay WH, Morales S, Carter EA, Britton WJ, Kutter E, Chan H-K. Jet nebulization of bacteriophages with different tail morphologies – Structural effects. Int J Pharm. 2019;554:322-6.
194. Flint R, Laucirica DR, Chan H-K, Chang BJ, Stick SM, Kicic A. Stability Considerations for Bacteriophages in Liquid Formulations Designed for Nebulization. Cells. 2023;12(16).
195. Chang RYK, Kwok PCL, Khanal D, Morales S, Kutter E, Li J, Chan H-K. Inhalable bacteriophage powders: Glass transition temperature and bioactivity stabilization. Bioeng Transl Med. 2020;5(2):e10159.
196. Ke W-R, Chang RYK, Chan H-K. Engineering the right formulation for enhanced drug delivery. Adv Drug Del Rev. 2022;191:114561.

197. Vandenheuvel D, Singh A, Vandersteegen K, Klumpp J, Lavigne R, Van den Mooter G. Feasibility of spray drying bacteriophages into respirable powders to combat pulmonary bacterial infections. Eur J Pharm Biopharm. 2013;84(3):578-82.
198. Vandenheuvel D, Meeus J, Lavigne R, Van den Mooter G. Instability of bacteriophages in spray-dried trehalose powders is caused by crystallization of the matrix. Int J Pharm. 2014;472(1):202-5.
199. Leung SSY, Parumasivam T, Gao FG, Carter EA, Carrigy NB, Vehring R, Finlay WH, Morales S, Britton WJ, Kutter E, Chan H-K. Effects of storage conditions on the stability of spray dried, inhalable bacteriophage powders. Int J Pharm. 2017;521(1):141-9.
200. Chang RYK, Wallin M, Kutter E, Morales S, Britton W, Li J, Chan H-K. Storage stability of inhalable phage powders containing lactose at ambient conditions. Int J Pharm. 2019;560:11-8.
201. Chang RYK, Chen K, Wang J, Wallin M, Britton W, Morales S, Kutter E, Li J, Chan H-K. Proof-of-principle study in a murine lung infection model of antipseudomonal activity of phage PEV20 in a dry-powder formulation. Antimicrobial Agents and Chemotherapy. 2018;62(2):10.1128/aac. 01714-17.
202. Steckel H, Müller BW. In vitro evaluation of dry powder inhalers I: drug deposition of commonly used devices. International Journal of Pharmaceutics. 1997;154(1):19-29.
203. Patton JS, Byron PR. Inhaling medicines: delivering drugs to the body through the lungs. Nature reviews Drug discovery. 2007;6(1):67-74.
204. Costantino HR, Langer R, Klibanov AM. Solid‐phase aggregation of proteins under pharmaceutically relevant conditions. Journal of pharmaceutical sciences. 1994;83(12):1662-9.
205. Hancock BC, Zografi G. Characteristics and significance of the amorphous state in pharmaceutical systems. Journal of pharmaceutical sciences. 1997;86(1):1-12.
206. Abedon ST, Kuhl SJ, Blasdel BG, Kutter EM. Phage treatment of human infections. Bacteriophage. 2011;1(2):66-85.
207. Coelho JM, Marto J, Bento C, Martins I. Microbiological Quality and Stability of Pharmaceutical Products in Europe: Discrepancies, Regulatory Perspectives and Challenges. 2025.
208. Muralidhara BK, Wong M. Critical considerations in the formulation development of parenteral biologic drugs. Drug Discov Today. 2020;25(3):574-81.
209. Leung SSY, Parumasivam T, Nguyen A, Gengenbach T, Carter EA, Carrigy NB, Wang H, Vehring R, Finlay WH, Morales S, Britton WJ, Kutter E, Chan H-K. Effect of storage temperature on the stability of spray dried bacteriophage powders. Eur J Pharm Biopharm. 2018;127:213-22.
210. Chang RYK, Chan H-K. Advancements in Particle Engineering for Inhalation Delivery of Small Molecules and Biotherapeutics. Pharm Res. 2022;39(12):3047-61.
211. Chang RYK, Wallin M, Kutter E, Morales S, Britton W, Li J, Chan HK. Storage stability of inhalable phage powders containing lactose at ambient conditions. Int J Pharm. 2019;560:11-8.
212. Qiu Z, Stowell JG, Morris KR, Byrn SR, Pinal R. Kinetic study of the Maillard reaction between metoclopramide hydrochloride and lactose. International journal of pharmaceutics. 2005;303(1-2):20-30.
213. Hardy JM, Dunstan RA, Grinter R, Belousoff MJ, Wang J, Pickard D, Venugopal H, Dougan G, Lithgow T, Coulibaly F. The architecture and stabilisation of flagellotropic tailed bacteriophages. Nature Communications. 2020;11(1):3748.
214. Cardarelli L, Pell LG, Neudecker P, Pirani N, Liu A, Baker LA, Rubinstein JL, Maxwell KL, Davidson AR. Phages have adapted the same protein fold to fulfill multiple functions in virion assembly. Proc Natl Acad Sci U S A. 2010;107(32):14384-9.
215. Mahony J, Alqarni M, Stockdale S, Spinelli S, Feyereisen M, Cambillau C, Sinderen Dv. Functional and structural dissection of the tape measure protein of lactococcal phage TP901-1. Sci Rep. 2016;6(1):36667.

216. Ke W-R, Kwok PCL, Khanal D, Chang RYK, Chan H-K. Co-spray dried hydrophobic drug formulations with crystalline lactose for inhalation aerosol delivery. Int J Pharm. 2021;602:120608.
217. Ke W-R, Chang RYK, Kwok PCL, Chen D, Chan H-K. Spray drying lactose from organic solvent suspensions for aerosol delivery to the lungs. Int J Pharm. 2020;591:119984.
218. Lin Y, Yoon Kyung Chang R, Britton WJ, Morales S, Kutter E, Li J, Chan H-K. Storage stability of phage-ciprofloxacin combination powders against Pseudomonas aeruginosa respiratory infections. Int J Pharm. 2020;591:119952.
219. Heljo VP, Nordberg A, Tenho M, Virtanen T, Jouppila K, Salonen J, Maunu SL, Juppo AM. The Effect of Water Plasticization on the Molecular Mobility and Crystallization Tendency of Amorphous Disaccharides. Pharm Res. 2012;29(10):2684-97.
220. Surana R, Pyne A, Suryanarayanan R. Effect of Aging on the Physical Properties of Amorphous Trehalose. Pharm Res. 2004;21(5):867-74.
221. Chen L, Okuda T, Lu X-Y, Chan H-K. Amorphous powders for inhalation drug delivery. Adv Drug Del Rev. 2016;100:102-15.
222. Chang RYK, Chow MYT, Wang Y, Liu C, Hong Q, Morales S, McLachlan AJ, Kutter E, Li J, Chan H-K. The effects of different doses of inhaled bacteriophage therapy for Pseudomonas aeruginosa pulmonary infections in mice. Clin Microbiol Infect. 2022;28(7):983-9.
223. Newman S, Chan H-K. In Vitro / In Vivo Comparisons in Pulmonary Drug Delivery. J Aerosol Med Pulm Drug Deliv. 2008;21:77-84.
224. Alhajj N, O'Reilly NJ, Cathcart H. Leucine as an excipient in spray dried powder for inhalation. Drug Discov Today. 2021;26(10):2384-96.
225. Chang RYK, Chen L, Chen D, Chan H-K. Overcoming challenges for development of amorphous powders for inhalation. Expert Opin Drug Deliv. 2020;17(11):1583-95.
226. Leung SSY, Chan H-K. Emerging antibiotic alternatives: From antimicrobial peptides to bacteriophage therapies. Adv Drug Del Rev. 2022;191:114594.
227. Mensink MA, Frijlink HW, van der Voort Maarschalk K, Hinrichs WL. Inulin, a flexible oligosaccharide I: Review of its physicochemical characteristics. Carbohydrate polymers. 2015;130:405-19.
228. Ergin F. Effect of freeze drying, spray drying and electrospraying on the morphological, thermal, and structural properties of powders containing phage Felix O1 and activity of phage Felix O1 during storage. Powder Technology. 2022;404:117516.
229. Carrigy NB, Liang L, Wang H, Kariuki S, Nagel TE, Connerton IF, Vehring R. Trileucine and pullulan improve anti-campylobacter bacteriophage stability in engineered spray-dried microparticles. Annals of biomedical engineering. 2020;48(4):1169-80.
230. Durda-Masny M, Gozdzik-Spychalska J, John A, Czainski W, Strozewska W, Pawlowska N, Wlizlo J, Batura-Gabryel H, Szwed A. The determinants of survival among adults with cystic fibrosis-a cohort study. J Physiol Anthropol. 2021;40(1):19.
231. Qin S, Xiao W, Zhou C, Pu Q, Deng X, Lan L, Liang H, Song X, Wu M. Pseudomonas aeruginosa: pathogenesis, virulence factors, antibiotic resistance, interaction with host, technology advances and emerging therapeutics. Signal Transduct Target Ther. 2022;7(1):199.
232. Barman S, Kurnaz LB, Leighton R, Hossain MW, Decho AW, Tang C. Intrinsic antimicrobial resistance: Molecular biomaterials to combat microbial biofilms and bacterial persisters. Biomaterials. 2024;311:122690.
233. Clokie MR, Millard AD, Letarov AV, Heaphy S. Phages in nature. Bacteriophage. 2011;1(1):31-45.
234. Nilsson AS. Phage therapy--constraints and possibilities. Ups J Med Sci. 2014;119(2):192-8.

235. Hong Q, Chang RYK, Assafiri O, Morales S, Chan HK. Optimizing in vitro phage-ciprofloxacin combination formulation for respiratory therapy of multi-drug resistant Pseudomonas aeruginosa infections. Int J Pharm. 2024;652:123853.
236. Zhang Y, Wang R, Hu Q, Lv N, Zhang L, Yang Z, Zhou Y, Wang X. Characterization of Pseudomonas aeruginosa bacteriophages and control hemorrhagic pneumonia on a mice model. Front Microbiol. 2024;15:1396774.
237. Ashworth EA, Wright RCT, Shears RK, Wong JKL, Hassan A, Hall JPJ, Kadioglu A, Fothergill JL. Exploiting lung adaptation and phage steering to clear pan-resistant Pseudomonas aeruginosa infections in vivo. Nat Commun. 2024;15(1):1547.
238. S SM, Abdellatif GR, Abu Zaid AS, Aziz RK, Aboshanab KM. In Vitro and Pre-Clinical Evaluation of Locally Isolated Phages, vB_Pae_SMP1 and vB_Pae_SMP5, Formulated as Hydrogels against Carbapenem-Resistant Pseudomonas aeruginosa. Viruses. 2022;14(12).
239. Rubalskii E, Ruemke S, Salmoukas C, Boyle EC, Warnecke G, Tudorache I, Shrestha M, Schmitto JD, Martens A, Rojas SV, Ziesing S, Bochkareva S, Kuehn C, Haverich A. Bacteriophage Therapy for Critical Infections Related to Cardiothoracic Surgery. Antibiotics (Basel). 2020;9(5).
240. Stacey HJ, De Soir S, Jones JD. The Safety and Efficacy of Phage Therapy: A Systematic Review of Clinical and Safety Trials. Antibiotics (Basel). 2022;11(10).
241. Chang RYK, Chow MYT, Wang Y, Liu C, Hong Q, Morales S, McLachlan AJ, Kutter E, Li J, Chan HK. The effects of different doses of inhaled bacteriophage therapy for Pseudomonas aeruginosa pulmonary infections in mice. Clin Microbiol Infect. 2022;28(7):983-9.
242. Chan BK, Stanley GL, Kortright KE, Vill AC, Modak M, Ott IM, Sun Y, Würstle S, Grun CN, Kazmierczak BI. Personalized inhaled bacteriophage therapy for treatment of multidrug-resistant Pseudomonas aeruginosa in cystic fibrosis. Nature Medicine. 2025:1-8.
243. Nainwal N. Treatment of respiratory viral infections through inhalation therapeutics: Challenges and opportunities. Pulm Pharmacol Ther. 2022;77:102170.
244. Semler DD, Goudie AD, Finlay WH, Dennis JJ. Aerosol phage therapy efficacy in Burkholderia cepacia complex respiratory infections. Antimicrob Agents Chemother. 2014;58(7):4005-13.
245. Debarbieux L, Leduc D, Maura D, Morello E, Criscuolo A, Grossi O, Balloy V, Touqui L. Bacteriophages can treat and prevent Pseudomonas aeruginosa lung infections. The Journal of infectious diseases. 2010;201(7):1096-104.
246. Morello E, Saussereau E, Maura D, Huerre M, Touqui L, Debarbieux L. Pulmonary bacteriophage therapy on Pseudomonas aeruginosa cystic fibrosis strains: first steps towards treatment and prevention. PloS one. 2011;6(2):e16963.
247. Duyvejonck H, Merabishvili M, Vaneechoutte M, de Soir S, Wright R, Friman VP, Verbeken G, De Vos D, Pirnay JP, Van Mechelen E, Vermeulen SJT. Evaluation of the Stability of Bacteriophages in Different Solutions Suitable for the Production of Magistral Preparations in Belgium. Viruses. 2021;13(5).
248. Hua Y, Luo T, Yang Y, Dong D, Wang R, Wang Y, Xu M, Guo X, Hu F, He P. Phage therapy as a promising new treatment for lung infection caused by carbapenem-resistant Acinetobacter baumannii in mice. Frontiers in microbiology. 2018;8:2659.
249. Takemura-Uchiyama I, Uchiyama J, Osanai M, Morimoto N, Asagiri T, Ujihara T, Daibata M, Sugiura T, Matsuzaki S. Experimental phage therapy against lethal lung-derived septicemia caused by Staphylococcus aureus in mice. Microbes and Infection. 2014;16(6):512-7.
250. Brom JA, Petrikis RG, Pielak GJ. How Sugars Protect Dry Protein Structure. Biochemistry. 2023;62(5):1044-52.
251. Polito C, Martin GS. Albumin: physiologic and clinical effects on lung function. Minerva Anestesiol. 2013;79(10):1180-6.

252. Woods A, Patel A, Spina D, Riffo-Vasquez Y, Babin-Morgan A, De Rosales R, Sunassee K, Clark S, Collins H, Bruce K. In vivo biocompatibility, clearance, and biodistribution of albumin vehicles for pulmonary drug delivery. Journal of Controlled Release. 2015;210:1-9.
253. Seo J, Lee C, Hwang HS, Kim B, Thao LQ, Lee ES, Oh KT, Lim J-L, Choi H-G, Youn YS. Therapeutic advantage of inhaled tacrolimus-bound albumin nanoparticles in a bleomycin-induced pulmonary fibrosis mouse model. Pulmonary pharmacology & therapeutics. 2016;36:53-61.
254. Kratz F. Albumin as a drug carrier: design of prodrugs, drug conjugates and nanoparticles. Journal of controlled release. 2008;132(3):171-83.
255. Stafford C, Lobel S, Fruge B, Moffitt J, Hoff R, Fadel H. Anaphylaxis to human serum albumin. Annals of allergy. 1988;61(2):85-8.
256. Beavers C, Flinchum D, Ayyoubi MT. Severe intraoperative albumin transfusion reaction and review of the literature. Laboratory Medicine. 2013;44(4):e129-e31.
257. Cao Y, Khanal D, Kim J, Chang RYK, Byun AS, Morales S, Banaszak Holl MM, Chan HK. Stability of bacteriophages in organic solvents for formulations. Int J Pharm. 2023;646:123505.
258. Boel E, Koekoekx R, Dedroog S, Babkin I, Vetrano MR, Clasen C, Van den Mooter G. Unraveling Particle Formation: From Single Droplet Drying to Spray Drying and Electrospraying. Pharmaceutics. 2020;12(7).
259. Chow MYT, Qiu Y, Liao Q, Kwok PCL, Chow SF, Chan HK, Lam JKW. High siRNA loading powder for inhalation prepared by co-spray drying with human serum albumin. Int J Pharm. 2019;572:118818.
260. Vehring R, Foss WR, Lechuga-Ballesteros D. Particle formation in spray drying. Journal of aerosol science. 2007;38(7):728-46.
261. Lintingre E, Lequeux F, Talini L, Tsapis N. Control of particle morphology in the spray drying of colloidal suspensions. Soft Matter. 2016;12(36):7435-44.
262. Leung SS, Tang P, Zhou QT, Tong Z, Leung C, Decharaksa J, Yang R, Chan HK. De-agglomeration Effect of the US Pharmacopeia and Alberta Throats on Carrier-Based Powders in Commercial Inhalation Products. AAPS J. 2015;17(6):1407-16.
263. Smith S, Rowbotham NJ. Inhaled anti-pseudomonal antibiotics for long-term therapy in cystic fibrosis. Cochrane Database Syst Rev. 2022;11(11):CD001021.
264. Chew NY, Chan HK. Use of solid corrugated particles to enhance powder aerosol performance. Pharm Res. 2001;18(11):1570-7.
265. Chew NY, Tang P, Chan HK, Raper JA. How much particle surface corrugation is sufficient to improve aerosol performance of powders? Pharm Res. 2005;22(1):148-52.
266. Maa YF, Nguyen PA, Hsu SW. Spray-drying of air-liquid interface sensitive recombinant human growth hormone. J Pharm Sci. 1998;87(2):152-9.
267. Wang W. Instability, stabilization, and formulation of liquid protein pharmaceuticals. Int J Pharm. 1999;185(2):129-88.
268. Monkos K. Determination of the glass-transition temperature of proteins from a viscometric approach. Int J Biol Macromol. 2015;74:1-4.
269. Crowe JH, Carpenter JF, Crowe LM. The role of vitrification in anhydrobiosis. Annu Rev Physiol. 1998;60:73-103.

# Chapter 6

Conclusion and future directions

## Conclusions

This thesis presents a comprehensive and integrated approach to optimizing bacteriophage therapy for Pseudomonas aeruginosa through strategic treatment design and advanced pharmaceutical formulation science. The research has successfully addressed two critical challenges limiting the clinical translation of phage therapeutics: the development of resistance-minimizing treatment strategies and the creation of stable, effective delivery systems for pulmonary administration.

The investigation of sequential versus simultaneous phage treatment strategies revealed that sequential administration targeting distinct bacterial receptors represents a superior therapeutic approach. Initiating treatment with LPS-targeting phages followed by TFP-targeting phages achieved substantial bacterial reductions exceeding 3-$\log_{10}$ within 48 hours at low multiplicities of infection while effectively minimizing resistance development. This strategy successfully exploited fitness costs associated with resistance mutations, as demonstrated through comprehensive resistance profiling and atomic force microscopy infrared spectroscopy analysis that elucidated molecular adaptations including LPS truncation and TFP glycosylation. These findings establish sequential phage therapy as a promising and scientifically-grounded strategy for combating antibiotic-resistant infections.

From a pharmaceutical formulation perspective, this research has made significant advances in developing stable dry powder systems for long-term phage storage and pulmonary delivery. The systematic investigation of polyvinylpyrrolidone-based matrices established novel formulation principles distinct from traditional saccharide-based systems, demonstrating that high-molecular-weight PVPs can maintain phage viability within 1 $\log_{10}$ loss over 180 days under ambient storage conditions. Importantly, these formulations showed

humidity tolerance with successful long-term stability achieved at temperatures up to 22°C and 33% relative humidity when adequate thermal offsets were maintained, offering potential for reduced cold-chain dependency in phage therapeutic distribution.

The four-year stability study represents the first demonstration that phage powder formulations can maintain acceptable biological activity over extended storage periods. The critical role of excipient selection was clearly established, with formulations containing ≥70% lactose providing robust glassy matrices that protect phage viability while leucine enhancement ensures moisture resistance and dispersibility. Although some formulations experienced titer losses exceeding 2 $\log_{10}$ and aerosol performance decreased over time, the maintenance of fine particle fractions around 40% combined with the inherent auto-dosing potential of phages suggests these formulations remain therapeutically viable for treating multidrug-resistant bacterial infections.

The development of human serum albumin and lactose-based formulations further advanced the field by introducing HSA as a performance-enhancing excipient for inhalable phage powders. The optimized formulations achieved exceptional aerosol performance with fine particle fractions exceeding 50% while minimizing phage titer loss to less than 1 $\log_{10}$. The incorporation of HSA not only enhanced powder dispersion characteristics but also effectively mitigated lactose recrystallization, establishing a promising platform for phage delivery that balances both pharmaceutical performance and biological preservation.

Collectively, this research has established an integrated framework for phage therapy optimization that successfully bridges therapeutic strategy considerations with advanced pharmaceutical formulation science. The demonstration that sequential treatment protocols can minimize resistance development while optimized formulation systems ensure long-term

stability and effective delivery addresses two of the most significant barriers to clinical implementation of phage therapeutics. The findings provide both fundamental scientific insights into phage-bacterial interactions and resistance mechanisms, as well as practical solutions for pharmaceutical development that can accelerate the translation of phage therapy from laboratory research to clinical application.

The integrated approach presented in this thesis represents a paradigm shift from treating therapeutic strategy and formulation development as separate research domains to recognizing their interconnected nature in successful therapeutic development. This comprehensive framework provides a foundation for future research and development efforts in bacteriophage therapeutics, offering evidence-based strategies for both optimizing treatment protocols and creating stable, effective delivery systems. As antibiotic resistance continues to pose growing threats to global health, the advances presented in this thesis contribute essential knowledge and practical solutions for implementing phage therapy as a viable alternative to conventional antimicrobial treatments, particularly for challenging respiratory infections caused by multidrug-resistant Pseudomonas aeruginosa.

## Future directions

The immediate priority involves comprehensive animal model validation using mouse pneumonia models infected with *P. aeruginosa* to compare HSA-lactose formulations against traditional lactose-leucine platforms. Key experiments should include pharmacokinetic studies tracking phage distribution and clearance in infected lung tissues, dose-response studies establishing optimal MOI ranges in *vivo*, and direct comparison of simultaneous versus sequential phage administration efficacy. Additional studies must evaluate treatment outcomes across different infection severities, assess immune responses to various formulation excipients, and determine the relationship between in vitro stability data and in *vivo* therapeutic performance.

Critical experiments must investigate how different formulations affect phage structural integrity at the molecular level using cryo-electron microscopy and small-angle X-ray scattering to visualize phage morphology before and after spray drying. Specific studies should determine how various molecular weight PVP grades affect preservation of tail fibre proteins responsible for host recognition, characterize HSA protective mechanisms through protein-protein interaction analysis using techniques like surface plasmon resonance and isothermal titration calorimetry, and correlate structural changes with functional viability over extended storage periods. Advanced AFM-IR spectroscopy should be adapted to characterize phage structural changes, identifying optimal excipient combinations for preserving specific phage functionalities and developing structure-based formulation design principles that account for different phage morphologies.

Future research must expand resistance studies beyond current LPS and TFP targets to include additional receptor systems such as outer membrane proteins and flagella. Key experiments

should investigate temporal dynamics of resistance development in sequential versus simultaneous treatments using time-course sampling and fitness landscape analysis, employ whole-genome sequencing coupled with transcriptomics to identify alternative resistance mechanisms not detected in current gene-specific analyses, and use advanced microscopy techniques to visualize real-time phage-bacteria interactions during treatment. Studies should systematically characterize fitness costs associated with different resistance mechanisms and investigate how environmental stresses (osmotic, temperature, nutrient limitation) affect resistance development and stability.

Research should systematically explore co-formulation of multiple phage types with different structural requirements, investigating phage-phage interactions during storage and their effects on individual phage stability. Experiments must test combination formulations with antibiotics using checkerboard assays and time-kill studies to exploit fitness costs of phage resistance, develop and characterize responsive formulation systems using pH-sensitive polymers and protease-cleavable linkers that protect vulnerable phage structural domains, and create controlled-release studies using dissolution testing and phage release kinetics under simulated lung conditions. Additional studies should investigate competitive binding dynamics when multiple phages target the same bacterial strain and characterize the evolution of bacterial populations under multi-phage pressure.

# Appendix

Supplementary data, co-author declaration, conference proceedings, and publications during candidacy

## Appendix 1. Supplementary data from Chapter 2

### Supplementary Information

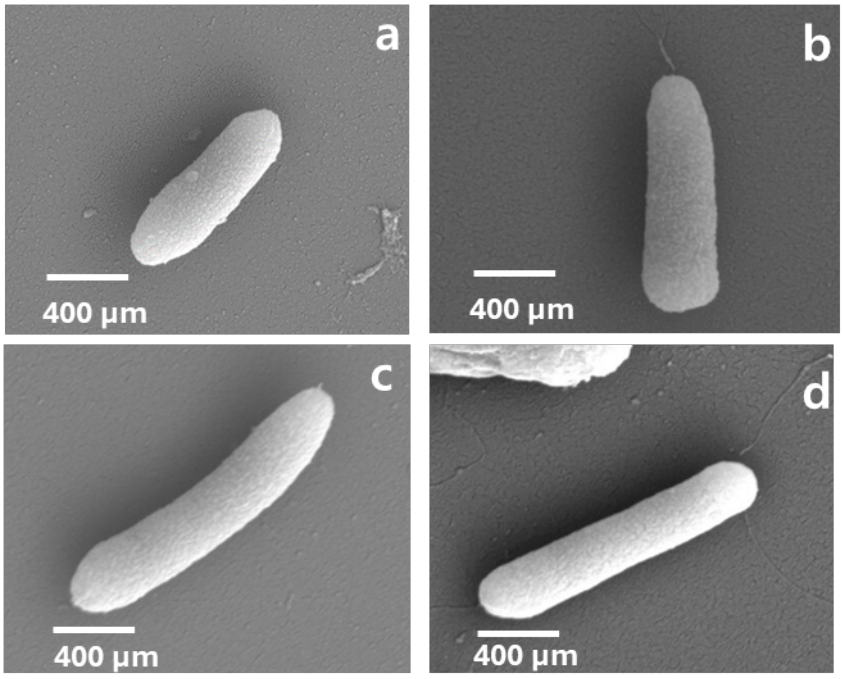


Figure 1. Scanning electron microscopy (SEM) images of resistant bacteria, showing morphological differences between (a) Phage cocktail-resistant strain, (b) Dobby-resistant strain, (c) MPK7-resistant strain, and (d) PAO1 control strain.

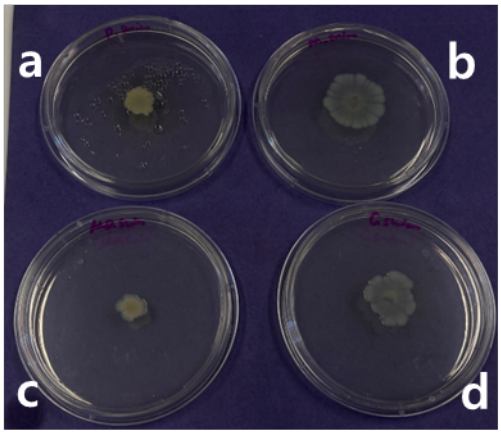


Figure 2. Swimming motility including (a) 24h-Dobby + MPK7-resistant strain, (b) 24h-MPK7-resistant strain, (c) 24h-Dobby-resistant strain, and (d) PAO1 control strain.

**Result**

Genomic analysis of three mutants isolated at the 24-hour time point focused on genes involved in LPS biosynthesis (lpxA, lpxC, and lpxD) and TFP function (pilT, pilU, and pilA). A mutation in the pilU gene was detected only in the 24-hour resistant isolates from the phage cocktail treatment (Table. S1).

Table 1. Genome analysis of resistant PAO1 mutants compared with wild-type PAO1

| Bacterial strain | Nucleotide position | Nucleotide substitution | Codon change | Amino acid change | Gene | Gene function |
|---|---|---|---|---|---|---|
| Dobby+MPK7 resistant bacteria | 438587 | T438587G | *TTA → TGA* | *Leu198** | *pilU* | pilus retraction |

## Appendix 2. Co-author declarations

Declaration from the co-authors of publications within this thesis as chapters are listed the following pages.

Prof. Hak-Kim Chan

Dr. Yue Cao

To whom it may concern,

I, Professor Hak-Kim Chan, declare that Mengyu Li was the primary researcher within the papers submitted in the thesis. All experimental work and manuscript presentations was conducted by Mengyu Li. I contributed as a supervisor on the experimental plan, data interpretation and editing on the following manuscript:

1. Li, M., Y. Cao, and H.K. Chan, Optimizing Performance of Inhalable Bacteriophage Powders using Human Serum Albumin (HSA). Int J Pharm, 2025. 678: p. 125709.

**Signed**: **Date**: 22/06/2025

To whom it may concern,

I, Dr. Yue Cao, declare that Mengyu Li was the primary researcher within the papers submitted in the thesis. All experimental work and manuscript presentations was conducted by Mengyu Li. I contributed as a supervisor on the experimental plan, data interpretation and editing on the following manuscript:

1. Li, M., Y. Cao, and H.K. Chan, Optimizing Performance of Inhalable Bacteriophage Powders using Human Serum Albumin (HSA). Int J Pharm, 2025. 678: p. 125709.

**Signed**: **Date**: 22/06/2025

## Appendix 3. Conference proceedings

1. Li, M., Morales, S., Chan, H.K. (2024) Presentation: Efficacy of Sequential Phage Application versus Phage Cocktail Approach in Reducing *Pseudomonas Aeruginosa* Virulence. Virus of Microbes, Perth, Australia
2. Li, M., Morales, S., Chan, H.K. (2022) Presentation: *Pseudomonas* phage cocktail powders for respiratory infections. Phage Bites Symposium, Sydney, Australia.
3. Li, M., Morales, S., Chan, H.K. (2022) Presentation: Phage Cocktail Powders for *Pseudomonas aeruginosa* Respiratory Infections. 5th World Bronchiectasis & NTM Conference, Prague.
4. Li, M, Hak-Kim Chan (2020). *Pseudomonas* Phage Cocktail Powders for Respiratory Infections. Drug Delivery to the Lung Conference, United Kingdom. **Appendix 3. Conference proceedings**

## Appendix 4. Publication during candidacy

1. Li, M., Y. Cao, and H.K. Chan, Optimizing Performance of Inhalable Bacteriophage Powders using Human Serum Albumin (HSA). Int J Pharm, 2025. 678: p. 125709.